



Terms and Conditions of Use of Digitised Theses from Trinity College Library Dublin

Copyright statement

All material supplied by Trinity College Library is protected by copyright (under the Copyright and Related Rights Act, 2000 as amended) and other relevant Intellectual Property Rights. By accessing and using a Digitised Thesis from Trinity College Library you acknowledge that all Intellectual Property Rights in any Works supplied are the sole and exclusive property of the copyright and/or other IPR holder. Specific copyright holders may not be explicitly identified. Use of materials from other sources within a thesis should not be construed as a claim over them.

A non-exclusive, non-transferable licence is hereby granted to those using or reproducing, in whole or in part, the material for valid purposes, providing the copyright owners are acknowledged using the normal conventions. Where specific permission to use material is required, this is identified and such permission must be sought from the copyright holder or agency cited.

Liability statement

By using a Digitised Thesis, I accept that Trinity College Dublin bears no legal responsibility for the accuracy, legality or comprehensiveness of materials contained within the thesis, and that Trinity College Dublin accepts no liability for indirect, consequential, or incidental, damages or losses arising from use of the thesis for whatever reason. Information located in a thesis may be subject to specific use constraints, details of which may not be explicitly described. It is the responsibility of potential and actual users to be aware of such constraints and to abide by them. By making use of material from a digitised thesis, you accept these copyright and disclaimer provisions. Where it is brought to the attention of Trinity College Library that there may be a breach of copyright or other restraint, it is the policy to withdraw or take down access to a thesis while the issue is being resolved.

Access Agreement

By using a Digitised Thesis from Trinity College Library you are bound by the following Terms & Conditions. Please read them carefully.

I have read and I understand the following statement: All material supplied via a Digitised Thesis from Trinity College Library is protected by copyright and other intellectual property rights, and duplication or sale of all or part of any of a thesis is not permitted, except that material may be duplicated by you for your research use or for educational purposes in electronic or print form providing the copyright owners are acknowledged using the normal conventions. You must obtain permission for any other use. Electronic or print copies may not be offered, whether for sale or otherwise to anyone. This copy has been supplied on the understanding that it is copyright material and that no quotation from the thesis may be published without proper acknowledgement.

**Role of infection and T cells in disease
pathogenesis in a model of
Alzheimer's disease**

Róisín M. McManus

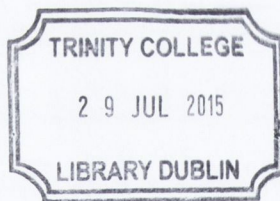


*A thesis submitted to Trinity College Dublin for the degree
of
Doctor of Philosophy*

**Supervisors: Prof. Kingston H.G. Mills
Prof. Marina A. Lynch**

**School of Biochemistry and Immunology
Trinity College Institute of Neuroscience
Trinity College Dublin**

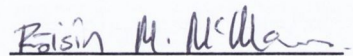
2015



Thesis 10624

Declaration of Authorship

This thesis is the sole work of the author, with the following exceptions; certain results were produced in collaboration with Dr. Tara Browne, Dr. Keith McQuillan, Dr. Kevin Walsh, Dr. Sarah Higgins and Dr. Mieszko Wilk. This work has not been submitted in whole or part to this or any other university for any other degree. The author gives permission to the library to lend or copy this work upon request.

A handwritten signature in black ink that reads "Róisín M. McManus". The signature is written in a cursive style and is underlined with a single horizontal line.

Róisín M. McManus

Abstract

Alzheimer's disease (AD) is a progressive neurodegenerative disease characterised by deposits of amyloid- β (A β) and neurofibrillary tangles. It has been suggested that inflammatory changes are associated with disease, however, it has not been established if these are a consequence of ongoing neurodegeneration or whether inflammation itself contributes to disease pathogenesis. T cells have been reported in the AD brain and clinical trials involving immunization with A β induced increased T cell infiltration into the brain and meningoencephalitis in some patients. In this study, the effect of A β -specific T cells was assessed *in vitro* and *in vivo*. It was observed that transfer of A β -specific Th1 cells increased numbers of T cells in the brain of APP/PS1 mice in comparison with wild type mice, and T cell infiltration enhanced A β deposition in the APP/PS1 mice. The *in vitro* studies revealed that A β -specific Th1 cells activate both microglia and astrocytes resulting in cytokine production, however, A β -specific Th17 cells preferentially activate astrocytes.

Recent studies suggest that exposure to infection can accelerate cognitive decline in AD patients, and pathogens have been detected in the post-mortem AD brain. However, the influence of infection on ongoing neuroinflammation and pathology remains poorly understood. In this study, the effect of a peripheral infection on AD-pathology in APP/PS1 mice was examined. There was significant infiltration of IFN- γ - and IL-17-producing T cells and NKT cells in older APP/PS1 mice 8 weeks after infection with the Gram-negative respiratory pathogen *Bordetella pertussis*, and this was accompanied by increased glial activation and A β deposition.

Current therapies for AD are limited and treat the symptoms of the disease as opposed to addressing the ongoing neuroinflammation or neurodegeneration. Previous studies indicated that infection enhanced T cell infiltration into the brain, therefore the effect of suppressing T cell migration by chronic treatment with FTY720 was investigated. However, analysis of the effect of FTY720 on clearance of infection revealed that chronic treatment with FTY720 prolonged the duration of infection with *B. pertussis*; this was associated with reduced influx of T cells into the lung and brain, and reduced infection-induced neuroinflammation. Treatment of APP/PS1 mice with FTY720 for the duration of infection restored blood-brain barrier (BBB) integrity reducing fibrinogen leakage into the parenchyma, and decreased T cell infiltration into the hippocampus. Furthermore, FTY720 attenuated the infection-induced increase in AD-pathology.

The data generated in this study demonstrate that T cells cause microglial and astrocytic activation which may contribute to the increase in A β deposition observed in APP/PS1 mice after transfer of A β -specific Th1 cells. The data suggest that infection may be a critical factor in the progression of AD and highlight an age-related vulnerability in APP/PS1 mice. This emphasises the importance of early diagnosis and treatment of infections in the elderly. Finally, the experiments with FTY720 suggest that stabilising the BBB and modulating T cell entry into the parenchyma may provide a future therapy for this disease. As FTY720 is a drug with multiple targets, it could prove an ideal therapy in AD where multiple pathways appear to be involved in disease progression.

Acknowledgements

I would first like to thank my supervisors Prof. Kingston Mills and Prof. Marina Lynch for their support and guidance during my time here in Trinity. The enthusiasm, drive and dedication you both have for your work has proved inspiring and I would like to thank you for the unique position of working in both of your labs. It has provided me with many opportunities and a chance to work with fantastic researchers, for which I am grateful.

I would like to thank Vivienne and Orla, you have both been invaluable throughout my PhD. Having you there made everything so much easier and I really appreciated it.

Thanks to Mieszko, Kevin, Sarah H and Tara for their help on the various experiments. I enjoyed working with and learning from you, and appreciated all of your help, especially with the big experiments and those long days in the lab! I would like to thank all the past and present members of MAL and KM lab, it's been a pleasure working with all of you. Special thanks to Barry and Gavin for all their help with the FACS and microscope work, you both helped me a lot (and at some critical times!) and I really appreciated it. In addition, thanks to the AH, TC and CC labs for their assistance with protocols and equipment.

I would like to thank the staff in the Biochemistry and Immunology Department, Physiology Department and TCIN for all your assistance over the last few years. I would like to acknowledge Catherine for her help with the financial bits and bobs, and I would also like to thank the Innovation Bursary for providing financial support.

I'd like to thank friends within Trinity and without, for their support and encouragement during my PhD. Last, but by no means least, special thanks go to my family. Mam, Dad, Eoin and Eilis your support over the course of my PhD and especially over the last few months has been amazing, and I truly couldn't have done it without you. I'm lucky to have you all.

Publications

McManus, R. M., K. H. Mills, and M. A. Lynch, 2015, T Cells-Protective or Pathogenic in Alzheimer's Disease?: J Neuroimmune Pharmacol. Epub 2015 May 10.

McManus, R. M., S. C. Higgins, K. H. Mills, and M. A. Lynch, 2014, Respiratory infection promotes T cell infiltration and amyloid-beta deposition in APP/PS1 mice: Neurobiol Aging, v. 35, p. 109-21.

Browne, T. C., K. McQuillan, **R. M. McManus**, J. A. O'Reilly, K. H. Mills, and M. A. Lynch, 2013, IFN- γ Production by amyloid β -specific Th1 cells promotes microglial activation and increases plaque burden in a mouse model of Alzheimer's disease: J Immunol, v. 190, p. 2241-51.

Table of Contents

Declaration of Authorship	i
Abstract	ii
Acknowledgements.....	iii
Publications	iv
List of Figures.....	xi
List of Tables	xvi
Abbreviations	xvii
Chapter 1 Introduction.....	1
1.1 Adaptive immunity.....	3
1.1.1 T cell induction	3
1.1.2 Th1 cells	7
1.1.3 Th2 cells	8
1.1.4 Th17 cells	8
1.1.5 Treg cells	9
1.1.6 CD8 ⁺ T cells	10
1.1.7 T cell memory	11
1.1.8 NKT cells	13
1.2 The central nervous system	13
1.2.1 The BBB and immune privilege	13
1.2.2 Maintaining the BBB; the role of tight junction proteins and pericytes...	15
1.2.3 T cell surveillance of the brain.....	18
1.2.4 T cell entry: a two-step process.....	18
1.2.5 Lymphatic drainage of the brain	23
1.3 Alzheimer’s disease.....	23
1.3.1 General background	23
1.3.2 Neurofibrillary tangles.....	26
1.3.3 Processing of APP to A β	27
1.3.4 AD mouse models.....	29
1.3.4.1 Tg2576	30

1.3.4.2 APP/PS1	30
1.3.4.3 3xTg-AD	31
1.4 CNS immune system	31
1.4.1 Microglial activation	31
1.4.2 Microglial activation in AD	34
1.4.3 Phagocytosis of amyloid	36
1.4.4 Microglia as APCs.....	37
1.4.5 Astrocytes in AD	40
1.4.6 Astrocytes as APCs.....	41
1.4.7 Increased BBB permeability in AD.....	42
1.4.8 Facilitated T cell entry through the BBB in AD	44
1.5 Future therapies for AD.....	46
1.5.1 Immunization.....	46
1.5.2 FTY720	48
1.6 Changes to the immune system with age and AD	51
1.6.1 Age-related changes in the immune system.....	51
1.6.2 Changes to the adaptive immune system in AD	52
1.7 Infection in AD.....	53
1.7.1 Infection in the elderly	53
1.7.2 Infection in AD	55
1.7.3 <i>Chlamydia pneumonia</i>	56
1.7.4 <i>Helicobacter pylori</i>	57
1.7.5 Spirochetes	58
1.7.6 HSV-1 and CMV	58
1.7.7 Infection in other neurodegenerative diseases	60
1.7.8 Animal models of systemic challenge	60
1.7.9 Other animal models of infection	61
1.7.10 <i>Bordetella pertussis</i>	62
1.8 Study aims	65
Chapter 2 Materials and Methods	67
2.1 Animals.....	69
2.2 Genotyping APP/PS1 mice	69

2.2.1 Isolation of DNA.....	69
2.2.2 Polymerase chain reaction (PCR) and identification of APPswe and PSEN1dE9 genes	70
2.3 Generation of A β -specific T cell lines and <i>in vivo</i> transfer.....	71
2.4 <i>B. pertussis</i> respiratory challenge	72
2.5 Immunization of mice against <i>B. pertussis</i>	73
2.6 FTY720 administration	73
2.7 Isolation of mononuclear cells from tissue.....	73
2.7.1 Isolation of mononuclear cells from CNS tissue.....	73
2.7.2 Isolation of cells from lung tissue.....	74
2.7.3 Isolation of cells from lymph node tissue	74
2.7.4 Flow cytometric analysis on cells prepared <i>ex vivo</i>	74
2.8 Preparation of tissue from mice	80
2.9 Detection of A β	80
2.10 Protein quantification	82
2.11 Immunohistochemical analysis.....	82
2.11.1 Coating of glass slides.....	82
2.11.2 Preparation of tissue sections for immunohistochemistry.....	82
2.11.3 Congo red identification of amyloid plaques	83
2.11.4 Fibrinogen staining	83
2.11.5 CD3 staining.....	84
2.12 Real-time PCR.....	84
2.12.1 RNA isolation	84
2.12.2 cDNA synthesis	85
2.12.3 RT-PCR	86
2.13 <i>In vitro</i> experiments	88
2.14 Ag-specific stimulation of lung or lymph node cells	88
2.15 Preparation and treatment of glia	88
2.16 Cell counts	89
2.17 Preparation and treatment of T cells.....	90
2.17.1 T cell polarization	90
2.17.2 Co-culture of T cells and glia	91
2.18 Analysis of cytokine and chemokine release using ELISA	91

2.19 Statistical analysis	93
Chapter 3 Aβ-specific T cells induce glial activation <i>in vitro</i> and infiltrate the brains of APP/PS1 mice <i>in vivo</i> triggering Aβ deposition	95
3.1 Introduction	97
3.2 Results	102
3.2.1 Th1 cells induce microglial activation	102
3.2.2 Th1 and Th17 cells induce activation of astrocytes	102
3.2.3 A β -specific Th1 cells induce microglial and astrocytic activation	103
3.2.4 A β -specific T cells infiltrate the brains of APP/PS1 mice.....	103
3.2.5 Increased A β deposition in the brains of APP/PS1 mice following transfer of A β -specific T cells	104
3.3 Discussion.....	122
Chapter 4 Infection with <i>B. pertussis</i> induces T cell infiltration and Aβ deposition in the brains of older APP/PS1 mice	130
4.1 Introduction	132
4.2 Results	135
4.2.1 Respiratory infection promotes T cell infiltration into the brains of APP/PS1 mice	135
4.2.2 Increased microglial and macrophage activation in previously infected APP/PS1 mice	136
4.2.3 Infection enhances A β accumulation in aged APP/PS1 mice.....	137
4.3 Discussion.....	150
Chapter 5 Treatment with FTY720 during infection with <i>B. pertussis</i> reduces T cell influx into the lung and exacerbates the infection	156
5.1 Introduction	158
5.2 Results	162
5.2.1 Chronic treatment with FTY720 significantly impairs the ability of mice to clear infection with <i>B. pertussis</i>	162
5.2.2 FTY720 treatment significantly suppresses T cell infiltration into the lungs of <i>B. pertussis</i> -infected mice.....	162
5.2.3 FTY720 treatment reduces the number of T cells in the mediastinal lymph nodes of <i>B. pertussis</i> -infected mice	164

5.2.4 Decreased Ag-specific response in lymph node and lung mononuclear cells prepared from FTY720-treated <i>B. pertussis</i> -infected mice.....	166
5.2.5 Decreased $\gamma\delta$ T cell and NKT cell influx into the lungs of FTY720-treated <i>B. pertussis</i> -infected mice	166
5.2.6 Increased inflammatory cells infiltrate into the lung of FTY720-treated mice during infection with <i>B. pertussis</i>	167
5.2.7 Chemokine and cytokine expression significantly reduced in lung tissue from FTY720-treated <i>B. pertussis</i> -infected mice.....	167
5.2.8 FTY720 does not impair clearance of <i>B. pertussis</i> in immunised mice..	168
5.2.9 Immunization with Pw increases effector memory T cell infiltration into the lungs of <i>B. pertussis</i> -infected mice	169
5.3 Discussion.....	200
Chapter 6 FTY720 treatment during infection with <i>B. pertussis</i> attenuates the infection-induced increase in AD-pathology in APP/PS1 mice	208
6.1 Introduction	210
6.2 Results	214
6.2.1 Chronic treatment with FTY720 during infection with <i>B. pertussis</i> significantly reduces infection-induced neuroinflammation	214
6.2.2 Infection of APP/PS1 mice with <i>B. pertussis</i>	214
6.2.3 Respiratory infection induces T cell infiltration into the brains of APP/PS1 mice	215
6.2.4 FTY720 promotes BBB integrity in APP/PS1 mice	216
6.2.5 FTY720 reduces neuroinflammation in <i>B. pertussis</i> -infected APP/PS1 mice	217
6.2.6 FTY720 reduces A β burden in <i>B. pertussis</i> -infected APP/PS1 mice	217
6.3 Discussion.....	239
Chapter 7 General Discussion	245
7.1 General Discussion	247
7.2 Limitations of the study	256
7.3 Future work.....	257
Chapter 8 Bibliography.....	259

Appendix I Solutions	305
Appendix II Materials.....	309
Appendix III Addresses.....	312

List of Figures

Chapter 1

Figure 1.1 Activation of a naïve T cell by an APC	6
Figure 1.2 CD4 ⁺ T cell differentiation and function.....	10
Figure 1.3 T cell memory.....	12
Figure 1.4 The blood-brain barrier.....	17
Figure 1.5 T cell migration into the brain; a two-step process	22
Figure 1.6 Processing of APP.....	29
Figure 1.7 M1 and M2 activation of myeloid cells in mouse	34
Figure 1.8 Proposed role of T cells in Alzheimer's disease.	42
Figure 1.9 FTY720 prevents T cell egress from the lymph node.....	51
Figure 1.10 Innate and adaptive immune responses to infection with <i>B. pertussis</i>	64

Chapter 2

Figure 2.1 Percoll separation to isolate mononuclear cells from the CNS	77
---	----

Chapter 3

Figure 3.1 T cells polarised <i>in vitro</i> to Th1, Th2 and Th17 subtype	105
Figure 3.2 T cells polarised to the Th1 subtype induce microglial activation..	106
Figure 3.3 Th2 cells do not induce microglial activation.....	107
Figure 3.4 Th17 cells do not induce a pro-inflammatory microglial response	108
Figure 3.5 Th1 cells induce activation of astrocytes	109
Figure 3.6 Th2 cells do not induce astrocytic activation.....	110
Figure 3.7 Th17 cells induce a pro-inflammatory response in purified astrocytic cultures	111
Figure 3.8 A β -specific T cells polarised <i>in vitro</i> to Th1, Th2 and Th17 subtype.....	112
Figure 3.9 A β -specific Th1 cells induce activation of microglial cells	113
Figure 3.10 Incubation with A β -specific Th2 cells does not induce microglial activation.....	114

Figure 3.11 A β -specific Th17 cells do not cause microglial activation <i>in vitro</i>	115
Figure 3.12 A β -specific Th1 cells induce astrocytic activation.....	116
Figure 3.13 A β -specific Th2 cells do not induce astrocytic activation	117
Figure 3.14 A β -specific Th17 cells induce astrocyte IL-6 release.....	118
Figure 3.15 A β -specific Th1 cells migrate into the brain of APP/PS1 mice.....	119
Figure 3.16 Increased chemokine expression in APP/PS1 mice injected with A β - specific Th1 cells.....	120
Figure 3.17 A β -specific Th1 cells increase A β deposition in APP/PS1 mice.....	121

Chapter 4

Figure 4.1 Infection induces T cell infiltration into the brain of older APP/PS1 mice	138
Figure 4.2 Respiratory infection induces IFN- γ ⁺ and IL-17 ⁺ CD4 ⁺ T cell infiltration into the brain of APP/PS1 mice	139
Figure 4.3 Increased IFN- γ ⁺ and IL-17 ⁺ CD8 ⁺ T cells in the brains of APP/PS1 mice following infection with <i>B. pertussis</i>	140
Figure 4.4 Infection with <i>B. pertussis</i> increases infiltration of IFN- γ ⁺ and IL-17 ⁺ NKT cells	141
Figure 4.5 T cells infiltrate the hippocampus of <i>B. pertussis</i> -infected APP/PS1 mice	142
Figure 4.6 Chemokine expression in cortical tissue from older APP/PS1 is exacerbated by infection with <i>B. pertussis</i>	143
Figure 4.7 CD11b and GFAP expression is enhanced in cortical tissue from older <i>B. pertussis</i> -infected APP/PS1 mice	144
Figure 4.8 Increased microglial activation in APP/PS1 mice.....	145
Figure 4.9 The increased macrophage activation in APP/PS1 is exacerbated by infection with <i>B. pertussis</i>	146
Figure 4.10 Cytokine expression increased in older APP/PS1 mice.....	147
Figure 4.11 Infection increases A β plaque number in older APP/PS1 mice	148
Figure 4.12 Insoluble A β ₄₀ increased 56 days post-infection in older APP/PS1 mice	149

Chapter 5

Figure 5.1 Chronic FTY720 treatment significantly impairs clearance of infection with <i>B. pertussis</i>	172
Figure 5.2 FTY720 treatment suppresses T cell infiltration into the lungs of <i>B. pertussis</i> -infected mice	174
Figure 5.3 FTY720 reduces naïve and central memory T cell infiltration into the lungs of <i>B. pertussis</i> -infected mice	175
Figure 5.4 CD49d ⁺ T cells infiltrate the lungs of <i>B. pertussis</i> -infected mice, with the absolute number but not the frequency reduced by treatment with FTY720	176
Figure 5.5 FTY720 treatment suppresses IFN- γ ⁺ and IL-17 ⁺ cell infiltration into the lungs of <i>B. pertussis</i> -infected mice	177
Figure 5.6 FTY720 treatment reduces the number of T cells in the mediastinal lymph nodes of <i>B. pertussis</i> -infected mice	179
Figure 5.7 FTY720 reduces the number of naïve and central memory CD4 ⁺ T cells in lymph nodes of <i>B. pertussis</i> -infected mice on day 28 post-infection	180
Figure 5.8 Effector memory CD8 ⁺ T cells unaffected by FTY720 treatment in the lymph nodes of <i>B. pertussis</i> -infected mice	181
Figure 5.9 Number of CD49d ⁺ T cells increased in the lymph nodes of FTY720-treated <i>B. pertussis</i> -infected mice on day 60 post-infection.....	182
Figure 5.10 FTY720 treatment suppresses IFN- γ ⁺ and IL-17 ⁺ T cell numbers in the lymph node of <i>B. pertussis</i> -infected mice	183
Figure 5.11 Decreased Ag-specific response by lung T cells from FTY720-treated <i>B. pertussis</i> -infected mice	184
Figure 5.12 FTY720 treatment suppresses $\gamma\delta$ T cell infiltration into the lungs of <i>B. pertussis</i> -infected mice	185
Figure 5.13 FTY720 treatment suppresses $\gamma\delta$ T cell numbers in the lymph nodes of <i>B. pertussis</i> -infected mice	186
Figure 5.14 FTY720 treatment alters IFN- γ ⁺ NKT cell infiltration into the lungs of <i>B. pertussis</i> -infected mice	187

Figure 5.15 FTY720 treatment suppresses IFN- γ ⁺ and IL-17 ⁺ NK and NKT cell populations in the mediastinal lymph nodes of <i>B. pertussis</i> -infected mice	188
Figure 5.16 FTY720 treatment suppresses B cell infiltration into the lungs of <i>B. pertussis</i> -infected mice	189
Figure 5.17 FTY720 treatment increases innate cell infiltration into the lungs of <i>B. pertussis</i> -infected mice	190
Figure 5.18 Decreased chemokine expression in the lungs of FTY720-treated infected mice.....	191
Figure 5.19 Decreased cytokine expression in the lungs of FTY720-treated infected mice.....	192
Figure 5.20 Delayed anti-inflammatory cytokine expression in the lungs of FTY720-treated infected mice.....	193
Figure 5.21 Expression of tight junction proteins in the lungs of <i>B. pertussis</i> -infected mice.....	194
Figure 5.22 FTY720 treatment does not affect the protective efficacy of Pa or Pw in mice	195
Figure 5.23 FTY720 treatment suppresses B cell and T cell infiltration into the lungs of immunised <i>B. pertussis</i> -infected mice	196
Figure 5.24 Immunization with Pw increases recruitment of CD4 ⁺ T cells into the lung following <i>B. pertussis</i> infection, and this is suppressed by FTY720.....	197
Figure 5.25 Immunization with Pw increases effector memory T cell infiltration into the lungs of <i>B. pertussis</i> -infected mice.....	198
Figure 5.26 FTY720 treatment suppresses naïve and central memory CD8 ⁺ T cell infiltration into the lungs of <i>B. pertussis</i> -infected mice.....	199

Chapter 6

Figure 6.1 Chronic treatment with FTY720 during infection with <i>B. pertussis</i> reduces infection-induced neuroinflammation.....	220
Figure 6.2 FTY720 induces the expression of IL-4 in the brain during infection with <i>B. pertussis</i>	221
Figure 6.3 Challenge with <i>B. pertussis</i> induces transient infection in mice.....	222

Figure 6.4 No evidence of genotype effect in response to <i>B. pertussis</i> -infection	223
Figure 6.5 Infection induces CD4 and CD8 T cell trafficking to the brains of APP/PS1 mice	224
Figure 6.6 Increased IFN- γ^+ and IL-17 $^+$ CD4 $^+$ T cells in the brains of APP/PS1 mice following <i>B. pertussis</i> -infection	225
Figure 6.7 Increased IFN- γ^+ and IL-17 $^+$ CD8 $^+$ T cells in the brains of APP/PS1 mice following infection with <i>B. pertussis</i>	226
Figure 6.8 FTY720 reduces T cell infiltration into the hippocampus of APP/PS1 mice	229
Figure 6.9 T cells found in close apposition to other brain cells in the hippocampus of APP/PS1 mice	230
Figure 6.10 Increased chemokine expression in APP/PS1 mice	231
Figure 6.11 FTY720 promotes BBB integrity, reducing fibrinogen immunoreactivity in the hippocampus of APP/PS1 mice	234
Figure 6.12 FTY720 treatment attenuates neuroinflammation in APP/PS1 mice	235
Figure 6.13 FTY720 treatment attenuates infection-induced A β deposition in APP/PS1 mice	237
Figure 6.14 FTY720 treatment attenuates infection-induced production of soluble A β_{40} and A β_{42} in APP/PS1 mice	238

Chapter 7

Figure 7.1 Proposed sequence of events leading to the increased deposition of A β in APP/PS1 mice during infection, and possible targets of FTY720	255
--	-----

List of Tables

Table 2.1 Primers used for DNA amplification	71
Table 2.2 Antibodies used in flow cytometry	78
Table 2.3 LSR Fortessa.....	79
Table 2.4 Gene expression assay numbers of the primers used in RT-PCR.....	87
Table 2.5 Cytokine expression using ELISA	93
Table 3.1 Results summary of microglial or astrocytic activation following incubation with T cells <i>in vitro</i>	128
Table 3.2 Results summary of microglial or astrocytic activation following incubation with A β -specific T cells <i>in vitro</i>	128

Abbreviations

ACT	Adenylate cyclase toxin	CCR	Chemokine C-C motif receptor
AD	Alzheimer's disease	CD	Cluster of differentiation
ADAM	A disintegrin and metalloprotease	cDNA	Complimentary deoxyribonucleic acid
Ag	Antigen	CFU	Colony forming units
AICD	APP intercellular domain	CMEC	Cerebral microvascular endothelial cells
AJ	Adherens junction	CMV	Cytomegalovirus
ANOVA	Analysis of variance	CNS	Central nervous system
APC	Antigen presenting cell	COX	Cyclooxygenase
APH-1	Anterior pharynx-defector-1	CSF	Cerebrospinal fluid
AP-1	Activator protein-1	CTF	C-terminal fragment
APO	Apolipoprotein	CTL	Cytotoxic lymphocyte
APOE4	Apolipoprotein E type 4	CTLA-4	Cytotoxic T lymphocyte antigen-4
APP	Amyloid precursor protein	CVO	Circumventricular organ
APP^{swe}	APP mice with the double Swedish mutation	CX3CL	C-X3-C motif chemokine ligand
Arg-1	Arginase-1	CX3CR	C-X3-C motif chemokine receptor
Aβ	Amyloid beta	CXCL	C-X-C motif chemokine ligand
B.P.	<i>Bordetella pertussis</i>	CXCR	C-X-C motif chemokine receptor
B220	Isoform of CD45R, 220 kDa expressed by B cells	DAMP	Danger-associated molecular pattern
BACE1	β -site APP cleaving enzyme 1	DAPI	40,6- diamidino-2-phenylindole
BBB	Blood-brain barrier	DC	Dendritic cell
BCA	Bicinchoninic acid	DEPC	Diethyl pyrocarbonate
BCSFB	Blood cerebrospinal fluid barrier	DG	Dystroglycan
BDV	Borna disease virus	dH₂O	Distilled water
BFA	Brefeldin A	DMEM	Dulbecco's modified eagle medium
BM	Basement membrane	DNA	Deoxyribonucleic acid
bp	Base pair	DPX	Dibutyl phthalate in xylene
BSA	Bovine serum albumin	EAE	Experimental autoimmune encephalomyelitis
C83	C-terminal fragment 83 residues long	EBAO	Ethidium bromide acridine orange
C99	C-terminal fragment 99 residues long	EDTA	Ethylenediaminetetraacetic acid
CAA	Cerebral amyloid angiopathy		
CaCl₂.2H₂O	Calcium chloride dihydrate		
CCL	Chemokine C-C motif ligand		

ELISA	Enzyme-linked immunosorbent assay	Ig	Immunoglobulin
FACS	Fluorescence activated cell sorting	IL	Interleukin
FBS	Fetal bovine serum	IL-12R2β	Interleukin-12 receptor beta
FDA	Food and Drug Administration	IL-1RA	Interleukin-1 receptor antagonist
Fe.SO₄.-7H₂O	Iron(II) sulfate heptahydrate	IL-4Rα1	Interleukin-4 receptor alpha 1
FHA	Filamentous hemagglutinin	ISF	Interstitial fluid
FIZZ-1	Found in inflammatory zone-1	JAM	Junctional adhesion molecule
FMO	Fluorescence minus one	KC	Keratinocyte derived-chemokine
FoxP3	Forkhead box P3	KCl	Potassium chloride
FTY720	Fingolimod/Gilenya; Novartis	KH₂PO₄	Potassium phosphate monobasic
GATA3	GATA binding protein 3	LFA-1	Lymphocyte function-associated antigen-1
GFAP	Glial fibrillary acidic protein	LOAD	Late-onset Alzheimer's disease
GFP	Green fluorescent protein	LPS	Lipopolysaccharide
GM-CSF	Granulocyte macrophage colony stimulating factor	M1	Classically-activated myeloid cells
GPCR	G-protein coupled receptor	M2	Alternatively-activated myeloid cells
H₂O₂	Hydrogen peroxide	MACS	Magnetic-activated cell sorting
H₂SO₄	Sulfuric acid	MAPK	Mitogen-activated protein kinases
HBSS	Hanks balanced salt solution	MCI	Mild cognitive impairment
HCl	Hydrochloric acid	MCP-1	Monocyte chemotactic protein-1
HK <i>B.P.</i>	Heat killed <i>B. pertussis</i>	M-CSF	Macrophage colony stimulating factor
HPLC	High-performance liquid chromatography	MgCl₂.6H₂O	Magnesium chloride hexahydrate
HR	Hazard ratio	MHC class I	Major histocompatibility complex class I
HRP	Horseradish peroxidase	MHC class II	Major histocompatibility complex class II
HSPG	Herparan sulphate proteoglycans	MHV	Mouse hepatitis virus
HSV-1	Herpes simplex virus type 1	MIP	Macrophage inflammatory protein
i.c.v.	Intracerebroventricular	MMP	Matrix metalloproteases
i.p.	Intraperitoneal	MMSE	Mini-mental state examination
i.v.	Intravenous	MR	Mannose receptor
ICAM	Intercellular adhesion molecule		
ICU	Intensive care unit		
IDE	Insulin-degrading enzyme		
IFN	Interferon		

MRI	Magnetic resonance imaging	PECAM	Platelet endothelial cell adhesion molecule
mRNA	Messenger ribonucleic acid	PEN	Presenilin enhancer
MS	Multiple sclerosis	PET	Positron emission tomography
mSOD1	Mutant superoxide dismutase 1	PFA	Paraformaldehyde
Na₂HPO₄	Disodium hydrogen phosphate	PI	Propidium iodide
NaCl	Sodium chloride	PIB	Pittsburgh compound B
NaN₃	Sodium azide	PMA	Phorbol myristate acetate
NaOH	Sodium hydroxide	Poly I:C	Polyinosinic-polycytidylic acid
NEP	Nephrilysin	PPAR-γ	Peroxisome proliferator-activated receptor-γ
NFAT	Nuclear factor of activated T cells	PRR	Pattern recognition receptor
NFTs	Neurofibrillary tangles	PS	Presenilin
NF-κB	Nuclear factor kappa B	PSEN1dE9	Presenilin 1 with exon 9 deleted
NGF	Nerve growth factor	PSGL-1	P-selectin glycoprotein ligand
NH₄Cl	Ammonium chloride	PT	Pertussis toxin
NK	Natural killer	Pw	Whole cell pertussis vaccine
NLR	NOD like receptor	RAGE	Receptor for advanced glycation endpoints
NLRP3	NOD-like receptor family, pyrin domain containing 3	RANTES	Regulated on activation, normal T cell expressed and secreted
NMDA	N-methyl-d-aspartate	RNA	Ribonucleic acid
NO	Nitric oxide	RORγT	RAR-related orphan receptor gamma T
NOD	Nucleotide-binding oligomerization domain	rpm	Revolutions per minute
NOS2	Nitric oxide synthase 2	RPMI	Roswell park memorial institute medium
OCT	Optimum cooling temperature compound	RT	Room temperature
OR	Odds ratio	s.c.	Subcutaneous
OVA	Ovalbumin	S1P	Sphingosine 1-phosphate
Pa	Acellular pertussis vaccine	S1P₁	Sphingosine 1-phosphate receptor 1
PAMP	Pathogen-associated molecular pattern	sAPP	Soluble APP
PBMC	Peripheral blood mononuclear cell	SCID	Severe combined immunodeficiency
PBS	Phosphate buffered saline	SDS	Sodium dodecyl sulphate
PBS-T	Phosphate buffered saline with Tween	SEM	Means with standard errors
PCR	Polymerase chain reaction	SIP	Stock isotonic percoll
PD-1	Programmed cell death-1	SR	Scavenger receptor
PD-L1	Programmed death-ligand 1		

STAT	Signal transducer and activator of transcription
T_{CM}	Central memory T cells
TCR	T cell receptor
TCRβJ	T cell receptor beta joining region
TCT	Tracheal cytotoxin
T_{EM}	Effector memory T cells
Tg	Transgenic
TGF-β	Transforming growth factor beta
Th	T helper
TJ	Tight junction
TLR	Toll-like receptor
TMEV	Theiler's murine encephalomyelitis
TNFα	Tumor necrosis factor alpha
Tr1	T regulatory 1 cells
Treg	Regulatory T cell
UTI	Urinary tract infection
VCAM-1	Vascular cell adhesion molecule-1
WT	Wild type
YM-1	Chitinase 3-like 3
ZO	Zonular occludens
γc	IL-2Rγ chain
γδ	Gamma delta TCR

Chapter 1

Introduction

1.1 Adaptive immunity

After exposure to an infectious agent, the innate immune system is the first defence; rapid acting and non-specific in nature, it can eliminate the pathogen in hours using pattern recognition receptors (PRRs) which recognise pathogens based on the conserved motifs they display on their cell surface called pathogen-associated molecular patterns (PAMPs). However if this defence is breached, the innate immune system works to contain the infection while the adaptive immune response is generated. The adaptive immune system is more efficient at eliminating infection as it develops specifically for each insult at a cost of taking days rather than hours to establish. The lymphocytes that develop have highly specialised antigen receptors on their cell surface that can respond to single antigens. Each lymphocyte has an antigen receptor with a specific, unique antigen-binding site. As there are billions of lymphocytes in the body, this results in a huge, diverse repertoire of antigen-specific cells available to recognize and respond to practically any antigen a person may be exposed to over their lifetime.

1.1.1 T cell induction

T cells are a subset of lymphocytes with antigen receptors that are specific for a unique antigen known as T cell receptors (TCR) however, the recognition and functional properties of this receptor are distinct. Over 90% of T cells have a TCR made up of a heterodimer; TCR α and TCR β , and a proportion have TCR γ : TCR δ heterodimers. T cell precursors develop in the bone marrow from which they migrate to the thymus where they mature. On maturation, the naïve T cell circulates through the lymphatic system, sampling antigen expressed on major histocompatibility complex (MHC) class I or class II receptors on dendritic cells (DC) until they recognize their specific antigen and become activated. The naïve T cell needs interleukin (IL)-7 and occasional interactions with self-peptide: self-MHC complexes to survive in the periphery, without these signals, the cell undergoes programmed cell death (Koenen et al., 2013). In mice, the pool of the naïve T cells in the periphery is continuously replenished via the thymus throughout the life of the mouse however, in humans this pool is maintained

through proliferation of naïve cells in the periphery only (den Braber et al., 2012).

Activation of a naïve T cell is a controlled process and a number of specific signals must occur for effective T cell activation (Fig 1.1). The TCR only recognizes its specific peptide when presented via a peptide: MHC complex on a DC, as only mature DCs can activate naïve T cells. The MHC complex must also recognise the TCR itself. The T cell has a co-receptor; CD4 or CD8 which binds the MHC complex of the TCR: MHC association increasing the sensitivity to antigen stimulation. Together this provides the first signal necessary for T cell activation. Activation of the TCR induces phosphorylation of tyrosine residues on CD3, allowing the intracellular protein ZAP-70 to bind which is in turn activated by Lck. This induces an intracellular signalling cascade resulting in the activation of protein kinase C- θ and calcineurin which ultimately leads to activation of nuclear factor kappa B (NF- κ B), nuclear factor of activated T cells (NFAT) and activator protein-1 (AP-1) transcription factors. Signalling through the TCR also induces a conformational change in lymphocyte function-associated antigen (LFA)-1, increasing its affinity for intercellular adhesion molecule (ICAM)-1 or -2 on the antigen presenting cell (APC) stabilising the T cell: APC interaction (Friedl and Gunzer, 2001). The second signal comes from the co-stimulatory receptor on the T cell; CD28. CD28 interacts with CD80 or CD86 (also termed B7.1 and B7.2) on the APC, resulting in increased expression of other co-stimulatory receptors while also activating NF- κ B, NFAT and AP-1 transcription factors. Together, the first and second signals induce IL-2 production by the T cell, triggering proliferation.

While these 2 signals are vital for activation of naïve T cells, other ligand – receptor interactions aid the process, such as CD40 on the DC which binds CD40L on the T cell. This interaction can signal bi-directionally, inducing T cell activation but also promoting CD80 and CD86 expression on the DC (Iezzi et al., 2009). These activated naïve T cells then leave the lymph node or spleen and migrate to the site of infection. Here the cells are re-stimulated by local APCs such as macrophages, inducing effector T cells that produce cytokines and chemokines

to mediate pathogen clearance. The T cell subtype generated will vary depending on the cytokine environment at the time of the reaction.

In order to control the magnitude of an immune response the expression of co-inhibitory receptors on T cells is induced during T cell activation which, unlike co-stimulatory receptors, negatively affects T cell responses (Chen and Flies, 2013). Indeed it is the balance between stimulatory and inhibitory signalling which can determine the immune response to a pathogen. Cytotoxic T lymphocyte antigen-4 (CTLA-4) is an inhibitory receptor that binds CD80 or CD86, and upregulation of CTLA-4 is associated with CD28 downregulation (Rudd et al., 2009). Programmed cell death-1 (PD-1) can also induce T cell inhibition by negatively regulating TCR signalling following ligation with its ligand, PD-L1 (Keir et al., 2008). At later stages of immune activation the expression of co-inhibitory receptors replaces the co-stimulatory receptor expression on the surface of T cells (Zhu et al., 2011). This ensures strict control of the adaptive immune system and allows contraction of the T cell response on resolution of infection.

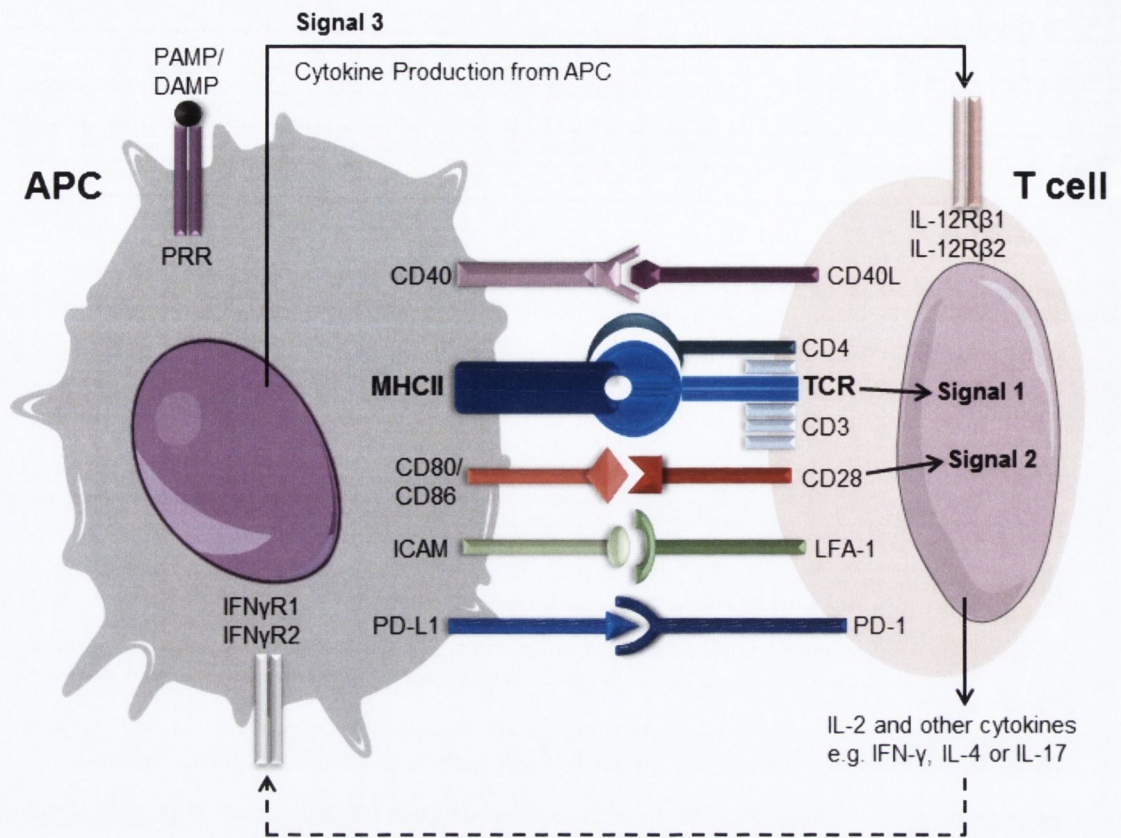


Figure 1.1 Activation of a naïve T cell by an APC

Activation of a naïve T cell requires three signals from an APC. The first comes from the TCR: MHC II interaction; professional APCs such as DCs phagocytose pathogens and process them into peptides, loading one into the groove of an MHC class II complex to present to a naïve T cell. If the TCR recognizes the peptide and MHC class II complex it becomes activated, binding of the co-receptor CD4 to the MHC class II induces the T cell to become much more sensitive to the antigen presented, thus enhancing the signal generated. Signalling induces a conformational change in lymphocyte function-associated antigen (LFA)-1 increasing its affinity for intercellular adhesion molecule (ICAM)-1 or -2 stabilising the T cell: APC interaction. The second signal comes from the co-stimulatory receptor CD28 on the T cell binding either CD80 or CD86 on the APC. Activation of the TCR and CD28 together induce production of IL-2 which functions in an autocrine manner on T cell inducing cell differentiation, and maintaining survival. Additional signalling occurs between the APC and T cell; CD40 binding CD40L can signal bi-directionally promoting cell activation. The APC also produces cytokines in response to the pathogen via activation of PRRs, which influences the polarisation of the T cell and is the third signal. The activated T cell can now produce cytokines e.g. IFN- γ , IL-4 or IL-17. T cell activation is also modulated by co-inhibitory receptors e.g. programmed cell death (PD)-1, which binds programmed death-ligand 1 (PD-L1) and negatively regulates T cell function, thus maintaining control over the magnitude of the adaptive immune response. PRR, pattern recognition receptor; PAMP, pathogen-associated molecular pattern; DAMP, danger-associated molecular pattern.

1.1.2 Th1 cells

T helper (Th) cells express the CD4 co-receptor and only recognize their cognate antigen presented via an MHC class II complex on an APC. Th cells are not cytotoxic or phagocytic on their own instead, as their name suggests, their main role is to help other cells carry out these functions. In order to provide the most efficient immune response, the particular cytokines that a pathogen induces are central to the type of adaptive immune response generated.

T cells activated in the presence of IL-12 and interferon (IFN)- γ differentiate to the Th1 subtype (Fig 1.2). Natural killer (NK) cells are a source of IFN- γ , and DCs and macrophages can produce IL-12 in response to certain pathogens (Walsh and Mills, 2013). IFN- γ signals via signal transducer and activator of transcription (STAT)-1 inducing the expression of the T-bet transcription factor. In turn, T-bet induces IL-12R2 β which binds and is activated by IL-12. IL-12 signals via STAT4 and together with T-bet, induces T cell production of IFN- γ which can feedback onto the T cell committing the differentiation to Th1.

Th1 cells predominantly mediate immunity to intracellular pathogens or tumours (Mills, 2008). Macrophages can ingest and phagocytose pathogens, however, in some instances the pathogen is not killed and can maintain a chronic infection in the macrophage. In this case, activation by Th1 cells can promote the macrophage into further microbial killing (Walsh and Mills, 2013) or if necessary, apoptosis. Once T cells recognise antigen presented by DCs or macrophages, they become activated and provide two signals necessary for further macrophage activation. The Th1 cell produces considerable amounts of IFN- γ and provides CD40L to interact with CD40 on the macrophage which together, activate the cell and convert it into an extremely effective antimicrobial cell. CD40 signalling also enhances MHC class II, CD80 and CD86 expression, making the macrophage a more efficient APC. Activated macrophages increase their cell-surface expression of CD40 and tumour necrosis factor α (TNF α) receptor and increase production of TNF α . This functions in a positive feedback loop, and with

IFN- γ , can enhance the production of reactive oxygen species creating a potent antimicrobial cell.

1.1.3 Th2 cells

Development of Th2 cells is induced by IL-4 (Fig 1.2). IL-4 signals via STAT6 to trigger the expression of the GATA3 transcription factor. GATA3 in turn promotes the expression and production of IL-4 and IL-13 by the T cell, thus a positive feedback loop is established via IL-4 and GATA3 signalling, committing the cell to the Th2 subtype.

Th2 cells secrete IL-4, IL-5 and IL-13 which can stimulate basophils, eosinophils and mast cells. IL-4 production from Th2 is important in B cell activation and immunoglobulin (Ig) class switching (Finlay et al., 2014; Paul and Zhu, 2010). IL-4 and IL-10 production by Th2 cells can also inhibit the development of Th1 cells, although IL-10 can also be secreted by DCs and regulatory T (Treg) cells (Walsh and Mills, 2013).

1.1.4 Th17 cells

For many years it was believed that CD4⁺ T cells could be divided into one of two subsets; Th1 or Th2 cells which mediated pro- or anti-inflammatory responses respectively and as a result, balanced each other. However, the discovery of Th17 and Treg cells has considerably changed this model. It was initially believed that IL-23 was important for the development of Th17 cells, though it was subsequently demonstrated that naïve T cells do not express a receptor for IL-23 (Harrington et al., 2005) and produce little IL-17 in response to IL-23 *in vitro* (Langrish et al., 2005). It has since been established that the role of IL-23 is in the survival and expansion of Th17 cells rather than their initial differentiation, transforming growth factor (TGF)- β and IL-6 were instead found to have a central role in Th17 differentiation (Mangan et al., 2006; Veldhoen et al., 2006). $\gamma\delta$ T cells have also been implicated in the production of IL-17 by CD4⁺ T cells (Sutton et al., 2009) and both IL-4 and IFN- γ inhibit Th17 differentiation (Harrington et al., 2005; Mangan et al., 2006). On activation, Th17 cells secrete numerous

cytokines including IL-17A, IL-17F, IL-6, IL-21, IL-22 and TNF α (Mills, 2008) and ROR γ T (an orphan nuclear hormone receptor) is the signature transcription factor for Th17 cells (Fig 1.2). These cells are important in mediating protection by inducing neutrophil recruitment to the sites of infection or inflammation, however, IL-17⁺ T cells have also been implicated in autoimmunity, in particular in experimental autoimmune encephalomyelitis (EAE) (Mills, 2008).

1.1.5 Treg cells

Treg cells form a heterogeneous population comprising natural and inducible Treg cells that function to suppress the immune response. Natural Treg cells are CD4⁺CD25⁺FoxP3⁺ cells, which develop in the thymus before migration to the periphery where they suppress the activity of autoreactive T cells (Mills, 2004). In contrast, inducible Treg cells are CD4⁺CD25⁺FoxP3⁺ cells generated in the periphery from naïve T cells on interaction with mature DCs, though the cytokine environment at the time of this reaction is different from that which induces Th1, Th2 or Th17 cells. IL-10-secreting Treg cells produced in this manner are known as T regulatory 1 cells (Tr1), whereas those that produce TGF- β are termed Th3 cells. Tr1 and Th3 cells predominantly mediate their immunosuppressive effects via cytokines especially IL-10 and TGF- β , which can inhibit the function of APCs to stimulate T cells, or directly inhibit Th1 cells (Mills, 2004). Treg cells also mediate suppression via cell contact, and can facilitate the killing of APCs and effector T cells via granzyme B (Josefowicz et al., 2012).

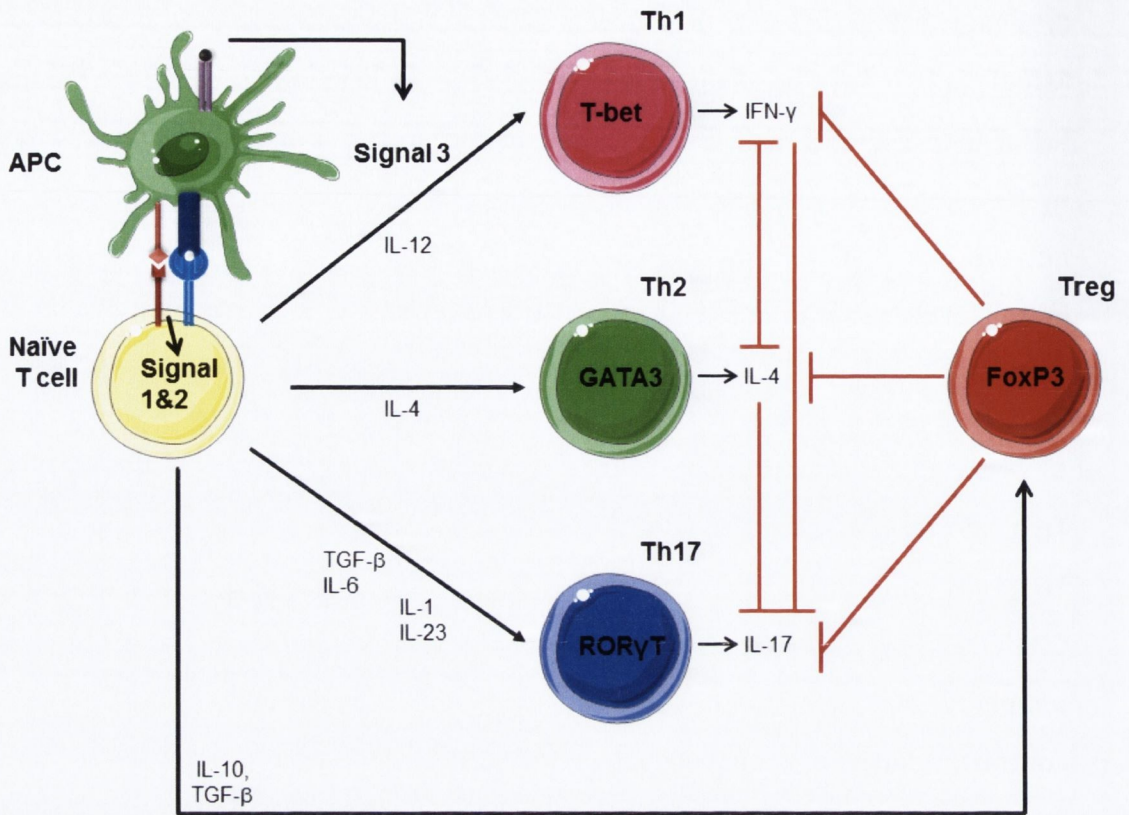


Figure 1.2 CD4⁺ T cell differentiation and function

T cells activated in the presence of IL-12 differentiate to the Th1 subtype. IL-12 signals via STAT4 enhancing the expression of T-bet, inducing T cell production of IFN- γ . Th1 cells predominantly mediate immunity to intracellular pathogens or tumours. Th2 cells are induced by IL-4, which signals via STAT6 to trigger the expression of GATA3. Th2 cells secrete IL-4, IL-5, IL-10 and IL-13 and are important in mediating immunity against extracellular pathogens, but also have a role in allergy. TGF- β and IL-6 induce Th17 differentiation by promoting the expression of ROR γ T where IL-1 and IL-23 enhances cell expansion. Th17 cells secrete numerous cytokines including IL-17A, IL-17F and IL-6. These cells induce neutrophil recruitment and have been implicated in many autoimmune diseases. Inducible Treg cells are CD4⁺ cells generated in the periphery in the presence of IL-10 and TGF- β and express FoxP3. Treg cells can regulate or inhibit Th1, Th2 and Th17 cells along with APC cell responses.

1.1.6 CD8⁺ T cells

CD8⁺ T cells are activated by recognizing their cognate antigen presented via MHC class I. MHC class I is expressed by all nucleated cells, and typically presents self-antigen. However, once the cell becomes infected by a virus, it is the viral antigens which become displayed on the MHC class I, thus CD8⁺ T cells are critical in mediating protection against intracellular pathogens, especially viral infections. Activation occurs in a similar manner to CD4⁺ T cells however, unlike

Th cells, naïve CD8⁺ T cells need more co-stimulatory activity from the mature DC and if the DC is not sufficiently activated, can require the help of a CD4⁺ effector T cell. The effector CD4⁺ T cell can interact with the same APC via MHC class II; this can increase the expression of co-stimulatory molecules and provide cytokines such as IL-2 to aid CD8⁺ T cell activation and differentiation into cytotoxic lymphocytes (CTLs). CTLs produce IFN- γ , which can prevent viral replication. CTLs also kill infected cells in a highly polarised manner by coordinating the delivery of perforin and granzymes directly into the targeted cell, sparing any uninfected cells nearby. In addition, CTLs can upregulate Fas ligand (CD95L), initiating cell death by binding to Fas (CD95) on the target cell (Harty et al., 2000).

1.1.7 T cell memory

During immune challenge, a naïve T cell differentiates into effector T cells, though the majority of these cells undergo apoptosis on resolution of infection. Memory T cells also differentiate from naïve T cells during immune challenge, however, they are long-lived cells poised to quickly respond should they encounter the antigen from the primary stimulus again, as memory T cells are much more sensitive to antigen-stimulation than naïve cells. Memory T cells exist in two distinct populations: central memory and effector memory T cells. Central memory T cells (T_{CM}) express CD44, CD62L and CCR7 and circulate in the lymphoid organs. Effector memory T cells (T_{EM}) do not express CD62L or CCR7 and preferentially circulate in non-lymphoid tissues (Weng et al., 2012). On activation, T_{EM} matures very quickly into an effector cell, producing IFN- γ or IL-4 early after re-stimulation, enabling these cells to carry out rapid effector functions at the site of inflammation. In contrast, activation of T_{CM} takes longer than T_{EM} to differentiate into effector T cells, they do not express much cytokine immediately after activation, but this is a quicker response than naïve T cell activation and they have better proliferative capacity than T_{EM} (Lanzavecchia and Sallusto, 2005). Memory CD4 T cells need IL-7, but can survive without encountering their antigen again.

It has been suggested that memory T cells are intermediates at different stages of differentiation, and the strength and duration of antigenic stimulation influences these dynamics (Lanzavecchia and Sallusto, 2005). During a primary immune response, high antigen stimulation via MHC class II on the DC along with co-stimulatory molecule induces effector T cells, an event which occurs early in infection, and T_{EM} may be generated at this time (Fig 1.3). At later stages of challenge the T cells that become activated proliferate less, perhaps due to competition and decreased stimulatory capacity of the DCs. Thus T_{CM} cells are not activated as intensely and do not lose CD62L nor lymphoid homing capacity (Catron et al., 2006).

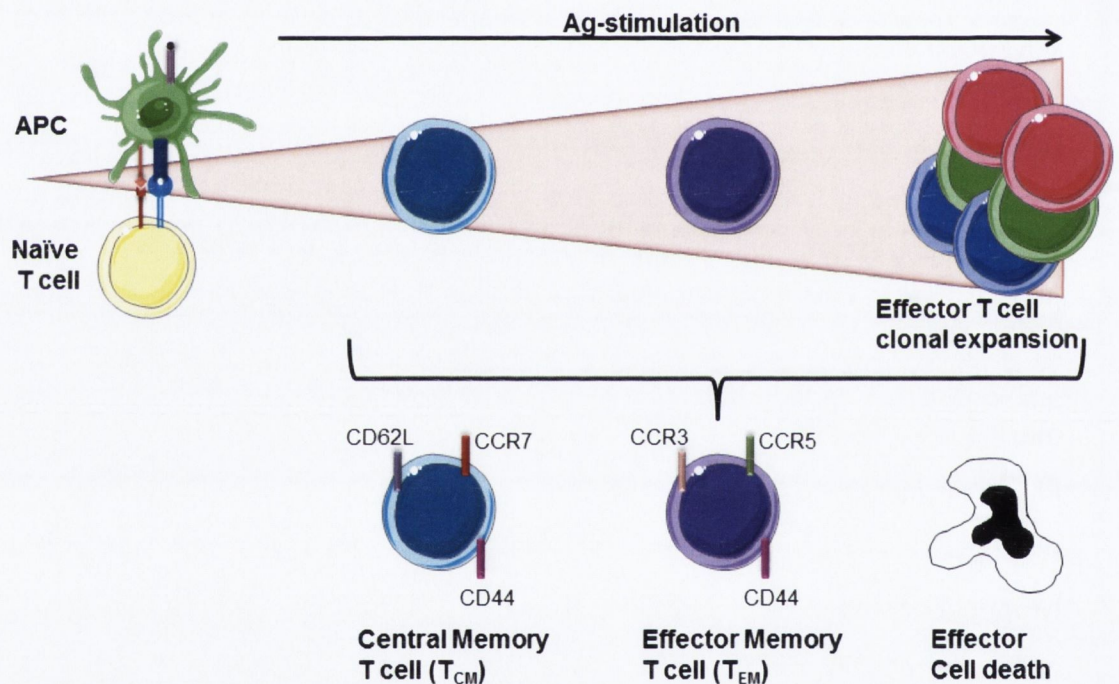


Figure 1.3 T cell memory

The strength of antigen stimulation via the TCR, co-stimulatory expression and cytokine expression determines T cell differentiation during an immune response. Effector T cells are produced by strong stimulation across all parameters, though the majority undergo apoptosis at resolution of infection. Memory T cells are also induced during immune challenge, and are ready to respond should they encounter their specific antigen again. Central memory T cells (T_{CM}) are activated less intensely than effector T cells and never lose CD62L expression, express CD44, CCR7 and circulate in the lymphoid organs. Effector memory T cells (T_{EM}) do not express CD62L or CCR7, instead can express receptors for inflammatory chemokines (e.g. CCR3, CCR5) and preferentially circulate in non-lymphoid tissues. On activation, T_{EM} differentiate quickly into effector cells. T_{CM} activation takes longer than T_{EM} but these cells have better proliferative capacity.

1.1.8 NKT cells

NKT cells are derived in the thymus and are a heterogeneous population that express a TCR and typical NK cell surface markers, such as NK1.1 in mice. Instead of binding MHC class I or II, the TCR on NKT cells binds CD1d, a non-classical MHC class I molecule. The TCR recognizes glyco-lipid antigen only e.g. α -galactosylceramide, which allows these cells to recognise glyco-lipid fragments from microorganisms forming an adaptive immune response. On activation, NKT cells can release various cytokines including IFN- γ , IL-10, TNF α and mouse NKT cells can produce IL-17 (Berzins et al., 2011). Defects in NKT cell function have been implicated in the development of autoimmune disease and cancer.

1.2 The central nervous system

The central nervous system (CNS) includes the brain and spinal cord, and is comprised of neurons and glial cells in a 1:1 ratio (Azevedo et al., 2009). Glial cells are non-neuronal cells and can be divided into three main groups: oligodendrocytes, astrocytes and microglia. Oligodendrocytes myelinate the neurons of the CNS. Each process of an oligodendrocyte can myelinate one segment of a neuronal axon, and oligodendrocytes can myelinate numerous axons simultaneously (Nave, 2010). Astrocytes are large, star shaped glial cells that have an important role in maintaining homeostasis within in the CNS, as these cells maintain the pH and extracellular ion concentration. Astrocytes also form part of the BBB, using their end feet to support the vascular endothelium (Dong and Benveniste, 2001). Microglia are the principal innate immune cells of the brain, and are often considered to be the macrophage equivalent of the CNS. These cells are efficient phagocytes and can produce cytokines and chemokines on activation. How microglia function as innate immune cells will be discussed in detail below.

1.2.1 The BBB and immune privilege

The brain was once considered to be a strictly immunologically privileged site. In 1921 Shirai observed that rat tumour grew well after transplantation to the brain

parenchyma, but not after transplant under the skin or into muscle (Shirai, 1921). This finding was replicated 2 years later, though it was found that if part of the spleen was transplanted with the tumour, tumour growth was inhibited (Murphy and Sturm, 1923). This led the authors to suggest that immune cells were unable to migrate into the parenchyma which facilitated tumour growth. It was also considered at this time that the absence of a lymphatic system prevented the generation of immune responses in the brain (Medawar, 1948). However, it has since been demonstrated tumours can be cleared from the CNS, this process is just delayed (Finsen et al., 1991), importantly clearance was associated with infiltration of T cells and activation of both microglia and astrocytes in the surrounding brain tissue. It is now accepted that immune privilege of the brain is not absolute. Rather than stating no immunosurveillance occurs within the CNS, it is now accepted that any immune response is tightly controlled and is compartmentalised i.e. more strictly regulated in the parenchyma than other brain regions such as the ventricles, meninges or choroid plexus, which respond to insult like the periphery (Galea et al., 2007). Importantly, any privilege the brain has declines with age or in inflammatory or infectious conditions.

The discovery of the BBB added considerable weight to the theory that the CNS was an immunologically privileged site. A series of studies from 1885 to 1913 demonstrated that dyes injected into the periphery did not stain the brain, and similarly when dye was injected into the brain it did not leak into the periphery (Bechmann et al., 2007). It was thus concluded that “brain capillaries must hold back certain molecules” (Lewandowski, 1900). The BBB is a tightly regulated, rather than absolute, structure. The BBB effectively protects the brain from pathogens or insult due to the presence of tight junction proteins between the endothelial cells of the vasculature, providing high electrical resistance from large molecules entering the CNS. Indeed the electrical resistance of the CNS vasculature is higher than that of the endothelial cells in many other regions of the body (Anderson and Van Itallie, 2009). The brain endothelium has other unique features in comparison to endothelial cells of the periphery, including greater numbers of mitochondria, no fenestrations and little pinocytotic activity

(Hawkins and Davis, 2005). The basement membrane and astrocyte foot processes support these endothelial cells, and constitutes another barrier between the blood and brain cells (Wraith and Nicholson, 2012). Not all areas of the brain have a BBB; in certain areas the blood capillaries are fenestrated, these regions are known as circumventricular organs (CVOs). CVOs allow peptide hormones to be released from the brain into the blood, and facilitate molecules communicating with neurons without disrupting the BBB. Areas of the brain that are classified as CVOs include the pineal gland, the posterior pituitary and the lamina terminalis (Weiss et al., 2009).

1.2.2 Maintaining the BBB; the role of tight junction proteins and pericytes

Occludin, claudin-3, claudin-5 and junctional adhesion molecule (JAM) are transmembrane proteins which make up the tight junctions (TJ) between the endothelial cells of the BBB. Occludin and claudin are proteins with four transmembrane domains and two extracellular loops that span the cleft between endothelial cells (Hawkins and Davis, 2005), whereas JAM is a single membrane spanning chain. Claudin-5 in particular is important in maintaining the integrity of the BBB, as knocking out this protein results in enhanced permeability and loss of BBB integrity in mice (Nitta et al., 2003). There are a number of cytosolic proteins called zonular occludens (ZO)-1, ZO-2 and ZO-3 which act together in multi-protein complexes, binding the TJ proteins intracellularly to the actin cytoskeleton (Weiss et al., 2009) (Fig 1.4). The adherens junction (AJ) is also located between the endothelial cells of the BBB, these are calcium sensitive cadherin proteins which promote barrier integrity and contribute to the regulation of TJ proteins (Hawkins and Davis, 2005; Weiss et al., 2009). Together the TJ and AJ proteins act as a zipper between each endothelial cell, limiting the permeability of solutes and molecules from the blood into the brain.

Endothelial cells are ensheathed by the basal lamina, a 30-40 nm membrane composed of layers of extracellular matrix proteins including collagen, proteoglycans and glycoproteins (Hawkins and Davis, 2005; Weiss et al., 2009). This is subsequently encapsulated by astrocyte end feet, which together make up the glia limitans and support the BBB. This region can also be referred

to as the neurovascular unit, when it also considers the pericytes within the basal membrane and the neurons which innervate and thus perhaps regulate BBB function (Hawkins and Davis, 2005).

Pericytes are cells embedded within the vascular basement membrane and are ubiquitously expressed along blood vessels, however, the vasculature of the CNS has the highest coverage of pericytes with an endothelial cell: pericyte ratio of 1:1-3:1 (Armulik et al., 2011; Mathiisen et al., 2010). Pericytes maintain contact with the endothelial cells of the vasculature through gaps in the basement membrane, with up to 1,000 contacts described for a single endothelial cell (Armulik et al., 2011). These cells have an important role in regulating the BBB, enhancing its integrity *in vitro* (Nakagawa et al., 2009) and pericyte deficiency in mice results in BBB permeability with reduced polarisation of astrocyte end feet at the BBB, increased capillary diameter and abnormal endothelial cell shape and structure (Armulik et al., 2010; Hellstrom et al., 2001). Pericyte deficiency is also associated with a reduction in TJ proteins, with an increase in the expression of leukocyte adhesion molecules and greater numbers of leukocytes infiltrating into the CNS parenchyma (Bell et al., 2010; Daneman et al., 2010). The absence of pericytes in mice results in increased expression of pro-inflammatory cytokines in the CNS, microglial activation and neuronal loss, in addition to memory impairments (Bell et al., 2010). Importantly, these changes were preceded by vascular damage and BBB disruption in the pericyte-deficient mice.

During periods of neuroinflammation the BBB can lose its integrity, becoming “leaky”. Compromised TJs have been reported in Multiple sclerosis (MS) lesions, with loss of occludin and ZO-1 (Kirk et al., 2003; Leech et al., 2007; Plumb et al., 2002), which is associated with fibrinogen leakage into the perivascular space and even into the parenchyma. It has been demonstrated that infiltration of inflammatory immune cells into the perivascular space is associated with loss of TJ proteins (Bolton et al., 1998; Boven et al., 2000). Pro-inflammatory cytokines such as TNF α , IL-1 β , IL-17 and IFN- γ have also been implicated in reducing the expression of TJ proteins of endothelial cells (Kebir et al., 2007; Minagar and Alexander, 2003), which facilitates entry of large

molecules and cells into the perivascular space. In addition, pro-inflammatory cytokines can affect pericytes, increasing their expression of MCP-1, IP-10, VCAM-1, ICAM-1 and MHC class II, along with altering pericyte migration and proliferation (Balabanov et al., 1999; Jansson et al., 2014; Tigges et al., 2013). The BBB can also be compromised after hypoxic or ischemic insults, in tumour vasculature and with drug use (Hawkins and Davis, 2005).

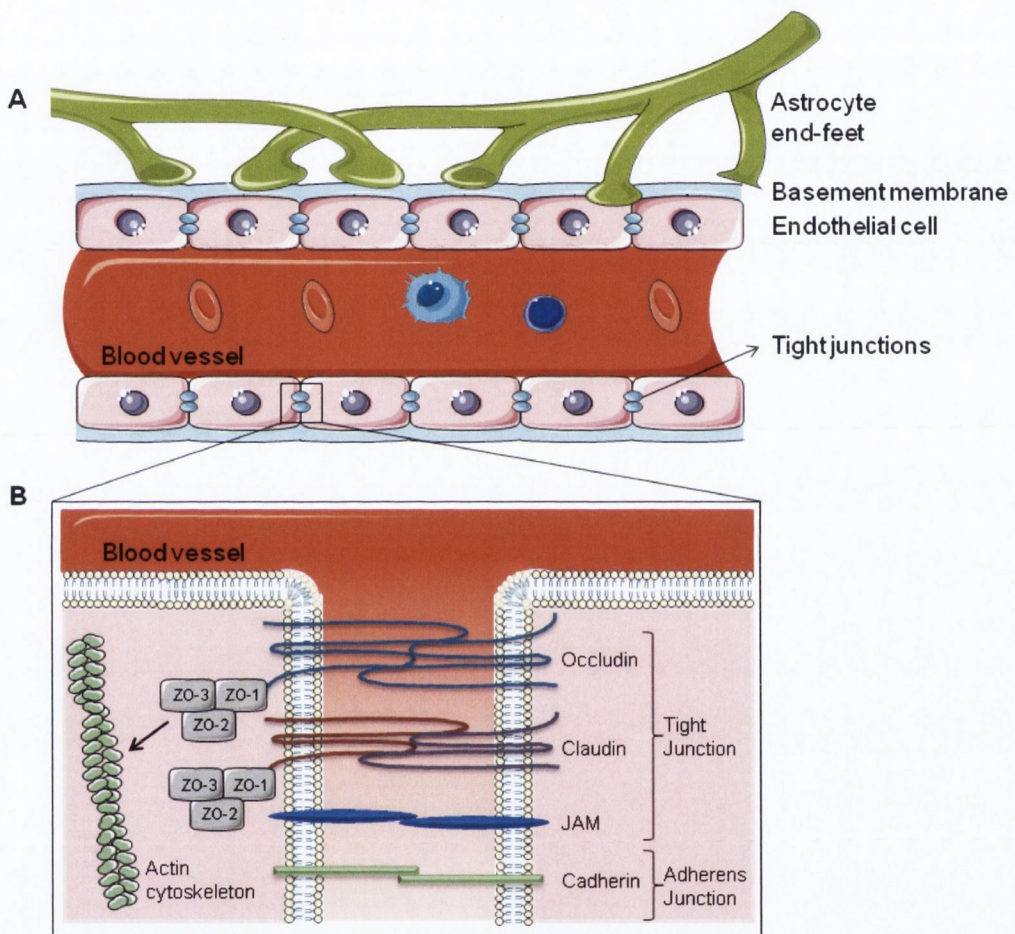


Figure 1.4 The blood-brain barrier

(A) The blood-brain barrier (BBB) is created by vascular endothelial cells which are not fenestrated and have tight junction proteins with high electrical resistance to prevent solutes or large molecules entering the brain parenchyma. The endothelial cells are supported by the basement membrane (which contains pericytes) and astrocyte end feet. (B) The tight junction proteins of the BBB include occludin, claudin-3 and -5 and junctional adhesion molecule (JAM). These are bound intracellularly by zonular occludens (ZO)-1, -2 and -3, which interacts with the actin cytoskeleton. Cadherin proteins make up the adherens junction promoting barrier integrity. Together these proteins act as a zipper or fence to regulate the diffusion of molecules into the brain.

1.2.3 T cell surveillance of the brain

While it was previously believed that lymphocytes do not infiltrate the brain, it is now established that T cells routinely enter the CNS for immunosurveillance (Hickey, 2001). There are approximately 150,000 lymphocytes circulating in the cerebrospinal fluid (CSF) of healthy individuals at any given time (Engelhardt and Ransohoff, 2005), it is estimated that these cells are replenished twice per day before re-entering the blood stream. Over 80% of the T cells in the CSF are CD4⁺, one-third of which are T_{EM} cells, and two-thirds are T_{CM} (Kivisakk et al., 2003). T cells in the CSF survey the brain by searching for their specific, cognate antigen presented by macrophages in the subarachnoid or perivascular space or by pericytes in the basal lamina membrane (Engelhardt and Ransohoff, 2005; Owens et al., 2008). DCs are also located in the perivascular and meningeal space, where they present antigen to T cells mediating their infiltration into the brain. Interestingly, increasing the number of DCs at these locations results in enhanced T cell influx into the brain (Greter et al., 2005). Entry into the parenchyma is dependent on the T cell recognising its specific antigen, if this occurs the T cell mounts an inflammatory response recruiting more immune cells, which together infiltrate into the brain parenchyma by breaching the glia limitans (Wraith and Nicholson, 2012).

1.2.4 T cell entry: a two-step process

Migration of immune cells through the vascular endothelial layer is a complex process involving a number of adhesion molecules binding the lymphocyte to the endothelial cell. This process occurs in five stages: rolling, activation, arrest and crawling before transendothelial migration (Engelhardt and Ransohoff, 2005, 2012). The immune cell (e.g. T cell) transiently makes contact with the endothelial cell via selectins (L-, E- or P-selectin) present on the vascular endothelium binding their respective ligand i.e. P-selectin glycoprotein ligand (PSGL-1). This initially tethers the cell, which rolls along the endothelium. The T cell can now respond to chemotactic factors present on the endothelial surface, these chemokines deliver signals to the immune cells via G-protein coupled receptors (GPCR) that in turn induce conformational changes to integrins (α 4-

and β 1-integrins) present on the T cell surface increasing both their affinity and avidity. The cell comes to an arrest when these high affinity, high avidity integrins bind their respective ligands present on the endothelial cell surface; ICAM-1, ICAM-2 and vascular cell adhesion molecule (VCAM)-1. This leads to strengthened cell adhesion, and the T cell begins to crawl along the endothelium searching for a site to undergo diapedesis. The cell crawling is mediated by LFA-1 on the T cell binding ICAM-1 and -2. It has been suggested the endothelium may form “docking structures” with increased ICAM-1 and VCAM-1, which help extravasation of the cell (Carman, 2009). The T cell can now migrate across the endothelium using one of two mechanisms: paracellular or transcellular diapedesis. Paracellular diapedesis occurs through the gap between two adjacent cells, and is thought to be mediated by recruitment of platelet endothelial cell adhesion molecule (PECAM) and JAM proteins (Engelhardt and Ransohoff, 2012). Transcellular diapedesis occurs through the formation of a transient pore within the cell. While both pathways are used in other regions of the body for infiltration or extravasation of immune cells, within the brain it appears that the transcellular pathway is favoured, sparing the TJ proteins of the BBB which would have to open and subsequently reseal after the cell passed through (Carman, 2009; Engelhardt and Ransohoff, 2012).

During neuroinflammation the expression of P-selectin can be increased on the endothelial cell surface, triggering T cell extravasation into the perivascular space (Engelhardt and Ransohoff, 2012). Upregulation of ICAM-1 and VCAM-1 can also be observed. In addition, numerous chemokines are produced by the inflamed brain, thus facilitating enhanced influx of immune cells which have the corresponding chemokine receptors (Engelhardt and Ransohoff, 2005).

The T cell is now in the basement membrane which can include the perivascular space depending on the size of the blood vessel. Blood vessels on the surface of the CNS are found in the subarachnoid space, as the vessel projects further into the brain the subarachnoid space becomes continuous with the perivascular space, located between the basement membrane of the astrocyte end feet and the basement membrane of vascular endothelial cells of

postcapillary venules (Owens et al., 2008). As the blood vessel passes deeper into the brain at the level of capillaries, the two basement membranes form a “gliovascular” membrane thus closing the perivascular space. The T cells must recognise antigen in this perivascular area or subarachnoid space to progress across the glia limitans and into the brain parenchyma (Engelhardt and Ransohoff, 2005; Owens et al., 2008). This two-step process of immune cell infiltration into the brain ensures strict control over what cells gain access, protecting the parenchyma from unnecessary inflammation. Pericytes, perivascular macrophages or DCs located at the meninges or endothelial basement membrane can activate antigen-specific T cells promoting their entry into the parenchyma (Engelhardt and Ransohoff, 2005; Greter et al., 2005). Activation of these T cells can induce further immune cell infiltration into the perivascular space, resulting in the production of matrix metalloproteases (MMP), which are critical for final extravasation across the glia limitans and into the parenchyma (Fig 1.5). Studies in EAE reveal that MMP-2 and MMP-9 in particular are important for cleaving dystroglycan, which binds the astrocyte end feet to the basement membrane thus allowing the T cell to breach the glia limitans and enter into the brain (Agrawal et al., 2006).

Peripheral immune cells can also infiltrate the brain through the epithelial blood CSF barrier (BCSFB) (Engelhardt et al., 2001). The choroid plexus produces CSF in the brain, is located in the ventricles and consists of capillaries encased in an endothelial layer. The cells of these capillaries are fenestrated allowing free movement of molecules into the choroid plexus, however, the cells of the choroid plexus endothelium are not fenestrated with TJ proteins to prevent movement of solutes into the CSF and is the functional BCSFB. These TJs are also made up of occludin and claudin transmembrane proteins (Owens et al., 2008). It has been suggested that any T cells in the CSF migrated through the BCSFB, and is the preferential site for immunosurveillance of the CNS in the absence of neuroinflammation (Engelhardt and Ransohoff, 2012). During neuroinflammation, the endothelial cells of the BCSFB also upregulate ICAM-1 and VCAM-1 facilitating T cell influx into the CSF (Engelhardt and Ransohoff, 2005). Once in the CSF, the T cell can enter the brain parenchyma by breaching

the ependymal layer of the ventricle, indeed it has been demonstrated in mice that Th1 and Th17 cells can infiltrate the brain parenchyma using this pathway (Fisher et al., 2014; Reboldi et al., 2009). Unfortunately, little is known about the exact mechanisms of T cells crossing the BCSFB, into the CSF and into the parenchyma.

Most of the information on T cell entry into the CNS is based *in vitro* or *in vivo* studies, and it remains to be established whether similar interactions occur in the human brain. T cell migration to the human CNS is minimal in healthy individuals, and is lower than T cell surveillance of peripheral organs (Hickey, 2001; Ousman and Kubes, 2012), however, T cell infiltration into the CNS is increased in AD (Togo et al., 2002) and in other neurodegenerative conditions such as MS (Fletcher et al., 2010), Parkinson's disease and motor neuron disease (Appel et al., 2010). Indeed T cells have proved important in learning and memory function as severe combined immunodeficiency (SCID), nude or Rag deficient mice that lack T cells display cognitive deficits, which was attenuated by T cell transfer (Filiano et al., 2014; Kipnis et al., 2004; Radjavi et al., 2014).

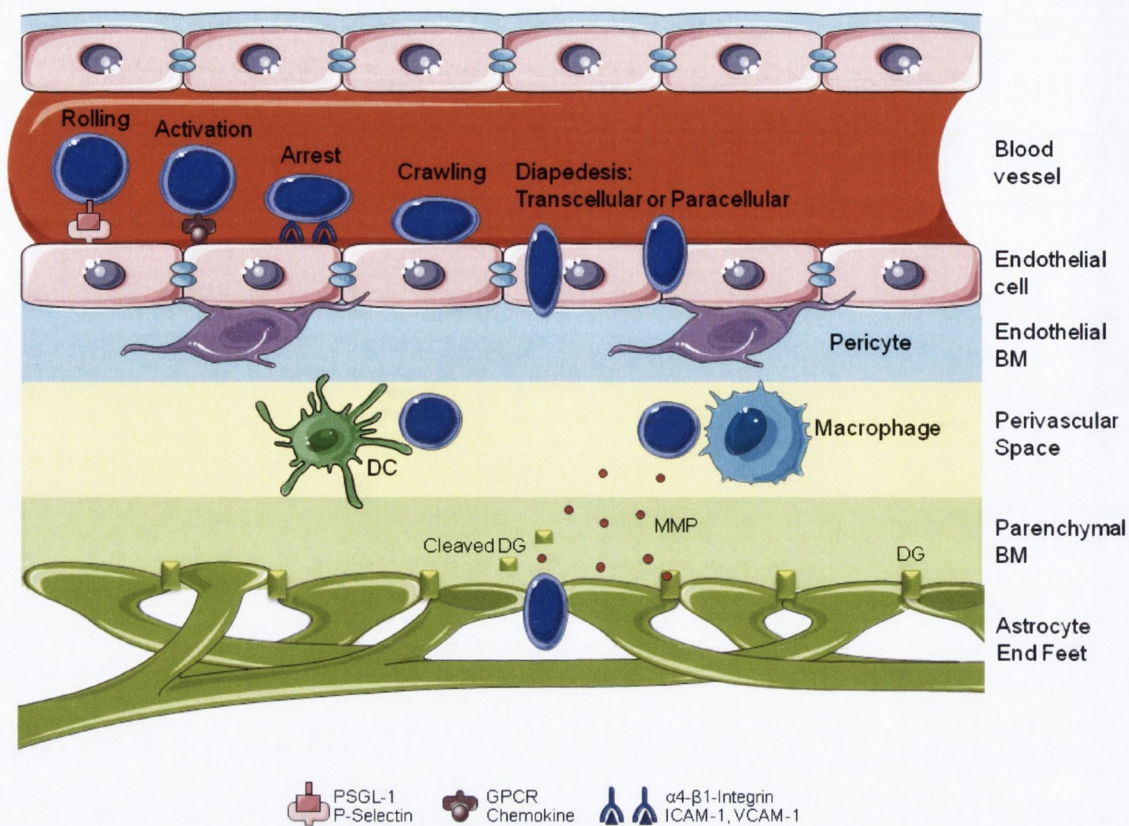


Figure 1.5 T cell migration into the brain; a two-step process

Cell migration into the parenchyma occurs in two steps; extravasation across the endothelium into the perivascular space, then migration through the glia limitans into the parenchyma. Migration of immune cells (e.g. T cell) through the endothelial layer occurs in five stages. (1. Rolling) The T cell transiently make contact with P-selectin present on the vascular endothelium binding P-selectin glycoprotein ligand (PSGL-1) tethering the cell allowing it to roll along the endothelium. (2. Activation) The T cell can now respond to chemotactic factors activating the cell, inducing conformational changes to $\alpha 4$ - $\beta 1$ -integrins increasing their affinity and avidity. (3. Arrest) Binding of the high affinity, avidity integrins to their respective ligands; intracellular adhesion molecule (ICAM)-1, ICAM-2 and vascular cell adhesion molecule (VCAM)-1 brings the cell to arrest. This results in strengthened cell adhesion and (4. Crawling) the T cell begins to crawl along the endothelium, via leukocyte-function associated antigen (LFA)-1 on the T cell binding ICAM-1 and -2, searching for a site to undergo diapedesis. (5. Diapedesis) The T cell migrates across the endothelium by paracellular or transcellular diapedesis. After moving through the endothelial basement membrane, the T cell is now located in the perivascular space. The T cell must be activated here by an APC to induce recruitment of other immune cells, and the production of matrix metalloproteases (MMP)-2 and -9. MMPs cleave dystroglycan (DG), which anchors the astrocyte end feet to the parenchymal basement membrane, allowing the T cell to cross the glia limitans and infiltrate into the parenchyma. BM, Basement membrane.

1.2.5 Lymphatic drainage of the brain

Although the brain does not have typical lymphatic drainage, interstitial fluid (ISF) from the parenchyma drains out of the brain along the basement membrane of the capillaries to the artery basement membrane. From here, the solutes can drain along the carotid arteries to the cervical lymph nodes (Weller et al., 2009). This pathway is aided by vascular pulsations as drainage does not occur in dead animals, however, cells are unable to migrate out of the brain along this pathway (Carare et al., 2008) which would typically occur in any other organ, thus maintaining the immune privilege of the brain.

The choroid plexus produces over 500 ml of CSF per day, which is continuously reabsorbed as capacity of the ventricles and subarachnoid spaces in humans is 140 ml. Studies in rodents and other animals reveal that the CSF passes through the subarachnoid space to the cribriform plate, then to the nasal submucosa before entering the cervical lymph nodes (Weller et al., 2009). Humans have larger arachnoid villi than rodents, thus much of the CSF in humans is drained into venous blood from the arachnoid villi and granulations.

The movement of solutes and antigen through the blood and CSF to locations including the cervical lymph node allow the generation of antigen-specific lymphocyte responses here when necessary. In addition, perivascular macrophages are phagocytic (Carare et al., 2008; Owens et al., 2008) thus uptake of antigen by these and other phagocytes along the drainage pathway in turn facilitates activation of any incoming Ag-specific T cells which have been primed in the cervical lymph node and are attempting to infiltrate the brain.

1.3 Alzheimer's disease

1.3.1 General background

In 1906 Alois Alzheimer described the first case of AD, although the disease was not officially named until 1910 (Maurer et al., 1997). Auguste D was examined by Alois Alzheimer in 1901, when she was admitted to hospital due to memory and

behavioural problems. Alzheimer followed the case until her death at which point he examined her brain for neuropathology, where he described miliary foci (now known as senile plaques) and clumps of intracellular fibrils or neurofibrillary tangles (NFTs). In 1984 A β was identified as the main component of the senile plaques (Glennner and Wong, 1984), and two years later it was discovered that abnormally phosphorylated tau was the main constituent of NFTs in AD (Grundke-Iqbal et al., 1986). Today AD is the most common neurodegenerative disease and accounts for 60-80% of all dementia cases (Thies and Bleiler, 2013). It is a progressive disease characterised by NFTs and deposits of A β , which are associated with dystrophic neurons, reactive astrocytes and activated microglia. A β also accumulates in the vasculature of the brain which is known as cerebral amyloid angiopathy (CAA) affecting from 80-100% of AD patients (Carrano et al., 2011). It is estimated that dementia affects 44 million people worldwide, and this figure is expected to reach over 135 million by 2050 (Prince et al., 2014).

The “amyloid hypothesis” is the most-studied theory in relation to AD; this suggests that the accumulation of A β is the primary influence in disease initiation and progression (Hardy and Selkoe, 2002). Constant and increasing presence of A β is believed to trigger an array of downstream effects including formation of A β plaques, tau hyperphosphorylation (resulting in NFTs), inflammation and loss of neurons. A β plaques can also be associated with degenerating neurons, which are termed neuritic plaques. It has recently been proposed that the process leading to AD begins 20 to 25 years before the onset of symptoms (Bateman et al., 2012). The areas of the brain most affected in this disease are the limbic cortex and hippocampus. Neuronal and synaptic loss in these areas is primarily responsible for the memory and behavioural disturbances observed in AD.

Almost 1% of all AD cases are genetic, a result of inherited missense mutations in the genes for either *APP*, *PSEN1* or *PSEN2* (Selkoe, 2012) and disease is typically early-onset occurring before the age of 60. The *APP* gene codes for amyloid precursor protein (APP), a 695 amino acid long protein which

A β is cleaved from. *PSEN1* and *PSEN2* code for presenilin-1 and -2 respectively, which form the catalytic component of γ -secretase; one of the enzymes that cleaves APP into A β . All mutations in APP that are associated with AD development change the amino acids found within or beside the A β region, favouring cleavage of APP through the amyloidogenic pathway (Hardy and Selkoe, 2002; Selkoe, 2012). In addition, the AD-associated mutations in γ -secretase enhance production of A β_{42} over A β_{40} (De Strooper, 2007). The *APP* gene is located on chromosome 21, and in trisomy 21 (Down's syndrome) A β_{42} begins to accumulate from 12 years of age, ultimately resulting in A β -plaques, NFTs and is indistinguishable from AD (Selkoe, 2001).

The majority of AD cases are sporadic, late-onset AD (LOAD), typically occurring after the age of 60 where the main genetic risk factor is the apolipoprotein E ϵ 4 (*APOE4*) allele. Carrying the *APOE4* allele not only increases the risk of developing AD, but also decreases the age of onset, as *APOE4* is associated with impaired A β clearance ultimately resulting in increased A β deposition (Castellano et al., 2011). Under normal conditions ApoE-lipoproteins bind A β , facilitating A β clearance, but ApoE4 has a lower binding affinity than the other isoforms thus impairing removal of A β (Liu et al., 2013). A β can also be metabolised by enzymes in the brain such as insulin-degrading enzyme (IDE) or neprilysin (NEP). It has been suggested that A β metabolism is impaired in LOAD as the protein level and activity of NEP is decreased in sporadic AD (Wang et al., 2010) and patients with the *APOE4* allele have decreased IDE messenger ribonucleic acid (mRNA) and protein (Cook et al., 2003). APP mice which overexpress IDE or NEP have significantly reduced A β -plaque burden, which was associated with decreased microglial and astrocyte activation (Leissring et al., 2003). As a result, impaired clearance or degradation of A β is thought to have a key role in A β accumulation, especially in sporadic AD (Wang et al., 2006), where disease onset is likely due to a combination of genetic and environmental factors; as risk factors include infection, sedentary lifestyle and obesity (Heneka et al., 2014). Regardless of whether AD develops as genetic early-onset or LOAD, the resulting pathology, behavioural and memory disturbances remain indistinguishable. The consistent similarity is the increased production or

decreased metabolism of A β , which occurs years before development of clinical symptoms (Bateman et al., 2012).

Diagnosis of AD is difficult as the only definite hallmarks of the disease are in the brain and thus unavailable for examination until after death. Nevertheless, a range of tests are available to aid diagnosis. The Mini-Mental State Exam (MMSE) is a test to assess cognitive function; the scores range from 0-30 with a score of over 26 considered to be in the normal range. People with mild, moderate, moderately severe and severe AD score 21-26, 14-20, 10-14 and below 10 respectively (Handels et al., 2013). The diagnostic criteria can also include biomarkers in CSF (increased tau but decreased A β_{42}), molecular imaging with positron emission topography (PET; amyloid plaques retain Pittsburgh compound B; PIB) and magnetic resonance imaging (MRI; demonstrates brain atrophy) (Handels et al., 2013; Perrin et al., 2009).

1.3.2 Neurofibrillary tangles

NFTs are formed from tau which has become hyperphosphorylated causing it to aggregate into fibres, which form either straight or paired helical filaments and is a feature of many neurodegenerative diseases including AD, Pick's disease and frontotemporal dementia with Parkinsonism (Gotz et al., 2004). Under normal conditions tau binds to the microtubules of neurons and functions in their assembly and stabilisation. During the course of AD, tau becomes hyperphosphorylated which leads to dissociation from the microtubules and relocation to the somatodendritic area from the axonal compartment (Gotz et al., 2004). Tau mutations can occur in humans, and are associated with neuronal degeneration and the development of dementia, however, this occurs without any A β accumulation or plaque formation (Selkoe, 2001). In AD, A β -deposits accumulate early in disease with secondary NFT from tau filaments forming gradually afterwards (Perrin et al., 2009). Moreover, it has been demonstrated that soluble A β oligomers can induce tau hyperphosphorylation and induce degeneration of hippocampal neurites (Jin et al., 2011), similar results have also been obtained using fibrillar A β (Gamblin et al., 2003). Microglial activation

precedes NFT formation in Tau-transgenic mice (P301S) (Yoshiyama et al., 2007) where immunosuppression attenuated the formation of tau pathology. Interestingly, injection of A β into the brains of P301L-transgenic mice induces a 5-fold increase in NFTs when assessed 3 weeks later (Gotz et al., 2001).

1.3.3 Processing of APP to A β

The APP protein has a single transmembrane domain with a large extracellular and small intracellular cytoplasmic domain. It is ubiquitously expressed throughout the body in three main isoforms: APP₆₉₅, APP₇₅₁ and APP₇₇₀, where APP₆₉₅ is predominantly expressed in the brain (Turner et al., 2003). APP participates in neuronal function; mediating adhesion, neurotrophic activity and intercellular signalling. Mice deficient in APP display reactive gliosis with impaired locomotor activity (Zheng et al., 1995). In addition, these mice have impaired long-term potentiation and cognitive deficits (Dawson et al., 1999).

APP can be cleaved via one of two pathways; the amyloidogenic or non-amyloidogenic pathway (Fig 1.6). Three proteases are involved in APP processing; α -, β - or γ -secretases which were so named before their molecular identities known (Kummer and Heneka, 2014). Cleavage of APP by α -secretase at the plasma membrane initiates the non-amyloidogenic pathway and is the favoured pathway in non-neuronal cells (Haass et al., 2012). APP is cut between position 16 and 17 of the A β sequence which results in a C-terminal fragment which is 83 residues long (known as α -CTF or C83) and soluble APP α (sAPP α), thus preventing the cleavage of APP into A β (Kummer and Heneka, 2014; Nunan and Small, 2000). C83 is subsequently cleaved by γ -secretase, producing the APP intercellular domain (AICD) and the short peptide p3, which contains the C-terminal region of A β . Members of the ADAM family of proteases (zinc metalloproteases, named from a disintegrin and metalloprotease) can act as α -secretase, in neurons it is thought that the ADAM10 protease primarily mediates this activity (Kuhn et al., 2010), though ADAM17 and ADAM19 can also function as α -secretase (Haass et al., 2012). γ -secretase is a protein complex which includes presenilin-1, -2, nicastrin, anterior pharynx-defector (APH)-1 and

presenilin enhancer (PEN)-2, with presenilin-1 and-2 forming the catalytic domain of γ -secretase.

Processing of APP via the amyloidogenic pathway predominantly occurs in neurons, which contain greater amounts of BACE1 (β -site APP cleaving enzyme 1) (Haass et al., 2012). In the amyloidogenic pathway, APP is internalised to the endosomes where β -secretase (BACE1) cleaves APP before the first position of the A β residue leaving the C-terminal fragment which is 99 residues long (C99 or β -CTF) and sAPP β (Kummer and Heneka, 2014; Nunan and Small, 2000). β -secretase can alternatively cleave the protein between position 10 and 11 of the A β site. C99 is cleaved by γ -secretase within the transmembrane domain of APP at varying locations generating A β fragments that range from 37 to 43 residues long and AICD. The mechanism of γ -secretase cleavage still remains to be fully elucidated, but it is thought to occur in a step-wise fashion, starting at residues 48 or 49 before cleaving at 45 or 46 with a final cleavage at position 38, 40 or 42, thus producing peptides of varying lengths (Haass et al., 2012). The peptides are released extracellularly into the CSF, ISF or plasma (Kummer and Heneka, 2014). In AD there is an increase in overall A β production but in particular, A β that is 42 residues long (A β_{42}) leading to a shift in the ratio of A β_{42} :A β_{40} (Haass and Selkoe, 2007), moreover, A β_{42} has a greater tendency to aggregate than A β_{40} . A β can also undergo post-translational modifications such as nitration or phosphorylation, which increases the ability of peptide aggregation (Kummer and Heneka, 2014).

It has previously been said that “A β is both cause and effect in AD” (Selkoe, 2012). The general sequence of events in the development of AD is that due to increased production or reduced degradation, A β begins to accumulate in the extracellular space. A β_{42} is prone to aggregation first forming oligomers and diffuse plaques which start to affect synaptic function and induce microglial and astrocyte activation. Amyloid plaques begin to form, leading to neuronal injury and hyperphosphorylation of tau ultimately resulting in chronic glial activation, widespread neuronal dysfunction and cell death which presents as dementia in the AD patient (Haass and Selkoe, 2007; Hardy and Selkoe, 2002).

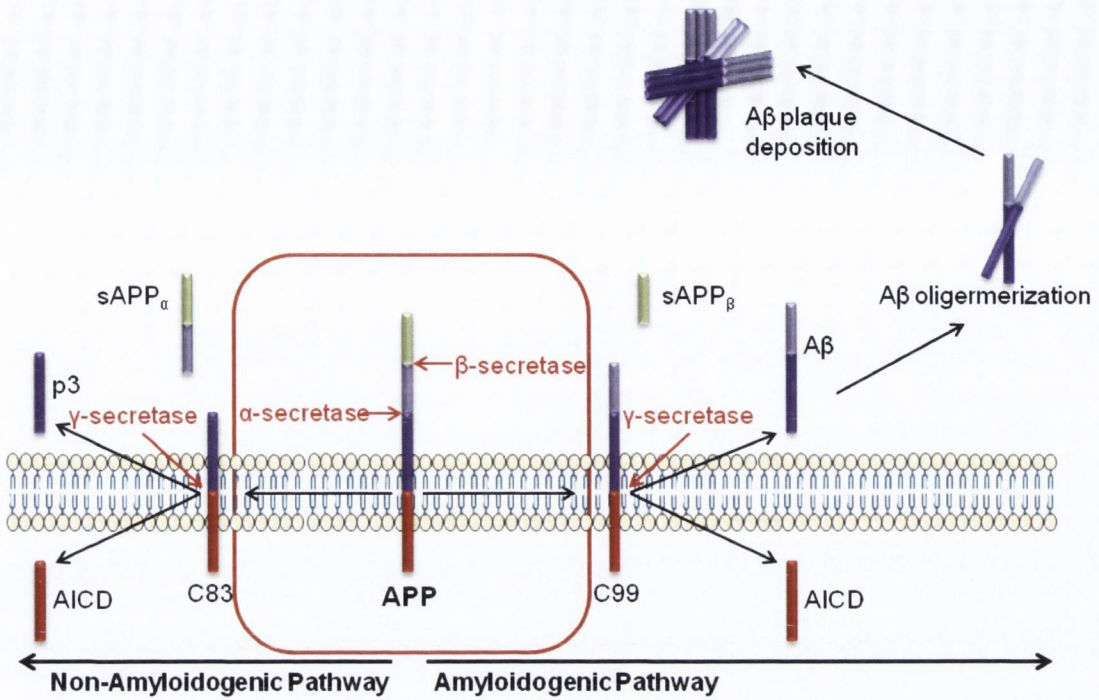


Figure 1.6 Processing of APP

Non-amyloidogenic pathway: APP is cleaved by α -secretase at the plasma membrane resulting in an 83 residue C-terminal fragment (C83) and soluble APP α (sAPP α), preventing the cleavage of APP into A β . C83 is cleaved by γ -secretase producing the short peptide p3, and APP intercellular domain (AICD). Amyloidogenic pathway: APP is internalised to the endosomes, β -secretase cleaves APP producing C99 and sAPP β . C99 is cleaved by γ -secretase generating A β fragments that range from 38 to 42 residues long and AICD. The peptides are released extracellularly into the CSF, ISF or plasma.

1.3.4 AD mouse models

The initial animal models of AD tried to replicate the pathology by injecting or infusing rodents with A β or with the core of plaques from AD patients, which resulted in some diffuse amyloid plaques located in the vicinity of the injection site (Frautschy et al., 1992; Frautschy et al., 1996) along with neuronal damage and cognitive deficits (Nakamura et al., 2001). However, the identification of genes involved in the development of inherited AD facilitated the creation of genetically modified mice which replicated more of the neuropathological characteristics of AD including A β -plaque development, glial activation and cognitive deficits. Using transgenic models has helped identify mechanisms and key players in this disease, and are central in designing drug targets or therapeutic approaches for AD.

1.3.4.1 Tg2576

A commonly used AD-mouse model is Tg2576 mice which express APP₆₉₅ with the Swedish double mutation (K670N and M671L) which favours APP processing through the β -secretase pathway (Citron et al., 1992) under the control of a hamster prion protein promoter. These mice develop cognitive deficits by 9–10 months of age which was associated with increased production of A β ₄₀ and A β ₄₂ and Congo red positive plaques throughout the cortex and limbic structures at 11-13 months of age (Hsiao et al., 1996; Westerman et al., 2002). Tg2576 mice do not develop NFTs. Other models which manipulate APP only include APP23 mice which are a similar strain, but the APP_{swe} gene is under the control of a different promoter and PDAPP mice where APP contains a V717F mutation (Gotz and Ittner, 2008).

1.3.4.2 APP/PS1

One of the most frequently used mouse models of AD is the APP_{swe}/PS1dE9 mouse that express humanised APP₆₉₅ with the Swedish double mutation (K595N and M596L in APP₆₉₅ which corresponds to amino acid positions K670N and M671L in APP₇₇₀ (Citron et al., 1992)) and human presenilin 1 with exon-9 deleted (PS1; APP/PS1) that enhances production of A β ₄₂. Both mutations have been implicated in familial early onset AD (Mullan et al., 1992; Perez-Tur et al., 1995) and are expressed under the mouse prion protein promoter in the APP/PS1 mouse model (Jankowsky et al., 2004). Due to the presence of two mutated genes APP/PS1 mice have greater production of A β ₄₂ than APP_{swe} transgenic mice, amyloid plaques are evident in APP/PS1 by 6 months, though there have been reports of plaques by 4 months (Gengler et al., 2010), and they are widespread throughout the brain by 9 months (Jankowsky et al., 2004). APP/PS1 mice also exhibit other features of AD, including microglial and astrocyte activation (Gallagher et al., 2012; Gallagher et al., 2013; Kelly et al., 2013) and memory impairment (Cao et al., 2007; Gallagher et al., 2013; Jankowsky et al., 2005). Interestingly, A β production does not reach a plateau in these mice and continues to accumulate up to 24 month of age (Minogue et al., 2014).

1.3.4.3 3xTg-AD

The only AD-mouse model to have both A β and tau pathology are 3xTg-AD mice which express APP₆₉₅ with the Swedish double mutation, mutated PS1 (M146V) and tau (P301L). The PS1 (M146V) mutation is associated with familial AD, and results in increased production of A β ₄₂ (Duff et al., 1996), the P301L mutation in tau is associated with familial early-onset dementia resulting in atrophy of the frontal, temporal and parietal cortex and widespread neurofibrillary tau tangles (Mirra et al., 1999). As a result of these mutations, 3xTg-AD mice have enhanced synaptic dysfunction at 6 months, intraneuronal A β accumulates at 6 months forming extracellular A β plaques at 12 months, with the appearance of NFTs at 12 months (Oddo et al., 2003).

1.4 CNS immune system

1.4.1 Microglial activation

Microglia are the principal innate immune cells in the brain and represent approximately 10% of cells in the CNS. While considered by many to be the macrophage of the brain, microglia are ontogenically distinct and derive from primitive myeloid progenitors in the yolk sac which migrate into the developing brain and give rise to microglia (Ginhoux et al., 2010). It was originally believed that the microglial population was maintained by infiltration of peripheral bone marrow-derived myeloid cells (Simard et al., 2006) however, it is now understood that microglia are maintained through *in situ* self-renewal (Ajami et al., 2007). Macrophages can infiltrate the brain (Ajami et al., 2011), and while microglia and macrophages share many cell surface characteristics (Guillemin and Brew, 2004) these cells are functionally distinct (London et al., 2013). In their resting state microglia, have a ramified appearance and use motile processes to survey their microenvironment (Nimmerjahn et al., 2005). Many factors within the brain contribute to maintaining microglia in a quiescent state, including the presence of the BBB which regulates the movement of large molecules and cell infiltrates into the parenchyma. Microglia express CD200 receptor and CX3CR1

which bind CD200L and CX3CL1 respectively. These ligands are expressed on neurons and astrocytes, and it has been demonstrated that the interaction modulates microglial activation (Lynch, 2014). Loss of CD200 occurs with age and in AD, and it has been demonstrated that absence of CD200 results in increased microglial activation and enhanced responsiveness to inflammatory stimuli (Cox et al., 2012; Denieffe et al., 2013; Lynch, 2014).

As innate immune cells, microglia are the first line of defence within the brain and can respond to pathogens (specifically, PAMPS) via PRRs, additionally microglia from mice express mRNA for Toll-like receptor (TLR) 1-9 (Olson and Miller, 2004). Microglial activation can occur as a result of numerous triggers including tissue damage, inflammation and infection. On activation, microglia change morphology by retracting their branches forming an amoeboid shape and upregulate the expression of many cell surface markers. There are a number of microglial subtypes, which differ principally in their function (Lynch, 2009; Perry et al., 2007). Upon activation, these cells can act as APCs, but they can become phagocytic or secretory and are capable of releasing numerous cytokines, chemokines and other neurotrophic factors.

In an effort to characterise microglial activation many researchers have investigated whether microglia respond to stimuli in a similar manner to macrophages which have broadly defined activation states; the classically-activated (M1) or alternatively-activated (M2) state. The activation states are largely identified by the cell surface markers expressed or cytokines produced. During a pro-inflammatory response macrophages can produce TNF α , IL-1 β and nitric oxide (NO) which is consistent with M1 activation. M2 is considered to be anti-inflammatory, playing a role in tissue repair and healing with IL-10 production and an up-regulation in the expression of mannose receptor and arginase-1 (Mantovani et al., 2013; Martinez and Gordon, 2014). These subtypes are stimulated *in vitro* using IFN- γ or lipopolysaccharide (LPS) to induce M1 and IL-4 and IL-13 to induce M2, thus M1 activation is often associated with Th1 cells and M2 activation with Th2 cells (Goldmann and Prinz, 2013). IFN- γ treated microglia secrete TNF α and IL-6 with increased CD86 and MHC class II expression

in vitro and intracerebroventricular (i.c.v.) injection of IFN- γ increases MHC class II and TNF α expression in the brain, along with enhancing the proportion of CD11b⁺ cells expressing CD86 or CD68 (Denieffe et al., 2013; Kelly et al., 2013). In contrast, treatment of microglia with IL-4 induced expression of arginase-1, mannose receptor, Chitinase 3-like 3 (also known as YM-1) and found in inflammatory zone (FIZZ)-1 (Michelucci et al., 2009). Therefore microglia can adopt M1 or M2 responses (Fig 1.7), however, in the brain the primary source of IFN- γ is from infiltrating immune cells, whose influx is highly controlled in normal conditions.

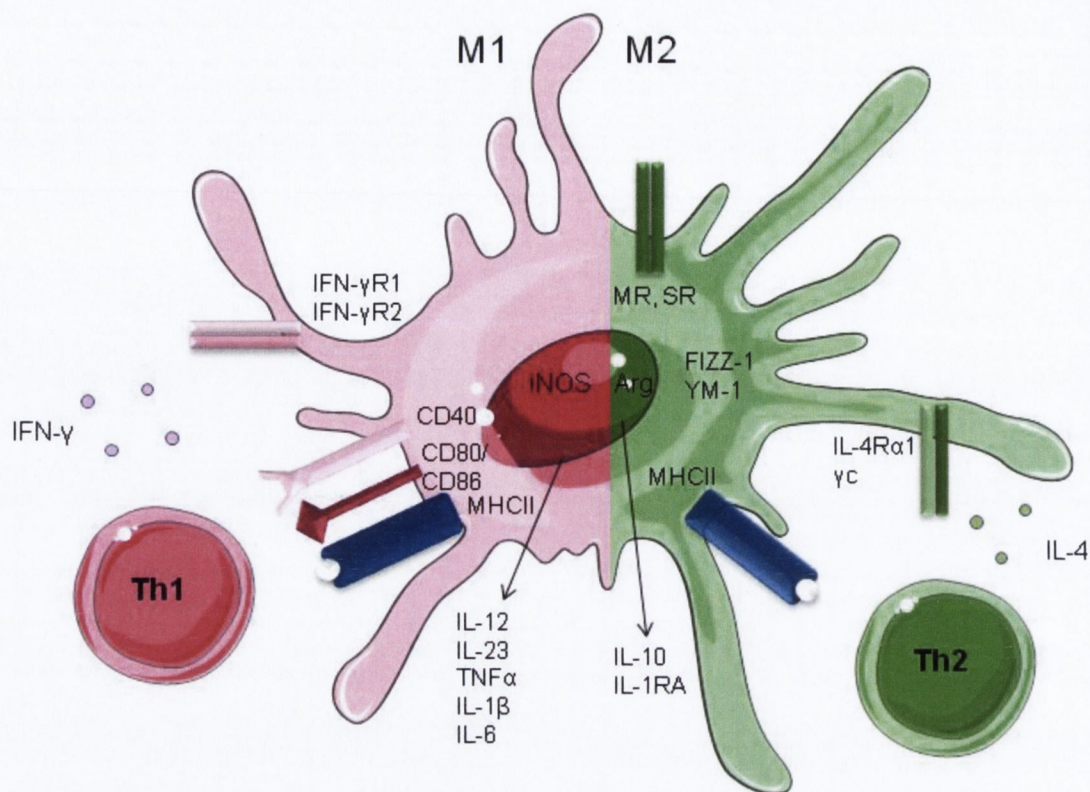


Figure 1.7 M1 and M2 activation of myeloid cells in mouse

M1 activation is induced *in vitro* using IFN- γ or LPS, as a result it is associated with a pro-inflammatory response and with Th1 cells which are a source of IFN- γ . Cell activation is characterised by determining cytokine secretion and the markers expressed on the cell surface. For M1 activation common cytokines produced are IL-12, IL-23, TNF α , IL-1 β and IL-6. These cells express MHC class II, CD80, CD86 and CD40 with increased expression of iNOS mRNA. M2 activation is anti-inflammatory, and is associated with healing, repair and Th2 cells which produce anti-inflammatory cytokines. M2 is achieved *in vitro* using IL-4 or IL-13 cytokines. It is characterised by an increase in IL-10 and IL-1RA release, cell surface expression of MHC class II, mannose receptor (MR) or scavenger receptors (SR) and increased mRNA expression of arginase, found in inflammatory zone (FIZZ)-1 and YM-1. γ c, IL-2R γ chain.

1.4.2 Microglial activation in AD

Microglia are sensitive to endogenous danger-associated molecular patterns (DAMPs), including A β , which can activate microglia through many receptors including CD14, TLR2 and TLR4 (Reed-Geaghan et al., 2009) and the expression of CD14 and TLR2 is increased in AD (Landreth and Reed-Geaghan, 2009).

Treatment of microglia *in vitro* with A β induces M1 activation increasing the expression of IL-1 β , IL-6, TNF α and cyclooxygenase (COX)-2 (Michelucci et al., 2009) and release of IL-1 β and TNF α into the supernatant along with increased MHC class II expression (Lyons et al., 2007b). Injection of A β i.c.v. results in IL-1 β and TNF α production *in vivo* with expression of MHC class II (Lyons et al., 2007b). Importantly, pro-inflammatory cytokines can promote the expression and activity of β -secretases and γ -secretases (Liao et al., 2004; Sastre et al., 2008). As activated microglia have been found in the brain of AD patients with dementia or those with mild cognitive impairment (MCI) (Cagnin et al., 2001; Okello et al., 2009), microglial activation may result in increased production of A β and accelerate the progression of AD (Glass et al., 2010).

A β can also activate the NOD-like receptor, pyrin domain containing 3 (NLRP3) inflammasome (Halle et al., 2008) which can result in activation of caspase-1, mediating the cleavage of pro-IL-1 β and pro-IL-18 into their mature cytokines. Indeed, APP/PS1 mice deficient in NLRP3 or caspase-1 have reduced amyloid plaque burden and were protected from spatial memory deficits which was associated with a shift to M2 activation in the brain (Heneka et al., 2013). IL-1 β is a potent inducer of inflammation and cell damage and its expression, along with IL-6 and IL-18, is increased in the brains of AD patients (Griffin et al., 1989; Ojala et al., 2009; Wood et al., 1993). Further evidence of pro-inflammatory signalling in AD comes from Vom Berg and colleagues who demonstrated that the concentration of IL-12p40 is increased in the CSF of AD patients, and microglia from APP/PS1 mice produce more IL-12p40 than wild type (WT) littermates (Vom Berg et al., 2012). Furthermore, APP/PS1 mice lacking IL-12p40 have reduced amyloid plaque deposition with decreased microglial and astrocyte activation. IL-1 β , IL-6, IL-18 and IL-12p40 can influence the adaptive immune response (Lalor et al., 2011; Mills, 2008), however, the combination of these cytokines with other factors released by activated microglia such as reactive oxygen species, can trigger neuronal cell death (Rogers et al., 2002). This can initiate a vicious cycle of chronic microglial activation, whereby dying neurons release DAMPs and further activate microglia.

1.4.3 Phagocytosis of amyloid

Microglia are capable of phagocytosing amyloid using many receptors including $\alpha 6\beta 1$ integrin, CD36, CD47, receptor for advanced glycation endpoints (RAGE) and scavenger receptors (Bamberger et al., 2003; Tahara et al., 2006). However, it has been proposed that in AD, failure of microglia to clear extracellular amyloid is central to the initial accumulation of A β (Weiner and Frenkel, 2006). Fibrillar A β can induce microglial phagocytosis, however the presence of oligomeric A β impairs phagocytic activity (Pan et al., 2011). Interestingly, this group demonstrated oligomeric A β induced a greater inflammatory environment than fibrillar A β , which resulted in decreased expression of microglial phagocytosis receptors. Pre-treatment of microglial cells with IL-1 β , TNF α , IFN- γ or monocyte chemoattractant protein (MCP)-1 also inhibits phagocytosis (Koenigsnecht-Talboo and Landreth, 2005) which, together, suggests it is the inflammatory environment in AD (particularly that induced by oligomeric A β) which inhibits up take of amyloid. This is in line with other reports which demonstrate that microglia have phagocytic activity *in vitro*, but this is impaired in AD as ultrastructural analysis could not detect amyloid fibrils in the lysosomal compartment of microglia in the AD brain (Frackowiak et al., 1992).

It has been revealed that microglia become dysfunctional with age. This is exacerbated in the presence of amyloid as microglia from AD brains have shorter telomeres, indicating senescence and cells surrounding A β -plaques are dystrophic with a fragmented cytoplasm, beaded processes and spheroidal swellings (Flanary et al., 2007; Miller and Streit, 2007). Microglial functions are also altered in APP/PS1 mice, which displayed reduced motility and an impaired phagocytic capacity (Krabbe et al., 2013).

Efforts to shift the phenotype of microglia from M1 to M2 and thus increase phagocytic activity have proved promising. Treatment of microglia with IL-4, IL-10, ibuprofen or COX-2 inhibitors can restore phagocytosis in cells pre-treated with pro-inflammatory cytokines (Koenigsnecht-Talboo and Landreth, 2005) as can inhibition of NK- κ B or the use of a free radical scavenger (Pan et al.,

2011). Treatment with the peroxisome proliferator-activated receptor (PPAR)- γ agonist, pioglitazone, increases A β degradation by microglia and astrocytes *in vitro* and *in vivo*, reducing A β deposits after just 9 days treatment in APP/PS1 mice; this was associated with a shift to M2 activation in the brain, along with an attenuation of cognitive deficits (Mandrekar-Colucci et al., 2012). In addition *Nlrp3*^{-/-} or *Caspase1*^{-/-} mice have decreased IL-1 β in the brain and a microglial shift to the M2 phenotype that are more efficient phagocytes (Heneka et al., 2013).

Macrophages infiltrate the AD brain, and have been found co-localised with A β -deposits (Fiala et al., 2002). It has been suggested that macrophage influx may be beneficial in AD as macrophages are better than microglia at degrading A β (Majumdar et al., 2008). In addition, Tg2576 mice deficient in CCR2 have exacerbated amyloid pathology which was associated with reduced numbers of microglia and macrophages surrounding A β plaques (El Khoury et al., 2007). However, it has been reported that macrophages prepared from AD patients exhibit decreased A β phagocytosis and degradation and are more vulnerable to A β induced apoptosis (Fiala et al., 2005; Mizwicki et al., 2012) and therefore they may contribute to the progression of AD.

1.4.4 Microglia as APCs

It has been demonstrated that the microglia surrounding amyloid plaques in AD are activated, expressing MHC class II and CD40 (McGeer et al., 1989; McGeer et al., 1987; Perlmutter et al., 1992; Togo et al., 2000). As T cell infiltration is also increased in AD (Hartwig, 1995; McGeer et al., 1989; Parachikova et al., 2007; Pirttila et al., 1992; Rogers et al., 1988; Togo et al., 2002; Town et al., 2005), it is possible that the microglia in their enhanced APC state can interact with T cells. The ability of microglia to act as APCs is examined more frequently in the context of MS and EAE where large numbers of T cells influx the brain, which is associated with increased MHC class II, CD80 and CD40 on microglia (Chastain et al., 2011; Murphy et al., 2010). While this area is still developing in relation to AD, studies in EAE provide a useful context.

IFN- γ is a potent inducer of M1 activation and microglia treated *in vitro* with IFN- γ increase their expression of MHC class II, CD86, CD40 and ICAM-1 on the cell surface, enhancing the APC capabilities of the cell (Aloisi et al., 2000a; Aloisi et al., 1998; McQuillan et al., 2010). Furthermore, IFN- γ can induce production of CXCL10, CCL2 and CCL5, thus facilitating immune cell recruitment (Rock et al., 2005). A β can also induce the APC phenotype, increasing CD40 and CD86 on the cell surface, which is further enhanced with IFN- γ treatment (McQuillan et al., 2010). Microglia treated with IL-17 produce significant amounts of MCP-1, MCP-5, macrophage inflammatory protein (MIP)-2 and keratinocyte derived-chemokine (KC) (Sarma et al., 2009) which have lymphocyte chemotactic properties (Rollins, 1997). While IL-17 treatment is not as effective as IFN- γ at inducing APC co-stimulatory receptors, IL-17 and IFN- γ together increases the expression of ICAM-1 and VCAM-1 adhesion molecules (Kawanokuchi et al., 2008).

Treatment of microglia with supernatants produced by Th1 cells mimicked the effect of IFN- γ (namely increased MHC class II, CD40, CD86 and ICAM-1), but also upregulated CD80 and increased the production of TNF α , IL-6 and CXCL10 over that induced by IFN- γ alone (Prajeeth et al., 2014; Séguin et al., 2003). As co-incubation with an α -IFN- γ antibody only partially blocked the Th1 supernatant effects (Séguin et al., 2003), it is clear that activation of microglia by Th1 cells is a complex process and requires multiple signals from the T cell. Incubation with supernatants from Th2 (Séguin et al., 2003) or Th17 cells (Prajeeth et al., 2014) was without effect. While microglia are strongly influenced by soluble factors released from T cells, it seems likely that cell-cell contact is necessary to induce a potent signal to the glial cell.

A number of studies have examined the effect of T cell co-incubation on microglia activation. It has been found that ovalbumin (OVA)-specific Th1, but not Th2 cells induced expression of MHC class II, CD40, CD80 and ICAM-1 on microglia (Aloisi et al., 2000a; Wolf et al., 2001). Furthermore, co-incubation with α -IFN- γ reduced the expression of microglial MHC class II and T cell-produced IL-2 (Aloisi et al., 2000a). Microglia are effective APCs; during *in vitro* infection with Theiler's murine encephalomyelitis virus (TMEV), these cells upregulate the

expression of MHC class II, CD80 and CD86 and can present both virus and myelin to CD4⁺ T cells, inducing T cell proliferation and cytokine secretion (Olson et al., 2001). TLR or IFN- γ stimulated microglia can also induce myelin specific CD4⁺ T cell proliferation and cytokine secretion *in vitro* (Olson and Miller, 2004), which was inhibited by blocking IL-12p40 (Constantinescu et al., 2005). In addition, it has been demonstrated that IFN- γ stimulated microglia are better APCs than IFN- γ stimulated astrocytes, inducing OVA-specific T cell production of IL-2 and IFN- γ with T cell proliferation (Aloisi et al., 1998) although without IFN- γ pre-treatment, proliferation was minimal.

The effect of A β -specific T cells on microglia in mixed glial cultures has been examined. It was found that glia can act as APCs for A β -specific Th1, Th2 and Th17 cells (McQuillan et al., 2010). A β -specific Th1 and Th17 cells increased MHC class II, CD86 and CD40 expression and production of TNF α , IL-6 and IL-1 β from A β -activated microglia (McQuillan et al., 2010). This response was greater than that observed when glia were treated with IFN- γ or IL-17 alone. However, incubation of A β -specific Th2 cells inhibited CD40 and CD86 on microglia induced by A β -specific Th1 cells and reduced production of IL-1 β and IL-6 by A β -specific Th17 cells (McQuillan et al., 2010). When supernatants from Th1 and Th2 cells were co-incubated with microglia, Th2 did not attenuate the Th1 cell-induced inflammatory effects (Séguin et al., 2003) suggesting that the mechanisms by which Th2 cells modulate Th1 and Th17 induced inflammation are mediated through cell-cell contact.

CD40 signalling in microglia has been implicated in the progression of AD. As mentioned previously, A β can induce expression of CD40 on microglia, however further treatment of these cells with CD40L induces significant production of TNF α , IL-6 and IL-1 β (Tan et al., 1999; Townsend et al., 2005). Microglia surrounding amyloid plaques in AD express CD40 (Togo et al., 2000) and APP^{swe} mice that lack CD40L or CD40 receptor have significantly reduced amyloid pathology throughout the brain which was associated with decreased microglia and astrocyte activation (Laporte et al., 2006; Tan et al., 2002). T cells are the likely source of CD40L though, during chronic inflammatory conditions, astrocytes can also upregulate CD40L (Calingasan et al., 2002). As a result of

these findings it has been suggested by Town and colleagues that microglia exist in one of two states when activated; “innate activation” which is phagocytic or “adaptive activation” which is the APC phenotype (Town et al., 2005; Townsend et al., 2005). Furthermore, microglia treated with CD40L *in vitro* have impaired phagocytic activity (Townsend et al., 2005) whereas these cells are more efficient APCs of A β -specific T cells and blocking CD40 in the co-incubation reduced the ability of pre-activated microglia to stimulate T cell cytokine production. Importantly it is suggested that when microglia adopt the APC phenotype this promotes inflammation, thus leading to enhanced AD-pathology (Fig 1.8). This is in line with other reports which demonstrate that microglia in AD are impaired at amyloid phagocytosis (Frackowiak et al., 1992).

1.4.5 Astrocytes in AD

Astrocytes are the most abundant glial cell of the CNS. They have many roles in the brain from maintaining homeostasis to modulating synaptic transmission and function via the release of gliotransmitters, growth factors and cytokines (Sofroniew and Vinters, 2010). In the healthy brain, astrocyte end feet cover 100% of the vasculature (Armulik et al., 2011). These cells also have a functional role between neurons and blood vessels, releasing vasoactive substances at their end feet in response to neuronal activity which can induce vasodilatation or vasoconstriction (Heneka et al., 2010). Furthermore, astrocytes can directly modulate the BBB, releasing pro-inflammatory cytokines which can increase BBB permeability, and conversely astrocytic production of TGF- β can enhance the integrity of the BBB (Nair et al., 2008). While astrocytes are not commonly associated with immune responses, emerging evidence demonstrates that these cells express TLRs and PPRs (Bowman et al., 2003; Jack et al., 2005), are capable of phagocytosis, including A β (Jones et al., 2013) and can readily produce pro-inflammatory cytokines on activation (Chastain et al., 2011; Dong and Benveniste, 2001). Astrocytes respond to insult, and do so by upregulating the expression of genes such as glial fibrillary acidic protein (GFAP), and inducing hypertrophy of the cell body and cell proliferation (Sofroniew and Vinters, 2010). Reactive astrogliosis is a feature of AD where astrocytes are found surrounding

amyloid plaques (Rodriguez et al., 2009; Sofroniew and Vinters, 2010) with substantial A β detected within the astrocytes (Nagele et al., 2004). Increased GFAP expression has also been associated with increased Braak stage (progression of NFTs) in AD patients (Simpson et al., 2010).

1.4.6 Astrocytes as APCs

Treatment of astrocytes *in vitro* with IFN- γ results in increased expression of MHC class II, CD80, CD86, CD40, ICAM-1 and VCAM-1 on the cell surface (Girvin et al., 2002; Soos et al., 1999; Tan et al., 1998). IFN- γ also induced CXCL10 (Carter et al., 2007). The ability of IL-17 to induce APC co-receptors on astrocytes is not well understood, however, astrocytes treated with IL-17 produce significant amounts of MCP-1, MCP-5, MIP-2 and KC (Sarma et al., 2009), in addition TNF α in combination with IL-17 or IFN- γ induces the expression of CXCL1, CXCL2, CXCL9, CXCL10, CXCL11 and CCL20 in astrocytes (Kang et al., 2004).

Astrocytes are capable of producing IL-12, IL-4, IL-23, IL-6 and TGF- β all of which can influence the adaptive immune response (Nair et al., 2008). Astrocytes can act as APCs inducing myelin- or OVA-specific T cell activation *in vitro* (Kort et al., 2006; Miljkovic et al., 2007; Teige et al., 2006) which was attenuated by blocking CD80 or CD86 (Tan et al., 1998) or pre-treating cells with IFN- β (Teige et al., 2006). Astrocytes are unable to induce Ag-specific T cell proliferation (Teige et al., 2006) unless cells have been pre-stimulated with IFN- γ (Aloisi et al., 1998; Nikcevich et al., 1997). Interestingly, blocking IL-12p40 signalling reduced the ability of IFN- γ activated astrocytes to induce T cell proliferation (Constantinescu et al., 2005). Furthermore, astrocytes surrounding lesions in MS express MHC class II, CD80 and CD86 (Zeinstra et al., 2003; Zeinstra et al., 2000).

In AD, the astrocytes surrounding amyloid plaques express ICAM-1 (Akiyama et al., 1993), but whether astrocytes express MHC or co-stimulatory molecules involved in activating T cells has not been investigated. However, it has been established that in mixed glial cultures, A β -specific Th1 and Th17 cells promoted MHC class II on CD11b⁻ astrocytes (McQuillan et al., 2010).

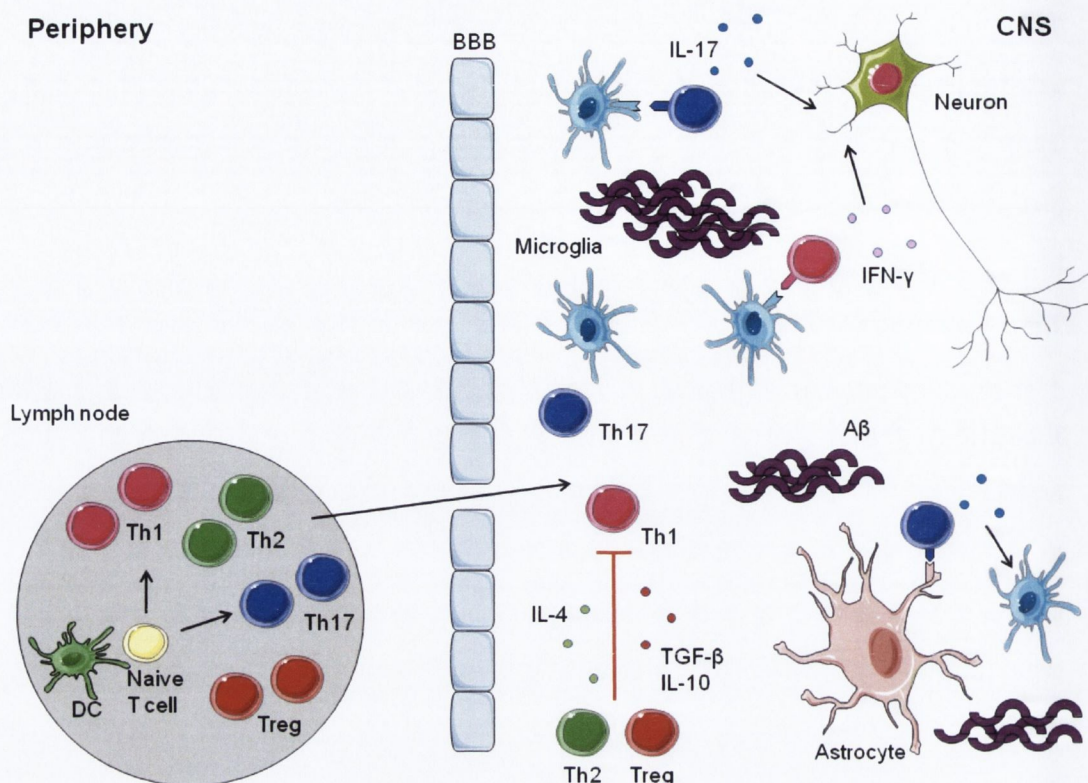


Figure 1.8 Proposed role of T cells in Alzheimer's disease.

CNS reactive T cells are activated or primed by dendritic cells (DC) in the lymph node. These cells migrate to the CNS and transverse the blood-brain barrier (BBB) by transendothelial migration. T cells are re-stimulated in the CNS by interacting with microglia or astrocytes acting as antigen presenting cells (APC) resulting in T cell activation and cytokine secretion. T cells have the capacity to modulate the activity of their APC and surrounding cells through contact and cytokine production. In cases of pro-inflammatory cytokine production, by Th1 and Th17 cell types, this may negatively affect nearby neurons or glial cells through the bystander effect thereby potentiating the inflammatory environment in AD. Induction of Th2 or Treg cells may suppress the neuroinflammation in AD by the secretion of anti-inflammatory cytokines or through cell-cell contact, thus providing a possible therapy for this disease.

1.4.7 Increased BBB permeability in AD

A meta-analysis on BBB changes revealed there is some loss in BBB integrity with normal aging, but this is significantly greater in patients with AD or vascular dementia (Farrall and Wardlaw, 2009). A number of reports have identified factors that contribute to the BBB permeability in AD. The vascular endothelial cells of AD patients are smaller and thinner than those of elderly healthy controls

(Zipser et al., 2007). Increases in IgG and the plasma proteins fibrinogen, thrombin and prothrombin have been reported in the AD brain, often appearing in association with A β deposits or activated microglia (Akiyama et al., 1992; Berzin et al., 2000; Fiala et al., 2002; Ryu and McLarnon, 2009). Furthermore, prothrombin changes corresponded with increased Braak stage, and was elevated in AD patients with the *APOE4* allele (Zipser et al., 2007). A separate study found an association between increased albumin extravasation in AD brain tissue with increased NFTs, and enhanced fibrinogen staining correlated with both increased NFTs and neuritic plaques (Viggars et al., 2011). High concentration of plasma proteins within the CNS is detrimental and can cause neurotoxicity and neuroinflammation (Zlokovic, 2011).

It has been demonstrated that AD patients have decreased ZO-1 at vascular endothelial cells. Interestingly, this co-localised with macrophage/monocyte infiltration at sites of TJ disruption (Fiala et al., 2002). In patients with CAA, there is a significant loss in the TJ proteins claudin-5, occludin and ZO-1 in A β -associated vessels (Carrano et al., 2011). Treatment of cerebral microvascular endothelial cells (CMEC) *in vitro* with A β reduces the protein and/or mRNA expression of claudin-5, occludin and ZO-1, resulting in increased barrier permeability (Carrano et al., 2011; Marco and Skaper, 2006; Tai et al., 2010), which was mediated in part by RAGE and MMPs (Kook et al., 2012). TNF α and IL-1 β can reduce the TJ protein expression of vascular endothelial cells (Kebir et al., 2007; Minagar and Alexander, 2003), both of which are increased in the circulation of AD patients along with IL-6, IL-18 and MCP-1 (Akiyama et al., 2000; Brosseron et al., 2014). Pro-inflammatory cytokines also increase the activity of MMP-9 in brain vascular endothelial cells (Harkness et al., 2000). Furthermore, MMP-9 is significantly increased in the plasma of AD patients (Lorenzl et al., 2003) and has been shown to disrupt the BBB directly by degrading ZO-1 which is an established MMP-9 substrate (Asahi et al., 2001).

In addition to the role of TJs in maintaining BBB integrity, an additional important factor is the presence of pericytes and the attachment of astrocytic end feet to the basement membrane. It was recently observed that both the

number and coverage of pericytes was significantly reduced in AD brain tissue (Sengillo et al., 2013). Furthermore, the reduction in pericyte coverage correlated with increased extravascular IgG and fibrin deposits. A β deposition along the vasculature is also associated with the retraction and swelling of astrocyte end feet (Merlini et al., 2011; Wilcock et al., 2009); one consequence of this is astrocytic detachment associated with a decrease in blood vessel-associated β -dystroglycan, and the leakage of IgG into the parenchyma (Merlini et al., 2011).

ApoE has been implicated in maintaining the BBB. Mice expressing *APOE4* or *APOE*^{-/-} mice have substantial BBB permeability demonstrated by enhanced leakage of IgG, thrombin and fibrin with increased activity of MMP-9 which was associated with decreased claudin-5, occludin and ZO-1 TJ proteins (Bell et al., 2012). Importantly, vascular dysfunction occurred before deficits in neuronal and synaptic changes were apparent which highlights the importance of an intact BBB with serious implications for AD patients carrying the *APOE4* allele.

Loss of TJ proteins and BBB permeability is also a feature of murine AD models; mice display increased gadolinium extravasation by MRI, greater fibrinogen staining, increased chemokine expression and decreased expression of TJ proteins (Biron et al., 2011; Minogue et al., 2014). Peripheral cell infiltration also occurs in the mouse brain, where T cell and macrophage influx is greater in older APP/PS1 mice (Jimenez et al., 2008; Kelly et al., 2013; Minogue et al., 2014).

1.4.8 Facilitated T cell entry through the BBB in AD

A number of studies have demonstrated that T cells from AD patients have an altered phenotype, which may aid migration across the BBB. MIP-1 α /CCL3 is significantly increased on T cells obtained from AD patients (Man et al., 2007) and this binds to CCR5 on the cells of the BBB resulting in transendothelial migration. This group have also shown that CCR5 expression on brain endothelial cells is increased in response to A β (Li et al., 2009). Similarly, CXCR2 is

overexpressed on T cells from AD patients (Liu et al., 2010) and this receptor is involved in cellular adhesion to the BBB, facilitating T cell migration into the brain. It has recently been demonstrated that expression of the chemokine receptors CCR2, CCR4, CCR5 and CCR6 is increased on CD4⁺ T cells from AD patients (Goldeck et al., 2013; Reale et al., 2008). Pellicano and colleagues also demonstrated an increase in CCR5 on T cells, where the T cell expression of CCR2 and CCR5 increased further after A β treatment in AD patients only (Pellicano et al., 2010). These receptors bind many chemokines including MCP-1/CCL2, MIP-1 α /CCL3, MIP-1 β /CCL4 and RANTES/CCL5 (Cartier et al., 2005) all of which are increased, with CXCL10, in the brains of AD patients (Streit et al., 2001; Tripathy et al., 2007, 2010; Xia et al., 2000; Xia et al., 1998).

CD14⁺ monocytes from AD patients also express increased CCR6 and CXCL1 (Goldeck et al., 2013; Zhang et al., 2013). It has been demonstrated that A β can induce monocyte adhesion to, and subsequent migration across a model BBB (Fiala et al., 1998; Gonzalez-Velasquez and Moss, 2008), and treatment of AD monocytes with α CXCL1 or α CXCR2 impairs migration in response to A β (Zhang et al., 2013). In addition, increased infiltration of macrophages has been observed in the AD brain, with macrophages located at the perivascular space and surrounding A β plaques (Fiala et al., 2002). Treatment of human monocytes with A β results in production of MIP-1 α /CCL3, MCP-1/CCL2, IL-8 and MIP-1 β /CCL4 along with the pro-inflammatory cytokines TNF α , IL-6 and IL-12 (Cartier et al., 2005; Fiala et al., 1998). Furthermore, peripheral blood mononuclear cells (PBMCs) from AD patients treated with A β produce significant amounts of MIP-1 β /CCL4 and RANTES/CCL5 and also IL-1 β , IL-6, IFN- γ , TNF α , IL-1RA and IL-10 (Pellicano et al., 2010).

As BBB permeability is increased in AD patients (Farrall and Wardlaw, 2009), the increased expression of chemokine receptors on T cells, together with their corresponding ligands in the AD brain further facilitates the recruitment of peripheral immune cells into the CNS, or at least into the perivascular space until T cells are further activated. It has been demonstrated that T cells from AD patients have increased reactivity to A β (Monsonogo et al., 2003; Saresella et al.,

2010; Saresella et al., 2012). Furthermore, A β drains from the brain along the perivascular pathway and, in the AD brain, A β accumulates adjacent to blood vessels (Carare et al., 2008; Nicoll et al., 2004). Therefore once in the perivascular space, the presence of A β provides an opportunity for stimulation of A β -specific T cells or activation of infiltrating monocytes. Given that monocytes and PBMCs produce numerous cytokines and chemokines after interaction with A β , as do T cells after Ag-stimulation, a vicious cycle of cell infiltration, inflammation and further cell recruitment may develop in the brains of AD patients. Importantly, T cell infiltration into the brain is enhanced in AD (Togo et al., 2002).

1.5 Future therapies for AD

1.5.1 Immunization

Immunization with A β to induce A β -specific antibodies is being investigated as an approach for the treatment of AD. Immunization with A β in the presence of an adjuvant induces an immune response against the peptide, inducing antibodies that may prevent further protein deposits, and even induce plaque breakdown. A clinical trial was initiated after positive findings in mouse models of AD which demonstrated reduced A β burden and behavioural deficits after immunization with A β and Freund's adjuvant (Janus et al., 2000; Schenk et al., 1999). Unfortunately the AN1792 trial, where A β was given with QS-21, was suspended in stage II due to the development of meningoencephalitis in several patients (Schenk, 2002). On post-mortem analysis, A β burden was decreased in AD patients who took part in the trial (Holmes et al., 2008). Furthermore, the microglia surrounding the residual plaques had increased MHC class II and CD68, with A β detected within the microglia (Boche and Nicoll, 2008), which rarely occurs in non-immunised AD patients. Interestingly, those patients with detectable titres of anti-A β antibodies 4.6 years after immunization had reduced functional decline in comparison with AD patients who received the placebo (Vellas et al., 2009). Many of the patients involved were diagnosed with

moderate AD, therefore immunization at earlier stages of disease onset may provide more functional benefits than later treatment.

The adjuvant used in the AN1792 trial, QS-21, stimulates Th1 type responses and this may have contributed to the development of meningoencephalitis and T cell infiltration into the brain (Wilcock and Colton, 2008). A β -specific Th1 cells enhance AD-like pathology in APP/PS1 mice when transferred intravenously (i.v.) (Browne et al., 2013). However, it has also been suggested that the key event mediating T cell-induced neuroinflammation is T cell activation and infiltration at the neurovasculature. When A β -specific Th1 cells are injected directly into the ventricle, the cells cross into the parenchyma at the ependymal layer only, and ultimately reduce plaque load in APP/PS1 mice (Fisher et al., 2014). Indeed it has been suggested by Schwartz and colleagues that T cell recruitment from the choroid plexus into the brain is a key step in the resolution of neuroinflammation (Schwartz and Baruch, 2014). Importantly they suggest that anti-inflammatory cytokines present in the CSF skew the infiltrating T cells to an anti-inflammatory or suppressive phenotype (i.e. Th2 or Treg), which is neuroprotective and capable of restoring homeostasis in the brain. However it has been demonstrated that AD patients have increased pro-inflammatory cytokines in their CSF including IL-12p40, TNF α , IL-6, IL-18 and MCP-1 (Akiyama et al., 2000; Brosseron et al., 2014; Vom Berg et al., 2012) which may prevent skewing of T cells to the anti-inflammatory subtype, and induce Th1 or Th17 cells instead.

The induction of an A β -specific Th2 or Treg type response could be more appropriate in vaccination studies given the anti-inflammatory function of these cells. A β immunization in Tg2576 mice with alum as an adjuvant successfully prevented deposition of plaques and cognitive deficits, though only when the vaccine was administered before substantial amyloid pathology had developed (Asuni et al., 2006). It has been observed that transfer of A β -specific Th2 cells is protective in 11 month-old APP/PS1 mice, reducing cognitive impairment and amyloid deposition at blood vessels (Cao et al., 2009). Conversely, transfer of A β -

specific Th2 cells was not sufficient to reduce neuroinflammation or plaque deposition in 6 month-old APP/PS1 mice (Browne et al., 2013).

The induction of a B cell only response through immunization with the B cell epitope, A β ₁₋₁₁, has proved successful in reducing plaque deposition and increasing survival in 3xTg-AD mice (Olkhanud et al., 2012). Another avenue of treatment currently being pursued in clinical trials is passive immunization which involves injecting humanised anti-A β antibodies i.v. into AD patients or injections of concentrated immunoglobulins (IVIg) from healthy individuals (Lambracht-Washington and Rosenberg, 2013; Wilcock and Colton, 2008). Direct injection of antibodies can negate the effects of immune senescence observed in elderly AD patients and avoid T cell-mediated encephalitis. These antibodies could reduce plaque burden by facilitating phagocytosis of amyloid or inhibiting A β aggregation, and the clinical trials are showing promising results by slowing cognitive decline in AD patients (Lambracht-Washington and Rosenberg, 2013). A potential risk of antibody-mediated therapy is that microhaemorrhages can occur, possibly as a result of increased antibody-bound A β in the blood, or due to further weakening of amyloid-associated vessels (Pfeifer et al., 2002).

Together the results indicate that activating the immune system by active or passive immunization could prove a promising therapy for AD. Importantly, the induction of an A β -specific Th2 response appears safer than Th1, though extreme caution must be taken with these treatments. Studies in animal models have shown that vaccination at late stages of amyloid accumulation is not protective, nor does it attenuate behavioural or cognitive defects, which reflects what might be observed in clinical trials. It is accepted that immunization before pathogen-induced infection is more efficient at preventing disease or illness than once the pathogen has already taken hold. As amyloid accumulation occurs decades before the development of AD symptoms, early treatment is vital.

1.5.2 FTY720

FTY720 (Fingolimod/Gilenya; Novartis) was derived from a chemical modification

of the metabolite myriocin isolated from the fungus *Isaria sinclairii*. Specifically, side chain functionalities were removed with the addition of a phenyl ring. FTY720 has immunosuppressant effects (Adachi et al., 1995; Suzuki et al., 1996); it was demonstrated that FTY720 could prolong organ graft survival and was associated with reduced lymphocyte infiltration into the grafted tissues due to increased T cell homing to the lymph nodes (Brinkmann and Lynch, 2002; Chiba et al., 1996; Chiba et al., 1998; Yanagawa et al., 1998). FTY720 is structurally similar to sphingosine-1-phosphate (S1P), a bioactive sphingolipid formed from sphingomyelin, a cell membrane constituent. Sphingomyelin is degraded by sphingomyelinase to produce ceramide, that is further metabolized by ceramidases to produce sphingosine, which is in turn phosphorylated by sphingosine kinase to produce S1P (Brinkmann, 2007). FTY720 is also phosphorylated by sphingosine kinase, which occurs extensively *in vivo*, and phosphorylated FTY720 can act on four of the five S1P receptors which are GPCRs (i.e. S1P₁, S1P₃, S1P₄ or S1P₅) (Brinkmann et al., 2002; Mandala et al., 2002). S1P₁ receptor is most highly expressed on cells of the immune and central nervous systems, and it is believed that FTY720 exerts its effect on lymphocyte sequestration by acting through this receptor (Brinkmann et al., 2010). T cells require S1P signalling through S1P₁ to override CCR7-mediated retention in the lymph node. This allows the T cell to egress along the S1P concentration gradient as S1P is found at low concentrations in the lymph node (5-20 nM) and high concentrations in the blood (100-1,000 nM) (Brinkmann et al., 2010; Rosen and Goetzl, 2005). However, FTY720 acts as a “functional antagonist” that leads to internalization of the S1P₁ receptor (Fig 1.9) thus preventing S1P₁ from responding to its natural agonist S1P; which retains T cells in the lymphoid organs (Brinkmann et al., 2010). Therefore FTY720 reduces the numbers of T cells in the circulation (Morris et al., 2005). It was first demonstrated in 2002 that FTY720 treatment reduced symptoms of disease in EAE (Brinkmann et al., 2002; Foster et al., 2007) and this led to a number of successful clinical trials that showed FTY720 reduced the relapse rate, MRI end points and progression of disability in MS patients (Kappos et al., 2006; Kappos et al., 2010). As a result, FTY720 received Food and Drug Administration (FDA) approval in 2010, with EU approval the following year and is now the first orally active immunomodulatory

drug available for the treatment of MS. There were minimal side effects from taking FTY720, although it was noted that there was an enhanced incidence of lower respiratory tract infections in MS patients that received FTY720 (Cohen et al., 2010; Kappos et al., 2010).

Another mechanism by which FTY720 exerts a protective effect in EAE is by acting on S1P₁ receptors on astrocytes (Choi et al., 2011), as the severity of EAE was reduced with a concomitant loss of FTY720 efficacy in transgenic mice lacking S1P₁ on astrocytes. S1P also has functions in the brain where it can induce astrocyte proliferation through pathways including activation of mitogen-activated protein kinases (MAPK) or Rho kinase (Malchinkhuu et al., 2003; Pébay et al., 2001; Sorensen et al., 2003) and neurogenesis through the MAPK pathway (Harada et al., 2004; Mizugishi et al., 2005).

Due to the efficacy of FTY720 in MS and EAE, this drug has also been tested as a possible treatment in other conditions such as stroke (Campos et al., 2013; Rolland et al., 2013) and diabetes (Moon et al., 2013; Penaranda et al., 2010). In animal experiments, FTY720 treatment attenuated the behavioural deficits induced by A β injection into the frontal cortex, hippocampus or ventricle (Asle-Rousta et al., 2013; Fukumoto et al., 2014; Hemmati et al., 2013). The effect of FTY720 in transgenic AD animal models has not been investigated.

Lymph Node

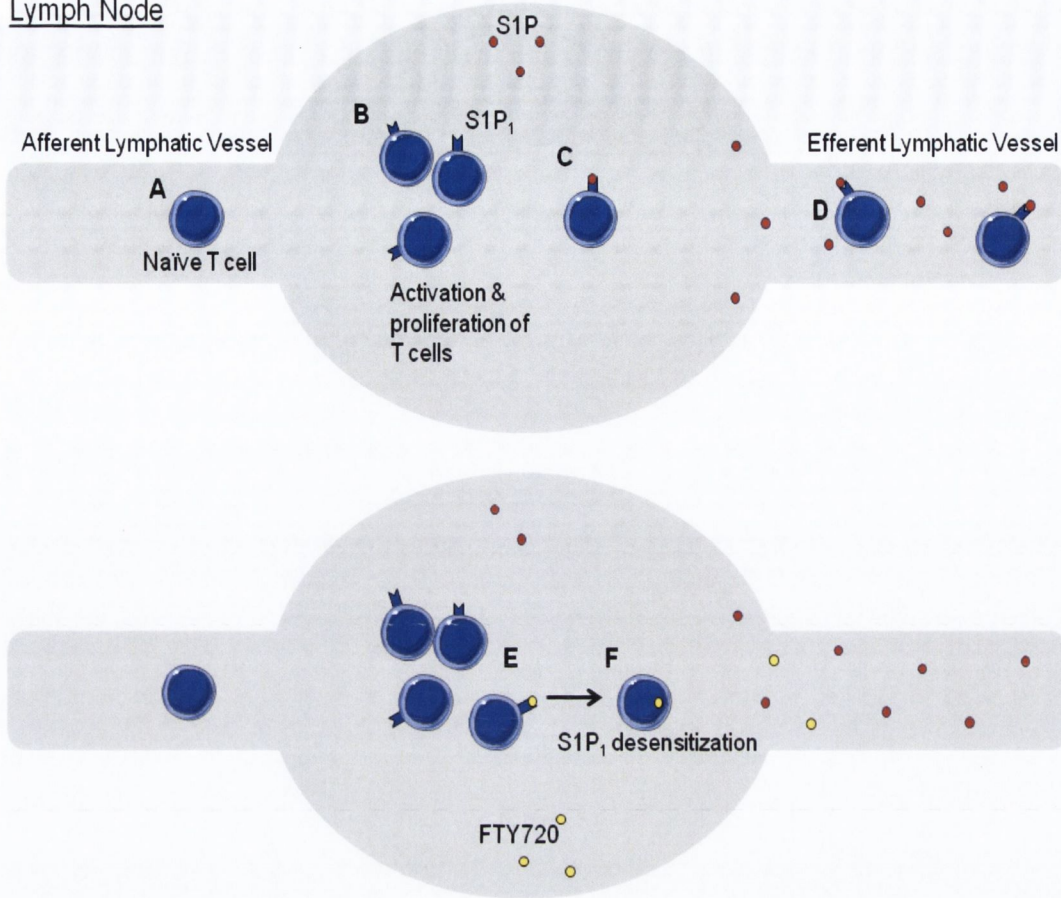


Figure 1.9 FTY720 prevents T cell egress from the lymph node

(A) Naïve T cells enter the lymph node through the afferent lymphatic vessel. (B) Upon antigen stimulation the naïve T cell become activated, proliferates and differentiates. (C) S1P binds to the S1P₁ receptor on the T cell (D) which allows the T cell to leave the lymph node. (E) However, FTY720 binds the S1P₁ receptor, which ultimately results in internalization and desensitization of the receptor. (F) This leaves the T cell unable to respond to S1P and thus remains trapped in the lymph node.

1.6 Changes to the immune system with age and AD

1.6.1 Age-related changes in the immune system

One of the most significant changes in the immune system with aging is the involution of the thymus, which results in decreased output of new T cells (Mackall et al., 1995; Naylor et al., 2005), though proliferation of the T cells in the periphery maintains the T cell pool (Mackall and Gress, 1997; Mackall et al., 1997). After the age of 65, the diversity of the TCR on naïve T cells drops

dramatically (Naylor et al., 2005) which limits the individuals' ability to induce a T cell response to new antigens. The T cells that have resided in the periphery for years are exposed to factors such as oxidative species that increase with age and may have a negative impact on immune function (Haynes and Swain, 2006). The decrease in naïve T cells in the elderly is associated with an increase in memory cells (Grubeck-Loebenstein and Wick, 2002; Pawelec et al., 2002), in particular clonally-expanded T cell subsets (Pawelec et al., 2004; Vasto et al., 2007) which may develop from repeated or chronic infections (Khan et al., 2002; Kovaïou et al., 2007). When the pool of memory T cells consists of expanded clones, there is a more restricted T cell repertoire and a reduced ability to respond to new antigens (Franceschi et al., 2000; Kovaïou et al., 2007). It has also been observed that the elderly have an impaired long term T cell response induced by vaccination (Kang et al., 2004). Changes in the Treg subsets have been reported, with cells from aged individuals less capable at preventing autoimmunity (Fessler et al., 2013). Altered Treg activity in aged mice is also associated with the reactivation of chronic infections (Lages et al., 2008). Indeed aging in humans is characterised by chronic, low-grade inflammation, known as "inflammaging", which is a significant risk factor for morbidity in the elderly (Franceschi and Campisi, 2014). Together, the changes in T cells and inflammaging may negatively impact on the ability of the elderly to mount an efficient immune response against infection, thus leaving them vulnerable to the effects of pathogens. This is particularly relevant in the context of newly-emerging infectious diseases.

1.6.2 Changes to the adaptive immune system in AD

A number of studies have shown that the activation state of T cells, and their responsiveness, is altered in AD. In addition to the increased reactivity of T cells from AD patients to A β (Monsonogo et al., 2003; Saresella et al., 2010; Saresella et al., 2012), there is also a skewing of the cells to Th17 and Th9 phenotypes (Saresella et al., 2011). An increase in circulating CD4⁺IFN- γ ⁺ and CD8⁺IFN- γ ⁺ T cells in AD patients has also been reported (Baglio et al., 2013; Fiala et al., 2005) and a decrease in CD4⁺PD-1⁺ T cells indicating a resistance to apoptosis in AD T

cells (Saresella et al., 2012). Indeed, a recent study demonstrated that T cells from patients with amnesic MCI, a preclinical stage of AD, had levels of CD45⁺IFN- γ ⁺ and CD45⁺IL-17⁺ lymphocytes in the CSF that were comparable to untreated patients with MS (Monson et al., 2014). Furthermore, the concentration of IFN- γ , IL-17 and IL-6 in the CSF was also unchanged between the groups. There is a shift in the circulating lymphocytes of AD patients, with decreased levels of naïve T cells and a corresponding increase in effector memory or terminally-differentiated CD4 and CD8 cells compared with age-matched controls (Larbi et al., 2009; Pellicanò et al., 2012; Saresella et al., 2011; Schindowski et al., 2007; Speciale et al., 2007). Furthermore, T cells from AD patients have shorter telomeres than healthy controls, suggesting a possible deterioration of the immune system (Panossian et al., 2003).

Together the data suggest that, in AD patients, the adaptive immune system undergoes chronic stimulation, perhaps by A β , resulting in earlier differentiation of T cells to their mature counterparts, and possibly undergoing senescence. These changes can have negative consequences on T cell-mediated inflammation and interaction with APCs. If the immune system of AD patients shows signs of immunosenescence, it can also have implications on the ability of patients to effectively respond to and control infection.

1.7 Infection in AD

1.7.1 Infection in the elderly

It is estimated that 40% of the population in Europe will be over 60 years of age by 2050 (Lutz et al., 1997) and the increase in life expectancy is associated with an increase in age-related diseases (Westendorp, 2006). The elderly are more prone to infection due to changes in the immune system with age (Kovaiou et al., 2007), and are susceptible to viral or bacterial infections that affect the respiratory tract and urinary tract while morbidity due to influenza is also increased with age (Caljouw et al., 2013; Castle, 2000; Engelhart et al., 2005; Gardner et al., 2006). Infection in older adults can present atypically, be

asymptomatic or non-specific (Crossley and Peterson, 1996; Löppönen et al., 2004; Tal et al., 2002). A recent study has found that bacterial and viral infectious burden correlates with MMSE scores of 24 or lower (Katan et al., 2013) which can indicate dementia. It has also been reported that 36% of the elderly with dementia had an infection that was previously undiagnosed or unidentified, and which was associated with lower MMSE scores (Hodgson et al., 2011). Bacteriuria was the most prevalent, and it has been reported previously that urinary tract infections (UTIs) are among the most common infection in nursing home patients, many of whom have dementia (Boockvar and Lachs, 2003; Engelhart et al., 2005) and are often unable to communicate their symptoms and ailments (McCloskey, 2004). This situation is confounded by the fact that the bacteria which cause UTIs in this age group are often more resistant to antibiotic therapy (Linhares et al., 2013). Studies have indicated that infections in this group result in increased disability (Barker et al., 1998; Caljouw et al., 2013) or enhanced functional decline post-infection (Büla et al., 2004), with a positive correlation between the number of infections and functional impairment.

It has recently been suggested that cases of severe sepsis in the elderly results in lasting cognitive impairment (Widmann and Heneka, 2014). Indeed those over 65 years old admitted to hospital with infection were twice as likely to develop dementia and the risk was similar regardless of infection severity (i.e. Hazard ratio (HR): pneumonia, 2.24; sepsis, 2.28; infection: 1.98 in comparison to those never hospitalised with infection). On average, dementia developed 2 years after hospitalisation with pneumonia (Shah et al., 2013). Interestingly a greater proportion of those admitted to the hospital had cognitive decline and co-morbidities including diabetes and heart disease before infection occurred. In addition, Guerra and colleagues examined the development of dementia in patients over 66 years old who survived hospitalisation in the intensive care unit (ICU) and demonstrated that infection in ICU patients was associated with an increased risk of developing dementia within 3 years (HR 1.44 vs. ICU survivors who did not develop infection). Other factors that increased the risk of dementia included length of hospital stay (HR 1.7), and neurologic dysfunction during illness (HR 2.38) (Guerra et al., 2012). Age was also a significant factor, with 33%

of those over 85 years old developing dementia in the follow-up period after a stay in ICU in comparison with just 7% of those between 66-69 years old.

1.7.2 Infection in AD

A number of studies have indicated that AD patients are more vulnerable to the effects of systemic infection. Delirium, which is often caused by infection, is considered to be a risk factor for developing dementia (Jackson et al., 2004; MacLulich et al., 2009; Rahkonen et al., 2001; Rahkonen et al., 2000). In a recent study which examined individuals over a 10-year period, the incidence of delirium was associated with an 8-fold increase in developing dementia (odds ratio (OR) 8.7), where delirium also corresponded with a worsening of cognition in those already diagnosed with dementia (OR 3.1) (Davis et al., 2012). Incidents of delirium in AD patients also result in greater cognitive decline (Fick et al., 2002; Fong et al., 2009). It has been established that two or more infections over a 4-year period increased by 2-fold the risk of developing AD (Dunn et al., 2005) and increased viral burden or general ill-health has also been associated with development of AD (Strandberg et al., 2004; Tilvis et al., 2004). Patients with AD are more likely to need emergency hospitalisation than non-demented age-matched controls, and the incidence of lower respiratory tract infections, pneumonia or UTIs is greater (Natalwala et al., 2008).

In AD patients, a resolved peripheral infection was associated with a significant cognitive decline when assessed 2 months later and this was accompanied by elevated IL-1 β in the serum (Holmes et al., 2003). When examined over a 6-month period, a significant association was found between an increased rate of cognitive decline in AD patients with elevated TNF α in the serum after a peripheral infection (Holmes et al., 2009). The estimated survival time with dementia is between 3.9 and 7.1 years after onset (Fitzpatrick et al., 2005), however, an 8-year follow-up study on patients with dementia revealed pneumonia doubles the risk of mortality, and an increased number of co-morbidities corresponded with an increased mortality risk in dementia patients (Van Dijk et al., 1996). Furthermore, pneumonia is a common cause of death in

AD (Fitzpatrick et al., 2005). In contrast, a history of vaccination against a number of different infectious diseases, including influenza, was associated with a significantly decreased risk of developing AD (Tyas et al., 2001; Verreault et al., 2001). Oral daily antibiotic treatment for 3 months in AD patients has also been shown to slow cognitive decline when assessed 6 months later (Loeb et al., 2004).

1.7.3 *Chlamydia pneumoniae*

A number of bacterial and viral pathogens have been implicated in the development or progression of AD (Itzhaki et al., 2004) including *Chlamydia pneumoniae*, spirochetes and herpes simplex virus type 1 (HSV-1). A recent study found that viral or bacterial infectious burden (established using serologies for human cytomegalovirus (CMV), HSV-1, *Borrelia burgdorferi*, *C. pneumoniae* or *Helicobacter pylori*) was associated with AD, moreover, significantly more AD patients than aged-matched controls were positive for 4 or 5 pathogens which was also associated with increased A β and pro-inflammatory cytokines in the serum (Bu et al., 2014).

C. pneumoniae is a Gram-negative intracellular bacteria which causes respiratory infections, its presence in the AD brain was first observed post-mortem in 1998 (Balin et al., 1998) and confirmed in several studies subsequently (Balin et al., 2008; Gérard et al., 2006; Gérard et al., 2005). AD patients have increased seropositivity to *C. pneumoniae* (Bu et al., 2014) furthermore, a recent meta-analysis found *C. pneumoniae* is associated with a 5-fold increase in the incidence of AD (Maheshwari and Eslick, 2014). Astrocytes, microglia and neurons can be infected with *C. pneumoniae* and, in the AD brain, infected cells were found proximal to AD-like pathology, where the organisms were both viable and metabolically active (Gérard et al., 2006). In addition, patients with the *APOE4* allele had an increased bacterial burden than their *APOE4* negative counterparts (Gérard et al., 2005) especially in the hippocampus and frontal cortex. ApoE-lipoproteins are capable of binding and neutralising LPS (de Bont et al., 1999), which is a constituent of, and secreted by, Gram-negative

bacteria including *C. pneumonia* (Di Pietro et al., 2013). ApoE4 binds LPS less effectively than other ApoE isoforms (den Hartigh et al., 2012) which may provide a mechanism by which *APOE4* carriers are more vulnerable to the effects of bacterial infection. Indeed, mice with the *APOE4* gene have increased pro-inflammatory cytokines in the brain following systemic administration of LPS (Lynch et al., 2003).

In vitro studies using neuronal cells demonstrate that *C. pneumonia* can maintain a chronic infection by inhibiting apoptosis in the host cell (Appelt et al., 2008) and it is suggested that inhibition of apoptosis could prolong the *C. pneumonia* infection in AD and as a result, contribute to neuroinflammation. Animal studies have revealed that intranasal inoculation of mice with *C. pneumonia* induced AD-like changes in the brain, with evidence of deposits of fibrillar A β associated with reactive glia in several brain areas, including the hippocampus (Little et al., 2004).

1.7.4 *Helicobacter pylori*

H. pylori is a Gram-negative bacterium which has also been linked to AD. *H. pylori* seropositivity is associated with decreased cognitive function in older adults (Beydoun et al., 2013). AD patients were found to have a higher prevalence of *H. pylori* than controls in samples taken from the gastric mucous membrane (Kountouras et al., 2006). Similarly, high *H. pylori* IgG levels were observed in the serum and/or CSF of individuals with AD (Kountouras et al., 2009a; Malaguarnera et al., 2004). AD patients with a *H. pylori* infection were found to have lower MMSE scores, and increased CSF tau levels than non-infected AD patients (Roubaud-Baudron et al., 2012). Furthermore *H. pylori* infection was a significant risk factor for developing dementia in a 20 year follow-up study (Roubaud Baudron et al., 2013). Eradication of *H. pylori* infection in AD patients resulted in improved cognition when tested two years later, in comparison with MMSE scores for the same individuals previously positive for this bacterium, while AD patients who were still positive for *H. pylori* had further declined over the two year period (Kountouras et al., 2009b). Eradication of *H. pylori* also reduced the mortality rate of AD patients in a 5-year follow up study (Kountouras et al.,

2010). It has recently been demonstrated that injection of *H. pylori* filtrates into rats impaired their spatial learning and memory, and increased the concentration of A β ₄₂ in the brain which was associated with increased expression of PSEN-2 (Wang et al., 2014).

1.7.5 Spirochetes

Spirochetes are Gram-negative, neurotropic bacteria which can either be associated with a host or are free living. A range of studies have reported that spirochetes were detected in significantly more post-mortem brains of AD patients than controls (Miklossy, 1993, 2011; Miklossy et al., 1994; Riviere et al., 2002) and it has been found that infection with spirochetes is associated with a 10-fold increase in the incidence of AD (Maheshwari and Eslick, 2014). Periodontitis is a risk factor for the development of AD (Kamer et al., 2008), indeed many of the spirochetes found in the AD brain were of the *Treponema* species which are periodontal pathogens (Riviere et al., 2002) and co-infection with different *Treponema* species occurred in some AD patients. In addition, LPS from the periodontal pathogen *P. gingivalis* had recently been detected in the AD brain (Poole et al., 2013). *B. burgdorferi*, another periodontal pathogen, can be found in the AD brain (MacDonald, 2007; Miklossy, 1993; Miklossy et al., 2004; Riviere et al., 2002), where it was co-localised with A β plaques (Miklossy et al., 2004) and AD patients also have increased seropositivity to *B. burgdorferi* (Bu et al., 2014). *B. burgdorferi* has also been found to induce A β deposition *in vitro* (Miklossy et al., 2006). It has been suggested that spirochete neuroinvasion may occur in an effort to evade detection by the immune system in the periphery (Livengood and Gilmore, 2006; Urosevic and Martins, 2008). Together, these results show that bacteria can invade the brain, with serious consequences for the development of AD.

1.7.6 HSV-1 and CMV

Certain viral infections have been reported to be associated with CNS pathology. HSV-1 is often a lifelong infection of the nervous system and is usually present in

a latent form, though re-activation can occur. HSV-1 has been found in the brains of both AD patients and control subjects (Jamieson et al., 1991; Jamieson et al., 1992; Wozniak et al., 2005). However, viral deoxyribonucleic acid (DNA) was found in the brain areas most affected in AD, including the hippocampus (Jamieson et al., 1991; Jamieson et al., 1992). It has been suggested that HSV-1 might contribute to pathogenesis of AD by inducing inflammation in the areas most vulnerable in AD, particularly when present in combination with other risk factors, such as genetic susceptibility (Honjo et al., 2009). Indeed HSV-1 infection induces APP processing in neuronal cells *in vitro*, producing A β that was in part mediated by activation of β - and γ -secretases (De Chiara et al., 2010; Piacentini et al., 2011). HSV-1 is a risk factor for development of AD in carriers of the *APOE4* allele; the frequency for this allele is higher in the HSV-1 infected AD population than the non-infected AD patients (Itzhaki et al., 1997). *APOE4* increases susceptibility to HSV-1 infection, as a much higher viral load was observed in *APOE4*-expressing mice after infection (Burgos et al., 2003; Burgos et al., 2006). A possible explanation for the link between infection and *APOE4* carriers is evident from studies which revealed that HSV-1 outcompetes ApoE4 for binding to cell surface heparan sulphate proteoglycans (HSPG). This allows HSV-1 to bind to the cell and become internalized via endocytosis or fusing with the host cell membrane (Itzhaki and Wozniak, 2006; Itzhaki et al., 2004; WuDunn and Spear, 1989).

Like HSV-1, CMV is a latent lifelong infection, and this virus was recently reported to be linked with AD-pathology, specifically NFTs in the brain (Lurain et al., 2013). Furthermore, HSV-1 or CMV viral burden was associated with cognitive impairments in the elderly as assessed by decreased MMSE scores (Strandberg et al., 2004). A recent study has also found that CMV seropositivity was associated with an increased risk of developing AD and greater rate of cognitive decline in a 5-year follow-up study (Barnes et al., 2014). This is consistent with a report that found an association between CMV and progression to AD (Carbone et al., 2014). The frequency of CMV seropositivity is higher in AD patients (Bu et al., 2014), in addition, PBMCs from CMV⁺ AD patients have

increased reactivity and produced more IFN- γ after stimulation than PBMCs from CMV⁻ AD patients or CMV⁺ controls (Westman et al., 2014).

1.7.7 Infection in other neurodegenerative diseases

The role of systemic or peripheral infection in other neurodegenerative or neuroinflammatory diseases has been investigated. One-third of relapses in MS were associated with a systemic infection - typically respiratory tract infections (Buljevac et al., 2002; Buljevac et al., 2003; Sibley et al., 1985). Importantly, infection-induced relapses led to a more sustained deficit in patients with increased immune activation, which was not accompanied with changes in BBB permeability (Buljevac et al., 2002). This is consistent with studies in EAE, where staphylococcal enterotoxins (Schiffenbauer et al., 1993) or streptococcus pneumonia (Herrmann et al., 2006) aggravated clinical symptoms.

Up to one third of stroke patients were observed to have a pre-existing infection (Emsley and Hopkins, 2008), with an association between infection and poor stroke outcome (Dénes et al., 2010; Muhammad et al., 2011). It has also been suggested that chronic infection with specific pathogens, including *C. pneumonia* or *H. pylori* increase the risk of stroke (Grau et al., 2010). Indeed the risk of having a stroke is highest in the first 3 days post onset of infection, and the infection-induced risk lasts for up to 3 months (Clayton et al., 2008; Smeeth et al., 2004).

1.7.8 Animal models of systemic challenge

A number of animal studies have investigated the influence of a systemic challenge on the CNS. A single intraperitoneal (i.p.) LPS injection induced activation of microglia and TNF α production in the CNS, and upregulation of these markers was evident 10 months post-injection (Qin et al., 2007). Furthermore, neurodegeneration of dopaminergic neurons was also apparent 7-10 months after this single injection. It has recently been reported that LPS injected i.p. enhanced production of IL-6 in the brains of APP^{swe} mice, which

was associated with enhanced sickness behaviour and significantly increased BBB leakage (Takeda et al., 2013). Daily systemic LPS for 7 days induced amyloid deposition in the brain (Lee et al., 2008) and LPS administered weekly for 12 weeks in APP^{swe} mice increased APP expression and processing (Sheng et al., 2003), while LPS twice a week for 6 weeks in 3xTg-AD mice enhanced Tau tangle pathology (Kitazawa et al., 2005). LPS can also induce robust changes in the brain in Tg2576 and WT mice (Erickson and Banks, 2011; Sly et al., 2001). The concentrations of LPS used throughout these studies is quite variable, however, they suggest that a peripheral stimulus can have a considerable impact on the CNS. Similar to the studies with LPS, systemic injections of polyinosinic-polycytidylic acid (poly I:C) predisposes WT mice to develop AD pathology when injected during gestation, while injection in 3xTg-AD mice at 4 months enhanced A β deposition accompanied by neurodegeneration, characterised by dystrophic neurites, 11 months later (Krstic et al., 2012).

1.7.9 Other animal models of infection

A limited number of studies have examined the impact of other infectious pathogens in animal models of AD. Infection of 3xTg-AD mice with mouse hepatitis virus (MHV) induced marked tau pathology post-infection (Sy et al., 2011). However, infection of Tg2576 mice with streptococcus pneumonia 3 times over a 3 month period had no effect on the course of neurodegenerative disease, though importantly the mice were given antibiotics 12 hours post-infection, thus limiting the impact of infection (Ebert et al., 2010).

It is important to note that an infection which has a strong anti-inflammatory component may even be beneficial in AD, and it has recently been shown that infection of Tg2576 mice with *Toxoplasma gondii* at 3 months (which induced IL-10 and TGF- β) resulted in lower amyloid pathology 6 months post-infection (Jung et al., 2012).

1.7.10 *Bordetella pertussis*

Bordetella pertussis is a Gram-negative bacteria that causes whooping cough. While traditionally considered to be a strictly childhood disease, the incidence of *B. pertussis* is increasing worldwide and of significant concern is the finding that the incidence of *B. pertussis* is increasing in adults (Klein et al., 2012; McGuinness et al., 2013), and particularly those over 65 (Weston et al., 2012). It is estimated that 16 million people were infected in 2008 (Black et al., 2010) with recent outbreaks described in America, Australia and even Ireland ((CDC), 2012; Barret et al., 2010; Cherry, 2012; Roper and Surveillance Branch, 2009). In 1991 there were just 2,719 cases of *B. pertussis* in the US, which is in stark contrast to the 48,277 cases reported in 2012 (<http://www.cdc.gov/pertussis/fast-facts.html>). Adults over the age of 20 constituted 21.6% of these cases, and 10% of reported deaths from pertussis occurred in adults over 55 years of age. Adults, particularly the elderly, are at risk of developing *B. pertussis*-induced complications including pneumonia and can require hospitalisation (Cortese et al., 2007). It has been suggested that the incidence of *B. pertussis* is under-reported due to the absence of “classic” symptoms in adults such as the inspiratory whoop (Cortese et al., 2007). The increasing incidence of *B. pertussis* may be due to increased detection methods, but also due to the short lived immunity generated from the newer acellular pertussis vaccine (Pa), which replaced the whole cell pertussis vaccine (Pw) approximately 20 years ago, as the latter was very reactogenic (Mills et al., 2014).

B. pertussis secrete many virulence factors, such as pertussis toxin (PT), pertactin, LPS and tracheal cytotoxin (TCT), some of which bind to TLRs and NLRs (Fig 1.10). Studies in mice have revealed that IFN- γ is required for clearance of the bacteria from the lungs (Barbic et al., 1997; Mahon et al., 1997), though a role for IL-17 has also been established (Higgins et al., 2006; Ross et al., 2013). However, in an effort to subvert the host’s immune response, filamentous hemagglutinin (FHA) and adenylate cyclase toxin (ACT) produced by *B. pertussis* induces IL-10 and Treg cells which contribute to the persistent infection, though may also protect the host by limiting infection induced pathology (Higgins et al.,

2003). As a result, infection in mouse models typically takes 35 days to clear (McGuirk et al., 1998), and can last from weeks up to 4 or 5 months in humans (Cortese et al., 2007; McGuinness et al., 2013).

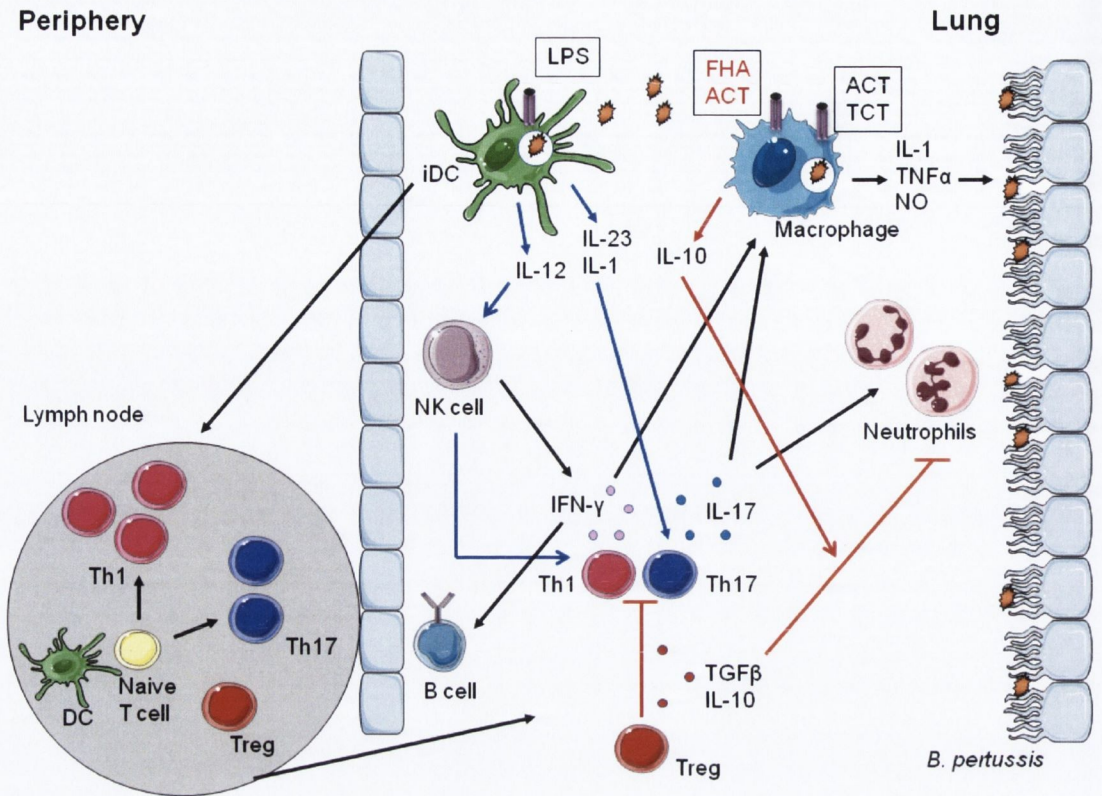


Figure 1.10 Innate and adaptive immune responses to infection with *B. pertussis*

On infection, *B. pertussis* binds to the cilia of the trachea, bronchi, and bronchioles and can be phagocytosed by resident macrophages and immature DCs within the lung. Early in disease further recruitment and infiltration of DCs and macrophages occurs, followed by NK cells and neutrophils. DCs migrate to the draining lymph node and present Ag to Ag-specific T cells, inducing activation of the adaptive immune response. Infiltration of $CD4^+$ and $CD8^+$ T cells occur in later stages of infection. $IFN-\gamma$ production by NK cells, and Th1 cells recruits and activates macrophages and neutrophils into killing *B. pertussis* via nitric oxide (NO) or reactive oxygen species. $IFN-\gamma$ also facilitates antibody secretion by B cells, opsonising the bacteria and targeting them for phagocytosis. In addition, IL-17 triggers neutrophil recruitment and activation. *B. pertussis* also produces a range of virulence factors, with pro- and anti-inflammatory effects. Lipopolysaccharide (LPS), adenylate cyclase toxin (ACT) and tracheal cytotoxin (TCT) induce pro-inflammatory cytokines that shape the adaptive immune response and facilitate removal of bacteria, but can also induce local lung pathology. However, filamentous hemagglutinin (FHA) and ACT induce IL-10 production by DCs and macrophages, and IL-10-producing Treg cells which together can inhibit the T cell response and limit infection induced pathology. Blue arrows represent cytokine production which shapes the inflammatory adaptive immune response; black arrows, effector/inflammatory immune response; red arrows, suppressive, anti-inflammatory responses. Figure adapted from Higgs et al., 2012.

1.8 Study aims

The aims of these studies were:

To examine the impact of Th1, Th2 and Th17 cells on glial activation *in vitro* and *in vivo* by transferring A β -specific Th1 cells into APP/PS1 and non-transgenic mice.

To investigate the influence of a peripheral infection with the respiratory pathogen *B. pertussis* on AD-like pathology in APP/PS1 mice, and to assess whether there was an age-related susceptibility to infection induced changes.

To determine whether chronic treatment with FTY720, which induces lymphocyte sequestration, impairs the ability of mice to resolve infection with *B. pertussis*.

To establish the effect of suppressing T cell migration into the brains of APP/PS1 mice by treating mice with FTY720 during infection with *B. pertussis*, and to examine whether this altered any infection-induced AD-pathology.

Chapter 2

Materials and Methods

2.1 Animals

APP^{swe}/PS1^{dE9} mice on a C57BL/6 background were obtained from the Jackson Laboratory, US and bred in a specific pathogen free unit in the Bioresources Unit, Trinity College Dublin. APP/PS1 mice and nontransgenic WT littermates were either 4 or 10 months old at onset of experiment. C57BL/6 mice (8 weeks old) were purchased from Harlan Laboratories, UK. GFP mice were on a C57BL/6 background, expressing GFP complementary DNA (cDNA) under a chicken β -actin promoter and CMV enhancer and were a gift from Matthew Campbell, School of Genetics and Microbiology. GFP mice were 6 months old when used for experimentation. All mice were maintained in groups under veterinary supervision and housed in individually ventilated cages under controlled conditions. The temperature was maintained at 22°–23°C with 12 h light-dark cycle, food (normal laboratory chow) and water was available *ad libitum*, and experimentation was carried out under a license granted by the Minister for Health and Children (Ireland) and with the appropriate ethical approval.

2.2 Genotyping APP/PS1 mice

2.2.1 Isolation of DNA

Ear punches or tail snips were taken from APP/PS1 mice and their WT littermates and either used directly or stored at -20°C until required. The DNA was isolated using a DNeasy[®] blood and tissue kit (Qiagen, US) which supplied all buffers necessary for the isolation. Tail snips (0.5 cm) or ear punches were placed in DNase/RNase free 1.5 ml Eppendorf tubes (Sarstedt, Germany) with buffer ATL (180 μ l) and Proteinase K (20 μ l) before overnight incubation at 56°C. Tubes were vortexed and buffer AL (200 μ l) was added. Samples were vortexed before addition of ethanol (96-100%; 200 μ l; Sigma-Aldrich, UK). The mixture was transferred to DNeasy Mini spin columns in 2 ml collection tubes which were centrifuged at 6,000 x g for 1 min at room temperature (RT). Flow through and collection tubes were discarded, the DNeasy Mini spin column was placed in a new 2 ml collection tube. Buffer AW1 (500 μ l) was added and samples

centrifuged for 1 min at 6,000 x g. The column was placed in a new 2 ml collection tube and buffer AW2 (500 µl) was added. The tubes were centrifuged at 20,000 x g for 3 min. The column was placed in a DNase/RNase free 1.5 ml microcentrifuge tube, and buffer AE was added directly onto the DNeasy membrane (100 µl). After 1 min incubation at RT, the tubes were centrifuged for 1 min at 6,000 x g to elute the DNA. DNA concentrations were quantified using a NanoDrop Spectrophotometer (ND-1000 v3.5, NanoDrop Technologies Inc., US).

2.2.2 Polymerase chain reaction (PCR) and identification of APP^{swe} and PSEN1^{dE9} genes

The presence of APP^{swe} and PSEN1^{dE9} genes was assessed using PCR. As a positive control, the expression of the prion gene was also assessed. Separate PCRs were carried out for each target gene. The mastermix was prepared to contain the following per sample: 1 µl of the forward primer (final concentration 0.5 µM; primer summary Table 2.1), 1 µl of the reverse primer (final concentration 0.5 µM; primer summary Table 2.1), 12.5 µl Go Taq[®] qPCR Mastermix (Promega; US) and 5.5 µl H₂O. DNA (5 µl of a 1 ng/µl solution) and the mastermix was added to new reaction tubes and placed in a thermocycler (MJ Research Peltier Thermal Cycler-200, Biosciences, Ireland). The amplification process was as follows: stage 1, 94°C for 3 min; stage 2, 94°C for 30 sec (denaturing step); stage 3, 52°C for 1 min (annealing step); stage 4, 72°C for 1 min (extension step); stage 5, repeat 2-4 for 35 cycles of amplification; stage 6, final extension step, 72°C for 2 min to ensure complete extension of PCR products.

A 1% (w/v) agarose gel (Life Technologies, Ireland) containing gel red (1:10,000 dilution; Biotium, US) was prepared, the samples (5 µl) and a 100 base pair (bp) ladder (5 µl; Promega; US) were loaded into individual wells. The samples were separated by application of 120 volts for 45 min. PCR products were visualized under an ultraviolet light and photographed using an ultraviolet transilluminator (Labworks Ultra Violet, Bioimaging Systems, US). APP/PS1 mice

were identified as having both the APP^{swe} and PSEN1^{dE9} genes, whereas WT mice had neither.

Table 2.1 Primers used for DNA amplification

Target	Primer Sequence	Size (bp)
APP^{swe} forward:	5'-AGGACTGACCACTCGACCAG-3'	377 bp product
APP^{swe} reverse:	5'-CGGGGGTCTAGTTCTGCAT-3'	
PSEN1^{dE9} forward:	5'-AATAGAGAACGGCAGGAGCA-3'	608 bp product
PSEN1^{dE9} reverse:	5'-GCCATGAGGGCACTAATCAT-3'	
Prion forward:	5'-CTAGGCCACAGAATTGAAAGATCT-3'	324 bp product
Prion reverse:	5'-GTAGGTGGAAATTCTAGCATCATCC-3'	

2.3 Generation of A β -specific T cell lines and *in vivo* transfer

Amyloid β_{1-42} (A β_{1-42} ; Life Technologies) was dissolved in high-performance liquid chromatography (HPLC)-grade water to provide a 12 mg/ml stock solution. It was diluted to 2 mg/ml using sterile phosphate buffered saline (PBS) and allowed to aggregate for 48 h at 37°C while it was agitated at 200 rpm. A β_{1-42} was used immediately or stored at -20°C. GFP mice were injected subcutaneously (s.c.) into the rear footpad with A β_{1-42} (75 μ g/mouse) and CpG (25 μ g/mouse) in a total volume of 50 μ l i.e. 25 μ l per foot. The mice were boosted after 21 days with A β_{1-42} (75 μ g/mouse) and CpG (25 μ g/mouse; Sigma-Genosys). After a further 7 days the draining popliteal lymph nodes and spleens were harvested. Lymph node and spleen tissue was dissociated through a sterile 70 μ m nylon mesh filter (Thermo Fisher Scientific, Ireland), washed with Roswell Park Memorial Institute solution (RPMI; Sigma-Aldrich, UK) supplemented with 1% penicillin-streptomycin, 1% L-glutamine and 10% fetal bovine serum (FBS) (Sigma-Aldrich, UK) and centrifuged at 1,200 rpm for 5 min. A cell count was performed and the cells were restimulated *ex vivo* at 2×10^6 cells per ml with

A β ₁₋₄₂ (25 μ g/ml) and IL-12 (10 ng/ml) to produce Th1 cells. After 4 days, IL-2 (5 ng/ml) was added and incubation continued for a further 7 days.

Cells were washed with complete RPMI, centrifuged at 1,200 rpm for 5 min and counted. Cells were injected i.v. into the tail vein of recipient mice at a concentration of 15×10^6 cells/mouse in 100 μ l PBS. Control mice were injected with 100 μ l PBS alone. The mice were perfused and culled, as described in section 2.7, after 14 days to assess migration of GFP⁺ cells into the brain or after 21 days to investigate changes in A β deposition.

2.4 B. pertussis respiratory challenge

B. pertussis infection of C57BL/6 or WT and APP/PS1 mice was induced by aerosol challenge as described (McGuirk et al., 1998). *B. pertussis* Wellcome 28 was streaked onto Bordet-Gengou agar plates and grown at 37°C for 4 days; bacteria were transferred to Stainer-Scholte liquid medium for 24 h at 37°C. Bacteria were resuspended at 1.7×10^{10} colony forming units (CFU)/ml in physiological saline containing 1% casein and administered by aerosol challenge over a period of 15 min using a nebulizer. This was followed by a rest period of 10 min before returning the mice to their cages. In a separate series of experiments, the bacteria were resuspended at 5×10^8 CFU/ml and administered by aerosol challenge over a period of 10 min using a different nebulizer (PARI GmbH, Germany), followed by a rest period of 10 min before returning to cages. Preliminary experimentation verified that infection with the different concentrations (i.e. 1.7×10^{10} or 5×10^8 CFU/ml) in the two different nebulizers produced similar bacterial loads in the lungs. Infection with the pathogen was confirmed by performing CFU counts on the lungs of mice at various time points post-infection. The lungs were aseptically removed and homogenized in 1 ml of sterile 1% casein on ice. Undiluted and serially-diluted lung homogenate was spread onto Bordet-Gengou agar plates, and the CFU was established after 5 days of incubation at 37°C. APP/PS1 mice and WT littermates were 4 or 10 months old on challenge with *B. pertussis* to investigate the effect of infection on the initial plaque development, or the period when plaques and

neuroinflammation was already apparent in this model. Mice were culled after 56 days (Chapter 4) or 70 days (Chapter 6) unless otherwise stated, as a result, mice were either 6 months or 12 months old at cull.

2.5 Immunization of mice against *B. pertussis*

Mice were immunised against *B. pertussis* using Pw (whole cell *B. pertussis* 41S, NIBSC, UK) or Pa (Infanrix®-IPV, GSK, Ireland). Mice were immunised i.p. with 1/50th of the human dose (100 µl/mouse) on day 0. A second (booster) immunization was administered on day 28. Treatment with FTY720 began on day 35, 7 days after the second immunization (as described in 2.6). Finally, on day 45 mice were infected with *B. pertussis* as described in 2.4.

2.6 FTY720 administration

C57BL/6 or WT and APP/PS1 mice received FTY720 (Santa-Cruz Biotechnology, US) daily in their drinking water at a concentration of 0.3 mg/kg. Control mice received untreated water only. Treatment with FTY720 began either 3 or 10 days before infection with *B. pertussis*, and continued daily for the duration of the experiment.

2.7 Isolation of mononuclear cells from tissue

2.7.1 Isolation of mononuclear cells from CNS tissue

APP/PS1 mice and nontransgenic littermates were anaesthetised with sodium pentobarbital (40 µl; Euthatal, Merial Animal Health, UK) and perfused intracardially with sterile ice-cold PBS (20 ml). The brain was removed and placed in complete RPMI solution. A single-cell suspension was prepared by passing the whole (i.e. not yet dissociated) brain tissue through a sterile 70 µm nylon mesh filter, washed with complete RPMI solution and centrifuged at 1,200 rpm for 5 min. The supernatant was removed and the remaining pellet was resuspended in complete RPMI (2 ml) containing collagenase D (1 mg/ml, Roche, Ireland) and

DNase I (10 µg/ml, Sigma-Aldrich, UK), and incubated for 1 h at 37°C with agitation. Cells were washed in complete RPMI and centrifuged at 1,200 rpm for 5 min. The supernatants were discarded and cells were resuspended in 1.088 g/ml Percoll (9 ml; Sigma-Aldrich, UK). This solution was underlayered with 1.122 g/ml Percoll (5 ml) and overlaid with 1.072 g/ml Percoll (9 ml), 1.030 g/ml Percoll (9 ml) and PBS (9 ml). Samples were centrifuged at 1,250 x g for 45 min. Mononuclear cells were removed from the 1.088:1.072 and 1.072:1.030 g/ml interfaces as described in Figure 2.1, washed twice in complete RPMI and counted.

2.7.2 Isolation of cells from lung tissue

C57BL/6 mice were euthanized with CO₂, the lung was aseptically removed and placed in 1% casein. The lung tissue was chopped bi-directionally and incubated in Hanks Balanced Salt Solution (HBSS; 1 ml, Sigma-Aldrich, UK) containing collagenase D (1 mg/ml) and DNase I (10 µg/ml) for 1 h at 37°C with agitation. A single cell suspension was prepared by passing the tissue through a sterile 70 µm nylon mesh filter, washed with complete RPMI and counted.

2.7.3 Isolation of cells from lymph node tissue

The mediastinal lymph node was removed, passed through a sterile 70 µm nylon mesh filter, and a cell count was performed.

2.7.4 Flow cytometric analysis on cells prepared ex vivo

Cell samples which were intended for intracellular staining to identify T cell subsets were centrifuged at 1,200 rpm for 5 min and cells were incubated in the presence of phorbol myristate acetate (PMA; 10 ng/ml; Sigma-Aldrich, UK), ionomycin (1 µg/ml; Sigma-Aldrich, UK) and brefeldin A (BFA; 5 µg/ml; Sigma-Aldrich, UK) for 5 h in complete RPMI at 37°C. Cells were centrifuged at 1,200 rpm for 5 min, resuspended in 50 µl PBS with 1:1000 LIVE/DEAD® Fixable Aqua Dead Cell Stain kit (Life Technologies, Ireland) for 20 min, washed with PBS, and resuspended in 50 µl fluorescence activated cell sorting (FACS) buffer (2% bovine

serum albumin (BSA) in PBS) containing CD16/CD32 FcγRIII (1:100) for 10 min to block low-affinity IgG receptors and thus prevent non-specific binding of antibodies. Cells were prepared for intracellular staining using a cell permeabilisation kit (Dako, Denmark). For surface labelling, cells were incubated in FACS buffer (50 µl/sample) containing the appropriate antibodies (CD45, CD3, CD4, CD8 and either CD49b or NK1.1; Table 2.1 for details) for 15 min at RT at a 1:100 dilution. Samples were fixed using IntraStain Reagent A (50 µl/sample; Dako, Denmark) or 2% paraformaldehyde (PFA; 50 µl/sample; Thermo Fisher Scientific, Ireland) for 15 min at RT, washed twice with FACS buffer, centrifuged at 1,200 rpm for 5 min and permeabilised with IntraStain Reagent B (50 µl/sample; Dako, Denmark) or 0.5% saponin (50 µl/sample; Sigma-Aldrich, UK) including intracellular antibodies (IFN-γ and IL-17A; Table 2.2 for details) for 15 min at RT in the dark. The cells were washed twice in FACS buffer and centrifuged at 1,200 rpm for 5 min. The appropriate compensation controls and fluorescence minus one (FMO) controls were also prepared during this time.

In separate FACS tubes, mononuclear cells from the CNS, which were not stimulated with PMA, ionomycin or BFA, were surface-stained to identify macrophage and microglial cells. These samples were blocked for 10 min with CD16/CD32 FcγRIII (1:100) to prevent non-specific low-affinity IgG receptors which are expressed on a range of cell types including APCs. Cells were incubated with the cell surface antibodies for 15 min (CD45, CD11b, CD80 and CD68; Table 2.2 for details) at a 1:100 dilution washed twice in FACS buffer and centrifuged at 1,200 rpm for 5 min. Propidium iodide (PI; Sigma-Aldrich, UK) was added (1:100) immediately before reading the samples and was used as a live/dead stain. The appropriate compensation controls and FMO controls were also prepared.

During infection of C57BL/6 mice with *B. pertussis*, mononuclear cells were stained to identify infiltrating CD4⁺, CD8⁺ and γδ⁺ T cells, B cells, NK cells and NKT cells into the lung, or expansion of immune cells in the mediastinal lymph node. These cells were divided and a proportion of the T cells were stained with CD44 and CD62L to identify naïve, central memory and effector memory subsets, while a separate group of cells were stimulated with PMA,

ionomycin and BFA for 5 h at 37°C before intracellular cytokine staining for IFN- γ and IL-17 as described above.

Flow cytometric analysis was performed on an LSR Fortessa (BD Biosciences, UK; Table 2.3 for details), and data acquired using Summit software (Dako, Denmark). The results were analysed using FlowJo software (Tree Star, US). T cells from the brain were identified as being negative for LIVE/DEAD[®] Fixable Aqua Dead Cell Stain, CD45⁺ and CD3⁺. T helper cells were identified as CD45⁺CD3⁺CD4⁺ cells, whereas cytotoxic T cells were identified as CD45⁺CD3⁺CD8⁺ cells. NKT cells were identified as CD45⁺CD3⁺NK1.1⁺ or CD3⁺CD49b⁺. In cells prepared from the brain, microglia were identified as CD11b⁺CD45^{low} cells and macrophages were identified as CD11b⁺CD45^{high} cells, according to criteria used in previous reports (Becher and Antel, 1996; Sedgwick et al., 1991) though a CD11b⁺CD45^{low/medium} population of microglial cells has been observed (Dick et al., 1997). In this study CD45, expression was found to be either high or low on the CD11b⁺ cells.

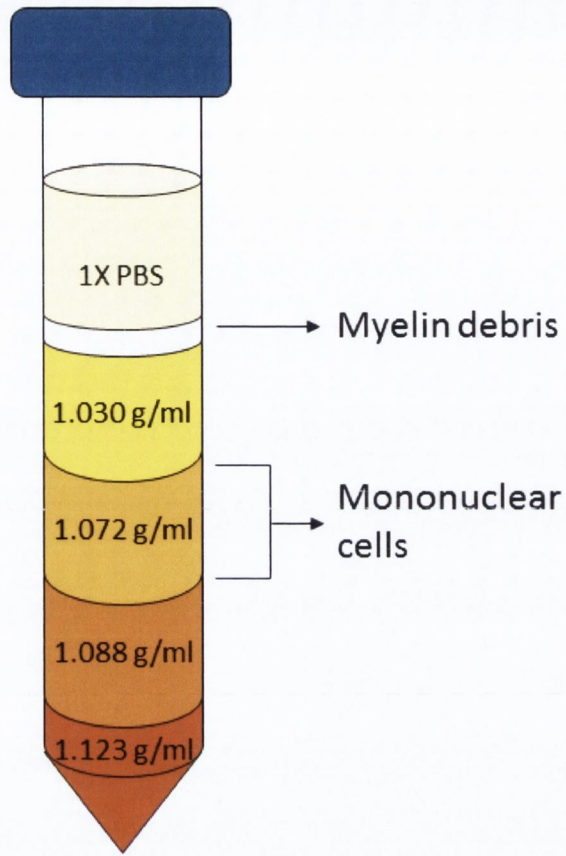


Figure 2.1 Percoll separation to isolate mononuclear cells from the CNS

Schematic representing the Percoll separation of cells. Shading is representative and does not reflect actual colour of Percoll layers, which are transparent. Mononuclear cells were obtained from the 1.088:1.072 and 1.072:1.030 g/ml interfaces, and the myelin debris was located at the 1.030 g/ml:PBS interface.

Table 2.2 Antibodies used in flow cytometry

FACS Antibody	Fluorescent Label	Dilution Factor	Supplier
B220	eFluor 605 NC	1/200	eBioscience
CD11b	A780	1/100	eBioscience
CD19	FITC, eFluor 450	1/400-600	eBioscience, BD Biosciences
CD3	APC, A780	1/100	BD Biosciences, eBioscience
CD4	A700	1/100	BD Biosciences, eBioscience
CD40	PE	1/100	BD Biosciences
CD44	PeCy7, eFluor 605 NC	1/100-200	eBioscience
CD45	eFluor 605 NC	1/100	eBioscience
CD49b	APC	1/200	eBioscience
CD49d	eF710	1/50	eBioscience
CD62L	PE-CF594	1/200	BD Biosciences
CD68	A488	1/100	AbD Serotec
CD8	A780, PeCy7, PE	1/100-600	eBioscience
CD80	V450	1/100	BD Biosciences
IFN-γ	PeCy7, PE-CF594	1/50-200	BD Biosciences
IL-17	V450, eFluor 450, FITC	1/50-400	BD Biosciences, eBioscience
LIVE/DEAD	Aqua	1/1000	Life Technologies
NK1.1	PerCPCy5.5	1/100	eBioscience
PI	PI	1/100	Sigma-Aldrich
$\gamma\delta$	PE-Cy5.5, APC	1/100-200	eBioscience

Table 2.3 LSR Fortessa

Fluorescent labels and filters for the 488nm, 633nm, 405nm and 551nm lasers.

(Laser) Filter	Channel	Fluorochrome
(488) 530/30	FL1	FITC, A 488, GFP
(488) 695/40	FL2	PerCP, PerCP-Cy5.5, PerCP-eFluor 710
(633) 670/30	FL3	APC, A 647, eFluor 660
(633) 730/45	FL4	A700
(633) 780/60	FL5	APC-Cy7, APC-H7, A780, APC-eFluor 780, APC-Vio 770
(405) 450/50	FL6	Brill Vio 421, V450, eF450, Pac Blue, Cell Trace Violet
(405) 525/50	FL7	Brill Vio 510, V500, Live/Dead Aqua, Qdot 525
(405) 610/20	FL8	Brill Vio 605, eFluor 605 NC, Qdot 605
(405) 660/20	FL9	Brill Vio 650, Qdot 655
(405) 710/50	FL10	Brill Vio 711, Qdot 705
(405) 780/60	FL11	Brill Vio 785, Qdot 800
(561) 582/15	FL12	PE
(561) 610/20	FL13	PI, PE-CF594, PE-TexasRed, PE-eFluor 610
(561) 670/30	FL14	PE-Cy5
(561) 710/50	FL15	PE-Cy5.5
(561) 780/60	FL16	PE-Cy7, PE-Alexa 750, PE-Vio 770

2.8 Preparation of tissue from mice

At the termination of the experiment, APP/PS1 and WT mice were anaesthetised with sodium pentobarbital (40 μ l; Euthatal, Merial Animal Health, UK) and perfused intracardially with ice-cold PBS (20 ml). The brains were rapidly removed and hemisected. A sagittal section of the brain was taken for immunohistochemical analysis, placed onto cork discs, covered with optimum cooling temperature compound (OCT) (Sakura Tissue- Tek, Netherlands), snap-frozen in isopropanol on dry ice and stored at -80°C . Cortical tissue was snap-frozen in liquid nitrogen and stored at -80°C for analysis of A β and cortical tissue was also snap-frozen for later mRNA analysis. The remaining brain tissue, which included the cortex and hippocampus, was used to prepare mononuclear cells for flow cytometric analysis as described in section 2.7.

2.9 Detection of A β

Snap-frozen cortical tissue was homogenised in 50mM sodium chloride (NaCl; pH 10) with 1% sodium dodecyl sulphate (SDS; Sigma-Aldrich) plus protease inhibitors which had a broad specificity for serine, cysteine, and acid proteases, and aminopeptidases (1:100, Sigma-Aldrich, UK) and centrifuged at 15,000 rpm for 40 min at 4°C . The supernatant, which was used for analysis of soluble A β , was taken and protein concentration assessed as described in 2.10. The samples were equalised to either 4 mg/ml or 5 mg/ml total protein using the homogenising buffer with 10X neutralising buffer (0.5M Tris/HCL, pH 6.8) with a final volume of 30 μ l per sample and stored at -20°C . For analysis of insoluble A β , the pellets were incubated in guanidine buffer (200 μ l; 5 M guanidine-HCl/50 mM Tris-HCl, pH 8, Sigma-Aldrich, UK) plus protease inhibitors (1:100) for 4 h at RT with agitation. Samples were centrifuged at 15,000 rpm for 30 min at 4°C and the supernatant samples were equalised to 0.1 mg/ml with guanidine buffer with a final volume of 30 μ l and stored at -20°C . Soluble and insoluble A β was assessed using "MSD[®] 96-well multi-spot 4G8 A β triple ultra-sensitive assay" kits according to the manufacturer's instructions (Meso Scale Discovery, US). Plates were blocked with 1% Blocker A (in 1X Tris Buffer; 150 μ l/well) for 1 h at RT with

vigorous shaking (300-1000 rpm). Plates were washed three times in 1X Tris wash buffer, and detection antibody solution was added (25 μ l/well; 60 μ l 50X SULFO-TAG 4G8 detection antibody, 30 μ l 100X Blocker G in 2910 μ l 1% Blocker A/1X Tris buffer). Standards were prepared by serial dilutions of recombinant human A β protein in 1% Blocker A/1X Tris buffer (A β ₁₋₃₈, 0-3,000 pg/ml; A β ₁₋₄₀, 0-10,000 pg/ml; A β ₁₋₄₂, 0-3,000 pg/ml). The soluble protein fraction was further diluted 1:30 using 1% Blocker A/1X Tris buffer, whereas the insoluble protein fraction was diluted a further 1:100 with 1% Blocker A/1X Tris buffer. Samples and standards were added to the 96-well plates (25 μ l/well), incubated for 2 h at RT with vigorous shaking, washed three times with 1X Tris buffer, and read in a Sector Imager plate reader (Meso Scale Discovery, US) immediately after addition of the 2X MSD read buffer (150 μ l/well). A β concentrations were calculated with reference to the standard curves and expressed as pg/ml.

In a separate series of experiments, soluble and insoluble A β was assessed using “MSD® A β peptide Panel 1 (4G8) V-PLEX” kits according to the manufacturer’s instructions (Meso Scale Discovery, US) as the previous kits were no longer commercially available. Plates were blocked with Diluent 35 (150 μ l/well) for 1 h at RT with vigorous shaking (300-1000 rpm). The plates were washed three times in 0.05% Tween-20 (Sigma-Aldrich) in PBS, and detection antibody solution was added (25 μ l/well; 60 μ l 50X SULFO-TAG anti-A β antibody, 30 μ l of A β ₄₀ blocker in 2910 μ l Diluent 100). Standards were prepared by serial dilutions of recombinant human A β protein in Diluent 35 (A β ₁₋₃₈, 0-10,675 pg/ml; A β ₁₋₄₀, 0-14,950 pg/ml; A β ₁₋₄₂, 0-1,333 pg/ml). The soluble protein fraction was further diluted 1:30 using Diluent 35, whereas the insoluble protein fraction was diluted a further 1:200 with Diluent 35. Samples and standards were added to the 96-well plates (25 μ l/well), incubated for 2 h at RT with vigorous shaking, washed three times with 0.05% Tween-20 in PBS, and read in a Sector Imager plate reader (Meso Scale Discovery, US) immediately after addition of the 2X MSD read buffer (150 μ l/well). A β concentrations were calculated with reference to the standard curves and expressed as pg/ml, however the data generated by Dr Keith McQuillan which appear in Fig 3.17 are expressed as pg/mg.

2.10 Protein quantification

Cortical tissue was homogenised in 50mM NaCl (pH 10) with 1% SDS plus protease inhibitors (1:100; as described in section 2.9). The protein concentrations were assessed using bicinchoninic acid (BCA) protein assay kit (Thermo Fisher Scientific, Ireland). Standards (0 mg/ml-1 mg/ml; BSA), and samples (diluted 1:5-50 as appropriate) were added to the 96-well plate in duplicate (25 µl/well). Pierce BCA reagent (200 µl/well; 1:50 Reagent B to Reagent A) was added to the plate and samples were incubated for 30 minutes at 37°C. The optical density was determined by measuring the absorbance at 562nm. Protein concentrations were calculated relative to the standard curve and were equalised in samples using the appropriate homogenisation buffer for the soluble and insoluble protein fractions, described in section 2.9.

2.11 Immunohistochemical analysis

2.11.1 Coating of glass slides

Glass slides (Thermo Fisher Scientific, Ireland) were coated prior to sectioning of tissue to ensure the tissue would adhere to the slide. Gelatine (2.5 g; Fluka, Switzerland) was dissolved in 500 ml dH₂O and heated. Chromium potassium sulphate (0.25 g; Sigma-Aldrich, UK) was added and solution heated to 60°C. The subbing solution was filtered through Whatman filter paper (Whatman International, UK) and clean glass slides were incubated in this solution for 1 min. Slides were removed and allowed to dry overnight.

2.11.2 Preparation of tissue sections for immunohistochemistry

The tissue was allowed to equilibrate to -20°C for 2 h prior to sectioning. Sagittal sections (10 µm thick) were prepared on the cryostat (Leica, Meyer, UK) and mounted on gelatine-coated glass slides (Fluka, Switzerland). This resulted in 3-4 sections per slide, and as the sections were not placed on the slides consecutively, each section on the slide represented a different part of the brain

tissue. The slides were allowed to dry for 20 min and stored at -20°C for later immunohistochemical analysis.

2.11.3 Congo red identification of amyloid plaques

Sections, which were allowed to equilibrate to RT for 30 min, were fixed in ice-cold methanol for 5 min, washed in PBS and incubated at RT for 20 min in saturated NaCl (200 ml; 80% ethanol in dH₂O) supplemented with sodium hydroxide (NaOH, 2 ml; 1 M). Sections were incubated in filtered Congo red solution (200 ml; 0.2% Congo red dye in saturated NaCl solution with 2 ml NaOH; 1 M; Sigma-Aldrich) for 30 min and rinsed in dH₂O. The slides were incubated in methyl green solution (1% in dH₂O; Sigma-Aldrich) for 30 sec, washed and dehydrated by dipping in 95%, 100% and 100% ethanol. Sections were dried, incubated in 100% xylene (3 x 5 min; Sigma-Aldrich) and mounted using dibutyl phthalate in xylene (DPX; RA Lamb, UK). Slides were allowed to dry overnight, stored at RT and later examined using an Olympus Ix51 light microscope (Olympus, Tokyo, Japan). Micrographs were taken using an Olympus UCMAD3 (Japan) at 10x magnification. Congo red plaques were quantified by counting the number of plaques per area of interest and averaging 3-8 sections (i.e. 1 or 2 slides containing 3-4 sections each) per mouse.

2.11.4 Fibrinogen staining

Sections, which were allowed to equilibrate to RT for 30 min, were fixed in 4% PFA for 1 h, washed (PBS containing 0.02% Triton X-100; 3 x 5 min washes; Sigma-Aldrich, UK) and blocked with 10% normal goat serum/4% BSA in wash buffer for 2 h. Sections were incubated with rabbit anti-human fibrinogen antibody (1:100 in block buffer; Dako, US), reported to cross-react with murine tissue, overnight at 4°C. Sections were washed (3 x 5 min washes) and incubated with Alexa Fluor 647 goat anti-rabbit secondary IgG (1:1000; Life Technologies, UK) for 2 h at RT. Sections were washed (3 x 5 min) and mounted onto glass slides (Vectashield with 40,6-diamidino-2-phenylindole (DAPI); Vector Laboratories, UK). Sections were viewed on a Leica SP8 confocal microscope

(Leica, Laboratory Instruments & Supplies Ltd, Ireland) at 40x magnification. Fibrinogen extravasation was quantified using Imaris imaging software (Bitplane, Switzerland) which calculated the area of fibrinogen reactivity per section, and 3-4 sections were averaged per mouse.

2.11.5 CD3 staining

Sections were allowed to equilibrate to RT for 30 min and subsequently fixed in 4% PFA for 1 h. The slides were washed with PBS (1 x 3 min) and submerged in Citrate buffer (2.1 g in 1L; pH 6; Sigma-Aldrich, UK) for 5 min in the microwave at full power with 5 min rest (x 2; total 20 min). Slides were washed in PBS (3 x 3 min) and incubated in 0.04% pepsin in 0.1 M HCl (Sigma-Aldrich, UK) for 20 min. Sections washed in PBS (1 x 3 min) and submerged in 1% Triton X-100/PBS (15 min). Samples were washed in PBS (1 x 3 min) and blocked with 10% normal goat serum (40 min; RT; Vector Laboratories, UK). Slides were incubated with rabbit anti-human CD3 antibody (1/250 in block buffer; Dako) reported to cross react with murine tissue, overnight at 4°C. Slides were washed in PBS (3 x 3 min) and incubated with Alexa Fluor 647 goat anti-rabbit secondary IgG (1:1000; Life Technologies, UK) for 2 h at RT. Samples were washed with PBS (3 x 3 min) and mounted onto glass slides (Vectashield with DAPI; Vector Laboratories, UK). Sections were viewed on a Leica SP8 confocal microscope at 20x magnification. CD3 influx into the parenchyma was quantified by counting the number of T cells which had infiltrated into the hippocampus and averaging 3-4 sections per mouse.

2.12 Real-time PCR

2.12.1 RNA isolation

Total RNA was extracted from snap-frozen cortical tissue or snap-frozen lung tissue. The tissue was weighed, allowed to thaw, and incubated in 350 µl RA1 and 3.5 µl β-mercaptoethanol before homogenisation using the hand-held homogeniser (Sigma-Aldrich, UK). The RNA was isolated according to the NucleoSpin® RNAII isolation kit (Macherey-Nagel Inc., Germany) which supplied

the reagents below. The homogenised tissue was filtered through NucleoSpin® Filter units (violet) into collecting tubes and centrifuged (11,000 x g; 1 min). The NucleoSpin® Filter columns were discarded and 70% ethanol (350 µl; prepared using diethyl pyrocarbonate (DEPC)-H₂O; Sigma-Aldrich) was added to the homogenised lysate, now in the flow through collecting tubes. NucleoSpin® column units (light blue), which bind the RNA, were placed into new 2 ml centrifuge tubes and the lysate/ethanol mixture was added and the columns centrifuged (8,000 x g; 30 s). The columns were placed in new collecting tubes, membrane desalting buffer was added (350 µl) and the samples were centrifuged (11,000 x g; 1 min). To digest the DNA, rDNase reaction mixture (95 µl; mixture containing 10 µl reconstituted rDNase and 90µl reaction buffer for rDNase per sample) was applied directly to the centre of the silica membrane of the column and incubated at RT for 15 min. The silica membrane was then washed and dried by adding RA2 buffer (200 µl) to the NucleoSpin® columns and centrifuged (8,000 x g; 30 s). The column was placed in a new collecting tube and washed with RA3 buffer (600 µl) and centrifuged (8,000 x g; 30 s). The flow-through was discarded and the column placed back in the same collecting tube. RA3 buffer (250 µl) was added to the NucleoSpin® columns and centrifuged (11,000 x g; 2 min). The column was placed in a new pre-labelled DNase/RNase free 1.5 ml microcentrifuge tube (NucleoSpin® RNA II). RNase-free water was applied to the silica membrane to elute the RNA (40 µl) and samples were centrifuged (11,000 x g; 1 min). The NucleoSpin® columns were discarded.

2.12.2 cDNA synthesis

Total RNA concentrations were determined using spectrophotometry (NanoDrop Spectrophotometer ND-1000), samples were equalised and cDNA synthesis was performed on 1 µg total RNA using a High Capacity cDNA RT kit (Applied Biosystems, Germany). The master mix was prepared from the reagents contained in the high-capacity cDNA kit (4 µl of 10X Reverse transcription buffer; 1.6 µl of 25X dNTPs; 4 µl of 10X random primers; 2 µl of MultiScribe reverse transcriptase (50 U/µl) and 8.4 µl of nuclease-free water per sample). The mastermix was added to the RNA in a 1:1 ratio, i.e. 20 µl of mastermix to 20 µl of

RNA (equalised to 1 µg total). The contents were mixed, spun in the mini centrifuge and placed in the thermal cycler (10 min at 25°C; 120 min at 37°C). The cDNA was stored at -20°C until required.

2.12.3 RT-PCR

Real-time PCR was performed for the detection of the primers listed in Table 2.4 using Taqman Gene Expression Assays (Applied Biosystems, Germany). The real-time PCR primers contained forward and reverse primers, and a FAM-labelled MGB Taqman probe for each gene (Applied Biosystems, Germany). Real-time PCR was conducted using an ABI Prism 7300 instrument (Applied Biosystems, Germany). A 25 µl volume was added to each well (2.5 µl of cDNA, 1.25 µl of each primer, 12.5 µl of SensiMix™ II Probe Mastermix (Bioline) and 7.5 µl of nuclease free H₂O). 18S ribosomal RNA was the endogenous control (VIC labelled Taqman probe, Applied Biosystems, Germany; Assay ID 4319413E). The cycles were as follows: stage 1, 50°C for 2 min; stage 2, 95°C for 10 min; stage 3, 95°C for 15 s and; stage 4, 60°C for 1 min. This was repeated for 40 cycles, after which the plate was removed and the data analysed using the 7500 Fast system V1.3.1 relative quantitative study (Applied Biosystems, Germany). Gene expression was calculated relative to the endogenous control and to the averaged relevant control samples giving an RQ value ($2^{-\Delta\Delta C_t}$, where C_t is the threshold cycle).

Table 2.4 Gene expression assay numbers of the primers used in RT-PCR

Gene Name	Taqman Gene Expression Assay number
Arginase-1	Mm00475988_m1
CCL2	Mm00441242_m1
CCL3	Mm00441258_m1
CCL5	Mm01302428_m1
CD11b (Itgam)	Mm00434455_m1
CD40	Mm0041895_m1
CD68	Mm03047340_m1
CD86	Mm01344638_m1
Claudin-5	Mm00727012_s1
CXCL1	Mm00433859_m1
CXCL10	Mm00445235_m1
GFAP	Mm01253033_m1
IL-10	Mm00439614_m1
IL-17a	Mm00439618_m1
IL-1β	Mm00434228_m1
IL-4	Mm00445259_m1
IL-6	Mm00446190_m1
Mannose receptor	Mm004485148_m1
NGF	Mm00443039_m1
NOS2	Mm00440502_m1
Occludin	Mm00500912_m1
TCRβ	Mm01166193_g1
TGFβ	Mm00441724_m1
TNFα	Mm00443258_m1

2.13 *In vitro* experiments

All cell culture work was carried out in a laminar flow hood using individually pre-packaged, sterile disposable plastic equipment, the outside of which was sterilised in 70% ethanol before bringing into the laminar flow hood. Where necessary, liquids were sterilised by membrane filtration, passing the solution through a 0.2 µm filter (Sigma-Aldrich, UK). For the brain dissections, all metal instruments used were sterilised by incubating overnight at 180°C, before subsequent treatment with 70% ethanol.

2.14 Ag-specific stimulation of lung or lymph node cells

Ag-specific immune responses were examined in lung and mediastinal lymph node cells of vehicle control- and FTY720-treated mice sacrificed 21 days after challenge with *B. pertussis*. Lung mononuclear cells were plated on 6-well plates for 2 h, non-adherent cells were removed and incubated with irradiated spleen cells (1:2 ratio) and heat killed *B. pertussis* (10^6 CFU/ml) or medium only for 72 h. Mediastinal lymph node cells were incubated with irradiated splenocytes at a 1:1 ratio, with heat killed *B. pertussis* (10^6 CFU/ml) or medium only for 72 h. Supernatants were removed and stored at -20°C for later analysis of IFN-γ and IL-17 in supernatant samples using enzyme-linked immunosorbent assay (ELISA).

2.15 Preparation and treatment of glia

Primary glial cells were prepared from 1 day-old C57BL/6 mice (Bioresources Unit, Trinity College, Dublin, Ireland). The animals were sacrificed by decapitation, the brain was dissected free and placed into a sterile Petri-dish (Sarstedt, Germany). Using a sterile scalpel, the brain tissue was chopped bi-directionally and incubated in warm Dulbecco's modified Eagle medium (DMEM; Sigma-Aldrich, UK) supplemented with FBS (10%; Life Technologies, UK) and penicillin-streptomycin (1%; Life Technologies, UK). The tissue was triturated and filtered through a 40 µm sterile nylon mesh filter using a sterile Pasteur pipette, into 50 ml Falcon tubes. The Falcon tubes were centrifuged at 1,200 rpm for 5 min at 20°C and the pellet was re-suspended in 5 ml DMEM. The glia were plated

in T25 flasks (Sigma-Aldrich) and incubated for 24 h (5% CO₂; Nuair Flow CO₂ incubator; Jencons, UK). Macrophage colony stimulating factor (M-CSF; 20 ng/ml, R&D Systems, US) and granulocyte macrophage colony stimulating factor (GM-CSF; 10 ng/ml, R&D Systems, US) were added to the media which was replaced every 3 days with enriched culture media for 10-14 days until the glia were confluent.

When the cells were confluent, the flasks were wrapped with Parafilm (VWR, Ireland), ensuring an air-tight seal around the neck and cap, and agitated at 200 rpm for 2 h at RT. The supernatants containing microglia were transferred into a 50 ml Falcon tube, centrifuged at 1,200 rpm for 5 min, resulting in a pellet of microglial cells. The pellet was re-suspended in 1 ml DMEM, and a cell count was performed. Microglial cells were plated at 3×10^5 cells/ml in 24-well plates. Cells were treated the following day.

Astrocytes, which remained adhered to the T25 flasks following agitation, were incubated with 2 ml of Trypsin-ethylenediamine tetraacetic acid (Trypsin-EDTA; Sigma-Aldrich, UK) for 5 min before adding 5 ml DMEM to inactivate the Trypsin-EDTA. The contents were poured into a 50 ml Falcon tube and centrifuged at 1,200 rpm for 5 min, resulting in a pellet of astrocytes. This pellet was re-suspended in 1 ml DMEM, and a cell count was performed. Astrocytes were plated at 3×10^5 cells/ml in 6-well plates. Cells were treated the following day.

2.16 Cell counts

Cell counts were performed by diluting cells with either Ethidium bromide acridine orange (EBAO) or Trypan blue (Sigma-Aldrich, UK). A 10 µl aliquot of cell suspension was placed on a haemocytometer (Hycor Biomedical, UK) and the number of viable cells which appear green under a fluorescent microscope (EBAO method) or appear white under a light microscope (trypan blue method) were counted.

2.17 Preparation and treatment of T cells

2.17.1 T cell polarization

T cells were prepared from 12 month-old C57BL/6 mice. The spleens were dissected free and filtered through a 70 μm sterile nylon mesh filter to create a single cell suspension. Red blood cells were lysed by incubating the splenocytes in ammonium chloride solution (1 ml; 0.87%; Sigma-Aldrich) for 2 min at RT. Cells were washed and centrifuged at 1,200 rpm for 5 min. CD4^+ T cells were isolated from the splenocytes using a magnetic activated cell sorter (MACS) column (Miltenyi Biotec, UK) and a CD4^+ T cell isolation kit (Miltenyi Biotec, UK). A cell count was performed, the cells were centrifuged and resuspended in 40 μl MACS buffer (0.5% BSA and 2 mM EDTA in PBS; Sigma-Aldrich, UK) per 10^7 total cells. Biotin-Antibody cocktail (10 μl per 10^7 total cells) was added and samples were incubated for 10 min at 4°C. MACS buffer (30 μl) and Anti-Biotin MicroBeads (20 μl) was added per 10^7 total cells and samples were incubated for a further 15 min at 4°C. Cells were washed with MACS buffer (1-2 ml) and centrifuged at 1,200 rpm for 5 min. Cells were resuspended in MACS buffer (500 μl per 10^8 total cells). The LS MACS column was rinsed with MACS buffer (3 ml) and the cell suspension was applied to the column. The entire flow-through was collected, and the column was washed 3 times, each with MACS buffer (3 ml). The flow-through containing enriched CD4^+ T cells was centrifuged at 1,200 rpm for 5 min. Cells were counted and plated at 2×10^6 cells/ml in X-Vivo media (Lonza, Switzerland) supplemented with 1% penicillin-streptomycin, 1% L-glutamine and 2 μl β -mercaptoethanol (Sigma-Aldrich, UK). These cells were stimulated *ex vivo* with $\alpha\text{CD3}/\alpha\text{CD28}$ antibody (1 $\mu\text{g}/\text{ml}$) and either IL-12 (10 ng/ml) to produce Th1 cells, IL-4 (10 ng/ml) and $\alpha\text{-IFN-}\gamma$ (5 $\mu\text{g}/\text{ml}$) to produce Th2 cells, or a cocktail of IL-1 β (10 ng/ml), IL-23 (10 ng/ml), $\alpha\text{-IFN-}\gamma$ (5 $\mu\text{g}/\text{ml}$) and TGF- β (5 ng/ml) to induce Th17 cells. On day 5, the supernatant was collected and stored for cytokine analysis using ELISA. The cells were counted and incubated with either isolated microglia or isolated astrocytes at a ratio of 1:2 (T cells: microglia/astrocytes; 1.5×10^5 cells/ml: 3×10^5 cells/ml) for 24 h.

To amplify the A β -specific T cells naturally present in the spleen, splenocytes were cultured with A β ₁₋₄₂ (15 μ g/ml) plus IL-12 (10 ng/ml) to differentiate Th1 cells, IL-4 (10 ng/ml) and α -IFN- γ (5 μ g/ml) to produce Th2 cells, or IL-1 β (10 ng/ml), IL-23 (10 ng/ml), α -IFN- γ (5 μ g/ml) and TGF- β (5 ng/ml) to induce Th17 cells. IL-2 (10 ng/ml) was added on the third day to the Th1 and Th2 cultures. On day 5 the supernatant was collected and stored for cytokine analysis using ELISA. The CD4⁺ T cells were isolated by MACS on day 5 as described, counted and incubated with either isolated microglia or isolated astrocytes at a ratio of 1:2 (T cells: microglia/astrocytes; 1.5 x 10⁵ cells/ml:3 x 10⁵ cells/ml) with A β ₁₋₄₂ (15 μ g/ml) for 24 h. Control glia were treated with A β ₁₋₄₂ alone.

A β ₁₋₄₂ used in cell culture was dissolved in HPLC-grade water to provide a 6 mg/ml stock solution, which was diluted to 1 mg/ml using sterile PBS and allowed to aggregate for 48 h at 37°C and with agitation of 200 rpm. A β ₁₋₄₂ was used immediately or stored at -20°C.

2.17.2 Co-culture of T cells and glia

T cells were co-incubated with isolated microglia or astrocytes for a period of 24 h (T cells: microglia/astrocytes; 1.5 x 10⁵ cells/ml: 3 x 10⁵ cells/ml). After the co-incubation, the T cells were collected separately by gently pipetting the medium which was centrifuged at 1,200 rpm for 5 min, and supernatants were removed and stored at -20°C in 1.5 ml tubes (Sarstedt, Germany). Microglia and astrocytes (which are both more adherent than T cells) were removed from the wells using Trypsin-EDTA (as described previously) and transferred to FACS tubes. These cells were FACS stained (as described in 2.7) for the appropriate cell markers to assess glial activation. Microglia were identified as CD11b⁺ cells whereas the purified astrocytes were CD11b⁻. The expression of CD40 on each of these cell populations was determined after the 24 h co-culture.

2.18 Analysis of cytokine and chemokine release using ELISA

96-well plates (Nunc-Immuno plate with Maxisorp surface, Sigma-Aldrich, UK) were coated with capture antibody (see Table 2.5 for details) and incubated

overnight at 4°C. The plates were washed 3 times using PBS containing 0.05% Tween-20 (PBS-T; pH 7.2-7.4). The plates were incubated in blocking buffer (100 µl reagent diluent; see Table 2.5) for 1-2 h and washed 3 times with PBS-T. Duplicate samples and standards were added to each well for 2 h at RT. Standards were prepared using serial dilutions of the recombinant protein in DMEM. The plates were washed 3 times using PBS-T and incubated in detection antibody (100 µl) for 2 h at RT. Plates were washed a further 3 times in PBS-T and incubated with horseradish peroxidase (HRP)- conjugated streptavidin (50 µl; 1:200 dilution in assay diluent, Table 2.5) for 20 min in the dark. Plates were washed 3 times in PBS-T and 100 µl substrate solution (1:1 H₂O₂:tetramethylbenzidine; R&D Systems, US) was added to each well. The reaction was stopped with 50 µl sulphuric acid (1 M H₂SO₄) and the optical density was determined by measuring the absorbance at 450 nm (Labsystem Multiskan RC, UK). A standard curve was constructed by plotting the standards against their absorption (GraphPad Prism v4.0; GraphPad Software, US). Protein concentrations from supernatants were expressed as pg/ml.

Table 2.5 Cytokine expression using ELISA

Cytokine	Reagent Diluent	Capture Antibody	Standards	Detection Antibody	Catalogue Number	Supplier
TNF α	1% BSA in PBS	0.8 μ g/ml in PBS	0-2 ng/ml	200 ng/ml in Reagent Diluent	DY410	R&D Systems
IL-6	1% BSA in PBS	2 μ g/ml in PBS	0-2 ng/ml	150 ng/ml in Reagent Diluent	DY406	R&D Systems
IFN- γ	1% BSA in PBS	4 μ g/ml in PBS	0-2 ng/ml	600 ng/ml in Reagent Diluent	DY485	R&D Systems
IL-5	1% BSA in PBS	1 μ g/ml in PBS	0-2 ng/ml	100 ng/ml in Reagent Diluent	DY405	R&D Systems
IL-13	1% BSA in PBS	4 μ g/ml in PBS	0-4 ng/ml	200 ng/ml in Reagent Diluent	DY413	R&D Systems
IL-17	1% BSA in PBS	2 μ g/ml in PBS	0-2 ng/ml	400 ng/ml in Reagent Diluent	DY421	R&D Systems

2.19 Statistical analysis

Statistical analysis was performed using GraphPad Prism or GB-STAT. Data were analysed using student's *t*-test for independent means, 1-way analysis of variance (ANOVA), followed by post hoc comparisons using Newman-Keuls test, 2-way ANOVA followed by Bonferroni post test or 3-way ANOVA followed by post hoc comparisons using Newman-Keuls test. Data are expressed as means with standard errors (SEM) and deemed statistically significant when $p < 0.05$.

Chapter 3

**A β -specific T cells induce glial
activation *in vitro* and infiltrate the
brains of APP/PS1 mice *in vivo*
triggering A β deposition**

3.1 Introduction

Microglia are resident tissue macrophages of the CNS and as such, are responsible for mediating the innate immune response within the brain and spinal cord. In their resting state, these cells use motile processes to survey their microenvironment (Nimmerjahn et al., 2005), have low expression of cell surface markers (such as MHC class II or co-stimulatory markers) with minimal production of cytokines or chemokines and are mainly involved in maintaining CNS homeostasis (Aguzzi et al., 2013; Goldmann and Prinz, 2013). Microglial activation can occur under a number of conditions ranging from tissue damage, inflammation or infectious insult. When this occurs, microglia retract their branches forming an amoeboid shape and upregulate the expression of many cell surface markers. Specific markers can distinguish whether the cell has entered a classically activated (M1) or alternatively activated (M2) state (Goldmann and Prinz, 2013; Saijo and Glass, 2011). While the division of M1 and M2 activation states is somewhat simplified, it corresponds with what is observed in macrophages, where M1 is typically associated with an acute, pro-inflammatory response with the production of TNF α , IL-6, IL-1 β and NO. M2 is considered to play a role in tissue repair and healing, and is anti-inflammatory in nature with evidence of increased IL-10 production and an upregulation in the expression of mannose receptor and arginase (Mantovani et al., 2013; Martinez and Gordon, 2014). These phenotypes are achieved *in vitro* using LPS or the Th1 cell-derived cytokine, IFN- γ , to polarize microglia to the M1 activation state, whereas Th2 cell-derived cytokines such as IL-4 and IL-13 induce M2 activation (Goldmann and Prinz, 2013; Lynch, 2014; Mantovani et al., 2013). Therefore M1 activation is often considered to be involved with the Th1 cell response, whereas Th2 cells are associated with the M2 state.

Activated microglia are co-localised with A β -containing plaques in post-mortem AD brain tissue (McGeer et al., 1987; Togo et al., 2000). These cells secrete pro-inflammatory cytokines, including IL-1 β and TNF α , in response to A β (Lue et al., 2001), both of which have been shown to enhance the expression and the activity of β -secretases and γ -secretases (Liao et al., 2004; Sastre et al., 2008) and increased protein and mRNA levels of these cytokines have been detected in

post-mortem AD brain tissue (Griffin et al., 1989; Rao et al., 2011; Wood et al., 1993). Therefore it has been suggested that M1 activated microglia may contribute to the processing of APP, the deposition of A β and progression of AD as a result (Glass et al., 2010; Lynch, 2014). Activated microglia express increased levels of MHC class II, CD40, CD80 and CD86 (Aloisi et al., 2000b; McQuillan et al., 2010; Prajeeth et al., 2014) which are necessary for antigen presentation to T cells and, in AD, the microglia associated with A β plaques express MHC class II (McGeer et al., 1987; Togo et al., 2000) and CD40 (Togo et al., 2000).

Astrocyte-mediated inflammation is another feature of AD. As the most abundant cell in the CNS, astrocytes are responsible for many essential, complex functions in maintaining homeostasis within the brain (Sofroniew and Vinters, 2010). In AD, development of A β plaques has been associated with activated astrocytes (Nagele et al., 2004) and increased GFAP expression is linked with increased Braak stage in AD patients (Simpson et al., 2010). While these glial cells are not often considered to have APC function, astrocytes express MHC class II *in vitro* and *in vivo* (Dong et al., 1999; Panek et al., 1992; Vass and Lassmann, 1990; Wong et al., 1984; Zeinstra et al., 2000), along with CD80 and CD86 (Nikceovich et al., 1997; Zeinstra et al., 2003). Additionally, astrocytes are capable of phagocytosing A β (Wyss-Coray et al., 2003) and do so via receptors including RAGE, CD36 and CD47 (Jones et al., 2013).

Under normal conditions, T cells which have previously encountered antigen routinely enter the brain (Becher et al., 2000; Hickey, 2001). Indeed antigen specificity is a critical step in T cell migration into the CNS, if T cells do not recognise antigen in the perivascular area or subarachnoid space there is no progression across the glia limitans into the brain parenchyma (Engelhardt and Ransohoff, 2005; Owens et al., 2008) The role of T cells in diseases of the CNS, particularly MS, is well established. Studies using the EAE model have revealed that Th1 cells infiltrate the CNS and facilitate the recruitment of other immune cells (O'Connor et al., 2008). In addition, IFN- γ ^{-/-} mice have delayed onset of disease which is associated with reduced infiltration of IL-17⁺ T cells to the CNS (Dungan et al., 2014). Th17 cells also have an important pathogenic role in disease progression (Fletcher et al., 2010; Sutton et al., 2009), the onset of EAE is

not only delayed in IL-17^{-/-} mice, but the severity is also considerably reduced (Komiyama et al., 2006).

Numerous reports have documented the presence of T cells in the post-mortem brain of AD patients (Hartwig, 1995; McGeer et al., 1989; Parachikova et al., 2007; Pirttila et al., 1992; Rogers et al., 1988; Togo et al., 2002; Town et al., 2005), and evidence of T cells in the hippocampus (Togo et al., 2002). AD patients have increased T cell reactivity to A β (Monsonogo et al., 2003; Saresella et al., 2010; Saresella et al., 2012) with an A β -specific Th17 response (Saresella et al., 2011). Additionally it appears that the peripheral immune response is altered in AD, where patients have a significant shift in T cell populations from naïve to effector memory or terminally-differentiated T cells (Larbi et al., 2009; Pellicanò et al., 2012; Saresella et al., 2011; Schindowski et al., 2007; Speciale et al., 2007). However, efforts to activate the immune system and immunize AD patients against A β (AN1792 trial) ultimately resulted in development of meningoencephalitis in 6% of patients (Schenk, 2002), probably due to induction of IFN- γ ⁺ cells by the Th1 adjuvant, QS-21, used in the trial (Wilcock and Colton, 2008).

T cells have also been documented in the brains of mouse AD models (Browne et al., 2013), and cell numbers infiltrating into the CNS were increased in 18 month-old APP/PS1 mice (Jimenez et al., 2008). *In vitro* studies reveal that microglia adopt a pro-inflammatory phenotype in response to the Th1 cell cytokine, IFN- γ or to supernatants derived from Th1 cell cultures (McQuillan et al., 2010; Prajeeth et al., 2014; Séguin et al., 2003). It is well established that microglia in mixed glial cultures can interact with, and are activated by T cells (McQuillan et al., 2010; Murphy et al., 2010) and a number of studies have shown that astrocytes are capable of acting as APCs for T cells (Constantinescu et al., 2005; Kort et al., 2006; Nikcevic et al., 1997; Soos et al., 1999; Soos et al., 1998; Tan et al., 1998). However, to date, the interaction between astrocytes and T cells has been examined predominantly in the context of EAE. The degree to which T cells can activate these individual glial cells is poorly understood,

particularly in the realm of AD. In addition, how microglia and astrocytes separately respond to the different T cell subtypes is yet to be fully investigated.

Study aims

The aims of this study were:

- 1) To establish whether isolated microglia and isolated astrocytes respond to Th1, Th2 or Th17 cells *in vitro*.
- 2) To investigate whether A β -specific T cells exert similar effects on these glial cells in an antigen presentation capacity.
- 3) To assess the effect of A β -specific T cells *in vivo* in APP/PS1 mice.

3.2 Results

3.2.1 Th1 cells induce microglial activation

It has been reported that Th1 cells and Th17 cells induce microglial activation in mixed glial cultures (McQuillan et al., 2010) and that this was regulated, in part, by Th2 cells. To investigate the effect of T cells on isolated microglia and astrocytes, purified microglia and purified astrocytes were co-incubated with polarised T cells at a ratio of 2:1 for 24 h. The microglial cells were prepared from 1-day old C57BL/6 mice as described in section 2.15. CD4⁺ T cells were polarised *in vitro* with α CD3 and α CD28 under Th1, Th2 or Th17-polarising conditions as detailed in 2.17.

T cells cultured under Th1-polarising conditions secreted high levels of IFN- γ , with low levels of IL-5 and IL-17 (Fig 3.1). Th2-polarised cells produced IL-5 with minimal IFN- γ or IL-17, while T cells incubated with Th17 polarising conditions produced high levels of IL-17 with low levels of IFN- γ or IL-5 (Fig 3.1). After 24 h co-incubation of glia with T cells, the supernatants were taken and concentrations of IL-6 and TNF α were measured using ELISA. CD11b⁺ cells expressing CD40 were quantified by FACS and expressed as a total population of cells expressing CD11b in the microglial cultures and CD11b⁻ cells expressing CD40 were quantified and expressed as a total population of CD11b⁻ cells for the astrocytic cultures. Incubation of microglia with Th1-polarised cells significantly increased the production of TNF α into the supernatant (Fig 3.2). An increase in CD11b⁺CD40⁺ cells was also observed (Fig 3.2B). Microglial cells were unresponsive to incubation with Th2- or Th17-polarised cells (Fig 3.3, 3.4).

3.2.2 Th1 and Th17 cells induce activation of astrocytes

Similar to that observed with microglia, incubation of astrocytes with Th1-polarised cells resulted in a significant production of IL-6 and TNF α into the supernatant, and a parallel increase in number of CD40⁺ astrocytes (Fig 3.5A, B). Astrocytes were unresponsive to incubation with Th2-polarised cells (Fig 3.6),

however, incubation with Th17-polarised cells increased supernatant concentration of IL-6 with a parallel increase in CD40 expression on the astrocytes (Fig 3.7A, B).

3.2.3 A β -specific Th1 cells induce microglial and astrocytic activation

A β -specific Th1, Th2 and Th17 cells were prepared as described in section 2.17 and evaluated for their impact on microglia and astrocytes. T cells incubated under Th1-polarising conditions secreted high levels of IFN- γ , with some IL-13 and low levels of IL-17 (Fig 3.8). Th2-polarised cells produced IL-13 with little IFN- γ and no IL-17, while T cells incubated with Th17 polarising conditions produced high levels of IL-17 with no IFN- γ (Fig 3.8). The A β -specific polarised T cells were incubated with microglia or astrocytes at a ratio of 2:1 in the presence of A β (15 μ g/ml; section 2.17.2 for details). A β -specific Th1 cells induced a significant production of TNF α and IL-6 in microglial co-cultures (Fig 3.9A) and while the expression of CD40 on microglial cells was increased after incubation with A β -specific Th1 cells, this did not reach statistical significance. As demonstrated for polyclonal T cells, microglia were unresponsive to incubation with A β -specific Th2 or Th17 cells (Fig 3.10, 3.11).

A β -specific Th1 cells induced a significant production of TNF α and IL-6 into the supernatant in astrocytic cultures (Fig 3.12A). While incubation with Th2-polarised cells did not induce any response (Fig 3.13), there was a significant increase in IL-6 in the supernatant after incubation of astrocytes with A β -specific Th17 cells for 24 h (Fig 3.14A).

3.2.4 A β -specific T cells infiltrate the brains of APP/PS1 mice

In order to examine the effect of A β -specific T cells *in vivo*, GFP⁺ A β -specific T cells were generated from GFP mice. GFP mice were immunized s.c. into the foot pad with CpG and A β on days 0 and 21. Cells were polarised with IL-12 *ex vivo* as described in section 2.3. Surviving T cells were washed and injected i.v. (15 x 10⁶ cells/mouse) into 6-7 month old WT and APP/PS1 mice. The mice were culled 14

days post-transfer to assess migration of the GFP⁺ cells into the brain. The number of CD45⁺CD3⁺ T cells was significantly increased in APP/PS1 in comparison with WT mice (Fig 3.15A), and the number of GFP⁺ cells was also significantly greater in APP/PS1 mice (Fig 3.15A). CD8⁺ and CD4⁺ T cells infiltrated the brain, and significantly more of these were IFN- γ ⁺ in APP/PS1 mice (Fig 3.15A).

The expression of chemokines, which are chemoattractant for T cells, was assessed in the brains of these mice using RNA extracted from snap-frozen cortical tissue. The expression of CCL3 and CXCL10 was significantly increased in APP/PS1 mice which received A β -specific Th1 cells in comparison with WT mice injected with A β -specific T cells (Fig 3.16A, B). The expression of CCL2 was also increased in APP/PS1 mice; however this did not reach statistical significance.

3.2.5 Increased A β deposition in the brains of APP/PS1 mice following transfer of A β -specific T cells

A β -specific Th1 cells were prepared and injected into recipient mice as described in section 2.3. Recipients of A β -specific T cells were culled 21 days post-transfer to assess changes in A β concentration in the brain. A β -containing plaques were quantified in the brains of 6 month-old mice as described previously (Jankowsky et al., 2004) and the number of A β -containing plaques in hippocampus and frontal cortex was significantly increased following transfer of A β -specific Th1 cells (Fig 3.17B). Consistently, the concentrations of insoluble A β ₄₀ and A β ₄₂ and soluble A β ₄₀ and A β ₄₂ were increased in APP/PS1 mice in comparison with WT, and the concentration was significantly greater after exposure to A β -specific Th1 cells (Fig 3.17C, D).

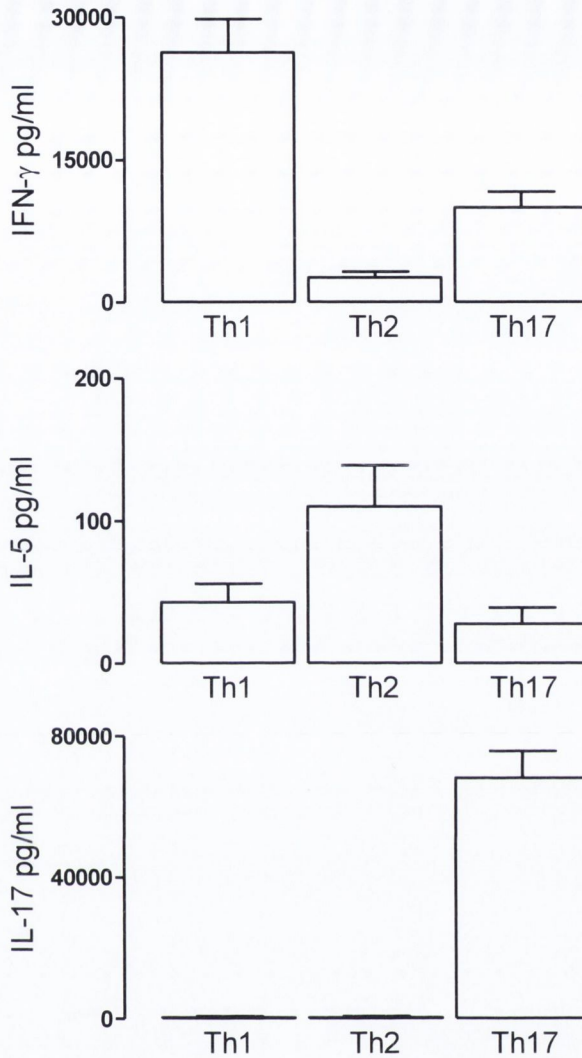


Figure 3.1 T cells polarised *in vitro* to Th1, Th2 and Th17 subtype.

CD4⁺ T cells isolated from the spleens of C57BL/6 mice were co-incubated with α CD3/ α CD28 antibody (1 μ g/ml) and either IL-12 (10 ng/ml) to produce Th1 cells, IL-4 (10 ng/ml) and α -IFN- γ (5 μ g/ml) to produce Th2 cells, or a cocktail of IL-1 β (10 ng/ml), IL-23 (10 ng/ml), α -IFN- γ (5 μ g/ml) and TGF- β (5 ng/ml) to induce Th17 cells. After 5 days supernatants were harvested and concentrations of IFN- γ , IL-5 and IL-17 were measured using ELISA. Values expressed as means \pm SEM, n = 5 independent *in vitro* experiments.

The data from Figures 3.1-14 were generated in collaboration with Dr. Tara Browne and also appear in her thesis in Chapter 5.

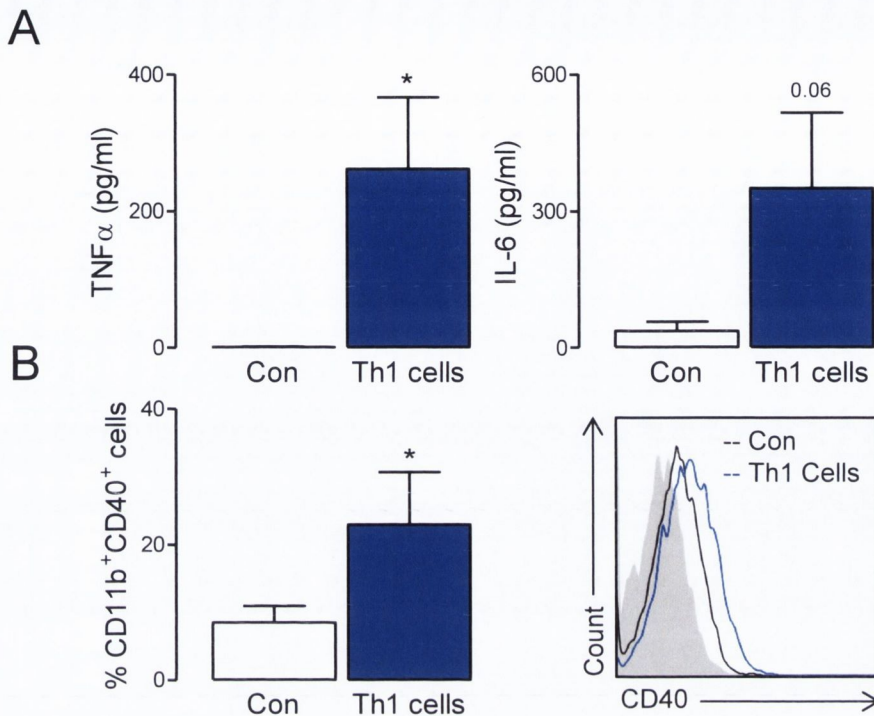


Figure 3.2 T cells polarised to the Th1 subtype induce microglial activation.

Microglia prepared from 1 day-old C57BL/6 mice were co-incubated with polarised T cells at a ratio of 2:1. After 24 h, supernatants were harvested and (A) concentrations of IL-6 and TNF α were measured using ELISA. The cells were surface-stained for CD11b and CD40, and flow cytometric analysis was performed. (B) CD11b⁺ cells expressing CD40 were quantified by FACS and expressed as a percentage of the total population of CD11b⁺ cells, with sample histogram of medium control (black), Th1 cell incubation (blue), FMO control (solid grey). * $p < 0.05$, $p = 0.06$; Student's t -test for independent means. Values expressed as means \pm SEM, $n = 5$ independent *in vitro* experiments. Con, Control.

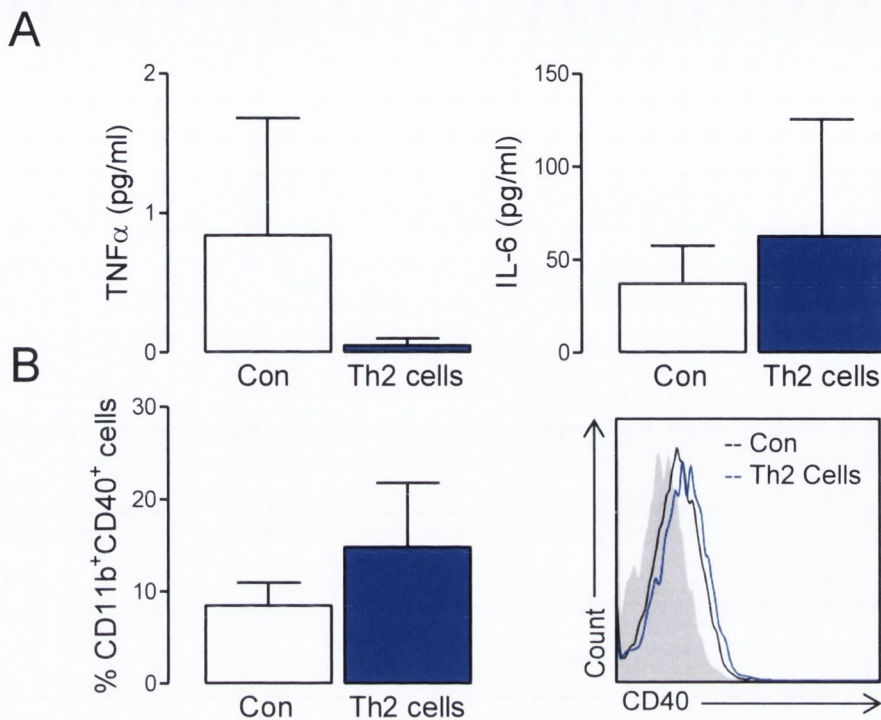


Figure 3.3 Th2 cells do not induce microglial activation.

Microglia prepared from 1 day-old C57BL/6 mice were co-incubated with polarised T cells at a ratio of 2:1. After 24 h, supernatants were harvested and (A) concentrations of IL-6 and TNF α were measured using ELISA. The cells were surface-stained for CD11b and CD40, and flow cytometric analysis was performed. (B) CD11b⁺ cells expressing CD40 were quantified by FACS and expressed as a percentage of the total population of CD11b⁺ cells, with sample histogram of medium control (black), Th2 cell incubation (blue), FMO control (solid grey). Values expressed as means \pm SEM, n = 5 independent *in vitro* experiments. Con, Control.

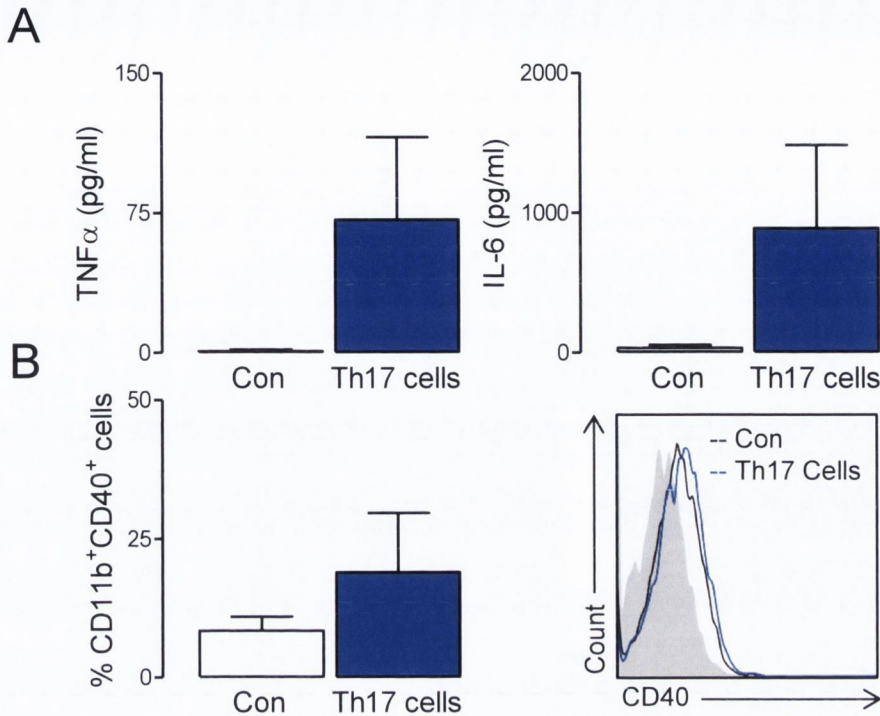


Figure 3.4 Th17 cells do not induce a pro-inflammatory microglial response.

Microglia prepared from 1 day-old C57BL/6 mice were co-incubated with polarised T cells at a ratio of 2:1. After 24 h, supernatants were harvested and (A) concentrations of IL-6 and TNF α were measured using ELISA. The cells were surface-stained for CD11b and CD40, and flow cytometric analysis was performed. (B) CD11b⁺ cells expressing CD40 were quantified by FACS and expressed as a percentage of the total population of CD11b⁺ cells, with sample histogram of medium control (black), Th17 cell incubation (blue), FMO control (solid grey). Values expressed as means \pm SEM, n = 5 independent *in vitro* experiments. Con, Control.

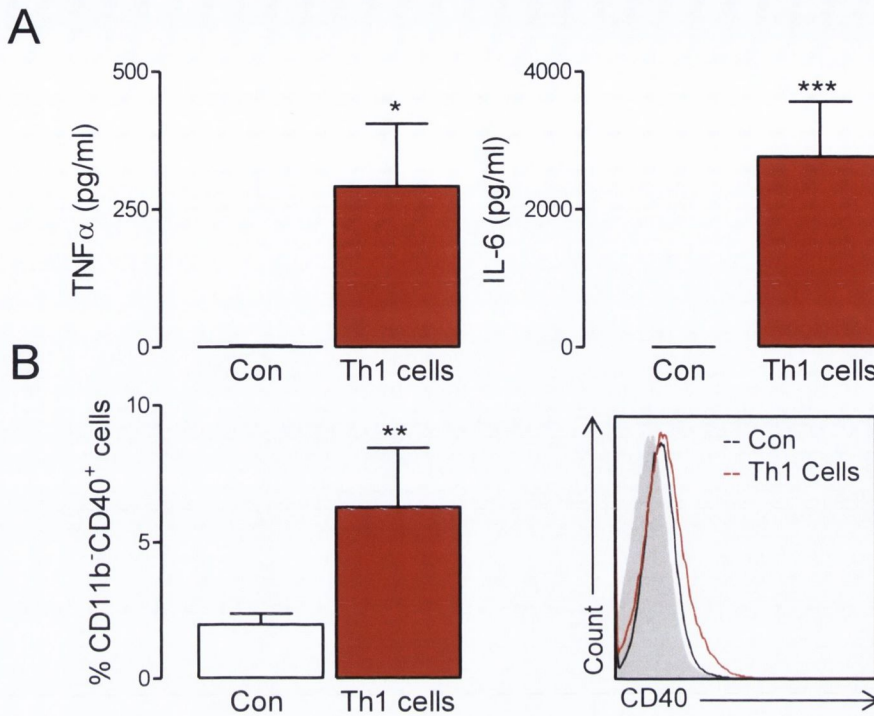


Figure 3.5 Th1 cells induce activation of astrocytes.

Astrocytes prepared from 1 day-old C57BL/6 mice were co-incubated with polarised T cells at a ratio of 2:1. After 24 h, supernatants were harvested and (A) concentrations of IL-6 and TNF α were measured using ELISA. The cells were surface-stained for CD11b and CD40, and flow cytometric analysis was performed. (B) CD11b⁻ cells expressing CD40 were quantified by FACS and expressed as a percentage of the total population of CD11b⁻ cells, with sample histogram of medium control (black), Th1 cell incubation (red), FMO control (solid grey). * $p < 0.05$, ** $p < 0.01$, *** $p < 0.001$; Student's t -test for independent means. Values expressed as means \pm SEM, $n = 5$ independent *in vitro* experiments. Con, Control.

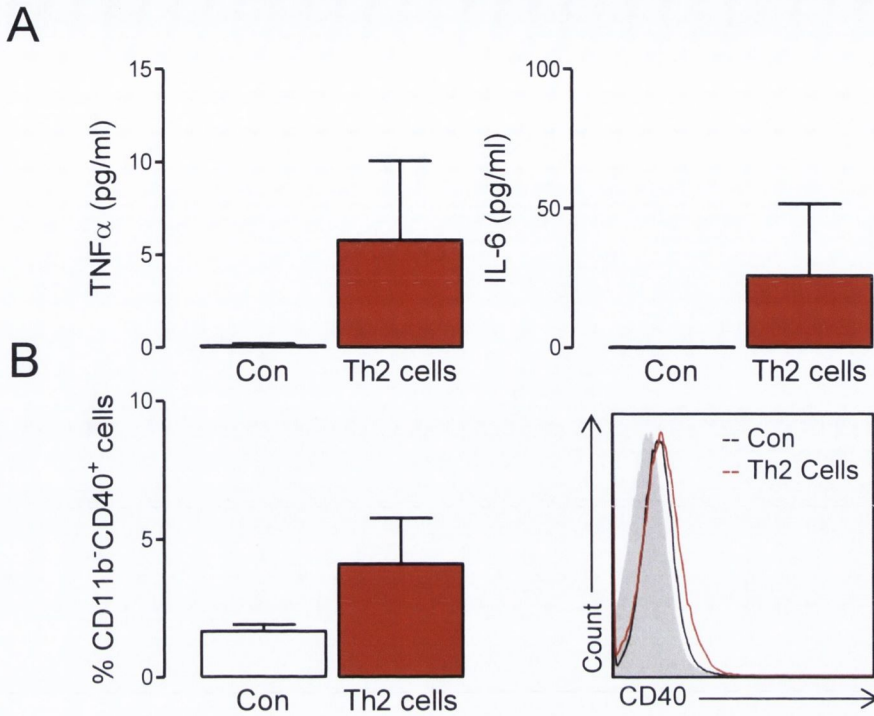


Figure 3.6 Th2 cells do not induce astrocytic activation.

Astrocytes prepared from 1 day-old C57BL/6 mice were co-incubated with polarised T cells at a ratio of 2:1. After 24 h, supernatants were harvested and (A) concentrations of IL-6 and TNF α were measured using ELISA. The cells were surface-stained for CD11b and CD40, and flow cytometric analysis was performed. (B) CD11b⁻ cells expressing CD40 were quantified by FACS and expressed as a percentage of the total population of CD11b⁻ cells, with sample histogram of medium control (black), Th2 cell incubation (red), FMO control (solid grey). Values expressed as means \pm SEM, n = 5 independent *in vitro* experiments. Con, Control.

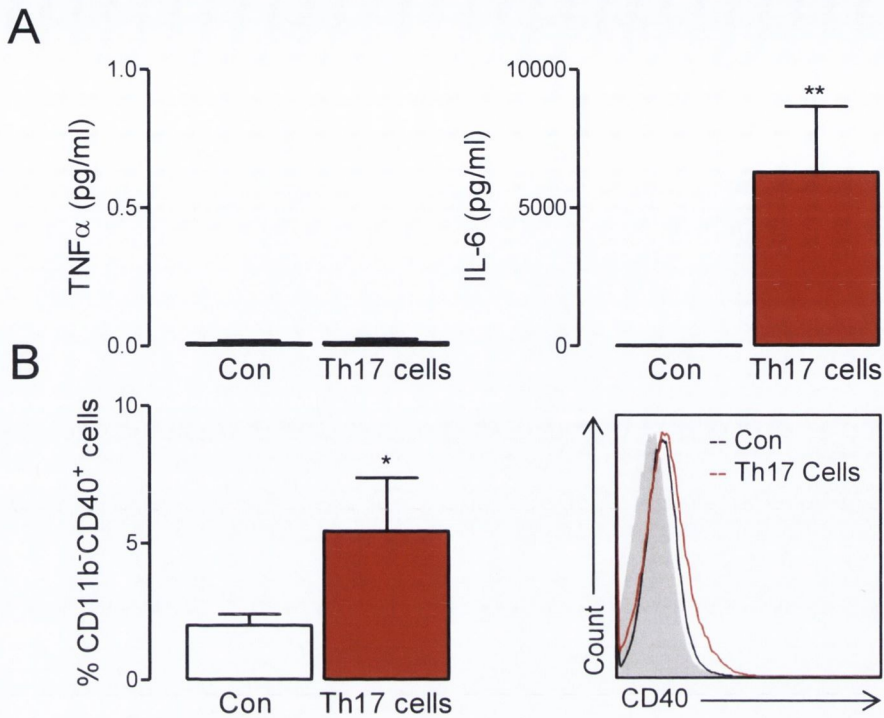


Figure 3.7 Th17 cells induce a pro-inflammatory response in purified astrocytic cultures.

Astrocytes prepared from 1 day-old C57BL/6 mice were co-incubated with polarised T cells at a ratio of 2:1. After 24 h, supernatants were harvested and (A) concentrations of IL-6 and TNF α (not detectable) were measured using ELISA. The cells were surface-stained for CD11b and CD40, and flow cytometric analysis was performed. (B) CD11b⁻ cells expressing CD40 were quantified by FACS and expressed as a percentage of the total population of CD11b⁻ cells, with sample histogram of medium control (black), Th17 cell incubation (red), FMO control (solid grey). * $p < 0.05$, ** $p < 0.01$; Student's *t*-test for independent means. Values expressed as means \pm SEM, $n = 5$ independent *in vitro* experiments. Con, Control.

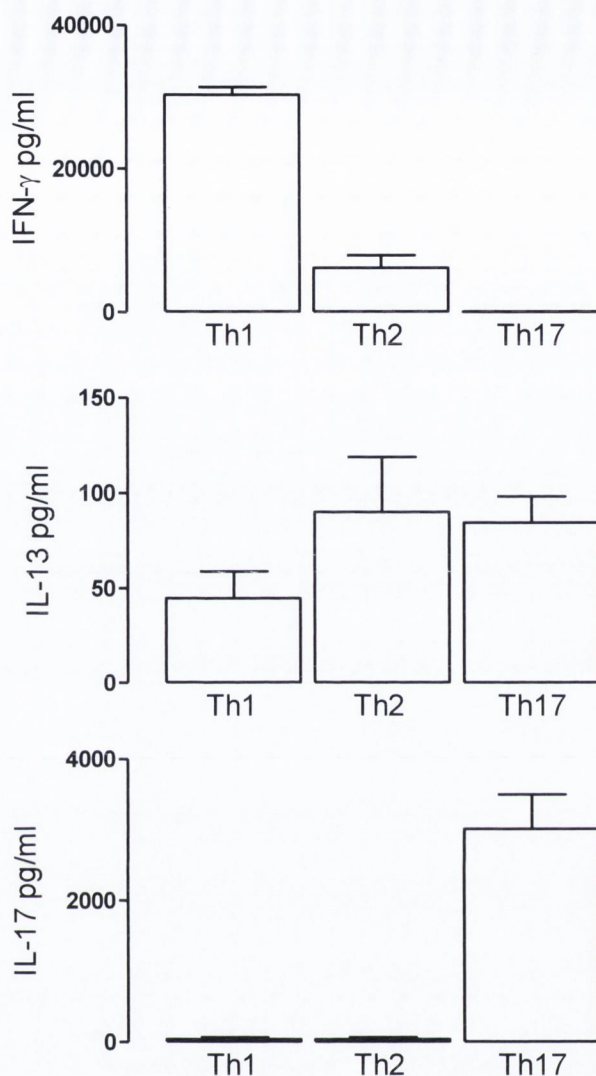


Figure 3.8 A β -specific T cells polarised *in vitro* to Th1, Th2 and Th17 subtype.

Splenocytes of C57BL/6 mice were co-incubated with A β (15 μ g/ml) and either IL-12 (10 ng/ml) to produce Th1 cells, IL-4 (10 ng/ml) and α -IFN- γ (5 μ g/ml) to produce Th2 cells, or a cocktail of IL-1 β (10 ng/ml), IL-23 (10 ng/ml), α -IFN- γ (5 μ g/ml) and TGF- β (5 ng/ml) to induce Th17 cells. After 5 days, supernatants were harvested and concentrations of IFN- γ , IL-13 and IL-17 were measured using ELISA. CD4⁺ T cells were isolated and used in co-culture experiments with either microglia or astrocytes. Values expressed as means \pm SEM, n = 5 independent *in vitro* experiments.

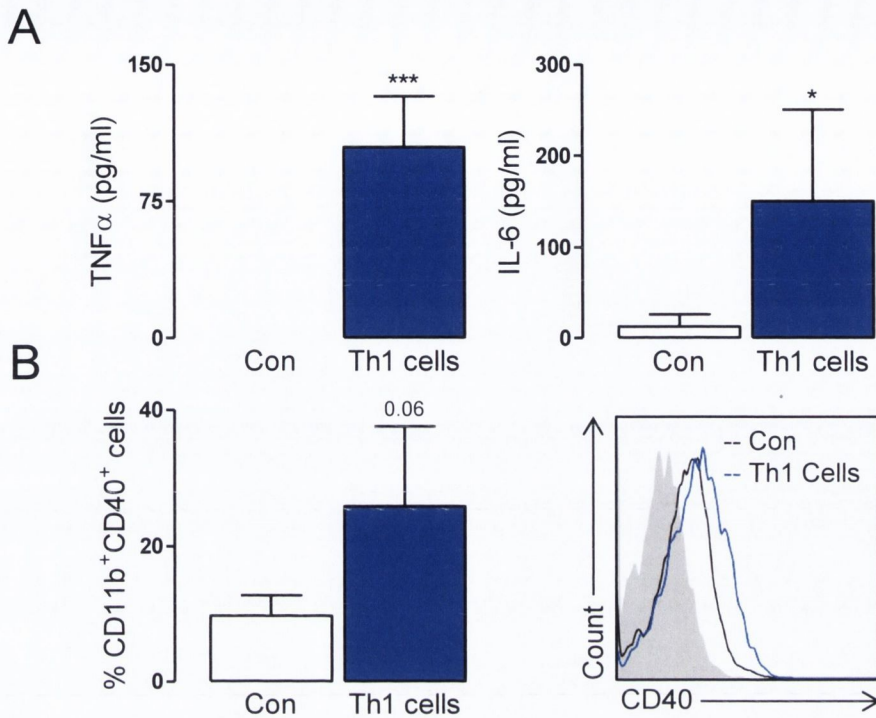


Figure 3.9 A β -specific Th1 cells induce activation of microglial cells.

Microglia prepared from 1 day-old C57BL/6 mice were co-incubated with A β (15 μ g/ml; control) or A β (15 μ g/ml) with polarised A β -specific T cells at a ratio of 2:1. After 24 h, supernatants were harvested and (A) concentrations of IL-6 and TNF α were measured using ELISA. The cells were surface-stained for CD11b and CD40, and flow cytometric analysis was performed. (B) CD11b⁺ cells expressing CD40 were quantified by FACS and expressed as a percentage of the total population of CD11b⁺ cells, with sample histogram of medium control (black), Th1 cell incubation (blue), FMO control (solid grey). * $p < 0.05$, *** $p < 0.001$, $p = 0.06$; Student's t -test for independent means. Values expressed as means \pm SEM, $n = 5$ independent *in vitro* experiments. Con, Control.

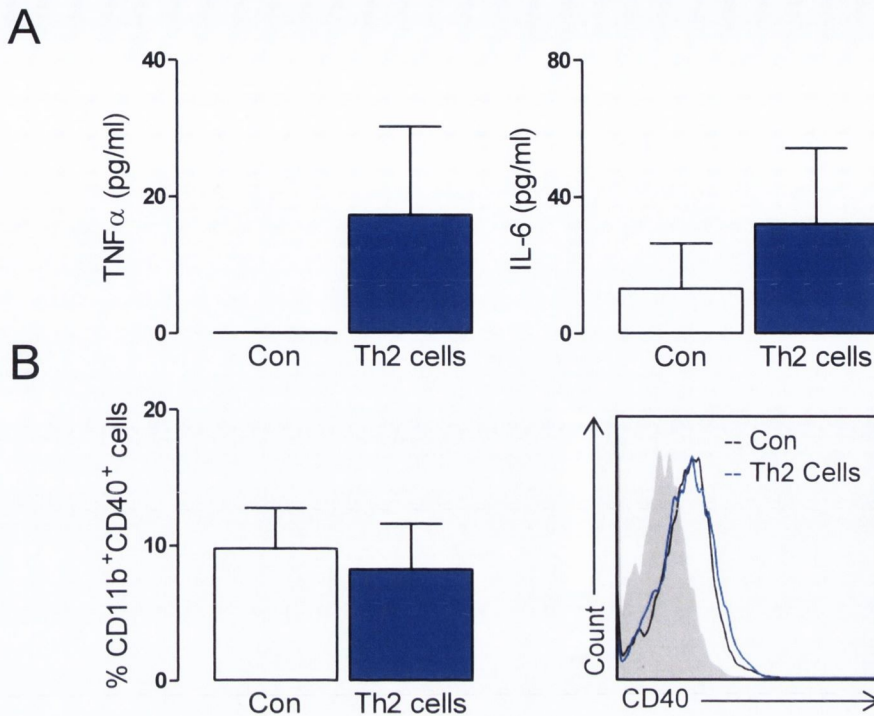


Figure 3.10 Incubation with A β -specific Th2 cells does not induce microglial activation.

Microglia prepared from 1 day-old C57BL/6 mice were co-incubated with A β (15 μ g/ml; control) or A β (15 μ g/ml) with polarised A β -specific T cells at a ratio of 2:1. After 24 h, supernatants were harvested and (A) concentrations of IL-6 and TNF α were measured using ELISA. The cells were surface-stained for CD11b and CD40, and flow cytometric analysis was performed. (B) CD11b⁺ cells expressing CD40 were quantified by FACS and expressed as a percentage of the total population of CD11b⁺ cells, with sample histogram of medium control (black), Th2 cell incubation (blue), FMO control (solid grey). Values expressed as means \pm SEM, n = 5 independent *in vitro* experiments. Con, Control.

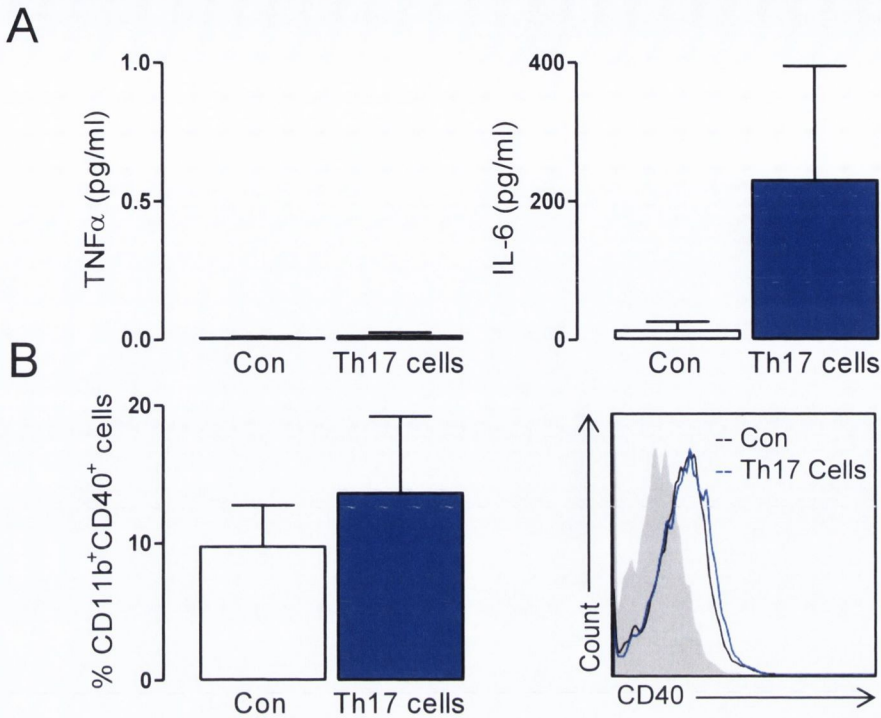


Figure 3.11 A β -specific Th17 cells do not cause microglial activation *in vitro*.

Microglia prepared from 1 day-old C57BL/6 mice were co-incubated with A β (15 μ g/ml; control) or A β (15 μ g/ml) with polarised A β -specific T cells at a ratio of 2:1. After 24 h, supernatants were harvested and (A) concentrations of IL-6 and TNF α (not detectable) were measured using ELISA. The cells were surface-stained for CD11b and CD40, and flow cytometric analysis was performed. (B) CD11b⁺ cells expressing CD40 were quantified by FACS and expressed as a percentage of the total population of CD11b⁺ cells, with sample histogram of medium control (black), Th17 cell incubation (blue), FMO control (solid grey). Values expressed as means \pm SEM, n = 5 independent *in vitro* experiments. Con, Control.

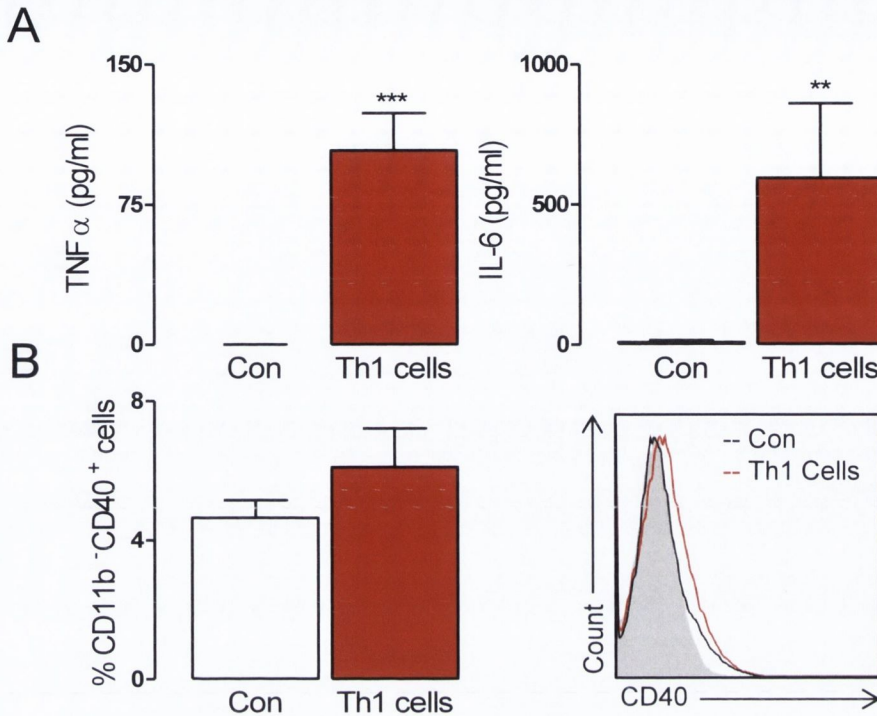


Figure 3.12 A β -specific Th1 cells induce astrocytic activation.

Astrocytes prepared from 1 day-old C57BL/6 mice were co-incubated with A β (15 μ g/ml; control) or A β (15 μ g/ml) with polarised A β -specific T cells at a ratio of 2:1. After 24 h, supernatants were harvested and (A) concentrations of IL-6 and TNF α were measured using ELISA. The cells were surface-stained for CD11b and CD40, and flow cytometric analysis was performed. (B) CD11b⁻ cells expressing CD40 were quantified by FACS and expressed as a percentage of the total population of CD11b⁻ cells, with sample histogram of medium control (black), Th1 cell incubation (red), FMO control (solid grey). ** $p < 0.01$, *** $p < 0.001$; Student's *t*-test for independent means. Values expressed as means \pm SEM, $n = 5$ independent *in vitro* experiments. Con, Control.

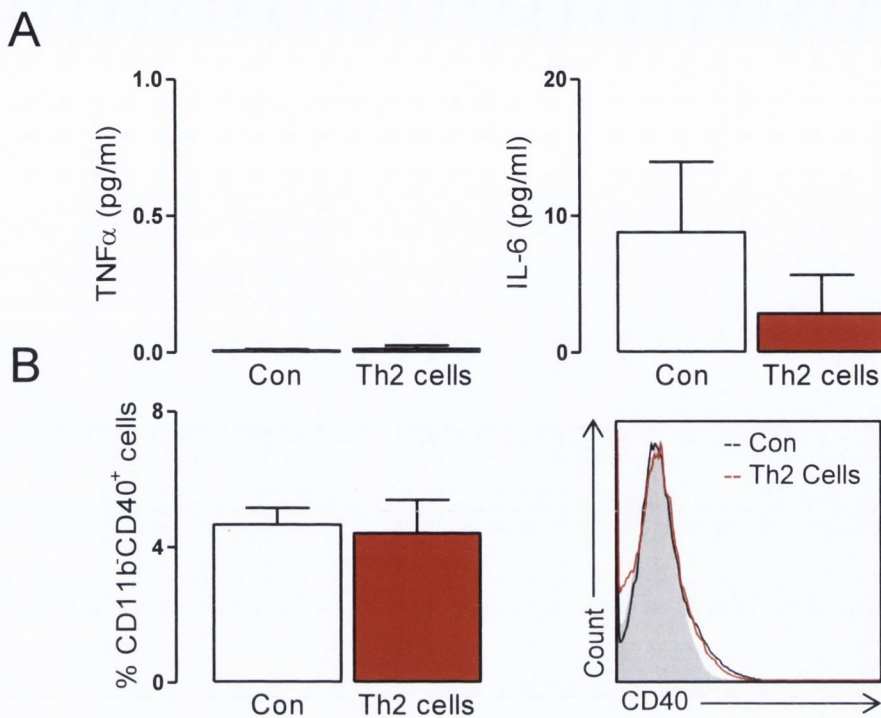


Figure 3.13 A β -specific Th2 cells do not induce astrocytic activation.

Astrocytes prepared from 1 day-old C57BL/6 mice were co-incubated with A β (15 μ g/ml; control) or A β (15 μ g/ml) with polarised A β -specific T cells at a ratio of 2:1. After 24 h, supernatants were harvested and (A) concentrations of IL-6 and TNF α (not detectable) were measured using ELISA. The cells were surface-stained for CD11b and CD40, and flow cytometric analysis was performed. (B) CD11b⁻ cells expressing CD40 were quantified by FACS and expressed as a percentage of the total population of CD11b⁻ cells, with sample histogram of medium control (black), Th2 cell incubation (red), FMO control (solid grey). Values expressed as means \pm SEM, n = 5 independent *in vitro* experiments. Con, Control.

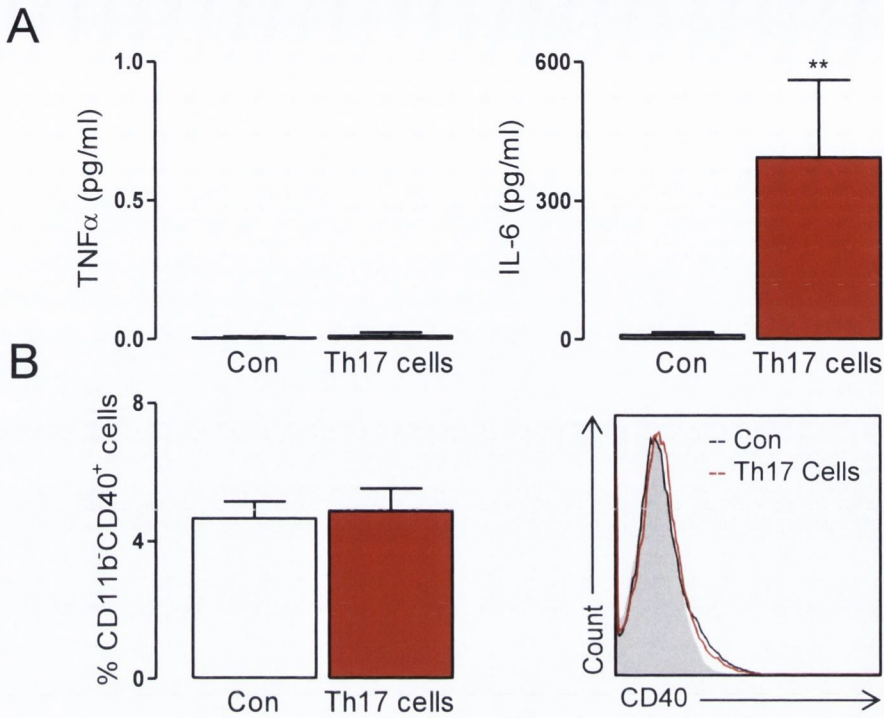


Figure 3.14 A β -specific Th17 cells induce astrocyte IL-6 release.

Astrocytes prepared from 1 day-old C57BL/6 mice were co-incubated A β (15 μ g/ml; control) or A β (15 μ g/ml) with polarised A β -specific T cells at a ratio of 2:1. After 24 h, supernatants were harvested and (A) concentrations of IL-6 and TNF α (not detectable) were measured using ELISA. The cells were surface-stained for CD11b and CD40, and flow cytometric analysis was performed. (B) CD11b⁻ cells expressing CD40 were quantified by FACS and expressed as a percentage of the total population of CD11b⁻ cells, with sample histogram of medium control (black), Th17 cell incubation (red), FMO control (solid grey). ** $p < 0.01$; Student's t -test for independent means. Values expressed as means \pm SEM, $n = 5$ independent *in vitro* experiments. Con, Control.

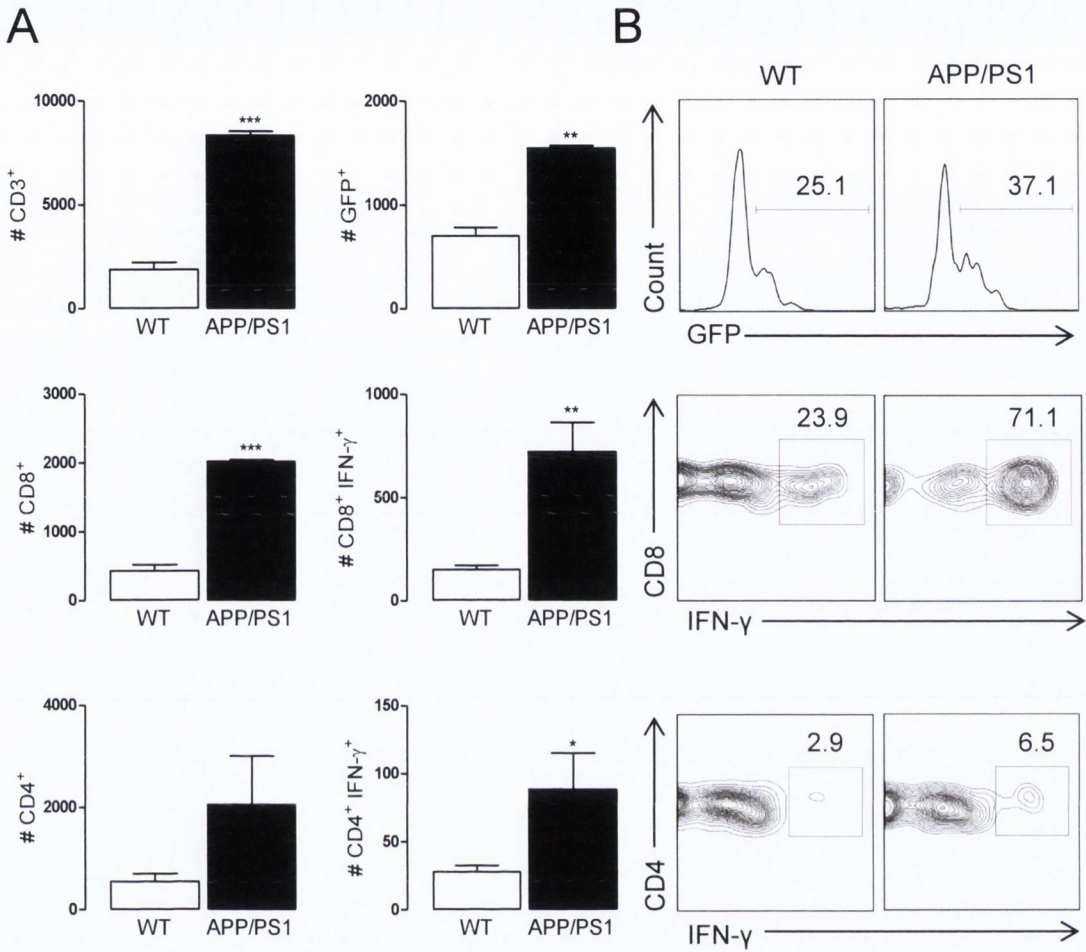


Figure 3.15 A β -specific Th1 cells migrate into the brain of APP/PS1 mice.

A β -specific Th1 cells were generated from GFP mice and injected i.v. into WT and APP/PS1 mice. Mice were sacrificed 2 weeks post-injection, and mononuclear cells were isolated from the brain. Cells were surface stained for CD3, CD4, and CD8 and intracellularly stained for IFN- γ . Flow cytometric analysis was then performed. (A) Results are mean absolute number of cells in the brain. (B) Sample FACS plots of GFP⁺ T cells (gated on CD3), CD8⁺IFN- γ ⁺, and CD4⁺IFN- γ ⁺ cells. * $p < 0.05$, ** $p < 0.01$, *** $p < 0.001$; Student's t -test for independent means. Data represent means \pm SEM from 1 experiment, $n = 4$.

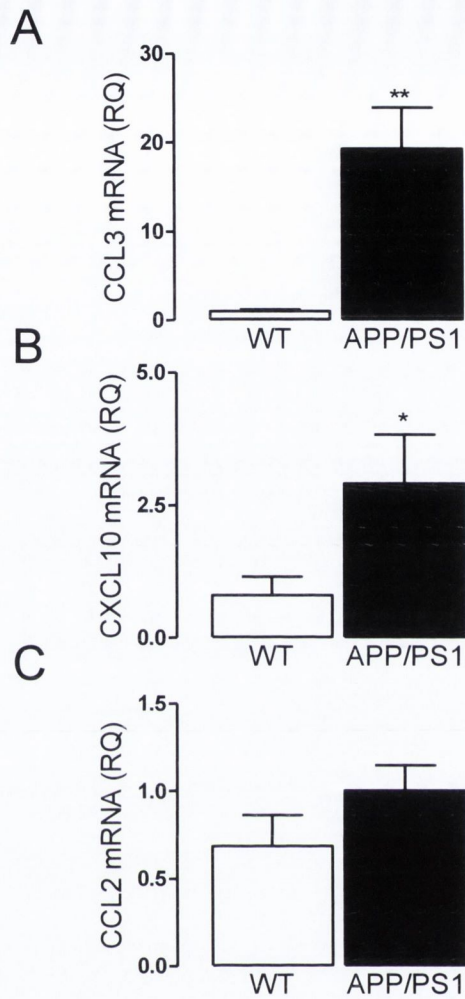


Figure 3.16 Increased chemokine expression in APP/PS1 mice injected with A β -specific Th1 cells.

RNA was extracted from snap-frozen cortical tissue 14 days post-injection with A β -specific Th1 cells. (A) CCL3, (B) CXCL10 and (C) CCL2 expression was assessed and values are expressed as relative quantities (RQ) normalised to the endogenous control gene, 18S, and relative to the averaged WT injected control group. * $p < 0.05$, ** $p < 0.01$; Student's t -test for independent means. Data represent means \pm SEM from 1 experiment, $n = 4$.

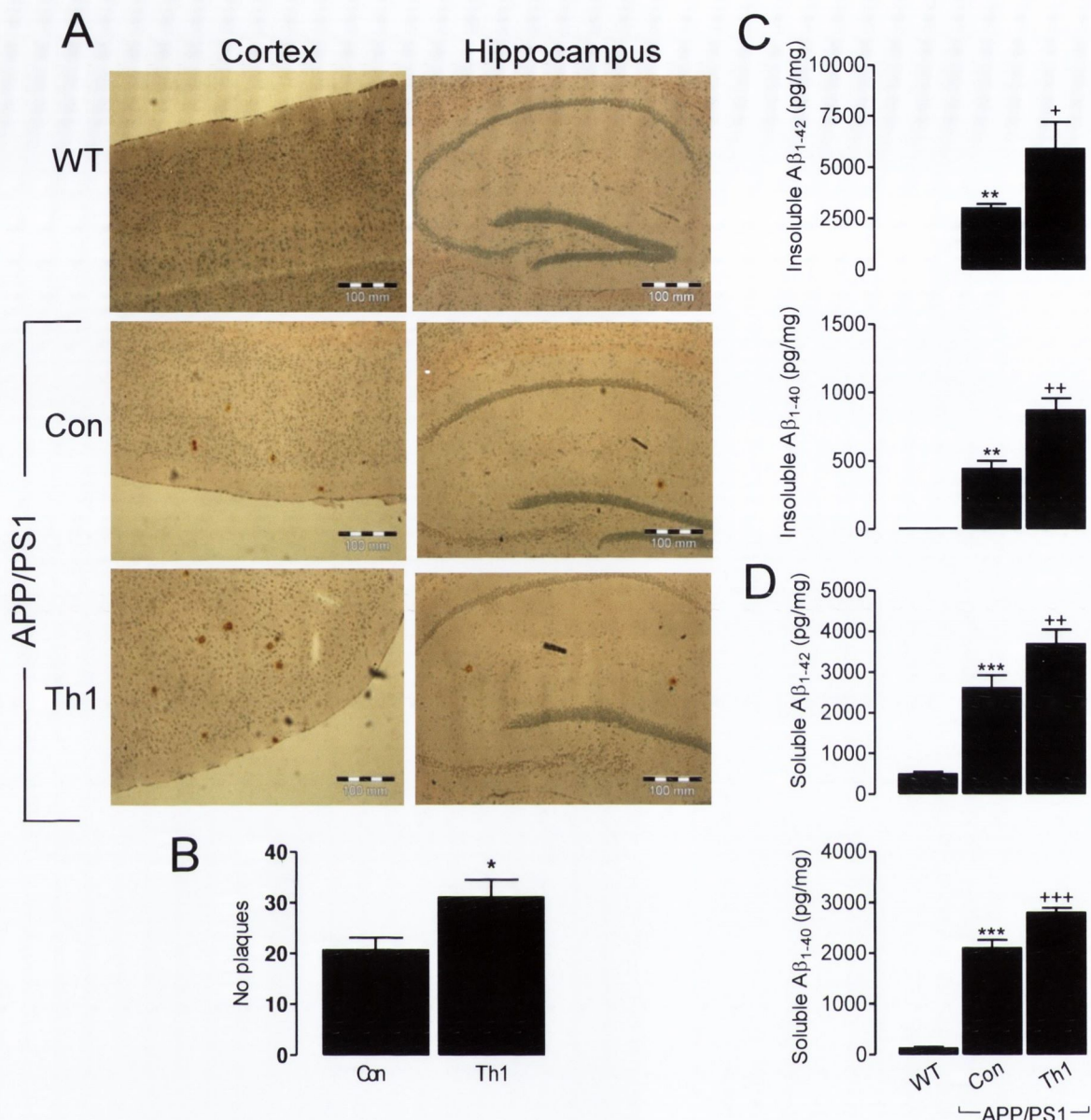


Figure 3.17 Aβ-specific Th1 cells increase Aβ deposition in APP/PS1 mice.

Aβ-specific Th1 cells were generated and injected i.v. into APP/PS1 mice. Mice were sacrificed 3 weeks post-injection, cryostat sections were stained with Congo red to assess Aβ plaques in hippocampus and frontal cortex (A), the average number of plaques per mouse was recorded (B). Amyloid levels were determined by Meso Scale from snap-frozen cortical tissue. The concentrations of insoluble Aβ₄₀ and Aβ₄₂ (C), soluble Aβ₄₀ and Aβ₄₂ (D) were established with reference to the standard curves. (B) * $p < 0.05$; Student's *t*-test for independent means. (C and D) * $p < 0.05$, ** $p < 0.01$, *** $p < 0.001$; ANOVA, APP/PS1 versus WT; + $p < 0.05$, ++ $p < 0.01$, +++ $p < 0.001$; ANOVA versus control untreated APP/PS1 mice ($n = 5-6$); representative of 2 experiments. Con, Control. These data were generated by Dr. Keith McQuillan who has kindly given me permission to also include here. They appear in his thesis in Figure 5.15.

3.3 Discussion

The influence of T cells on neuroinflammation was assessed *in vitro* and *in vivo*. The data demonstrates that Th1 cells are capable of inducing a pro-inflammatory response from purified microglia and astrocytes in culture, whereas Th17 cells preferentially activate astrocytes. Transfer of A β -specific Th1 cells resulted in increased infiltration of IFN- γ ⁺ T cells into the brains of APP/PS1 mice, which was accompanied by increased A β -containing plaque deposition.

A number of studies have demonstrated T cell-induced activation of microglia in mixed glial cultures (McQuillan et al., 2010; Murphy et al., 2010) and in astrocytic cultures (Constantinescu et al., 2005; Kort et al., 2006; Nikceovich et al., 1997; Soos et al., 1999; Soos et al., 1998; Tan et al., 1998), though many of these experiments have examined this interaction in the context of MS using myelin-specific T cells. In relation to AD, the effect of A β -specific Th1 cells on purified microglia and astrocytes has not been previously examined. The results described here show that microglia and astrocytes are activated following co-incubation with A β -specific or α CD3/ α CD28-activated Th1 cells. A β -specific Th1 cells induced a significant production of the pro-inflammatory cytokines IL-6 and TNF α from both purified microglia and astrocytes, and this was accompanied by increased expression of CD40 on the glial cells. This is consistent with previous studies from this laboratory where A β -specific Th1 cells increased co-stimulatory molecule expression and pro-inflammatory cytokine release from A β -activated microglia in mixed glial cultures (McQuillan et al., 2010). As pro-inflammatory cytokines can induce the production of A β *in vitro* when IFN- γ is present (Liao et al., 2004; Sastre et al., 2008), this may explain why transferred A β -specific Th1 cells increase microglial activation and A β accumulation in APP/PS1 mice. Conversely, A β -specific Th17 cells only induced IL-6 release from astrocytes, and α CD3/ α CD28 activated Th17 cells increased the expression of CD40 on astrocytes, along with IL-6 production. Astrocytes are a major source of IL-6 within the CNS (Van Wagoner et al., 1999) and it has been demonstrated that IL-17 can enhance IL-6 signalling in astrocytic cultures (Ma et al., 2010), providing an explanation for the finding that astrocytes, and not microglia, are reactive to

incubation with Th17 cells. These results are consistent with a recently published study, where Th1 cells, but not Th17 cells induced CD40 expression on microglia (Prajeeth et al., 2014). Furthermore, treatment of microglia with Th1-derived supernatants resulted in a pro-inflammatory response, whereas the microglial cells were unresponsive to Th17-derived supernatant. As a result, it is possible that the effect of A β -specific Th17 cells on cytokine production from mixed glia *in vitro* (McQuillan et al., 2010) may be a result of Th17 induced astrocytic activation, rather than a primary effect on microglia. However, it is important to note the A β -specific T cells were prepared differently in these studies.

A β -specific Th2 cells did not induce pro-inflammatory cytokines or co-stimulatory molecule expression on microglia or astrocytes, which is consistent in their association with M2, as opposed to M1, activation (Goldmann and Prinz, 2013). Microglia and astrocytes were similarly resistant to α CD3/ α CD28 stimulated Th2 cells. While A β -specific Th2 cells are capable of reducing Th1 induced glial activation *in vitro* (McQuillan et al., 2010), adoptive transfer of these cells was not sufficient to reduce A β -mediated inflammation in the APP/PS1 model (Browne et al., 2013). This is in conflict with a previous study which demonstrated that transfer of A β -specific Th2 cells was protective in 11 month-old APP/PS1 mice by reducing cognitive impairment when assessed 2 months after injection, and also reducing amyloid deposition at blood vessels (Cao et al., 2009). Importantly, there are many differences between these studies ranging from the method used to generate A β -specific T cells, the number of cells transferred and the age of recipient mice.

IFN- γ is a potent inducer of CD40 in microglial cells, with a critical role for TNF α as an intermediary in its induction (Nguyen and Benveniste, 2002). Ligation of CD40 with its ligand (CD40L/CD154) induces increased co-stimulatory molecule expression on APCs, such as MHC class II, CD80, CD86 and, to an even greater extent CD40; this was associated with pro-inflammatory cytokine production which included, but was not limited to, TNF α and IL-6 (Benveniste et al., 2004). It has been reported that incubating microglia with A β increases the expression of CD40, with a significant production of TNF α when these cells were

further treated with CD40L (Tan et al., 1999). Interestingly, APP^{swe} transgenic mice deficient in CD40 or CD40L have decreased amyloid pathology with reduced microgliosis and astrocytosis throughout the brain (Laporte et al., 2006; Tan et al., 2002). The obvious source of CD40L is CD40L-expressing T cells, however, in the absence of T cell infiltration to the CNS another source may be astrocytes, which express CD40L in chronic inflammatory conditions (Calingasan et al., 2002). Tissue prepared from AD patients have increased levels of CD40⁺ microglia, which was co-localised with MHC class II (Togo et al., 2000), where the CD40⁺ microglial cells were also associated with A β -plaques. Microglia treated with CD40L *in vitro* are reported to have decreased phagocytic activity (Townsend et al., 2005), and A β /CD40L treated microglia are more effective APCs to A β -specific T cells. Importantly, the authors suggest that in the presence of T cells, or co-stimulatory molecules, microglia exhibit an APC phenotype poor at phagocytosis, which in combination with pro-inflammatory T cell cytokine production could ultimately lead to enhanced A β deposition. Other reports have confirmed that microglia are capable of phagocytosing amyloid *in vitro*, however this was inhibited in the presence of pro-inflammatory cytokines (Koenigsnecht-Talboo and Landreth, 2005), and ultrastructural analysis of microglia from AD patients was unable to detect any amyloid fibrils in the lysosomal compartment of these cells (Frackowiak et al., 1992). Together with reports that pro-inflammatory cytokines increased the activity of β - and γ -secretases (Liao et al., 2004; Sastre et al., 2008), this suggests that in the AD brain the microglial cells are aiding the production, rather than facilitating the removal, of amyloid. The role of CD40-induced astrocyte activation is not well understood, however, studies in EAE demonstrate that treatment with an α -CD40 antibody reduced disease severity with decreased astrocyte-associated TNF α *in vivo* (Kim et al., 2011).

As predicted, adoptive transfer of GFP⁺ A β -specific Th1 cells revealed that T cells injected into the periphery crossed the BBB and entered the CNS, particularly in APP/PS1 mice. Indeed, a large portion of T cells found in the CNS following i.v. injection were IFN- γ ⁺ which is broadly consistent with the proposal that infiltration of Th1 cells occurs first in EAE and is followed by recruitment of

other immune cells (O'Connor et al., 2008). The number of T cells in the brain was significantly increased in APP/PS1 mice compared with WT mice; this may be due to the presence of A β in the brains of these mice, thus promoting antigen stimulation of the T cells. The expression of chemokines CCL3 and CXCL10 was significantly higher in cortical tissue prepared from the APP/PS1 mice which may facilitate T cell migration across the BBB. CCL3 and CXCL10 have known chemotactic properties (Agostini et al., 2000; Schall et al., 1993) and the expression of these chemokines has been reported in AD (Tripathy et al., 2007; Xia et al., 2000). Importantly, transfer of the A β -specific Th1 cells resulted in increased concentrations of A β in the brains of the APP/PS1 mice (Browne et al., 2013). Transfer of A β -specific Th1 cells also induced behavioural deficits in APP/PS1, compared with WT, mice whereas A β -specific Th17 cells did not induce similar deficits nor did these cells affect the deposition or concentration of A β within the brain (Browne et al., 2013). IFN- γ potently activates microglia (Benveniste et al., 2004; Downer et al., 2009) and, in the presence of other inflammatory cytokines, results in increased production of A β (Liao et al., 2004; Sastre et al., 2008). The importance of IFN- γ is underlined by the finding that neutralisation of IFN- γ attenuated Th1 cell-induced increases in both microglial activation and A β production *in vivo* (Browne et al., 2013). As A β also activates microglia (Clarke et al., 2007; Lyons et al., 2007a) it is possible that further activation with IFN- γ ⁺ Th1 cells results in chronic microglial activation leading to the enhanced production of A β with behavioural deficits in a feedback cycle.

These results are at variance with a recent study in which i.c.v. injection of A β -specific Th1 cells reduced plaque load in APP/PS1 mice when assessed 28 days post injection (Fisher et al., 2014). While the experimental design was different between the two studies, the authors suggest that by injecting the cells directly into the ventricle the T cells crossed at the ependymal layer of the ventricle only, therefore the brain's vasculature and epithelial layers were spared from T cell interaction, activation and resulting pathology. Fisher and colleagues, (Fisher et al., 2014) proposed that bypassing this step of cellular infiltration into the parenchyma allows the T cells to secrete a variety of proteins including

cytokines and neurotrophic factors, which ultimately prove beneficial to the APP/PS1 mice under these circumstances.

The results observed within this chapter go some way in explaining why immunization with synthetic A β ₄₂ in the AN1792 trial induced aseptic meningoencephalitis in some patients, and CD4⁺ and CD8⁺ T cell infiltration into the brain. While the vaccination was successful at reducing plaque deposition and behavioural impairments in animal models of AD (Janus et al., 2000; Schenk et al., 1999), the adjuvant used in these models was Freund's adjuvant. The adjuvant administered to AD patients, QS-21, induces an IFN- γ ⁺ Th1 response, but also results in greater TNF α production and T cell proliferation to the A β ₆₋₂₀ peptide (which contains the A β T cell epitope in mice (Wiessner et al., 2011)) than that induced by Freund's adjuvant (Cribbs et al., 2003). IFN- γ -secreting Th1 cells, as demonstrated by the data in this chapter, induces considerable microglial and astrocytic activation *in vitro*, and *in vivo* (Browne et al., 2013), ultimately resulting in enhanced A β deposition in APP/PS1 mice. Though the AN1792 trial failed, the data still proved encouraging for immunotherapy as a long term treatment for AD. Patients who developed anti-AN1792 antibodies had reduced functional decline compared with those that received the placebo (Vellas et al., 2009) which corresponds to the behavioural improvements demonstrated in the animal models (Janus et al., 2000). A β immunization with other adjuvants such as alum has proven successful in the Tg2576 model, though only when the vaccine was administered before plaque development (Asuni et al., 2006). Therefore an adjuvant which induces a Th2 based response, could prove more effective and importantly, safer for AD patients. Research is ongoing into other methods of immunization against A β and include passive immunization i.e. i.v. injecting anti-A β antibodies or injections of concentrated immunoglobulins (IVIg) from healthy individuals, to DNA immunization (Lambracht-Washington and Rosenberg, 2013; Wilcock and Colton, 2008). An important caveat in these studies is that treatment in clinical trials often starts too late. Amyloid deposition occurs in humans decades before the cognitive deficits of AD become apparent. Intervention at this late stage may slow disease

progression at best, highlighting the need for early, preclinical treatments of the disease.

Together, these results implicate Th1 cells in exacerbating neuroinflammation as a result of their interaction with microglia and astrocytes, whereas increased Th17 cell infiltration to the brain may enhance astrocyte-mediated neuroinflammation. It was observed that Th1 cells increased CD40 expression on both microglia and astrocytes, along with TNF α and IL-6 production into the supernatant. However, Th17 cells induced CD40 expression and IL-6 release from astrocytes alone. A β -specific Th1 cells had a similar effect on these cells by inducing cytokine release from the two glial populations, whereas A β -specific Th17 cells induced IL-6 release from astrocytes only. Incubation with Th2 cells had no effect on microglia or astrocytes. Transfer of A β -specific Th1 cells to APP/PS1 mice resulted in increased concentration and deposition of A β , which was associated with enhanced IFN- γ ⁺ T cell migration into the brain. Importantly, the proximity of A β plaques with microglia and astrocytes in the CNS provides increased opportunities for antigen stimulation of A β -specific T cells, thereby potentiating the neuroinflammation already observed at this age, and ultimately results in enhanced amyloid pathology.

Table 3.1 Results summary of microglial or astrocytic activation following incubation with T cells *in vitro*

	Marker	Th1	Th2	Th17
Microglia	TNF α	↑		
	IL-6			
	CD40	↑		
Astrocyte	TNF α	↑		
	IL-6	↑↑↑		↑↑
	CD40	↑↑		↑

Table 3.2 Results summary of microglial or astrocytic activation following incubation with A β -specific T cells *in vitro*

	Marker	A β Th1	A β Th2	A β Th17
Microglia	TNF α	↑↑↑		
	IL-6	↑		
	CD40			
Astrocyte	TNF α	↑↑↑		
	IL-6	↑↑		↑↑
	CD40			

Chapter 4

Infection with *B. pertussis* induces T cell infiltration and A β deposition in the brains of older APP/PS1 mice

4.1 Introduction

AD is the most common neurodegenerative disease and accounts for over two-thirds of all dementia cases. It is a progressive disease characterised by NFTs and deposits of A β . These protein deposits are associated with dystrophic neurons, reactive astrocytes and activated microglia. It is estimated that AD affects about 20 million people worldwide, and this figure is expected to reach over 100 million by 2050 (Williams, 2009).

Although the aetiology of AD is unknown, there is evidence to suggest that inflammatory responses play a role in the pathogenesis of AD (Mattson, 2004; Weiner and Frenkel, 2006). Pro-inflammatory cytokines and chemokines are increased in the post-mortem brains of AD patients or in animal models of AD (Akiyama et al., 2000; Streit et al., 2001). Activated microglia have been found in the brain of AD patients with dementia or patients with MCI (Cagnin et al., 2001; Okello et al., 2009) and these cells secrete pro-inflammatory cytokines, such as IL-1 β and TNF α . These cytokines promote expression and activity of β -secretases and γ -secretases (Liao et al., 2004; Sastre et al., 2008) and therefore microglial activation may contribute to deposition of A β and progression of AD (Glass et al., 2010). Activated microglia exhibit increased expression of MHC class II, CD40, CD80 and CD86 (Aloisi et al., 2000b; McQuillan et al., 2010) and, in AD, there is increased MHC class II and CD40 expression on microglia associated with A β plaques (McGeer et al., 1987; Togo et al., 2000), indicating enhanced APC function. Interestingly, there have been a number of reports demonstrating the presence of T cells in the brain of AD patients (Hartwig, 1995; McGeer et al., 1989; Parachikova et al., 2007; Pirttila et al., 1992; Togo et al., 2002; Town et al., 2005), since the original observation over 25 years ago (Rogers et al., 1988). Furthermore, inflammatory IFN- γ -secreting Th1 cells and IL-17-secreting Th17 cells have been shown to infiltrate the brain of aged APP/PS1 mice (Browne et al., 2013).

Although the environmental factors that precipitate the neurological changes associated with the development of AD are unclear, it has been suggested that infectious agents may be involved. HSV-1 and *C. pneumonia*, as

well as antibodies against these pathogens, have been found in the post-mortem brains (Hammond et al., 2010) or intrathecal samples (Wozniak et al., 2005) of AD patients. Indeed HSV-1 infection has been suggested to be a risk factor in carriers of the gene for APOE4 (Honjo et al., 2009; Itzhaki et al., 2004), while viral load is related to ApoE dosage especially ApoE4 (Burgos et al., 2006), and spirochetes particularly *B. burgdorferi* and oral *Treponema* (Honjo et al., 2009) and CMV (Barnes et al., 2014; Lurain et al., 2013) have also been implicated as playing a role in the pathogenesis of AD. Furthermore, a number of studies have shown that infections can accelerate cognitive decline in AD patients (Holmes et al., 2009; Holmes et al., 2003), but there is little understanding of the mechanisms which underlie this effect. Animal studies have revealed that intranasal inoculation of mice with *C. pneumoniae* induced AD-like changes in brain, with evidence of deposits of fibrillar A β associated with reactive glia in several brain areas including the hippocampus (Little et al., 2004). Similarly, peripheral challenge with the TLR agonists, LPS or poly I:C induced amyloid pathology in some (Krstic et al., 2012; Sheng et al., 2003), but not all (Kitazawa et al., 2005) animal models of AD. However, activation of the immune system may also prove beneficial in AD as administration of a vaccine (Butovsky et al., 2006; Olkhanud et al., 2012; Schenk et al., 1999) or TLR agonist (Michaud et al., 2013) was effective in clearing A β load and in some cases, preventing cognitive decline in mice. It has also been suggested that bone marrow-derived dendritic cells (Butovsky et al., 2007) and bone marrow-derived microglia-like cells (Simard et al., 2006) have an important role in plaque clearance.

In this study the influence of a peripheral infection with a respiratory pathogen *B. pertussis* on AD-like pathology was examined in APP/PS1 mice. *B. pertussis* is a Gram-negative bacteria that causes whooping cough, a persistent and sometimes fatal disease in young children, but also an emerging problem in adults and older people. Recent studies have shown that the prevalence of *B. pertussis* infection is high in adults and increasing at a significant rate, especially in those over 65 (Weston et al., 2012).

Study aims

The aims of this study were:

- 1) To establish whether APP/PS1 mice were more susceptible to the effects of a peripheral infection than WT animals.
- 2) To determine whether there was an age-related vulnerability to any infection-induced changes in APP/PS1 mice.
- 3) To investigate whether any change in AD-like pathology was accompanied by infiltration of peripheral immune cells.

4.2 Results

4.2.1 Respiratory infection promotes T cell infiltration into the brains of

APP/PS1 mice

Young (4 months) and older (10 months) WT and APP/PS1 mice were infected with *B. pertussis* by aerosol challenge with live bacteria. Evidence of successful infection was provided by performing CFU counts on lung homogenates removed from groups of mice 3 h and 21 days after challenge. The mean CFU counts were \log_{10} 4.7 and 3.0 at 3 h and 21 days respectively, which is consistent with previous studies from this laboratory (Dunne et al., 2010; Ross et al., 2013). Mice were killed 56 days post-infection, 3 weeks after the pathogen is normally cleared (McGuirk et al., 1998), thus the mice were 6 or 12 months-old at cull, and brain tissue was prepared for flow cytometry to assess infiltration of immune cells. The number of CD45⁺CD3⁺ T cells was doubled in brains of 12 month-old compared with 6 month-old mice, but was significantly greater in older *B. pertussis*-infected APP/PS1 mice when compared with genotype, age or non-infected controls (Fig 4.1A). Analysis of the T cell subtypes also showed that infection with *B. pertussis* caused a significant increase in the number of CD4⁺ and CD8⁺ T cells in the brain of older APP/PS1 mice (Fig 4.1B, C respectively) and there was an age-related increase in the number of CD8⁺ T cells in APP/PS1 mice at 12 months (Fig 4.1C). Intracellular cytokine staining revealed that a proportion of the brain infiltrating CD4⁺ T cells were IFN- γ ⁺ with overall significant increase in Th1-type cells in *B. pertussis*-infected mice (Fig 4.2A). Interestingly there was a significant increase in the number of IL-17⁺ and IFN- γ ⁺IL-17⁺ CD4⁺ T cells in *B. pertussis*-infected mice (Fig 4.2B, C). Similar results were obtained for CD8⁺ T cells, with an infection-induced increase in CD8⁺IFN- γ ⁺ T cells, especially in the older APP/PS1 mice (Fig 4.3A). The number of infiltrating IL-17⁺ and IFN- γ ⁺IL-17⁺ CD8⁺ T cells was also enhanced in brains of infected mice (Fig 4.3B, C).

There was also a significant increase in the number of CD45⁺NK1.1⁺CD3⁺ T cells in the brain of 12 month-old *B. pertussis*-infected APP/PS1 mice (Fig 4.4A)

and parallel significant increases in the numbers of these cells which were IFN- γ ⁺ (Fig 4.4B) and IL-17⁺ (Fig 4.4C).

The location of T cells was determined by staining cryostat sections for CD3 before assessment by confocal microscopy. CD3⁺ T cells were found throughout the hippocampus of older *B. pertussis*-infected APP/PS1 mice (Fig 4.5). Importantly, many of these cells were observed in the brain parenchyma.

The expression of chemokines, which are chemoattractant for T cells, was assessed using RNA extracted from snap-frozen cortical tissue. CCL3 was significantly increased in APP/PS1 mice even at 6 months and expression increased further with age, particularly in *B. pertussis*-infected APP/PS1 mice (Fig 4.6A). CXCL10 was significantly increased in older APP/PS1 mice (Fig 4.6B) and CCL5 expression was also increased in older APP/PS1 mice, especially after exposure to infection (Fig 4.6C).

4.2.2 Increased microglial and macrophage activation in previously infected APP/PS1 mice

Having demonstrated that peripheral infection promoted Th1 and Th17 infiltration into the brain, the effect of *B. pertussis* infection on microglia and astrocytes was assessed. Expression of CD11b mRNA, which is a marker of microglial activation, and GFAP mRNA, which is a marker of astrocytic activation, were increased in the cortex of 12 month-old APP/PS1 mice as previously reported (Gallagher et al., 2012; Gallagher et al., 2013), and infection with *B. pertussis* further increased expression of both markers (Fig 4.7A, B). In addition, the number of CD11b⁺CD45^{low} microglia expressing CD68 was increased in tissue prepared from 12 month-old APP/PS1 mice and this number was significantly enhanced post-infection in the older APP/PS1 (Fig 4.8B).

The expression of CD80 on microglia and macrophages was assessed as an indicator of their antigen-presenting capability and the number of CD11b⁺CD45^{low} microglia expressing CD80 was significantly increased in APP/PS1

mice, particularly older infected APP/PS1 mice, with an overall genotype effect observed (Fig 4.8A). The number of CD11b⁺CD45^{high}CD80⁺ macrophages was also significantly increased in preparations from older *B. pertussis*-infected APP/PS1 mice (Fig 4.9A). Mirroring the changes observed in microglia, infection caused a significant increase in the number of CD68⁺ macrophages in the older APP/PS1 mice, though infection also increased the number of these cells in younger *B. pertussis*-infected APP/PS1 mice (Fig 4.9B).

Activated microglia and macrophages produce inflammatory cytokines and, consistent with this, it was found that expression of TNF α , IL-1 β and IL-6 mRNA was significantly increased in cortical tissue prepared from older *B. pertussis*-infected APP/PS1 mice (Fig 4.10A-C); IL-1 β mRNA was also significantly increased in the older uninfected APP/PS1 mice (Fig 4.10B).

4.2.3 Infection enhances A β accumulation in aged APP/PS1 mice

Deposition of A β has been reported in APP/PS1 mice as young as 6 months of age (Jankowsky et al., 2004). Consistent with this, A β -containing plaques were found in the hippocampus and the frontal cortex in cryostat sections prepared from 6 month-old mice (Fig 4.11). Plaque number was significantly increased with age and interestingly, the number of A β -containing plaques was further significantly increased in both the hippocampus and frontal cortex of older mice post-infection with *B. pertussis* (Fig 4.11B, D). Analysis of insoluble A β ₄₀ and A β ₄₂ provided further evidence of age-related increases that were exacerbated in *B. pertussis*-infected older APP/PS1 mice (Fig 4.12C, D). Although soluble A β ₄₀ and A β ₄₂ both increased in an age-related manner (Fig 4.12A, B), no additional effect of infection was observed. These findings demonstrate that a peripheral infection of older APP/PS1 mice can enhance inflammatory T cell infiltration into the brain and this is associated with the enhanced A β burden.

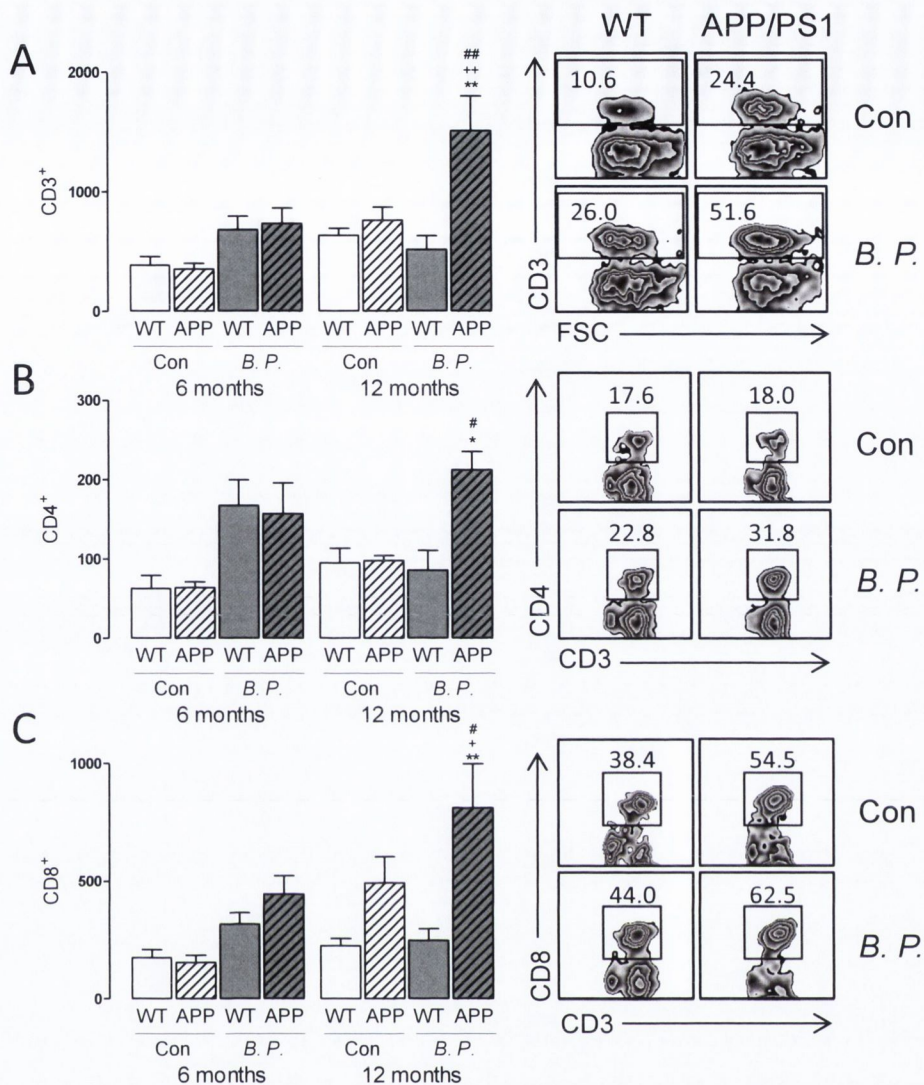


Figure 4.1 Infection induces T cell infiltration into the brain of older APP/PS1 mice.

Mice were infected with *B. pertussis* and culled 56 days post-infection. Mononuclear cells were isolated from the brains of WT and APP/PS1 mice, stained with LIVE/DEAD®, and surface-stained for CD45, CD3, CD4 and CD8. Flow cytometric analysis was performed. Results are mean absolute number of the indicated cells in the brain, with sample FACS plots of (A) CD45⁺CD3⁺ T cells, (B) CD45⁺CD3⁺CD4⁺ T cells and (C) CD45⁺CD3⁺CD8⁺ T cells where numbers in quadrants are percentage of positive cells. (A) CD45⁺CD3⁺ T cells; Age x genotype x infection interaction * $p < 0.05$, $F_{(1,43)}=4.22$; 3-way ANOVA. (B) CD45⁺CD3⁺CD4⁺ T cells; Infection effect *** $p < 0.001$, $F_{(1,41)}=16.68$; 3-way ANOVA. (C) CD45⁺CD3⁺CD8⁺ Age x genotype interaction ** $p < 0.01$, $F_{(1,42)}=8.56$ and infection effect ** $p < 0.01$, $F_{(1,42)}=9.91$; 3-way ANOVA. * $p < 0.05$, ** $p < 0.01$ in comparison to relevant genotype control; + $p < 0.05$, ++ $p < 0.01$ in comparison to relevant age control; # $p < 0.05$, ## $p < 0.01$ in comparison to relevant infection control; Newman-Keuls post hoc. Data represent means \pm SEM from 3 infection experiments, $n = 6-9$. Con, Control; *B.P.*, *B. pertussis*; FSC, Forward Scatter.

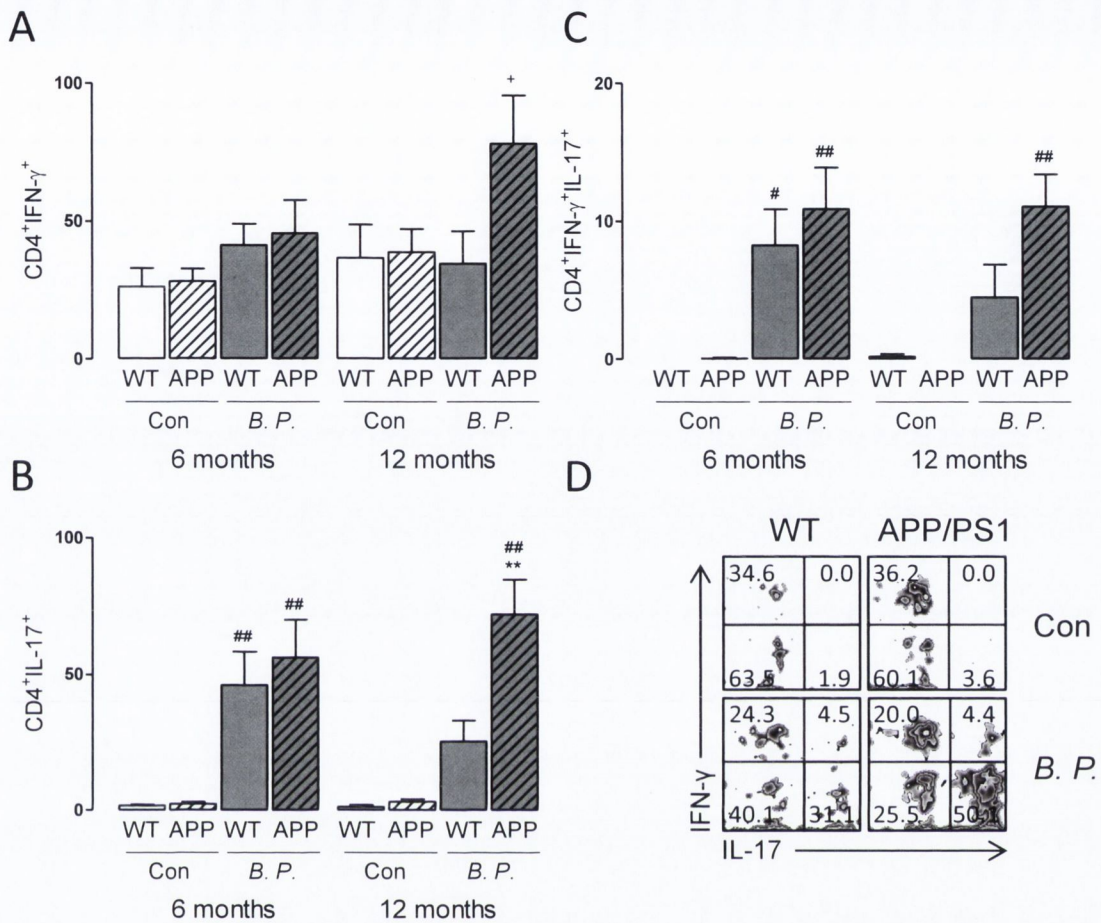


Figure 4.2 Respiratory infection induces IFN- γ ⁺ and IL-17⁺ CD4⁺ T cell infiltration into the brain of APP/PS1 mice.

CD4⁺T cells were intracellularly stained for IFN- γ and IL-17 and assessed by flow cytometry. Results are mean absolute number of the indicated cells in the brain. (A) CD4⁺IFN- γ ⁺; Infection effect * $p < 0.05$, $F_{(1,41)}=5.42$; 3-way ANOVA. (B) CD4⁺IL-17⁺; Genotype x infection interaction * $p < 0.05$, $F_{(1,42)}=4.58$; 3-way ANOVA. (C) CD4⁺IFN- γ ⁺IL-17⁺; Infection effect *** $p < 0.001$, $F_{(1,42)}=38.55$; 3-way ANOVA. ** $p < 0.01$ in comparison to relevant genotype control; + $p < 0.05$, ++ $p < 0.01$ in comparison to relevant age control; # $p < 0.05$, ## $p < 0.01$ in comparison to relevant infection control; Newman-Keuls post hoc. (D) Sample FACS plots of IFN- γ ⁺ and IL-17⁺ CD4⁺ T cells where numbers in quadrants are percentage of positive cells. Data represent means \pm SEM from 3 infection experiments, $n = 6-9$. Con, Control; B.P., *B. pertussis*.

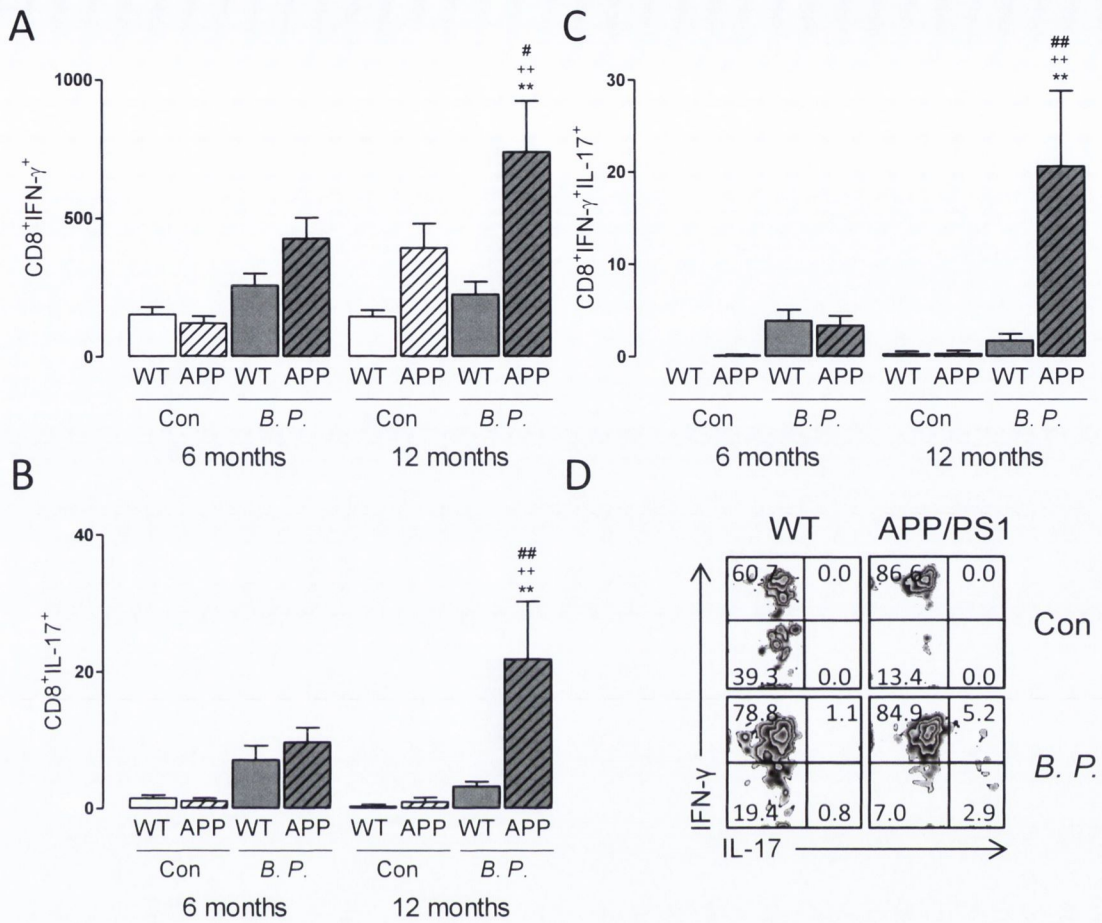


Figure 4.3 Increased IFN- γ ⁺ and IL-17⁺ CD8⁺ T cells in the brains of APP/PS1 mice following infection with *B. pertussis*.

CD8⁺ T cells were intracellularly stained for IFN- γ and IL-17 and assessed by flow cytometry. Results are mean absolute number of the indicated cells in the brain. (A) CD8⁺IFN- γ ⁺; Age x genotype interaction * $p < 0.05$, $F_{(1,42)}=6.66$; 3-way ANOVA. (B) CD8⁺IL-17⁺; Genotype x infection interaction * $p < 0.05$, $F_{(1,42)}=5.46$; 3-way ANOVA. (C) CD8⁺IFN- γ ⁺IL-17⁺; Age x genotype x infection interaction * $p < 0.05$, $F_{(1,43)}=4.32$; 3-way ANOVA. ** $p < 0.01$ in comparison to relevant genotype control; ++ $p < 0.01$ in comparison to relevant age control; # $p < 0.05$, ## $p < 0.01$ in comparison to relevant infection control; Newman-Keuls post hoc. (D) Sample FACS plots of IFN- γ ⁺ and IL-17⁺ CD8⁺ T cells where numbers in quadrants are percentage of positive cells. Data represent means \pm SEM from 3 infection experiments, $n = 6-9$. Con, Control; *B.P.*, *B. pertussis*.

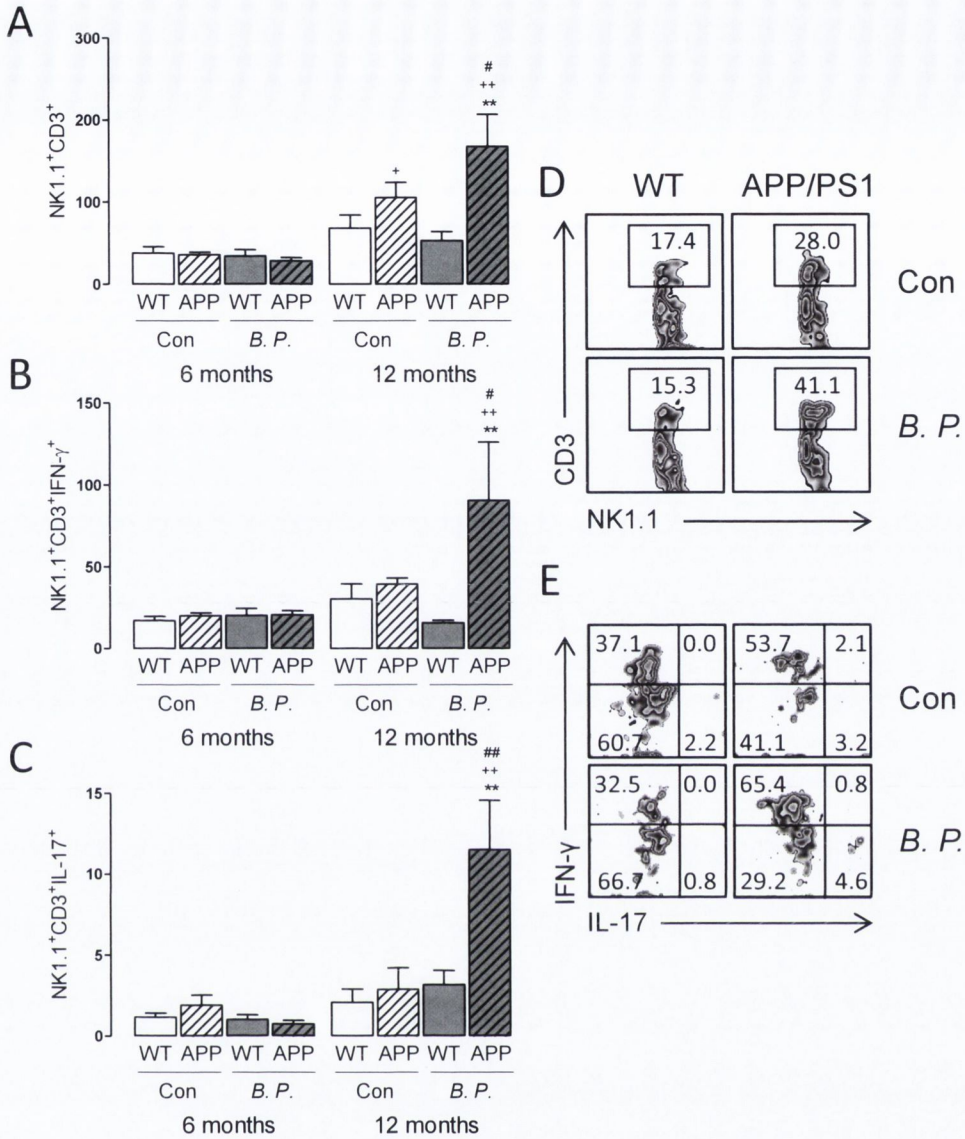


Figure 4.4 Infection with *B. pertussis* increases infiltration of IFN- γ ⁺ and IL-17⁺ NKT cells.

Mononuclear cells were prepared from the brain, stained with LIVE/DEAD[®], and surface-stained for CD45, NK1.1 and CD3. Cells were intracellularly stained for IFN- γ and IL-17, and assessed by FACS. Results are mean absolute number of the indicated cells in the brain. (A) CD45⁺NK1.1⁺CD3⁺ NKT cells; Age x genotype interaction *** $p < 0.001$, $F_{(1,44)}=12.96$; 3-way ANOVA. (B) IFN- γ ⁺ NKT cells; Age x genotype interaction * $p < 0.05$, $F_{(1,40)}=4.56$; 3-way ANOVA. (C) IL-17⁺ NKT cells; Age x genotype x infection interaction * $p < 0.05$, $F_{(1,43)}=6.38$; 3-way ANOVA. ** $p < 0.01$ in comparison to relevant genotype control; + $p < 0.05$, ++ $p < 0.01$ in comparison to relevant age control; # $p < 0.05$, ## $p < 0.01$ in comparison to relevant infection control; Newman-Keuls post hoc. (D) Sample FACS plots of NK1.1⁺ CD45⁺CD3⁺ T cells and (E) IFN- γ ⁺ and IL-17⁺ NKT cells where numbers in quadrants are percentage of positive cells. Data represent means \pm SEM from 3 infection experiments, $n = 6-9$. Con, Control; *B.P.*, *B. pertussis*.

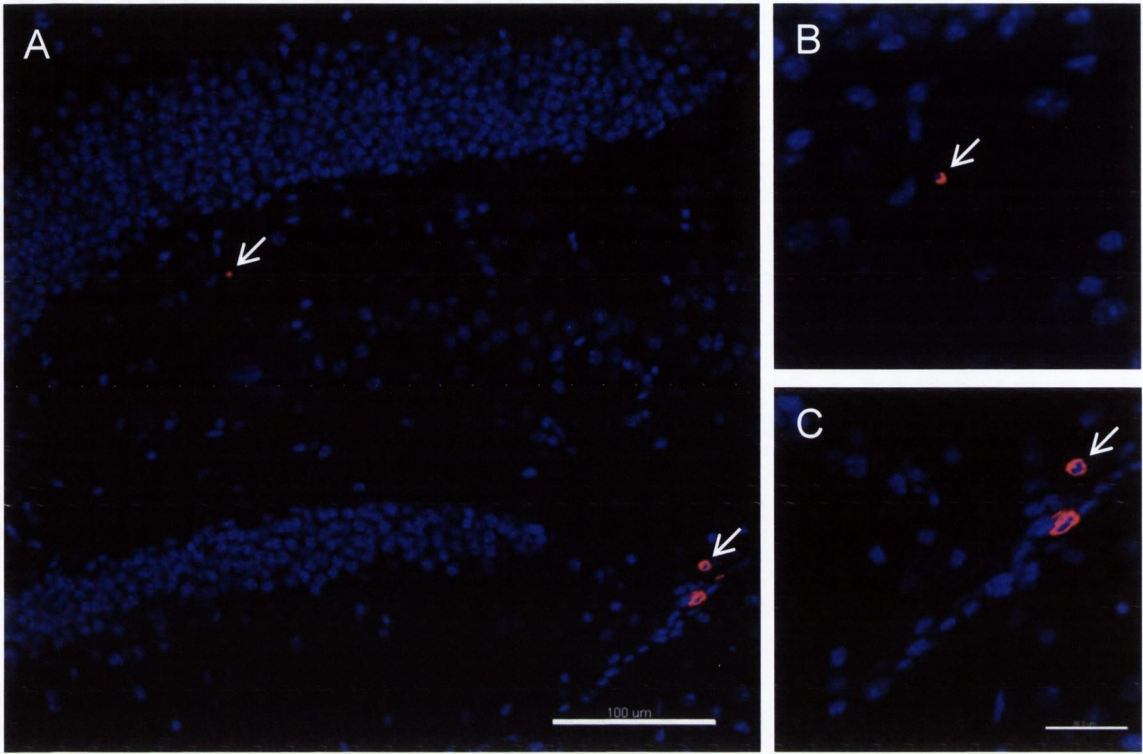


Figure 4.5 T cells infiltrate the hippocampus of *B. pertussis*-infected APP/PS1 mice.

Mice were infected with *B. pertussis* and culled 56 days post-infection. Cryostat sections were stained for CD3 (red) and DAPI (blue) and assessed by confocal microscopy to determine infiltrating T cells in the hippocampus. (A) Original magnification x20, scale bar = 100 μm. (B and C) enlarged panels, scale bar = 30 μm. Data are representative of 3 mice per experimental group.

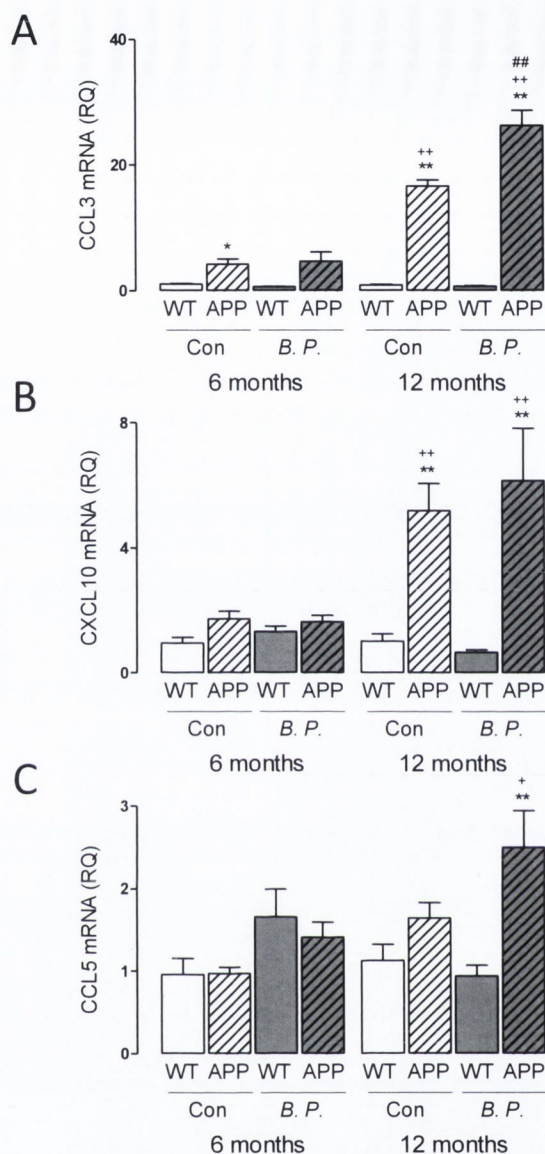


Figure 4.6 Chemokine expression in cortical tissue from older APP/PS1 is exacerbated by infection with *B. pertussis*.

RNA was extracted from snap-frozen cortical tissue 56 days post-infection. (A) CCL3, (B) CXCL10 and (C) CCL5 expression was assessed and values are expressed as relative quantities (RQ) normalised to the endogenous control gene, 18S, and relative to averaged young WT uninfected mice. (A) Age x genotype x infection interaction ** $p < 0.01$, $F_{(1,40)}=7.48$; 3-way ANOVA. (B) Age x genotype interaction *** $p < 0.001$, $F_{(1,41)}=20.13$; 3-way ANOVA. (C) Age x genotype interaction ** $p < 0.01$, $F_{(1,41)}=9.18$ and infection effect * $p < 0.05$, $F_{(1,41)}=5.67$; 3-way ANOVA. * $p < 0.05$, ** $p < 0.01$ in comparison to relevant genotype control; + $p < 0.05$, ** $p < 0.01$ in comparison to relevant age control; ### $p < 0.01$ in comparison to relevant infection control; Newman-Keuls post hoc. Data represent means \pm SEM from 3 infection experiments, $n = 6-9$. Con, Control; B.P., *B. pertussis*.

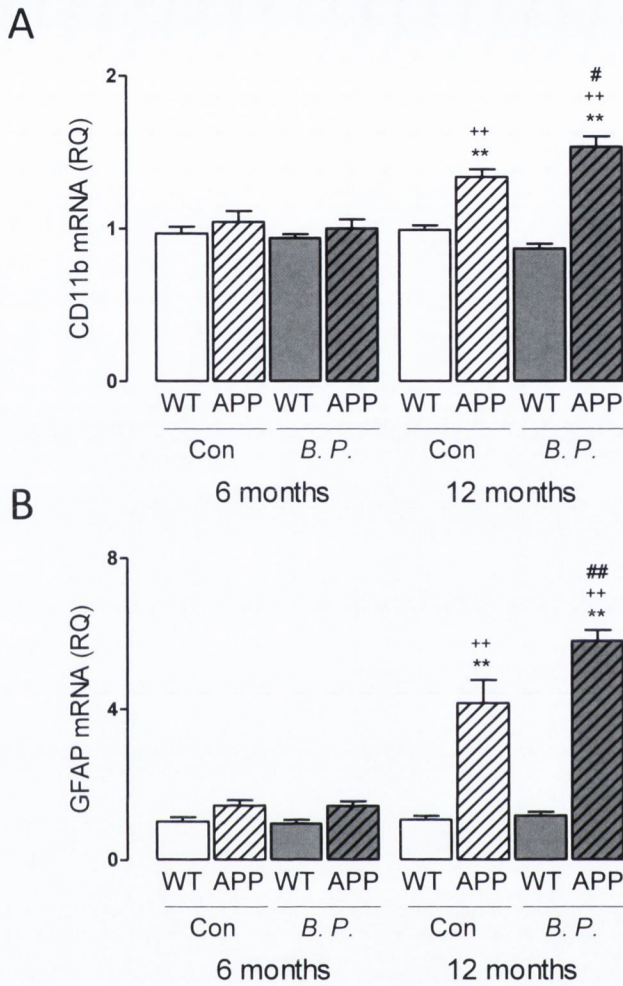


Figure 4.7 CD11b and GFAP expression is enhanced in cortical tissue from older *B. pertussis*-infected APP/PS1 mice.

RNA was extracted from snap-frozen cortical tissue and assessed for (A) CD11b and (B) GFAP expression. Values are expressed as relative quantities (RQ) normalised to the endogenous control gene, 18S, and relative to the averaged young WT uninfected control group. (A) Age x genotype x infection interaction * $p < 0.05$, $F_{(1,43)}=4.09$; 3-way ANOVA. (B) Age x genotype x infection interaction * $p < 0.05$, $F_{(1,42)}=4.26$; 3-way ANOVA. ** $p < 0.01$ in comparison to relevant genotype control; ++ $p < 0.01$ in comparison to relevant age control; # $p < 0.05$, ## $p < 0.01$ in comparison to relevant infection control; Newman-Keuls post hoc. Data represent means \pm SEM from 3 infection experiments, $n = 6-9$. Con, Control; *B.P.*, *B. pertussis*.

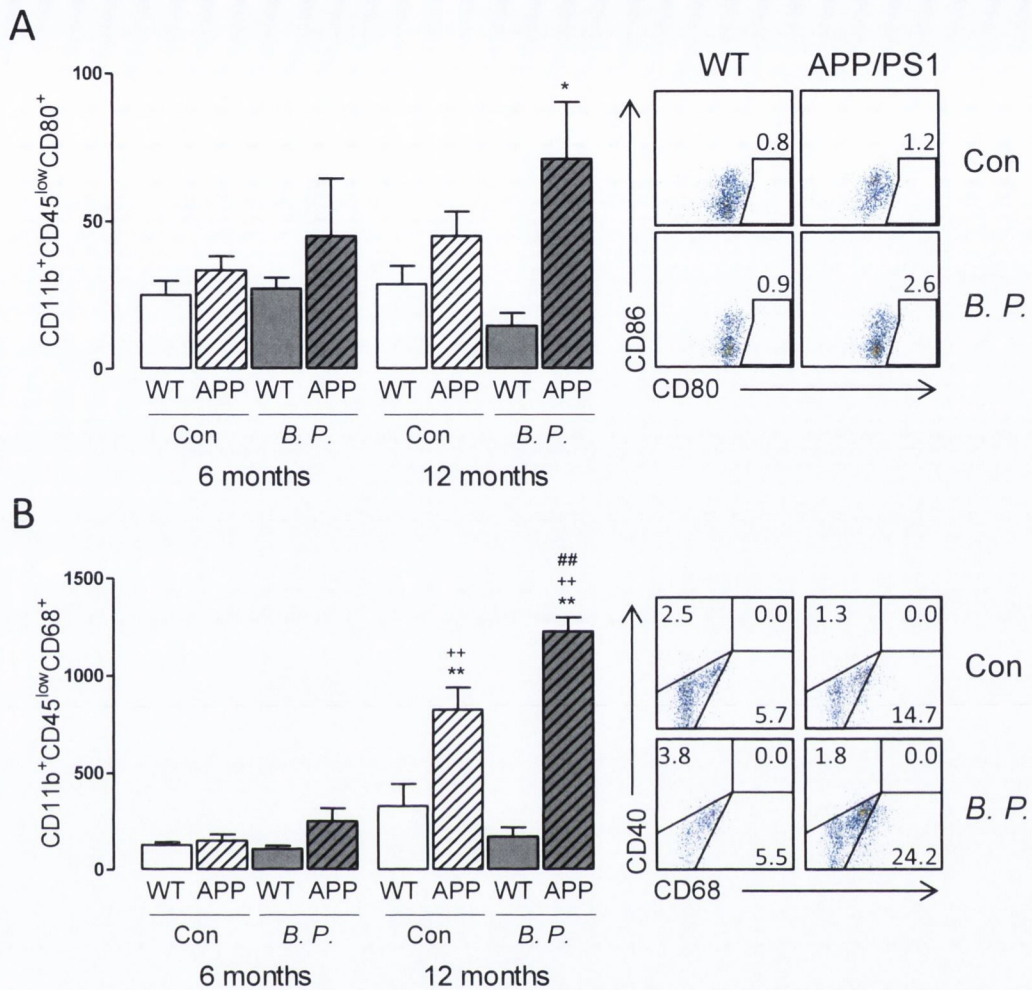


Figure 4.8 Increased microglial activation in APP/PS1 mice.

Mononuclear cells were isolated from the brains of WT and APP/PS1 mice, stained with PI, and surface-stained for CD45, CD11b, CD80 and CD68 and assessed by flow cytometry. Results are mean absolute number of the indicated cells in the brain. (A) CD11b⁺CD45^{low}CD80⁺; Genotype effect ** $p < 0.01$, $F_{(1,42)}=9.69$; 3-way ANOVA, and sample FACS plots of CD11b⁺CD45^{low}CD80⁺ cells. (B) CD11b⁺CD45^{low}CD68⁺; Age x genotype x infection interaction * $p < 0.05$, $F_{(1,43)}=5.53$; 3-way ANOVA and sample FACS plots of CD11b⁺CD45^{low}CD68⁺ cells. * $p < 0.05$, ** $p < 0.01$ in comparison to relevant genotype control; ** $p < 0.01$ in comparison to relevant age control; ### $p < 0.01$ in comparison to relevant infection control; Newman-Keuls post hoc. Numbers in quadrants are percentage of positive cells. Data represent means \pm SEM from 3 infection experiments, $n = 6-9$. Con, Control; B.P., *B. pertussis*.

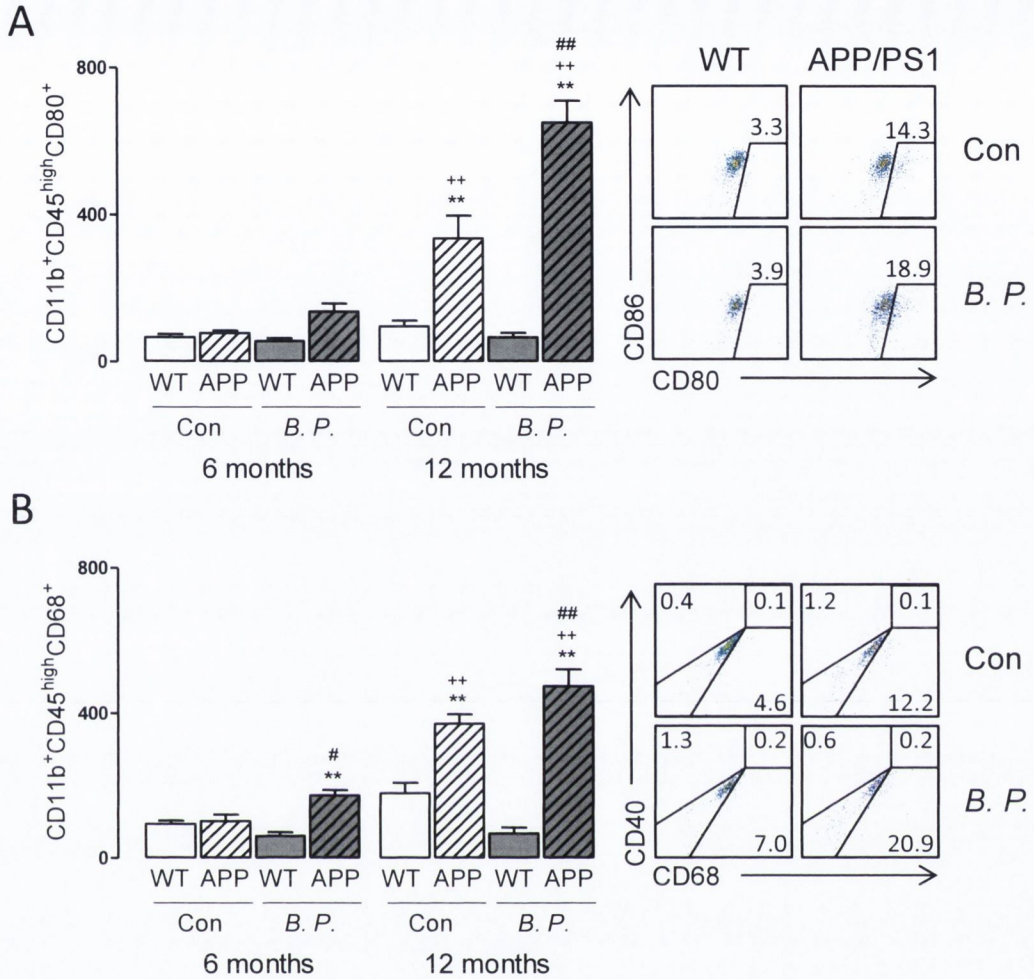


Figure 4.9 The increased macrophage activation in APP/PS1 is exacerbated by infection with *B. pertussis*.

Mononuclear cells prepared from WT and APP/PS1 mice were stained with PI, surface-stained for CD45, CD11b, CD80 and CD68, and assessed by flow cytometry. Results are mean absolute number of the indicated cells in the brain. (A) CD11b⁺CD45^{high}CD80⁺; Age x genotype x infection interaction ** $p < 0.01$, $F_{(1,41)}=10.73$; 3-way ANOVA with sample FACS plots of CD11b⁺CD45^{high}CD80⁺ cells. (B) CD11b⁺CD45^{high}CD68⁺; Age x genotype interaction *** $p < 0.001$, $F_{(1,39)}=50.44$ and genotype x infection interaction *** $p < 0.001$, $F_{(1,39)}=22.62$; 3-way ANOVA and sample FACS plots of CD11b⁺CD45^{high}CD68⁺ cells. ** $p < 0.01$ in comparison to relevant genotype control; ++ $p < 0.01$ in comparison to relevant age control; # $p < 0.05$, ## $p < 0.01$ in comparison to relevant infection control; Newman-Keuls post hoc. Numbers in quadrants are percentage of positive cells. Data represent means \pm SEM from 3 infection experiments, $n = 6-9$. Con, Control; *B.P.*, *B. pertussis*.

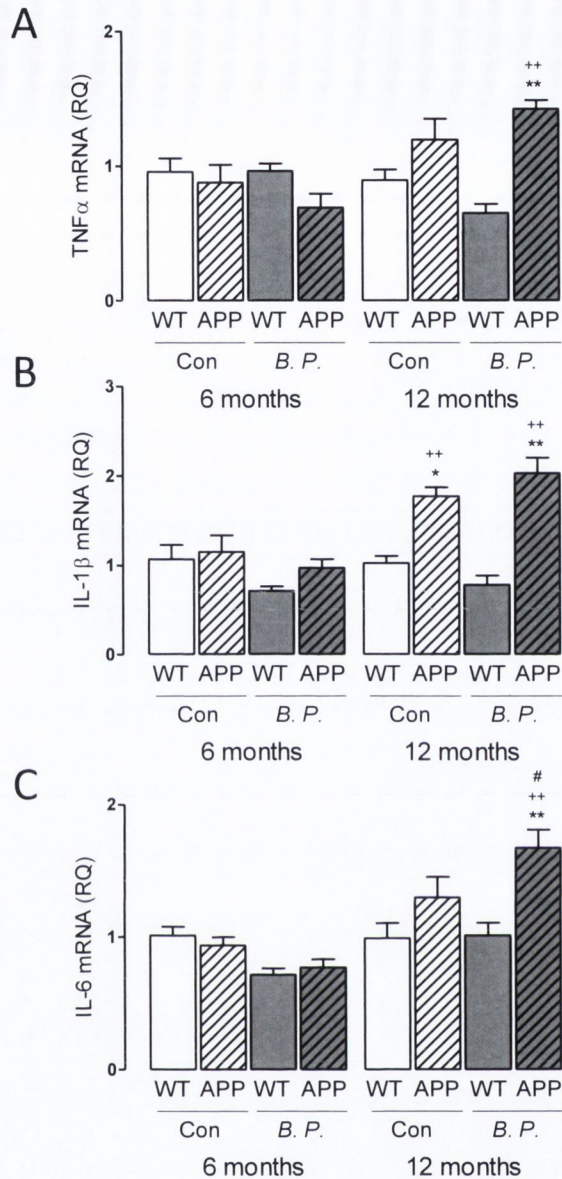


Figure 4.10 Cytokine expression increased in older APP/PS1 mice.

RNA was extracted from snap-frozen cortical tissue and assessed for (A) TNF α , (B) IL-1 β and (C) IL-6 expression. Values are expressed as relative quantities (RQ) normalised to the endogenous control gene, 18S, and relative to the averaged young WT uninfected control group. (A) Age x genotype x infection interaction * $p < 0.05$, $F_{(1,40)}=4.79$; 3-way ANOVA. (B) Age x genotype interaction *** $p < 0.001$, $F_{(1,41)}=17.42$; 3-way ANOVA. (C) Age x genotype interaction *** $p < 0.001$, $F_{(1,42)}=8.56$ and age x infection interaction ** $p < 0.01$, $F_{(1,41)}=11.12$; 3-way ANOVA. * $p < 0.05$, ** $p < 0.01$ in comparison to relevant genotype control; ** $p < 0.01$ in comparison to relevant age control; # $p < 0.05$ in comparison to relevant infection control; Newman-Keuls post hoc. Data represent means \pm SEM from 3 infection experiments, $n = 6-9$. Con, Control; *B.P.*, *B. pertussis*.

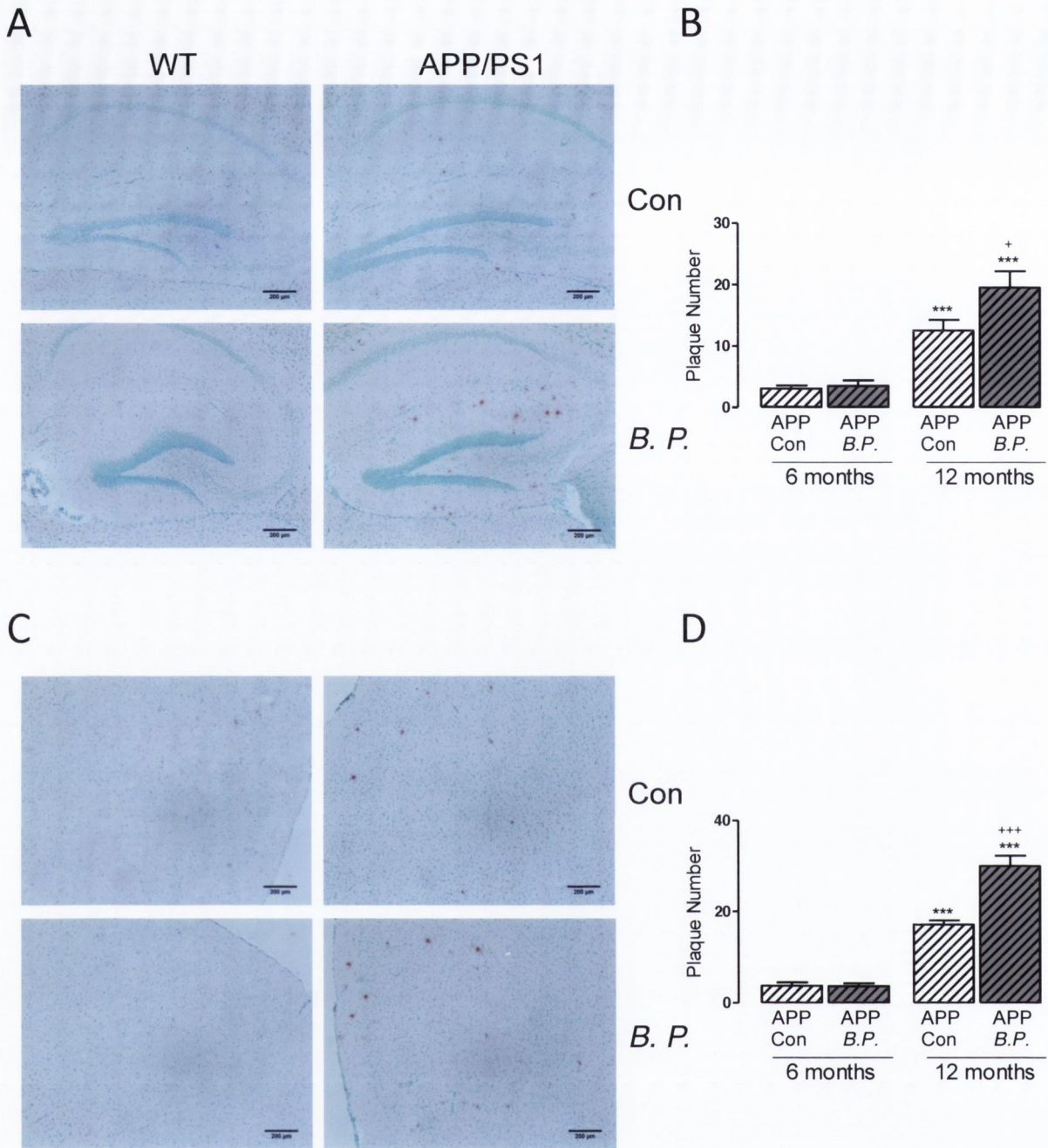


Figure 4.11 Infection increases A β plaque number in older APP/PS1 mice.

Cryostat sections were stained with Congo red to assess A β plaques in hippocampus (A) and frontal cortex (C), the average number of plaques per area of interest per mouse was recorded. (B) Mean number of plaques in the hippocampus; Age x infection interaction * $p < 0.05$, $F_{(1,23)}=4.87$; 2-way ANOVA. (D) Mean number of plaques in the frontal cortex; Age x infection interaction *** $p < 0.001$, $F_{(1,22)}=25.5$; 2-way ANOVA. *** $p < 0.001$ in comparison to relevant age control; + $p < 0.05$, *** $p < 0.001$ in comparison to relevant infection control; Newman-Keuls post hoc. Data represent means \pm SEM from 3 infection experiments, $n = 6-9$. Scale bar = 200 μ m. Con, Control; B.P., *B. pertussis*.

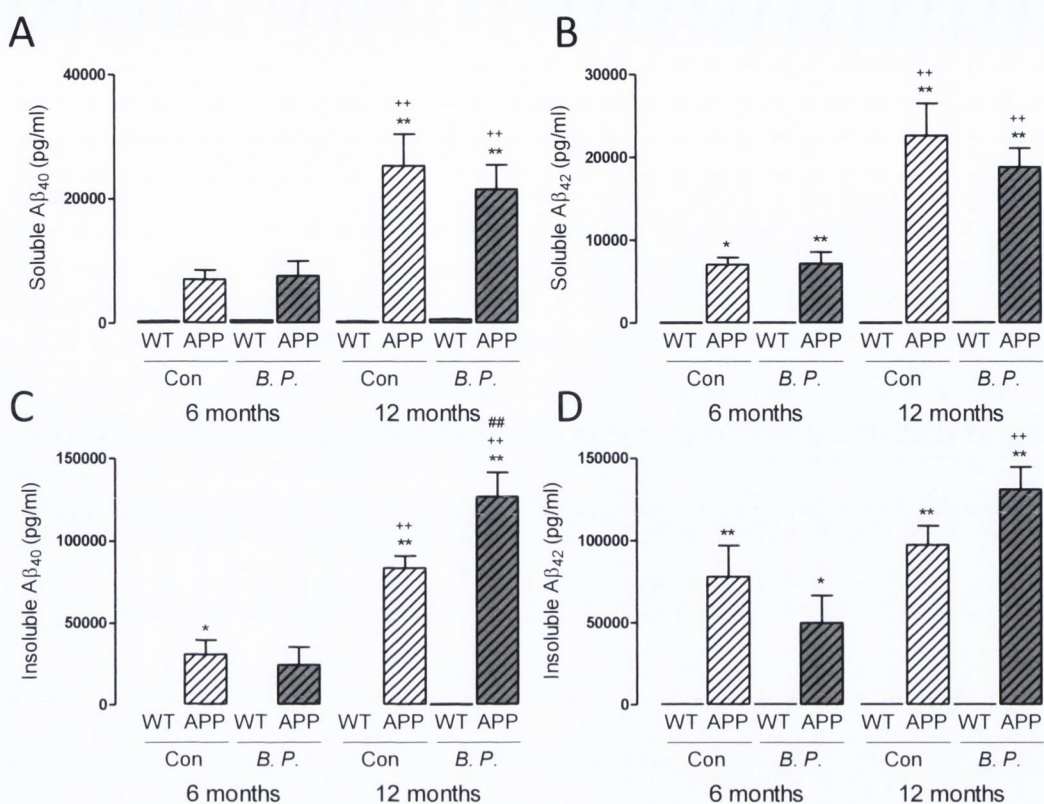


Figure 4.12 Insoluble A β_{40} increased 56 days post-infection in older APP/PS1 mice.

Mice were infected with *B. pertussis* and culled 56 days post-infection. Amyloid levels were determined by Meso Scale from snap-frozen cortical tissue. The concentrations of soluble A β_{40} (A) and A β_{42} (B), insoluble A β_{40} (C) and A β_{42} (D) were established with reference to the standard curves. (A) Age x genotype interaction *** $p < 0.001$, $F_{(1,40)}=22.46$; 3-way ANOVA. (B) Age x genotype interaction *** $p < 0.001$, $F_{(1,41)}=40.32$; 3-way ANOVA. (C) Age x genotype x infection interaction * $p < 0.05$, $F_{(1,43)}=4.99$; 3-way ANOVA. (D) Age x genotype interaction ** $p < 0.01$, $F_{(1,42)}=8.09$; 3-way ANOVA. * $p < 0.05$, ** $p < 0.01$ in comparison to relevant genotype control; ++ $p < 0.01$ in comparison to relevant age control; ## $p < 0.01$ in comparison to relevant infection control; Newman-Keuls post hoc. Data represent means \pm SEM from 3 infection experiments, $n = 6-9$. Con, Control; *B.P.*, *B. pertussis*.

4.3 Discussion

Infection is a risk factor for AD, therefore this study set out to investigate the effect of infection on the brains of APP/PS1 mice in comparison with their WT counterparts, and to establish whether there was an age-related susceptibility to any infection-induced changes. The significant new findings of this study are that infection of mice with a common human pathogen can induce lasting changes in the brain of older APP/PS1 mice. Specifically, a significant number of Th1 and Th17 cells were identified in the brains of 12 month-old APP/PS1 mice, after the resolution of respiratory infection, and this was accompanied by increases in glial activation and A β accumulation. These findings suggest that infection may be a major environmental factor in the progression of AD-like pathology.

T cell infiltration into the brain occurs under normal conditions and was consistently observed in this experiment, however, there was a marked infiltration of T cells, NKT cells and macrophages into the brain of older *B. pertussis*-infected APP/PS1 mice. CD4⁺ T cells and CD8⁺ T cells were detected in the brains of both infected and uninfected, 6 and 12 month-old, WT and APP/PS1 mice but the cell number was markedly enhanced in older *B. pertussis*-infected APP/PS1 mice. It is significant that the changes were observed 3 weeks after the infection is normally cleared, indicating an age- and genotype-related comorbidity. The infiltrating T cells were predominantly IFN- γ ⁺, although infection also triggered infiltration of IL-17⁺ T cells into the brains of mice which were exposed to *B. pertussis*. IFN- γ is a potent activator of microglia (Benveniste et al., 2004; Downer et al., 2009) and IFN- γ ⁺ T cells promote microglial activation *in vivo* (Browne et al., 2013) and *in vitro* (McQuillan et al., 2010) and as demonstrated in Chapter 3. Increased circulation of IFN- γ ⁺ T cells has also been reported in AD (Baglio et al., 2013; Fiala et al., 2005). Although IL-17⁺ T cells play a pivotal role in disease pathogenesis in EAE (Mills, 2008), their role in AD is less clear, though it has been reported that there is a skewing of T cells in AD to a Th17 phenotype (Saresella et al., 2011). The present data demonstrated that IL-17⁺ T cells infiltrate the brain, particularly in older *B. pertussis*-infected APP/PS1 mice. Like A β -specific Th1 cells, Th17 cells induce microglial activation *in vitro* in mixed glial

cultures (McQuillan et al., 2010) and therefore it seems reasonable to suggest that the presence of both IL-17⁺ and IFN- γ ⁺ T cells combine to trigger the marked increase in activated microglia observed in these mice. In this study, many of the T cells in the APP/PS1 brain were CD8⁺IFN- γ ⁺. While the role of CD8⁺ T cells in the progression of AD pathology remains to be established, it has been observed that a large proportion of the infiltrating peripheral cells in the human CNS are CD8⁺ T cells (Ousman and Kubes, 2012). Indeed these cells have been implicated in the progression of MS, with increased numbers of CD8⁺ T cells in the MS brain which were associated with plaques (Friese and Fugger, 2005). Consistent with the findings of the present study, CD3⁺ cells have been identified in brain tissue prepared from 18 month-old APP/PS1 mice, with little observed in 6 month-old APP/PS1 mice (Jimenez et al., 2008).

An increase in CD11b⁺CD45^{high}CD80⁺ and CD11b⁺CD45^{high}CD68⁺ macrophages was also observed in brains of *B. pertussis*-infected older APP/PS1 mice. It has been proposed that infiltrating macrophages play a role in phagocytosis of A β and therefore exert a protective effect (Town et al., 2008). However increased A β deposition paralleled macrophage number in the present study, suggesting that their phagocytic potential was limited despite the fact that expression of CD68, a lysosomal marker and proposed indicator of phagocytic function, was increased on macrophages. IFN- γ ⁺ NKT cells were also present in the brain of *B. pertussis*-infected older APP/PS1 mice. The role of NKT cells in AD has not been addressed although these cells have a protective function in EAE (Mars et al., 2008; Mayo et al., 2012), and in the mutant superoxide dismutase 1 G93A (mSOD1) mouse model of amyotrophic lateral sclerosis (Finkelstein et al., 2011). Overall, the significant finding is that infection drives the infiltration of several IFN- γ ⁺ immune cells particularly in older APP/PS1 mice and the evidence indicates that this is associated, ultimately, with increased A β pathology.

The first evidence suggesting that T cell infiltration occurred in AD was reported over 25 years ago (Rogers et al., 1988) and others have confirmed this observation (Hartwig, 1995; McGeer et al., 1989; Monsonigo et al., 2003; Parachikova et al., 2007; Pirtila et al., 1992; Togo et al., 2002; Town et al., 2005).

Interestingly, these cells have been identified in areas of the brain where amyloid pathology is evident including the hippocampus and limbic regions (Rogers et al., 1988; Togo et al., 2002) and have been found in close apposition to activated microglia (Togo et al., 2002). This suggests the existence of a causal relationship between T cells, microglial activation and amyloid pathology, which is consistent with the current data demonstrating parallel increases in T cell infiltration, microglial activation and increased A β accumulation. Importantly, recent work from this laboratory (part of which appears in Chapter 3) shows that injection of A β -specific Th1 cells into 6-7 month-old APP/PS1 mice induced microglial activation and increased A β deposition (Browne et al., 2013), substantiates this hypothesis.

Infiltration of immune cells may result from the creation of a chemotactic gradient as a consequence of increased expression of chemokines in the brain and this study found that there was an age- and genotype-related increase in expression of CCL3, CXCL10 and CCL5 that was enhanced in *B. pertussis*-infected mice and all 3 chemokines have established lymphocyte chemotactic properties (Agostini et al., 2000; Murooka et al., 2008; Schall et al., 1993). Indeed, increased expression of these chemokines has been reported in AD (Tripathy et al., 2007, 2010; Xia et al., 2000), while increased T cell expression of CCR2, CCR5 and CXCR2 has also been reported (Liu et al., 2010; Man et al., 2007; Reale et al., 2008). Infiltration of immune cells may also be a consequence of increased BBB permeability, which has been observed in aged animals (Blau et al., 2012) and APP/PS1 mice (Minogue et al., 2014) and which is known to occur following *B. pertussis* infection (Linthicum et al., 1982).

AD patients are more vulnerable to the effects of systemic infection with evidence of a significant decline in cognitive function associated with persistent increases in circulating inflammatory cytokines following peripheral infection (Holmes et al., 2009; Holmes et al., 2003). It is also recognized that the risk of developing AD is increased by infection or general ill-health (Dunn et al., 2005; Strandberg et al., 2004; Tilvis et al., 2004), whereas a protective effect of vaccination against infection has been reported (Tyas et al., 2001; Verreault et

al., 2001). Interestingly, the incidence of pertussis is increasing in developed countries, probably due to limited efficacy of the current vaccine and the increase is not only evident in infants, but also in adolescents and adults, including those over 50 (Klein et al., 2012; McGuinness et al., 2013). In the US alone, 29.9% of pertussis cases occurred in adolescents, with over 21% of cases occurring in adults in 2012 (<http://www.cdc.gov/pertussis/surv-reporting.html>).

The effect of peripheral infection on cognitive function was not assessed in this study, however, Takeda and colleagues have reported that LPS injected i.p. enhanced sickness behaviour in APP^{swe} mice (Takeda et al., 2013). Indeed it has been demonstrated that LPS induced memory impairments in WT mice (Lee et al., 2008), and in 3xTg-AD mice (Sy et al., 2011). In the present study, the more profound inflammatory effects induced by infection of older APP/PS1 mice included increased expression of inflammatory cytokines as well as glial activation. These changes were associated with increased concentrations of insoluble A β ₄₀ and A β ₄₂. This suggests that the underlying pathology endows a susceptibility to subsequent infection and enhances pathogenic processes and is broadly consistent with the findings that infection of 3xTg-AD mice with MHV induced marked tau pathology post-infection (Sy et al., 2011). Stahl and colleagues (2006) reported that intracerebral infection of Tg2576 mice with the neurotropic BDV resulted in a decrease in A β -containing plaques in the hippocampus (Stahl et al., 2006), however, A β deposits increased in the walls of cerebral vessels post-infection. An increase in microglial activation and increased expression of inflammatory cytokines was observed, prompting the authors to suggest that an inflammatory environment might enhance clearance of A β , which has been supported by some groups (Wilcock et al., 2011), but not by others (Koenigsknecht-Talboo and Landreth, 2005; Yamamoto et al., 2007). Indeed, it has been shown that an inflammatory environment, such as predominates in AD, inhibits efficient phagocytosis (Koenigsknecht-Talboo and Landreth, 2005) while the interaction of microglia with T cells has also been shown to switch microglia from a phagocytic to an APC phenotype (Townsend et al., 2005). Furthermore, IFN- γ has been shown to increase production of A β fragments (Liao et al., 2004; Sastre et al., 2008), which is important in the

present context because of the increased number of IFN- γ ⁺ cells in the brain of older APP/PS1 mice post-infection.

It is concluded that infection with a common human pathogen has persistent effects on inflammatory changes in the brain, particularly in older APP/PS1 mice. The evidence suggests that these changes are driven by infiltration of IFN- γ ⁺ and IL-17⁺ cells and result in exacerbated A β pathology. The data point to infection as a significant additional factor to the rapid progression of pathology in AD and highlight the importance of vaccination or treatment of infections in the elderly.

Chapter 5

**Treatment with FTY720 during
infection with *B. pertussis* reduces T
cell influx into the lung and
exacerbates the infection**

5.1 Introduction

The experiments in the previous chapter demonstrated that older APP/PS1 mice are more vulnerable to the effects of a respiratory infection, which induced increased T cell infiltration into the brain and ultimately resulted in enhanced A β deposition. Therefore, blocking T cell infiltration during infection with an immunomodulating drug like FTY720 may alleviate the infection-induced plaque burden in older APP/PS1 mice. Before undertaking this experiment it was first important to investigate whether FTY720 had an effect on the ability of mice to resolve infection with *B. pertussis*.

FTY720 is an immunosuppressant first described in 1995, and is derived from a modification of a metabolite isolated from the fungus *Isaria sinclairii* (Adachi et al., 1995; Suzuki et al., 1996). Early studies revealed that FTY720 was capable of prolonging organ graft survival (Brinkmann and Lynch, 2002; Chiba et al., 1996; Chiba et al., 1998; Yanagawa et al., 1998), which correlated with decreased lymphocyte infiltration into the grafted tissues due to the enhanced homing of T cells to the lymph nodes. Further studies demonstrated that FTY720 activates four subtypes of S1P receptors (Brinkmann et al., 2002; Mandala et al., 2002) and that the effects of FTY720 on lymphocyte sequestration are mediated by downregulating the S1P₁ receptor (Matloubian et al., 2004). In 2002 it was documented that FTY720 was effective at inhibiting the development of EAE (Brinkmann et al., 2002) and this has been replicated many times since (Chiba et al., 2011; Choi et al., 2011). After a number of clinical trials (Kappos et al., 2006; Kappos et al., 2010) FTY720 received FDA approval in 2010 for the treatment of MS and is now a widely available therapy for this disease. However, it was noted during the clinical trials that the incidence of lower respiratory tract infections was greater in patients that received FTY720 (Cohen et al., 2010; Kappos et al., 2010). In addition two fatal herpesvirus infections were reported in the phase III clinical trial (Cohen et al., 2010).

Due to the increased incidence of infections in patients taking FTY720, studies have been performed in animal models to examine the host's ability to

clear infection following FTY720 treatment, however, the literature remains conflicted on this issue. It has been reported that chronic treatment with FTY720 impairs the clearance of the enteropathogen *Citrobacter rodentium* (Murphy et al., 2012), the helminth *Nippostrongylus brasiliensis* (Thawer et al., 2014), and the protozoan parasite *Trypanosoma cruzi* (Dominguez et al., 2012). FTY720 treatment also reduces survival following infection with the murine adapted H1N1 influenza virus (Ntranos et al., 2014). FTY720 treatment during immunization impaired the vaccine-mediated protection against mycobacteria induced by the BCG vaccine (Connor et al., 2010). Interestingly, FTY720 does not seem to impair secondary infection (Thawer et al., 2014) or immune challenge when FTY720 treatment begins after vaccination (Connor et al., 2010). However, it has also been reported that FTY720 has no effect on infection with *Leishmania amazonensis* (Lopes et al., 2010). Furthermore, low doses of FTY720 did not alter the course of infection with the lymphocytic choriomeningitis virus (Walsh et al., 2010). In fact, FTY720 alleviates disease in a murine model of cerebral malaria (Finney et al., 2011; Nacer et al., 2012). To date there are no studies that have examined the effect of FTY720 on the progression or clearance of a bacterial infection of the respiratory tract.

B. pertussis is a Gram-negative respiratory pathogen and is the causative agent of whooping cough. *B. pertussis* can infect infants, adolescents and adults (Klein et al., 2012; McGuinness et al., 2013). Importantly, the incidence of infection is increasing worldwide, with recent outbreaks reported in America, Australia and Ireland ((CDC), 2012; Barret et al., 2010; Mills et al., 2014; Roper and Surveillance Branch, 2009). In America alone there were 48,277 reported cases of *B. pertussis* in 2012, a significant increase on the 2,719 cases reported in 1991 (<http://www.cdc.gov/pertussis/fast-facts.html>). In addition, 21.6% of these cases were in adults over 20 years old, with 10% of reported pertussis deaths occurring in adults over 55 years of age. It has been suggested that the incidence of *B. pertussis* is under-reported due to the lack of 'classic' symptoms, notably the inspiratory whoop in adolescents and adults (Cortese et al., 2007). The increasing incidence of *B. pertussis* may be due to increased detection methods, but also due to the short lived immunity generated from the newer Pa, which

replaced Pw approximately 20 years ago, due to safety concerns around the latter (Mills et al., 2014).

On infection, *B. pertussis* binds to the cilia of the trachea, bronchi, and bronchioles (Higgs et al., 2012) and can also be found intracellularly in macrophages and ciliated epithelial cells of the lung (Carbonetti et al., 2007; Hellwig et al., 1999; Lamberti et al., 2010; Paddock et al., 2008). The first cells to respond to *B. pertussis* are resident macrophages and immature DCs within the lung; early in disease these are accompanied by further recruitment and infiltration of DCs and macrophages, followed by NK cells and neutrophils (Byrne et al., 2004; Dunne et al., 2009; McGuirk et al., 1998; Ross et al., 2013). Infiltration of CD4⁺ and CD8⁺ T cells occurs in later stages of infection (McGuirk et al., 1998; Ross et al., 2013). Experiments using SCID mice, that lack mature T and B cells, and nude mice, that lack mature T cells, have revealed the importance of the adaptive immune response in the clearance of infection with *B. pertussis* (Barbic et al., 1997). In addition, Ig^{-/-} mice that lack mature B cells fail to clear infection (Mahon et al., 1997) and mice with an impaired IFN- γ response have persistent bacterial infection (Barbic et al., 1997; Mahon et al., 1997). IL-17 production is also required for effective clearance of the *B. pertussis* bacteria (Dunne et al., 2010; Higgins et al., 2006; Ross et al., 2013). *B. pertussis* produces a range of virulence factors, many of which subvert immune responses of the host. These include FHA and ACT that induce IL-10 production by DCs and macrophages, and IL-10-producing Treg cells which, together, can inhibit pro-inflammatory cytokine production, including IFN- γ , and thus contribute to persistent infection (McGuirk et al., 2002; McGuirk and Mills, 2000; Ross et al., 2004). However, this anti-inflammatory response may also protect the host by limiting infection-induced pathology (Higgins et al., 2003). As a result, infection in mouse models typically takes 35-42 days to clear (Dunne et al., 2010; McGuirk et al., 1998; Ross et al., 2013), though it can last from weeks up to 4 or 5 months in humans (Cortese et al., 2007; McGuinness et al., 2013).

Study aims

The aims of this study were:

- 1) To establish the effect of FTY720 on clearance of a primary infection with *B. pertussis*.
- 2) To investigate whether any changes in the bacterial load of FTY720-treated mice was accompanied by changes in the expansion of T cells in the lymph node or infiltration of T cells into the lung.
- 3) To examine whether FTY720 had a suppressive effect on T cell infiltration into the lung or bacterial clearance following *B. pertussis* challenge of immunised mice.

5.2 Results

5.2.1 Chronic treatment with FTY720 significantly impairs the ability of mice to clear infection with *B. pertussis*

Mice were infected with *B. pertussis* by aerosol challenge. One group was given FTY720 (0.3 mg/kg) daily for the duration of the experiment and treatment began either 3 or 10 days before mice were infected with *B. pertussis*. Vehicle control- and FTY720-treated mice were culled at a number of time points post-challenge. The course of infection was followed by determining the CFU counts at 3 h and 7, 21, 28, 42 and 60 days post-challenge. The mean CFU counts for vehicle control mice infected with *B. pertussis* were consistent with previous studies (Dunne et al., 2010; McGuirk et al., 1998; Ross et al., 2013). Chronic treatment with FTY720 decreased the ability of mice to clear infection, and a significantly higher bacterial load in the lungs of FTY720-treated mice was observed from days 28 to 60 post-challenge. Mice treated with FTY720 had 100-1500-fold more CFU in the lungs at later stages of infection with *B. pertussis* than vehicle control mice (Fig 5.1A, B).

5.2.2 FTY720 treatment significantly suppresses T cell infiltration into the lungs of *B. pertussis*-infected mice

The lungs of FTY720- and vehicle control-treated mice were prepared for flow cytometry to assess infiltration of immune cells. The cells were either stained immediately to determine memory T cell populations or stimulated with PMA, ionomycin and BFA for 5 h to investigate intracellular cytokine production. The number of CD3⁺ T cells in the lung significantly increased following infection with *B. pertussis* in vehicle control mice (Fig 5.2A) but the recruitment of T cells was reduced in FTY720-treated mice. At later stages of infection the total number of CD3⁺ T cells infiltrating the lungs of FTY720-treated *B. pertussis*-infected mice was increased, though not significantly, in comparison with naïve mice (Fig 5.2A). The number of CD3⁺CD4⁺ T cells and CD3⁺CD8⁺ T cells in the lung was significantly increased following infection with *B. pertussis* in vehicle control mice, and these populations were decreased in FTY720-treated mice (Fig 5.2B, C).

The number of CD3⁺ T cells expressing CD4 and CD8 was also assessed following stimulation of cells with PMA, ionomycin and BFA for 5 h. The number of CD3⁺CD4⁺ and CD3⁺CD8⁺ T cells in the lungs of vehicle control mice infected with *B. pertussis* was increased on day 7 but numbers declined thereafter (Fig 5.2F, G). Treatment with FTY720 significantly reduced the number of CD3⁺CD4⁺ T cells and CD3⁺CD8⁺ T cells in the lung following infection with *B. pertussis* (Fig 5.2F, G). Importantly, the T cell numbers in the lung was similar when the analysis was immediate (Fig 5.2A-D) or after 5 h stimulation (Fig 5.2E-H).

It has been demonstrated previously that FTY720 preferentially retains naïve and central memory T cell populations in the lymph node over effector memory cells (Brinkmann et al., 2010; Mehling et al., 2008). Here the number of CD62L⁺ (naïve), CD62L⁺CD44⁺ (T_{CM}) and CD44⁺ (T_{EM}) CD4⁺ T cells was significantly increased in vehicle control *B. pertussis*-infected mice for the duration of the infection (Fig 5.3A). In contrast, the number of naïve CD4⁺CD62L⁺ and CD4⁺CD62L⁺CD44⁺ T_{CM} cells in the lung was significantly lower in FTY720-treated mice following infection with *B. pertussis*, with minimal infiltration of either cell type observed (Fig 5.3A). Almost 95% of all CD4⁺ T cells in the lungs of FTY720-treated mice were CD44⁺ T_{EM} cells (Fig 5.3). The number of CD4⁺CD44⁺ T_{EM} cells was reduced in FTY720-treated mice in comparison with vehicle control-treated *B. pertussis*-infected mice on days 28 and 42 post-challenge, however on day 60 following infection this population of T cells increased significantly in FTY720-treated *B. pertussis*-infected mice (Fig 5.3A). This is in contrast with the vehicle control infected mice, where similar numbers of CD4⁺CD44⁺ T_{EM} cells were present in the lung from day 28 post-challenge (Fig 5.3).

Comparable results were obtained for CD8⁺ T cells, where the infiltration of naïve CD8⁺CD62L⁺, CD8⁺CD62L⁺CD44⁺ T_{CM} and CD8⁺CD44⁺ T_{EM} cells was significantly increased following infection (Fig 5.3B). However, the number of naïve CD8⁺CD62L⁺ and CD8⁺CD62L⁺CD44⁺ T_{CM} cells was significantly lower in the lungs of FTY720-treated *B. pertussis*-infected mice compared with vehicle control-treated *B. pertussis*-infected mice (Fig 5.3B).

The expression of CD49d, a marker of activated T cells, was determined on CD4⁺ and CD8⁺ infiltrating T cells in the lung. The proportion CD4⁺CD49d⁺ T cells was similar in vehicle control- and FTY720-treated *B. pertussis*-infected mice (Fig 5.4A, B), but the absolute number of CD4⁺CD49d⁺ T cells was significantly increased in vehicle control-treated *B. pertussis*-infected mice (Fig 5.5A). The proportion of CD8⁺CD49d⁺ T cells in the lung followed a similar trend, although on day 28 post-challenge, there was a greater proportion of CD8⁺CD49d⁺ T cells in FTY720-treated *B. pertussis*-infected mice than in vehicle control-treated *B. pertussis*-infected mice. A significant increase in the absolute number of CD8⁺CD49d⁺ T cells in the lungs of FTY720-treated *B. pertussis*-infected mice was observed on day 28 only (Fig 5.4). These findings demonstrate that FTY720 prevents infiltration of CD4⁺ and CD8⁺ naïve and T_{CM} cells into the lung. Influx of CD4⁺ T_{EM} cells is considerably delayed with FTY720 treatment, however FTY720 does not affect infiltration of CD8⁺ T_{EM} cells.

To investigate the effect of FTY720 on infiltrating Th1 and Th17 cells into the lung, cells prepared from the lung were stimulated for 5 h with PMA, ionomycin and BFA *ex vivo* and stained intracellularly for IFN- γ and IL-17. There was a considerable influx of IFN- γ ⁺ and IL-17⁺ T cells into the lung following challenge with *B. pertussis* (Fig 5.5). Treatment of mice with FTY720 reduced the numbers of IFN- γ ⁺ and IL-17⁺ CD4⁺ and CD8⁺ T cells in the lung (Fig 5.5).

5.2.3 FTY720 treatment reduces the number of T cells in the mediastinal lymph nodes of *B. pertussis*-infected mice

The mediastinal lymph nodes were also prepared for flow cytometric analysis and cells were either stained immediately to determine memory T cell populations or stimulated for 5 h with PMA, ionomycin and BFA to investigate intracellular cytokine production. The number of CD3⁺, CD3⁺CD4⁺ and CD3⁺CD8⁺ T cells was significantly increased in the lymph nodes of mice infected with *B. pertussis* (Fig 5.6) and FTY720 prevented the infection-induced increase in CD3⁺ and CD3⁺CD4⁺ T cells in the lymph node (Fig 5.6A, B). Analysis of PMA, ionomycin and BFA stimulated cells showed that the number of CD3⁺, CD3⁺CD4⁺ and CD3⁺CD8⁺ T cells in the lymph nodes was significantly lower in FTY720-treated

mice post-infection with *B. pertussis* (Fig 5.6E-G). Stimulation of the lymph node cells did not affect their viability.

The number of naïve CD4⁺CD62L⁺, CD4⁺CD62L⁺CD44⁺ T_{CM} and CD4⁺CD44⁺ T_{EM} cells was increased in the lymph nodes of vehicle control mice on day 28 post-challenge with *B. pertussis* (Fig 5.7A, B), perhaps due to infection-induced T cell expansion. However, FTY720 prevented the infection-induced increase in CD4⁺CD62L⁺ and CD4⁺CD62L⁺CD44⁺ T_{CM}, which remained comparable to uninfected mice (Fig 5.7A, B). On day 60 post-challenge the number of CD4⁺CD62L⁺ and CD4⁺CD62L⁺CD44⁺ T_{CM} cells were comparable in the vehicle control- and FTY720-treated infected groups, although CD4⁺CD44⁺ T_{EM} cells were significantly increased in FTY720-treated *B. pertussis*-infected mice (Fig 5.7E-G).

The number of CD8⁺CD62L⁺, CD8⁺CD62L⁺CD44⁺ T_{CM} and CD8⁺CD44⁺ T_{EM} cells was increased in the lymph nodes 28 days post-challenge with *B. pertussis* (Fig 5.8A-C), although the number of CD8⁺CD62L⁺ T cells was lower in mice treated with FTY720 (Fig 5.8A). The number of CD8⁺CD62L⁺ and CD8⁺CD62L⁺CD44⁺ T_{CM} cells was similar in the FTY720- and vehicle control-treated infected mice on day 60 post-challenge (Fig 5.8E, F), where CD8⁺CD44⁺ T_{EM} cells were significantly increased in FTY720-treated *B. pertussis*-infected mice (Fig 5.8G). The changes on day 60 were mirrored by an increase in the number of CD4⁺CD49d⁺ and CD8⁺CD49d⁺ T cells in the lymph nodes of FTY720-treated *B. pertussis*-infected mice (Fig 5.9A, B).

To investigate changes in Th1 and Th17 cells in the mediastinal lymph node, cells stimulated with PMA, ionomycin and BFA were stained intracellularly for IFN- γ and IL-17. The number of CD4⁺IFN- γ ⁺ and CD4⁺IL-17⁺ T cells was increased in the lymph nodes of mice following infection with *B. pertussis* and this was decreased in FTY720-treated mice (Fig 5.10A). However, on day 60 the number of CD4⁺IL-17⁺ T cells was significantly increased in FTY720-treated *B. pertussis*-infected mice. No significant change was observed in CD8⁺ T cells (Fig 5.10B).

5.2.4 Decreased Ag-specific response in lymph node and lung mononuclear cells prepared from FTY720-treated *B. pertussis*-infected mice

On day 21 post-infection with *B. pertussis*, the macrophage-depleted cells from the lungs (Fig 5.11A) or cells from the mediastinal lymph node (Fig 5.11B) of vehicle control- and FTY720-treated mice were incubated with APCs (1:2 ratio), heat-killed *B. pertussis* or medium only for 72 h. IFN- γ and IL-17 was quantified in the supernatants using ELISA. Re-stimulation of lung and lymph node mononuclear cells from *B. pertussis*-infected mice with heat killed *B. pertussis* significantly increased IFN- γ and IL-17 production into the supernatant (Fig 5.11A, B). However, the production of IFN- γ was significantly lower in lung cells prepared from FTY720-treated *B. pertussis*-infected mice (Fig 5.11A). In addition, IL-17 production was significantly reduced in the lymph node cells from FTY720-treated *B. pertussis*-infected mice (Fig 5.11B). These data are consistent with the reduction of Th1 and Th17 cells in FTY720-treated *B. pertussis*-infected mice.

5.2.5 Decreased $\gamma\delta$ T cell and NKT cell influx into the lungs of FTY720-treated *B. pertussis*-infected mice

It has been demonstrated that $\gamma\delta$ T cells infiltrate the lung early after infection with *B. pertussis* (McGuirk et al., 1998). The majority of $\gamma\delta$ T cell infiltration into the lung occurred on day 7 following challenge (Fig 5.12A), and treatment with FTY720 decreased this population in the lung and lymph node (Fig 5.12, 5.13). FTY720 significantly lowered the $\gamma\delta^+$ IFN- γ^+ T cell population in the lung and lymph node (Fig 5.12, 5.13) in addition, the number of $\gamma\delta^+$ IL-17 $^+$ T cells was reduced in the lungs of FTY720-treated *B. pertussis*-infected mice, though this did not reach statistical significance (Fig 5.12C). On day 60 post-challenge, the number of IFN- γ^+ and IL-17 $^+$ $\gamma\delta^+$ T cells was significantly increased in lymph nodes of FTY720-treated *B. pertussis*-infected mice (Fig 5.13B, C).

Previous studies from this laboratory demonstrated that NK cells infiltrate the lung early in the course of infection following challenge with *B. pertussis*. Influx of NK cells peaked on day 7 post-challenge and the number of NK cells was significantly increased in the lungs of FTY720-treated *B. pertussis*-infected mice

(Fig 5.14A). There was no effect of FTY720 on the number of IFN- γ ⁺ and IL-17⁺ NK cells in the lung however, the number of IFN- γ ⁺ NKT cells was significantly decreased in FTY720-treated *B. pertussis*-infected mice on day 7 post-challenge (Fig 5.14B, C). Infection with *B. pertussis* did not affect NK or NKT cells in the lymph nodes of vehicle control- and FTY720-treated mice (Fig 5.15). However, the number of IFN- γ ⁺ and IL-17⁺ NK cells and NKT cells was significantly increased on day 60 post-challenge in FTY720-treated mice (Fig 5.15B, C).

Analysis of infiltrating B cells into the lung revealed an increase in CD19⁺ and B220⁺ cells throughout the course of infection with *B. pertussis* (Fig 5.16A, B) with similar numbers observed for the CD19⁺ and B220⁺ populations. The effect of infection was attenuated in FTY720-treated *B. pertussis*-infected mice (Fig 5.16A, B). However, the population of B220⁺ cells in the lymph node increased significantly on day 60 post-challenge (Fig 5.16C).

5.2.6 Increased inflammatory cells infiltrate into the lung of FTY720-treated mice during infection with *B. pertussis*

Having demonstrated that FTY720 modulates the number of T cells and B cells in the lung following *B. pertussis*-infection, innate immune cell infiltration into the lung was examined. The number of macrophages (CD3⁻CD19⁻SSC^{int}FSC^{high}), but not neutrophils (CD3⁻CD19⁻SSC^{int}FSC^{int}), was increased in the lung of *B. pertussis*-infected mice on day 28 post-challenge, however, both populations were significantly increased in FTY720-treated mice on days 28 and 42 post-infection with *B. pertussis* (Fig 5.17A, B). The number of eosinophils (CD3⁻CD19⁻SSC^{high}FSC^{int}) was significantly increased in vehicle control mice on day 42 post-challenge (Fig 5.17C), but the number of eosinophils was significantly reduced in FTY720-treated *B. pertussis*-infected mice at this time point.

5.2.7 Chemokine and cytokine expression significantly reduced in lung tissue from FTY720-treated *B. pertussis*-infected mice

The mRNA expression of chemokines, which are chemoattractant for T cells, was assessed in snap-frozen lung tissue. CCL3, CXCL10 and CCL2 mRNA were significantly increased in the lungs of mice 7 days post-infection with *B. pertussis*

(Fig 5.18A-C). However, the expression of these chemokines did not increase in FTY720-treated *B. pertussis*-infected mice (Fig 5.18A-C), except for a small change in CCL3 expression on day 21 post-challenge (Fig 5.18A).

During the course of infection with *B. pertussis* the production of pro-inflammatory cytokines in the lung is important in the control and clearance of the bacteria (Higgs et al., 2012). The expression of TNF α , IL-1 β , NOS2 and IL-6 increased significantly in the lungs of mice 7 days post-challenge with *B. pertussis* (Fig 5.19A-D) and these were significantly decreased in FTY720-treated *B. pertussis*-infected mice (Fig 5.19A-D). Anti-inflammatory cytokines such as IL-10 and TGF- β , and Treg cells are also induced during the course of infection with *B. pertussis*. The expression of TGF β 1 and IL-10 was increased in the lung from day 7 post-infection with *B. pertussis* (Fig 5.20); however, this response was delayed in FTY720-treated *B. pertussis*-infected mice and did not appear until day 21 post-challenge (Fig 5.20B, C). The expression of the M2 marker, mannose receptor was significantly increased in the lungs of mice on day 21 post-infection with *B. pertussis* (Fig 5.20A), but was delayed until day 42 post-challenge in FTY720-treated *B. pertussis*-infected mice (Fig 5.20A).

It has previously been shown that FTY720 can increase the expression of the barrier-forming TJ proteins of endothelial cells (Natarajan et al., 2013) and therefore expression of claudin-5 and occludin was assessed. On day 42 post-challenge, occludin mRNA was increased in tissue prepared FTY720-treated *B. pertussis*-infected mice (Fig 5.21A, B), but no change was observed at other time points.

5.2.8 FTY720 does not impair clearance of *B. pertussis* in immunised mice

The results so far demonstrate that chronic treatment with FTY720 impairs the ability of mice to clear a primary infection with *B. pertussis* and this was associated with decreased T cell infiltration into the lung, and decreased T cell expansion in the lymph node. The ability of FTY720 to alter clearance of infection in immunised mice was addressed, using two licensed human pertussis vaccines; Pw and Pa. It has previously been demonstrated that vaccination with Pw is

more effective than Pa, and is associated with the induction of Th1 cells (Barnard et al., 1996; Redhead et al., 1993; Ross et al., 2013). Mice were immunised with Pw or Pa on day 0 and boosted on day 28. Treatment with FTY720 began on day 35 and mice were infected with *B. pertussis* on day 45. Mice were culled on day 3, 7 and 10 post-challenge. *B. pertussis* colonies were not detectable in either Pw- or Pa-immunised, vehicle control mice on day 7 or 10 post-challenge, and FTY720 did not affect bacterial load, nor enhance the duration of infection in mice immunised with Pw or Pa (Fig 5.22).

5.2.9 Immunization with Pw increases effector memory T cell infiltration into the lungs of *B. pertussis*-infected mice

Immunization did not enhance B cell infiltration into the lung on days 3 or 7 post-challenge, however, FTY720 treatment significantly reduced the B cell numbers in the lungs of Pa- and Pw-immunised *B. pertussis*-infected mice (Fig 5.23A, B). Immunization with Pw increased T cell infiltration into the lung on days 3 and 7 post-infection with *B. pertussis* to a significantly greater extent than mice immunised with Pa (Fig 5.23A, B). While FTY720 reduced the number of infiltrating T cells, there was still a significant T cell influx in Pw-immunised *B. pertussis*-infected mice (Fig 5.23A, B). CD3⁺CD4⁺ T cells were significantly increased in the lungs of mice immunised with Pw and subsequently challenged with *B. pertussis*, this was 3-fold greater than in Pa-immunised mice (Fig 5.24A, B). The number of CD3⁺CD4⁺ T cells was significantly lower in the lungs of FTY720-treated Pw- and Pa-immunised mice, although CD4⁺ T cells remained significantly higher in Pw-immunised FTY720-treated mice compared with Pa-immunised FTY720-treated mice (Fig 5.24A, B). CD3⁺CD8⁺ T cells were also lower with FTY720 treatment in Pw- and Pa-immunised mice, though these numbers were 2-fold higher in Pw-immunised FTY720-treated mice (Fig 5.24A, B).

The mice in this experiment were immunised and received a booster vaccination 4 weeks later, which confers protective immunity in the host. This leads to rapid clearance of *B. pertussis* bacteria just days after challenge (Higgins et al., 2006; Ross et al., 2013) as verified here. Therefore the memory phenotype of the cells infiltrating the lung was assessed. Immunization with Pw increased

the number of CD4⁺CD44⁺ T_{EM} cells in the lung on days 3 and 7 post-challenge, to a significantly greater extent than mice immunised with Pa (Fig 5.25A, B). The number of CD4⁺CD62L⁺ and CD4⁺CD62L⁺CD44⁺ T_{CM} cells infiltrating the lung was completely ablated in all FTY720-treated mice (Fig 5.25A, B). FTY720 reduced the number of CD4⁺CD44⁺ T_{EM} cells in the lung, however, CD4⁺CD44⁺ T_{EM} cells remained significantly increased in Pw- compared with Pa-immunised, FTY720-treated mice following infection (Fig 5.25A, B). Similar results were obtained for CD8⁺ T cells; immunization with Pw increased CD8⁺CD44⁺ T_{EM} cell influx into the lung (Fig 5.26A, B), however, the number of CD8⁺CD62L⁺ and CD8⁺CD62L⁺CD44⁺ T_{CM} cells infiltrating the lung was significantly lower with FTY720 treatment (Fig 5.26A, B). CD8⁺CD44⁺ T_{EM} cell infiltration was unaffected by FTY720. These findings demonstrate the effectiveness of immunization with Pw over Pa in mice and highlight that treatment with FTY720 only impairs clearance of a primary infection with *B. pertussis*, FTY720 does not prolong the duration of infection in previously immunised mice. The influx of effector T cells to the lung still occurs to a large degree with FTY720 treatment, and as a result the immunised mice can clear *B. pertussis* infection as normal.

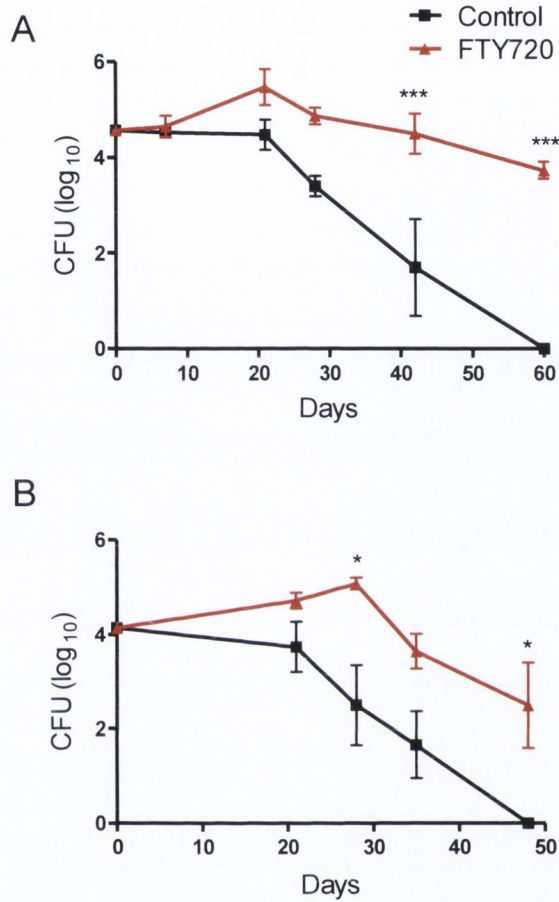


Figure 5.1 Chronic FTY720 treatment significantly impairs clearance of infection with *B. pertussis*.

Mice were treated with FTY720 daily, starting from day -10 (A) or day -3 (B). Vehicle control- and FTY720-treated mice were infected with *B. pertussis* at 5×10^8 CFU/ml on day 0 and sacrificed at various time points after infection. CFU counts were determined on lung homogenate. (A) FTY720 x time post-infection interaction *** $p < 0.001$; 2-way ANOVA. (B) FTY720 treatment effect *** $p < 0.001$, time post-infection effect *** $p < 0.001$; 2-way ANOVA. * $p < 0.05$, *** $p < 0.001$; Bonferroni post hoc. Data represent means \pm SEM, $n = 4$ per time point.

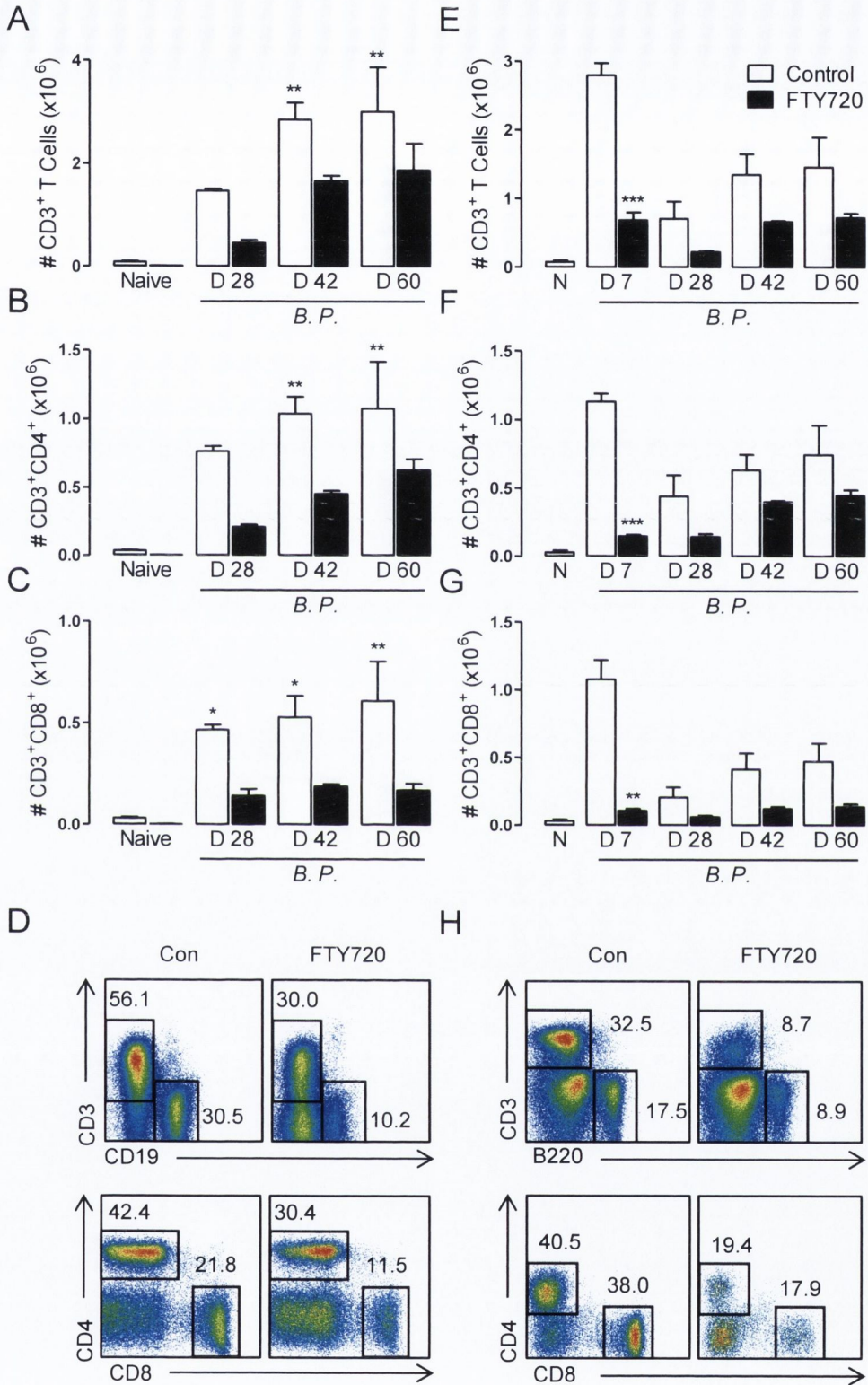


Figure 5.2 FTY720 treatment suppresses T cell infiltration into the lungs of *B. pertussis*-infected mice.

Vehicle control- and FTY720-treated mice were infected with *B. pertussis* and culled at various time points post-infection, a group of naïve uninfected vehicle control- and FTY720-treated mice were also culled on day 28 of the experiment. Cells were isolated from the lungs of mice, either stained with LIVE/DEAD, and surface-stained for CD3, CD4, and CD8 (A-C) or stimulated with PMA, ionomycin and BFA for 5 h, stained with LIVE/DEAD, and surface-stained for CD3, CD4 and CD8 (E-G). Flow cytometric analysis was performed. Results are mean absolute numbers of the indicated cells in the lung. (A-C)* $p < 0.05$, ** $p < 0.01$ in comparison to naïve uninfected control; Newman-Keuls post hoc (E) CD3⁺ T cells; FTY720 treatment x time post-infection interaction * $p < 0.05$; 2-way ANOVA, (F) CD3⁺CD4⁺ T cells; FTY720 treatment x time post-infection interaction * $p < 0.05$; 2-way ANOVA (G) CD3⁺CD8⁺ T cells; FTY720 treatment x time post-infection interaction ** $p < 0.01$; 2-way ANOVA. (E-G) ** $p < 0.01$, *** $p < 0.001$ in comparison to relevant *B. pertussis*-infected vehicle control mice; Bonferroni post hoc. Sample FACS plots of (D) CD3⁺, CD3⁺CD4⁺, and CD3⁺CD8⁺ T cells from lung cells immediately FACS stained, or (H) after 5 h stimulation, where numbers in quadrants are percentage of positive cells. Data represent means \pm SEM, $n = 4$ per time point, representative of 2 experiments. Con, control; *B.P.*, *B. pertussis*; D, Day; N, Naïve.

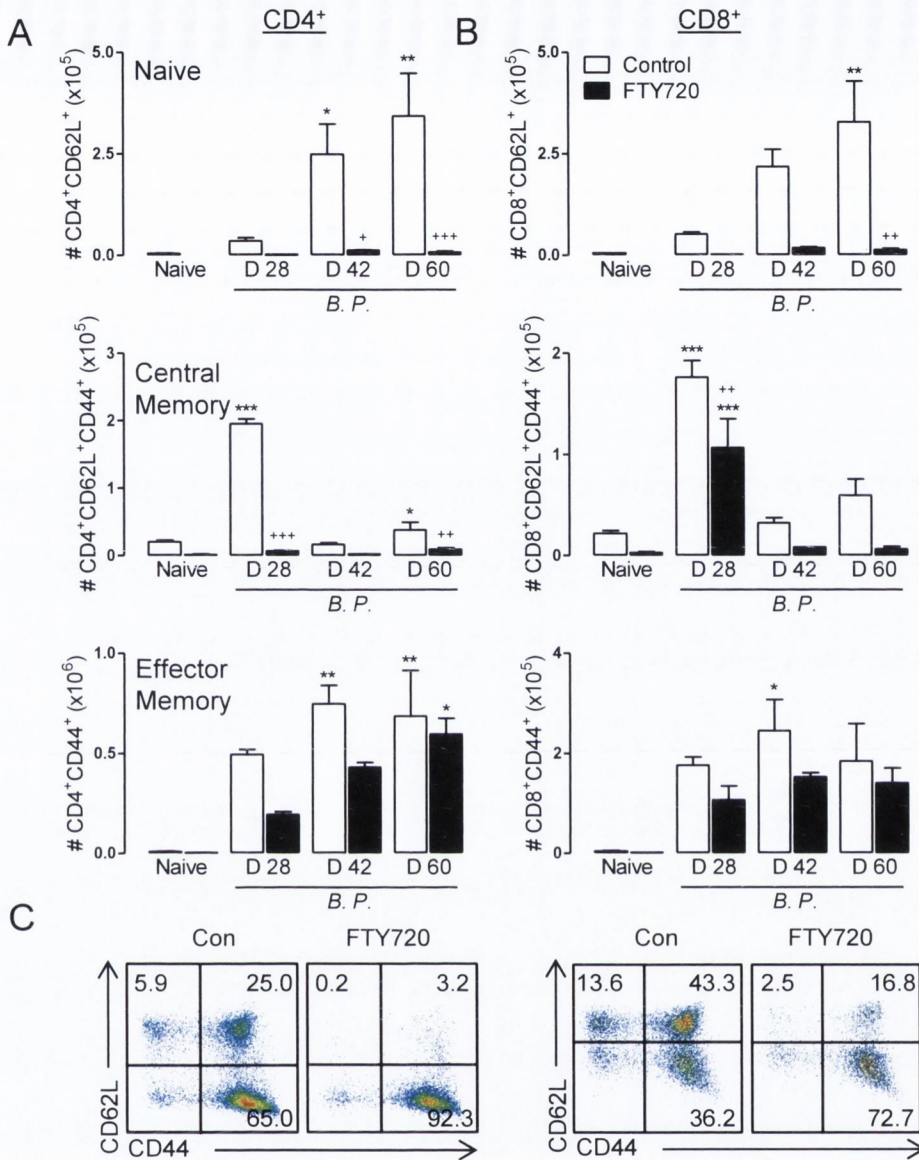


Figure 5.3 FTY720 reduces naïve and central memory T cell infiltration into the lungs of *B. pertussis*-infected mice.

(A) CD4⁺ and (B) CD8⁺ T cells were surface-stained for CD62L⁺ and CD44⁺ and assessed by flow cytometry to determine naïve (CD62L⁺), central memory (CD62L⁺CD44⁺) and effector memory (CD44⁺) populations. Results are mean absolute numbers of the indicated cells in the lung. * p < 0.05, ** p < 0.01, *** p < 0.001 in comparison to uninfected control; + p < 0.05, ++ p < 0.01, +++ p < 0.001, in comparison to relevant *B. pertussis*-infected vehicle control mice; Newman-Keuls post hoc. (C) Sample FACS plots of memory CD4⁺ and CD8⁺ T cells in the lung where numbers in quadrants are percentage of positive cells. Data represent means ± SEM, n = 4 per time point. Con, control; *B.P.*, *B. pertussis*; D, Day.

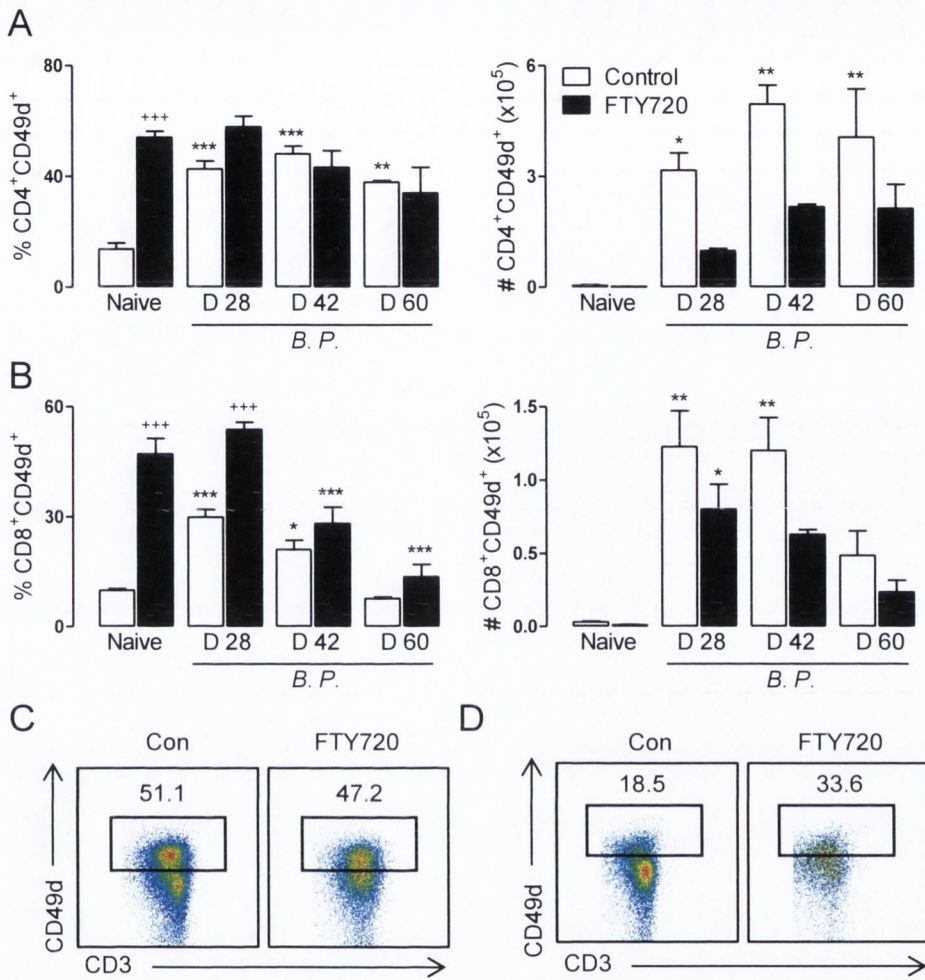


Figure 5.4 CD49d⁺ T cells infiltrate the lungs of *B. pertussis*-infected mice, with the absolute number but not the frequency reduced by treatment with FTY720.

(A) CD4⁺ and (B) CD8⁺ T cells were surface-stained for CD49d⁺ and assessed by flow cytometry. Results are mean percentage and absolute numbers of the indicated cells in the lung, with sample FACS plots of (C) CD4⁺CD49d⁺ and (D) CD8⁺CD49d⁺ T cells where numbers in quadrant are percentage of positive cells. * p < 0.05, ** p < 0.01, *** p < 0.001 in comparison to relevant uninfected control; *** p < 0.001 in comparison with relevant infected vehicle control mice; Newman-Keuls post hoc. Data represent means ± SEM, n = 4. Con, control; *B.P.*, *B. pertussis*; D, Day.

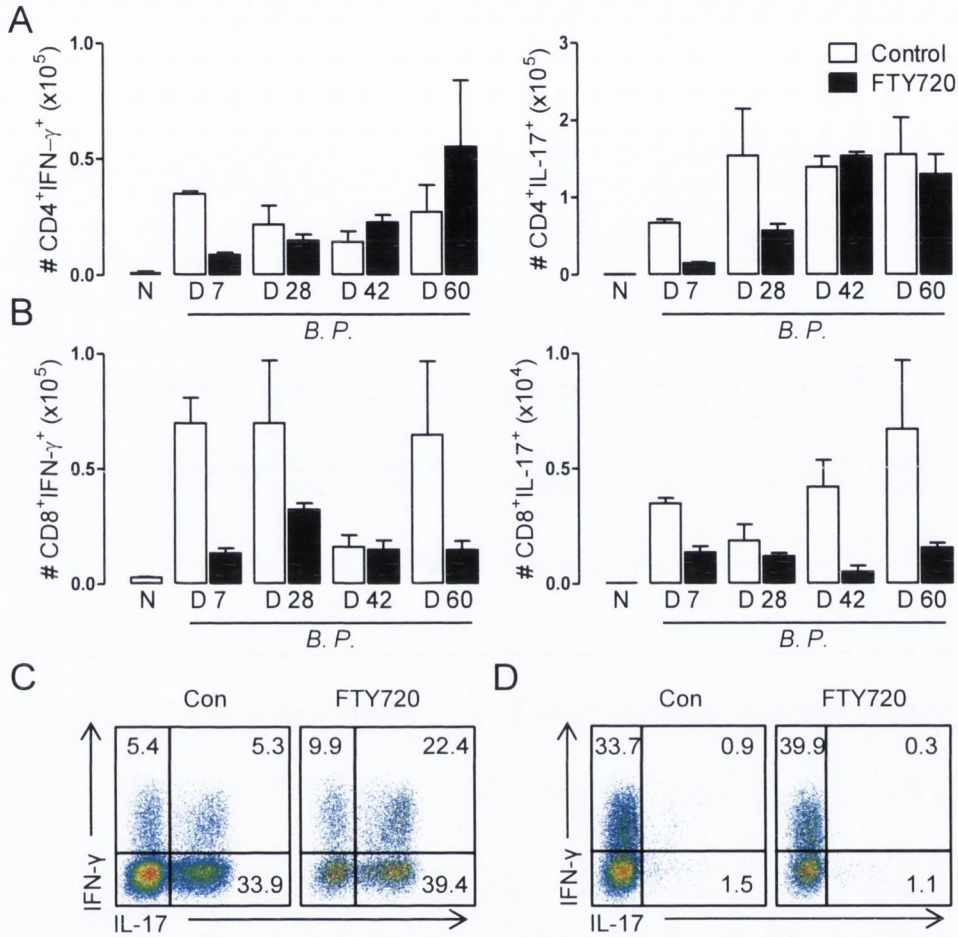


Figure 5.5 FTY720 treatment suppresses IFN- γ ⁺ and IL-17⁺ cell infiltration into the lungs of *B. pertussis*-infected mice.

CD4⁺ and CD8⁺ T cells were stimulated with PMA, ionomycin and BFA for 5 h, intracellularly stained for IFN- γ and IL-17 and assessed by flow cytometry. Results are mean absolute numbers of the indicated cells in the lung. (A) CD4⁺IFN- γ ⁺ T cells, CD4⁺IL-17⁺ T cells; time post-infection effect * $p < 0.05$; 2-way ANOVA. (B) CD8⁺IFN- γ ⁺ T cells; FTY720 treatment effect ** $p < 0.01$; 2-way ANOVA, CD8⁺IL-17⁺ T cells; FTY720 treatment effect ** $p < 0.01$; 2-way ANOVA. Sample FACS plots of (C) CD4⁺IFN- γ ⁺ or IL-17⁺ T cells, (D) CD8⁺IFN- γ ⁺ or IL-17⁺ T cells, numbers in quadrant are percentage of positive cells. Data represent means \pm SEM, $n = 4$ per time point, representative of 2 experiments. Con, control; D, Day; N, Naïve.

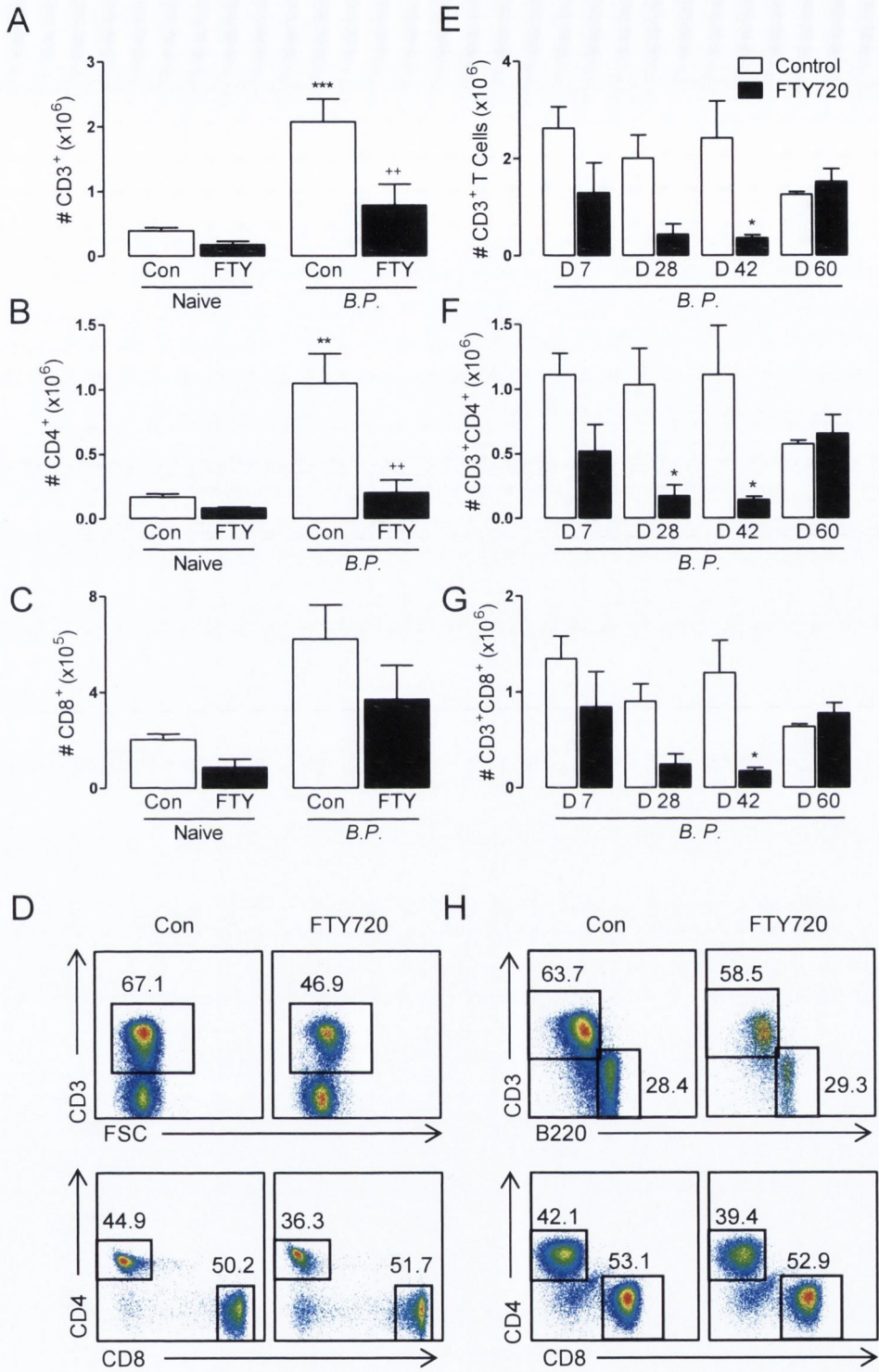


Figure 5.6 FTY720 treatment reduces the number of T cells in the mediastinal lymph nodes of *B. pertussis*-infected mice.

B. pertussis-infected and naïve uninfected vehicle control- and FTY720-treated mice were culled on day 28 (A-D) or various time points (E-H) post-infection. Cells were isolated from the mediastinal lymph nodes, either immediately stained with LIVE/DEAD, and surface-stained for CD3, CD4, and CD8 (A-D) or stimulated with PMA, ionomycin and BFA for 5 h, stained with LIVE/DEAD, and surface-stained for CD3, CD4 and CD8 (E-H). Flow cytometric analysis was performed. (A) CD3⁺ T cells; FTY720 treatment x *B. pertussis* infection interaction $p = 0.06$, FTY720 treatment effect * $p < 0.05$, *B. pertussis* infection effect ** $p < 0.01$; 2-way ANOVA. (B) CD3⁺CD4⁺ T cells; FTY720 treatment x *B. pertussis* infection interaction * $p < 0.05$; 2-way ANOVA. (C) CD3⁺CD8⁺ T cells; *B. pertussis* infection effect ** $p < 0.01$; 2-way ANOVA. (E) CD3⁺ T cells; FTY720 treatment effect ** $p < 0.01$; 2-way ANOVA (F) CD3⁺CD4⁺ T cells; FTY720 treatment effect *** $p < 0.001$; 2-way ANOVA, (G) CD3⁺CD8⁺ T cells; FTY720 treatment effect *** $p < 0.001$; 2-way ANOVA. Results are mean absolute numbers of the indicated cells in the lymph node with sample FACS plots of (D) CD3⁺, CD3⁺CD4⁺ and CD3⁺CD8⁺ T cells from immediate FACS stain, or (H) after 5 h stimulation, where numbers in quadrants are percentage of positive cells. (A-D) ** $p < 0.01$, *** $p < 0.001$ in comparison to uninfected control; ** $p < 0.01$, in comparison to relevant infected vehicle control mice; Bonferroni post hoc. (E-H) * $p < 0.05$ in comparison to relevant *B. pertussis*-infected vehicle control mice; Bonferroni post hoc. Data represent means \pm SEM, $n = 4$ per time point. Con, control; *B.P.*, *B. pertussis*; FTY, FTY720; D, Day; FSC, Forward scatter.

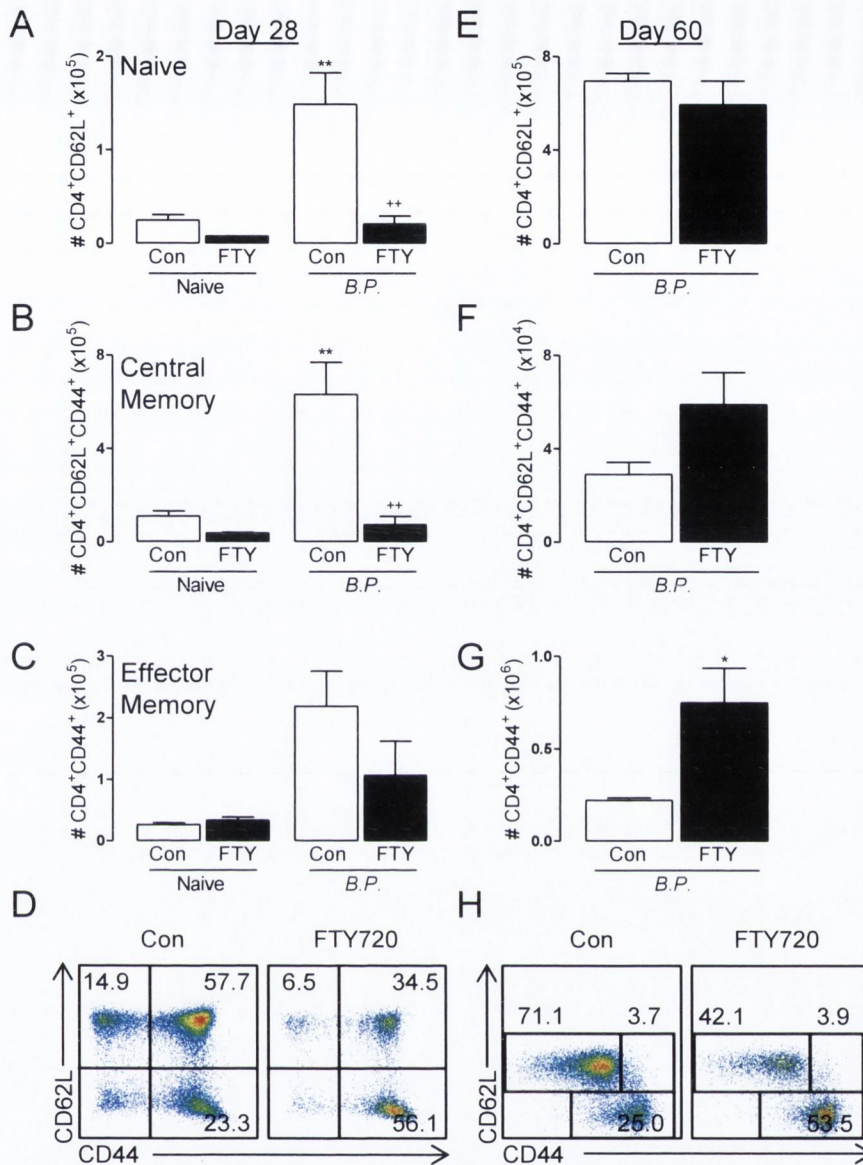


Figure 5.7 FTY720 reduces the number of naïve and central memory CD4⁺ T cells in lymph nodes of *B. pertussis*-infected mice on day 28 post-infection.

B. pertussis-infected and naïve uninfected vehicle control- and FTY720-treated mice were culled on day 28 (A-D) or day 60 (E-H) post-infection. CD4⁺ T cells were surface-stained for CD62L⁺ and CD44⁺ and assessed by flow cytometry. Results are mean absolute numbers of the indicated cells in the mediastinal lymph node, with representative FACS plots. (A) CD4⁺CD62L⁺; FTY720 x infection interaction * $p < 0.05$; 2-way ANOVA. (B) CD4⁺CD62L⁺CD44⁺; FTY720 x infection interaction * $p < 0.05$; 2-way ANOVA. (C) CD4⁺CD44⁺; infection effect * $p < 0.05$; 2-way ANOVA. ** $p < 0.01$ in comparison to uninfected control; ++ $p < 0.01$ in comparison to relevant *B. pertussis*-infected vehicle control mice; Bonferroni post hoc. (G) * $p < 0.05$; Student's *t*-test. Numbers in quadrants are percentage of positive cells. Data represent means \pm SEM, $n = 4$ per time point. Con, control; *B.P.*, *B. pertussis*; FTY, FTY720.

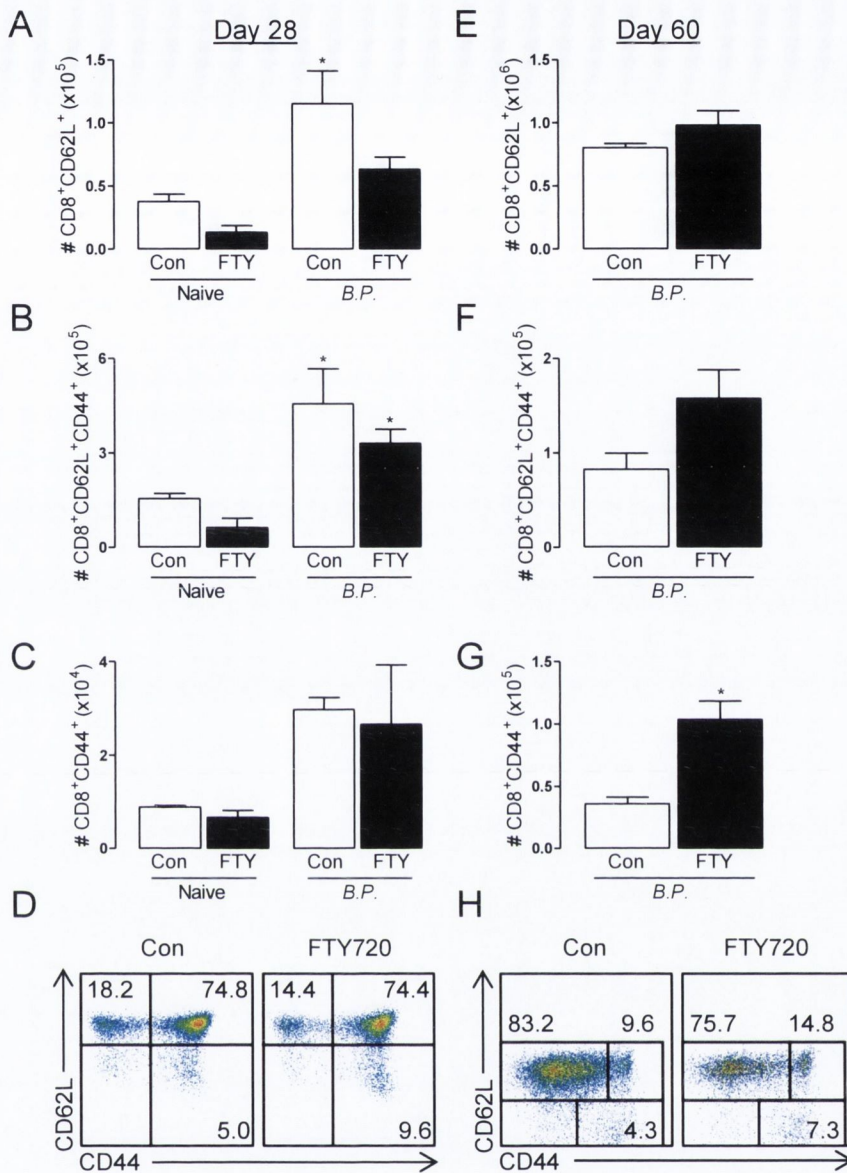


Figure 5.8 Effector memory CD8⁺ T cells unaffected by FTY720 treatment in the lymph nodes of *B. pertussis*-infected mice.

B. pertussis-infected and naïve uninfected vehicle control- and FTY720-treated mice were culled on day 28 (A-D) or day 60 (E-H) post-infection. CD8⁺ T cells were surface-stained for CD62L⁺ and CD44⁺ and assessed by flow cytometry. Results are mean absolute numbers of the indicated cells in the mediastinal lymph node with sample FACS plots. (A) CD8⁺CD62L⁺; FTY720 effect * $p < 0.05$, x infection effect * $p < 0.05$; 2-way ANOVA. (B) CD8⁺CD62L⁺CD44⁺; infection effect ** $p < 0.01$; 2-way ANOVA. (C) CD8⁺CD44⁺; infection effect * $p < 0.05$; 2-way ANOVA. * $p < 0.05$ in comparison to uninfected control; Bonferroni post hoc. (G) * $p < 0.05$; Student's *t*-test. Numbers in quadrants are percentage of positive cells. Data represent means \pm SEM, $n = 4$ per time point. Con, control; *B.P.*, *B. pertussis*; FTY, FTY720.

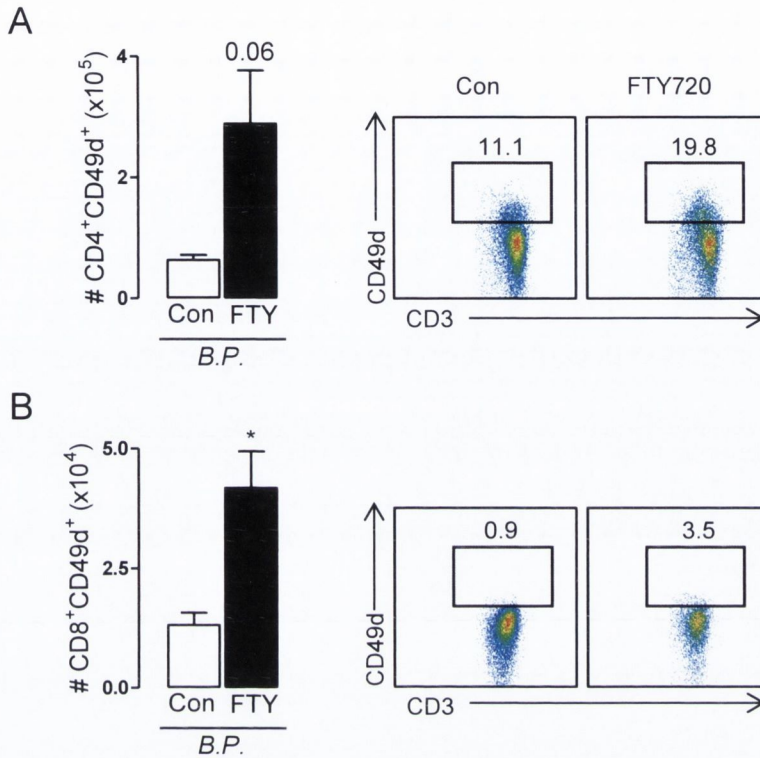


Figure 5.9 Number of CD49d⁺ T cells increased in the lymph nodes of FTY720-treated *B. pertussis*-infected mice on day 60 post-infection.

B. pertussis-infected vehicle control- and FTY720-treated mice were culled on day 60 post-infection. (A) CD4⁺ and (B) CD8⁺ T cells were surface-stained for CD49d and assessed by flow cytometry, with sample FACS plots of CD4⁺CD49d⁺ and CD8⁺CD49d⁺ T cells in the lymph node where numbers in quadrants are percentage of positive cells. Results are mean absolute numbers of the indicated cells in the mediastinal lymph node. p = 0.06, * p < 0.05; Student's t-test. Data represent means ± SEM, n = 4 per time point. Con, control; FTY, FTY720.

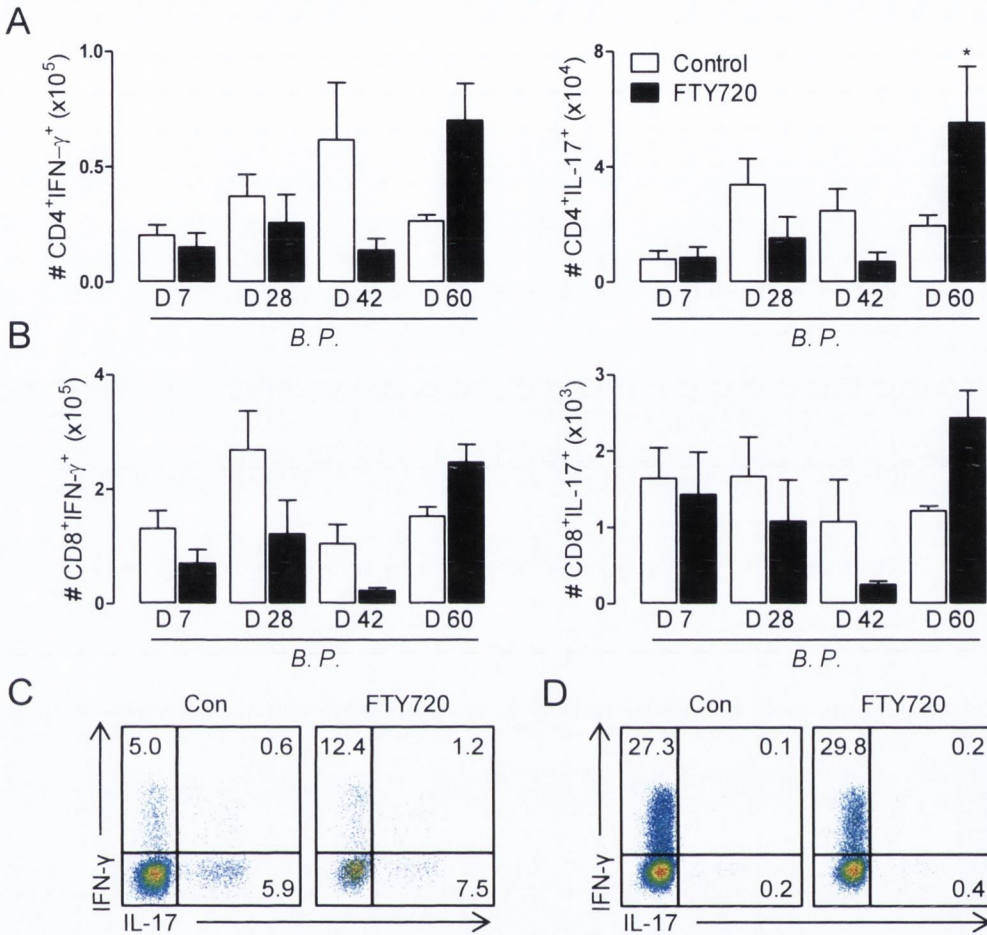


Figure 5.10 FTY720 treatment suppresses IFN- γ ⁺ and IL-17⁺ T cell numbers in the lymph node of *B. pertussis*-infected mice.

CD4⁺ and CD8⁺ T cells were stimulated with PMA, ionomycin and BFA, intracellularly stained for IFN- γ and IL-17 and assessed by flow cytometry. Results are mean absolute numbers of the indicated cells in the mediastinal lymph node. (A) CD4⁺IFN- γ ⁺ T cells; FTY720 treatment x time post-infection interaction * $p < 0.05$; 2-way ANOVA, CD4⁺IL-17⁺ T cells; FTY720 treatment x time post-infection interaction * $p < 0.05$; 2-way ANOVA. (B) CD8⁺IFN- γ ⁺ T cells; FTY720 treatment x time post-infection interaction * $p < 0.05$; 2-way ANOVA, CD8⁺IL-17⁺ T cells. Sample FACS plots of (C) CD4⁺IFN- γ ⁺ or IL-17⁺ T cells, (D) CD8⁺IFN- γ ⁺ or IL-17⁺ T cells, numbers in quadrant are percentage of positive cells. * $p < 0.05$ in comparison to relevant *B. pertussis*-infected vehicle control mice; Bonferroni post hoc. Data represent means \pm SEM, $n = 4$ per time point, representative of 2 experiments. Con, control; D, Day.

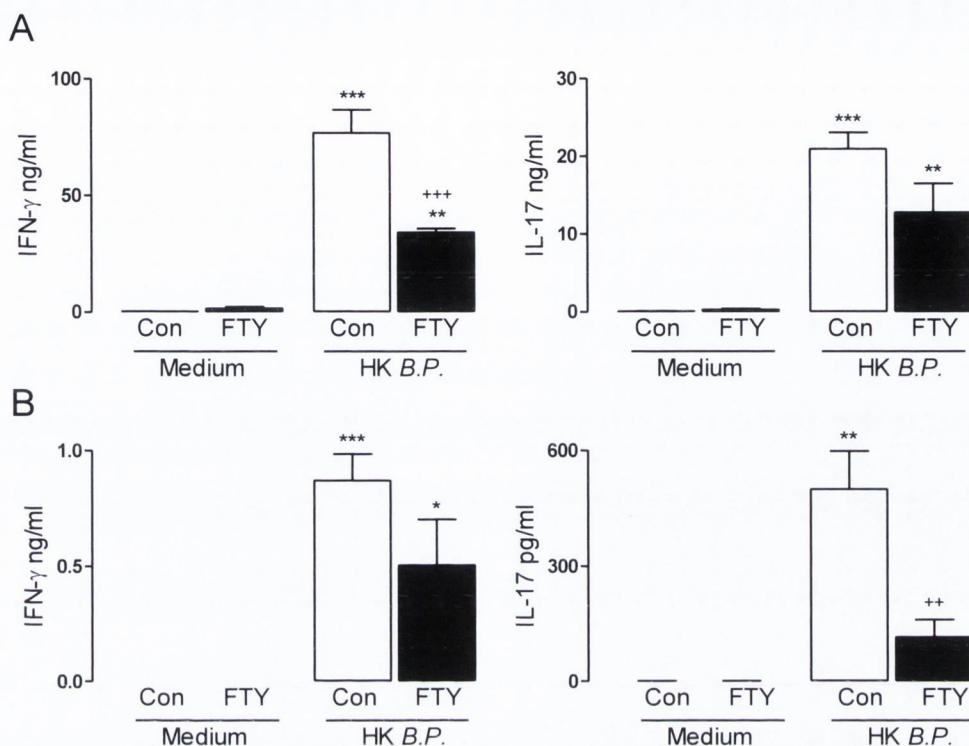


Figure 5.11 Decreased Ag-specific response by lung T cells from FTY720-treated *B. pertussis*-infected mice.

(A) Lung mononuclear cells from vehicle control- and FTY720-treated *B. pertussis* infected mice were prepared *ex vivo* on day 21 post-infection, incubated with irradiated spleen cells (APCs; 1:2 ratio), heat killed *B. pertussis* (HK *B.P.*) or medium only for 72 h. (B) Cells prepared from the mediastinal lymph node were incubated with APCs (1:1 ratio), HK *B.P.* or medium only for 72 h. IFN- γ and IL-17 was assessed in supernatant samples using ELISA. (A) IFN- γ concentration; FTY720-treatment x Ag-recall interaction ** $p < 0.01$; 2-way ANOVA, IL-17 concentration; FTY720-treatment x Ag-recall interaction $p = 0.08$, Ag-specific effect *** $p < 0.001$; 2-way ANOVA. (B) IFN- γ concentration; Ag-recall effect *** $p < 0.001$; 2-way ANOVA, IL-17 concentration; FTY720-treatment x Ag-recall interaction * $p < 0.05$; 2-way ANOVA. * $p < 0.05$, ** $p < 0.01$, *** $p < 0.001$ in comparison with relevant medium control; ++ $p < 0.01$, *** $p < 0.001$ in comparison with relevant FTY720 treatment control; Bonferroni post hoc. Data represent means \pm SEM, $n = 4$. Con, control; FTY, FTY720; HK *B.P.*, heat killed *B. pertussis*; D, Day.

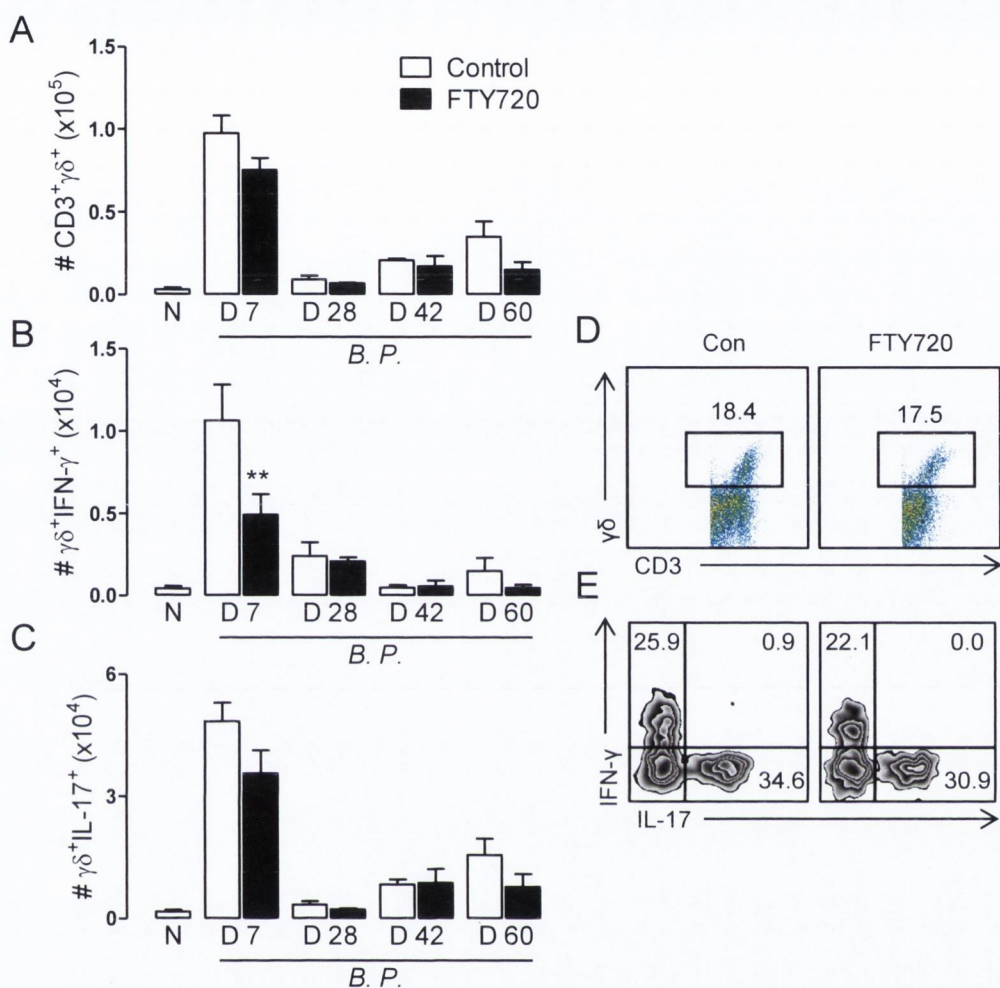


Figure 5.12 FTY720 treatment suppresses $\gamma\delta$ T cell infiltration into the lungs of *B. pertussis*-infected mice.

$\gamma\delta$ T cells were stimulated with PMA, ionomycin and BFA for 5 h, intracellularly stained for IFN- γ and IL-17 and assessed by flow cytometry. Results are mean absolute numbers of the indicated cells in the lung (A) $\gamma\delta$ T cells; FTY720 treatment effect * $p < 0.05$, time post-infection effect *** $p < 0.001$; 2-way ANOVA. (B) $\gamma\delta$ +IFN- γ ⁺ T cells; FTY720 treatment x time post-infection interaction * $p < 0.05$; 2-way ANOVA (C) $\gamma\delta$ +IL-17⁺ T cells; FTY720 treatment effect $p = 0.06$, time post-infection *** $p < 0.001$; 2-way ANOVA. Sample FACS plots of (D) $\gamma\delta$ T cells and (E) $\gamma\delta$ +IFN- γ ⁺ or IL-17⁺ T cells, numbers in quadrant are percentage of positive cells. ** $p < 0.01$ in comparison to relevant *B. pertussis*-infected vehicle control mice; Bonferroni post hoc. Data represent means \pm SEM, $n = 4$ per time point, representative of 2 experiments. Con, control; D, Day; N, Naïve.

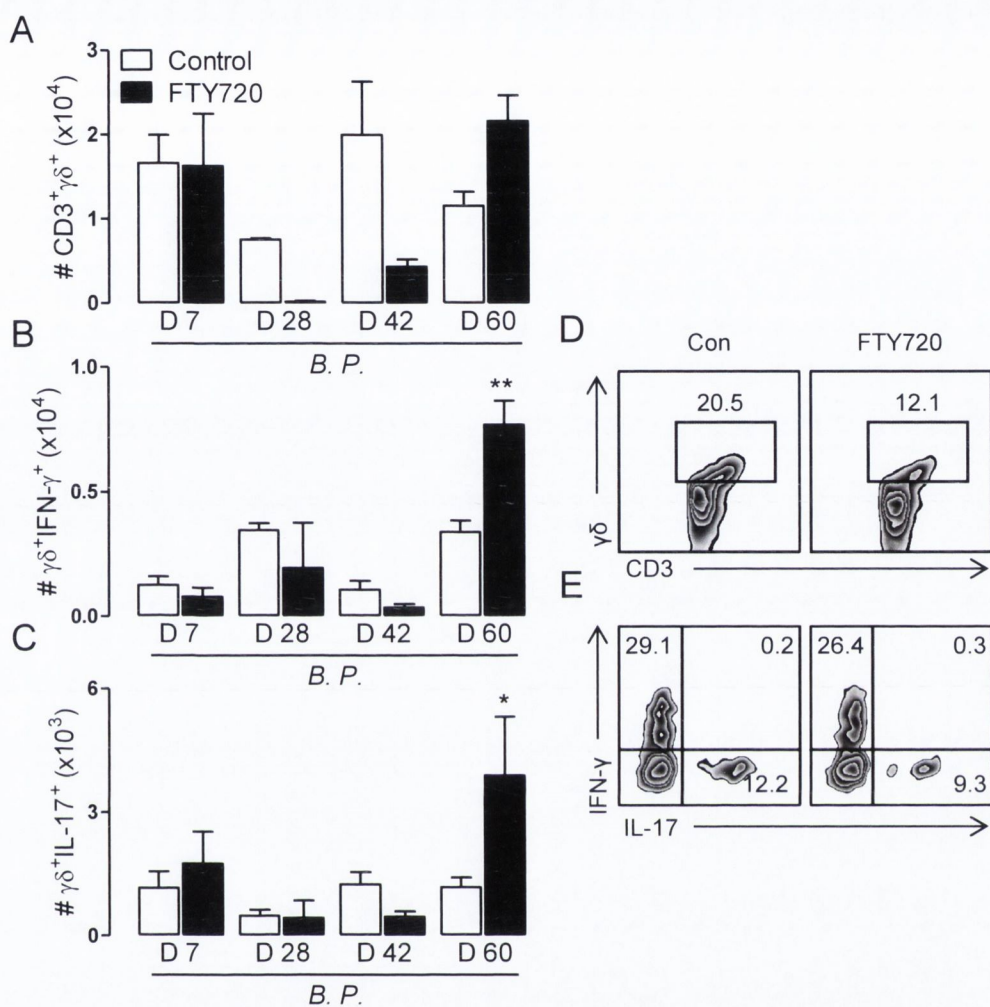


Figure 5.13 FTY720 treatment suppresses $\gamma\delta$ T cell numbers in the lymph nodes of *B. pertussis*-infected mice.

$\gamma\delta$ T cells were stimulated with PMA, ionomycin and BFA, intracellularly stained for IFN- γ and IL-17 and assessed by flow cytometry. Results are mean absolute numbers of the indicated cells in the mediastinal lymph node. (A) $\gamma\delta$ T cells; FTY720 treatment x time post-infection interaction * $p < 0.05$; 2-way ANOVA. (B) $\gamma\delta^+$ IFN- γ^+ T cells; FTY720 treatment x time post-infection interaction ** $p < 0.01$; 2-way ANOVA. (C) $\gamma\delta^+$ IL-17⁺ T cells; time post-infection effect * $p < 0.05$; 2-way ANOVA. * $p < 0.05$, ** $p < 0.01$ in comparison to relevant *B. pertussis*-infected vehicle control mice; Bonferroni post hoc. Numbers in quadrants are percentage of positive cells. Data represent means \pm SEM, $n = 4$ per time point, representative of 2 experiments. Con, control; D, Day.

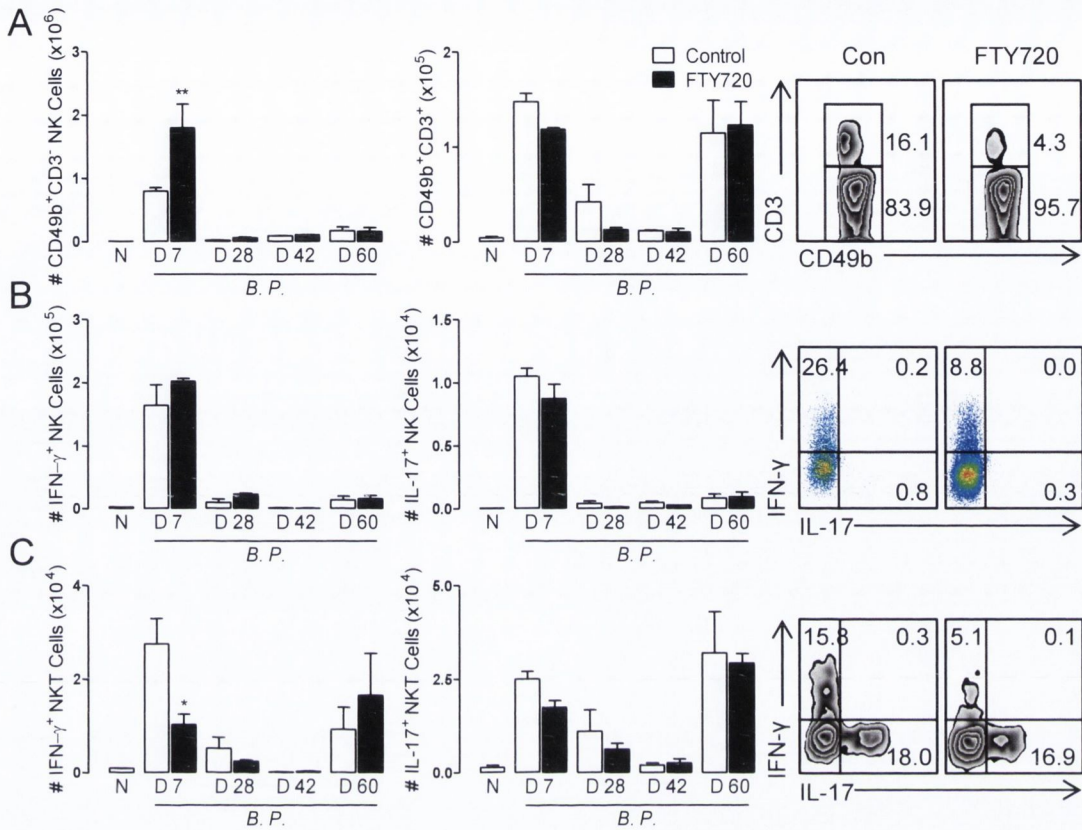


Figure 5.14 FTY720 treatment alters IFN- γ ⁺ NKT cell infiltration into the lungs of *B. pertussis*-infected mice.

Cells were prepared from the lung, stimulated with PMA, ionomycin and BFA for 5 h, stained with LIVE/DEAD, and surface-stained for CD49b and CD3. Cells were intracellularly stained for IFN- γ and IL-17, and assessed by FACS. Results are mean absolute numbers of the indicated cells in the lung with sample FACS plots, numbers in quadrants are percentage of positive cells. (A) CD49b⁺CD3⁻ NK cells; FTY720 treatment x time post-infection interaction ** $p < 0.01$; 2-way ANOVA. CD49b⁺CD3⁺ NKT cells; time post-infection effect *** $p < 0.001$; 2-way ANOVA (B) IFN- γ ⁺ NK cells; time post-infection effect *** $p < 0.001$; 2-way ANOVA, IL-17⁺ NK cells; time post-infection effect *** $p < 0.001$; 2-way ANOVA. (C) IFN- γ ⁺ NKT cells; FTY720 treatment x time post-infection interaction $p = 0.06$, time post-infection effect ** $p < 0.01$; 2-way ANOVA, IL-17⁺ NKT cells, time post-infection effect *** $p < 0.001$; 2-way ANOVA. * $p < 0.05$, ** $p < 0.01$ in comparison to relevant *B. pertussis*-infected vehicle control mice; Bonferroni post hoc. Data represent means \pm SEM, $n = 4$ per time point, representative of 2 experiments. Con, control; D, Day; N, Naïve.

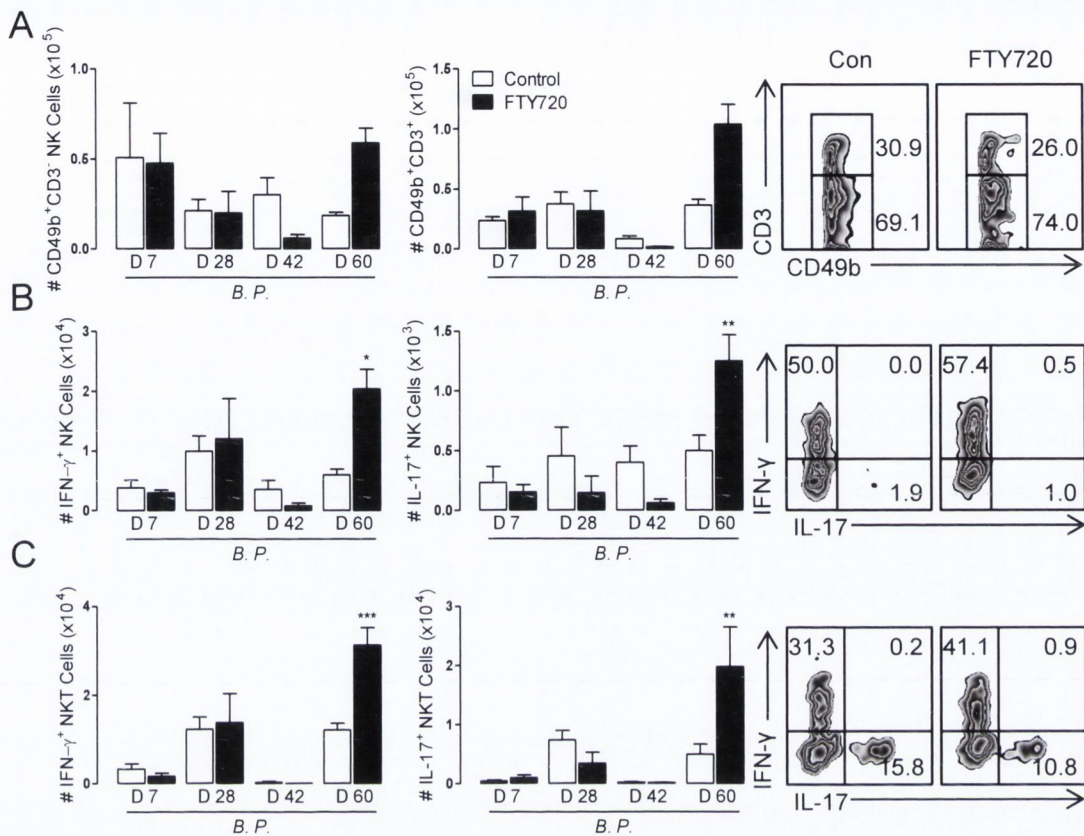


Figure 5.15 FTY720 treatment suppresses IFN- γ ⁺ and IL-17⁺ NK and NKT cell populations in the mediastinal lymph nodes of *B. pertussis*-infected mice.

Cells were prepared from the mediastinal lymph node, stained with LIVE/DEAD, and surface-stained for CD49b and CD3. Cells were intracellularly stained for IFN- γ and IL-17, and assessed by FACS. Results are mean absolute numbers of the indicated cells in the lymph node. (A) CD49b⁺CD3⁻ NK cells; CD49b⁺CD3⁺ NKT cells; time post-infection effect * $p < 0.05$; 2-way ANOVA (B) IFN- γ ⁺ NK cells; FTY720 treatment x time post-infection interaction * $p < 0.05$; 2-way ANOVA, IL-17⁺ NK cells; FTY720 treatment x time post-infection interaction ** $p < 0.01$; 2-way ANOVA. (C) IFN- γ ⁺ NKT cells; FTY720 treatment x time post-infection interaction ** $p < 0.01$, IL-17⁺ NKT cells; FTY720 treatment x time post-infection interaction ** $p < 0.01$; 2-way ANOVA. * $p < 0.05$, ** $p < 0.01$, *** $p < 0.001$ in comparison to relevant *B. pertussis*-infected vehicle control mice; Bonferroni post hoc. Numbers in quadrants are percentage of positive cells. Data represent means \pm SEM, $n = 4$ per time point, representative of 2 experiments. Con, control; D, Day.

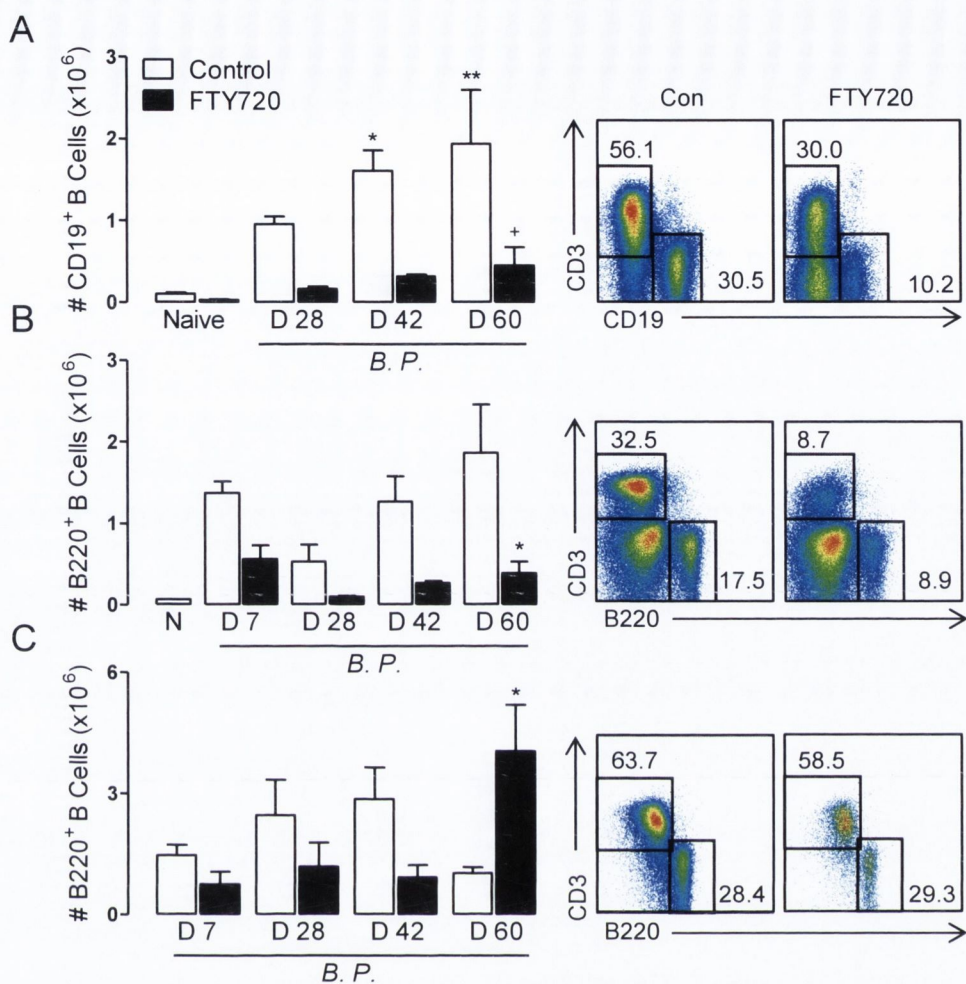


Figure 5.16 FTY720 treatment suppresses B cell infiltration into the lungs of *B. pertussis*-infected mice.

Vehicle control- and FTY720-treated mice were infected with *B. pertussis* and culled at various time points post-infection, a group of naïve uninfected control- and FTY720-treated mice were also culled on day 28. Cells were isolated from the lungs or mediastinal lymph nodes of mice, stained with LIVE/DEAD, and surface-stained for CD19 or B220, flow cytometric analysis was performed. Results are mean absolute numbers of the indicated cells with sample FACS plots of (A) lung CD19⁺ B cells, (B) lung B220⁺ B cells and (C) lymph node B220⁺ B cells, where numbers in quadrants are percentage of positive cells. (A) * $p < 0.05$, ** $p < 0.01$ in comparison to relevant uninfected control; + $p < 0.05$, in comparison to relevant vehicle control infected mice; Newman-Keuls post hoc. (B) FTY720 treatment effect *** $p < 0.001$; 2-way ANOVA. (C) FTY720 treatment x time post-infection interaction ** $p < 0.01$; 2-way ANOVA. (B and C) * $p < 0.05$ in comparison to relevant *B. pertussis*-infected vehicle control mice; Bonferroni post hoc. Data represent means \pm SEM, $n = 4$ per time point, representative of 2 experiments. Con, control; *B.P.*, *B. pertussis*; D, Day; FTY, FTY720.

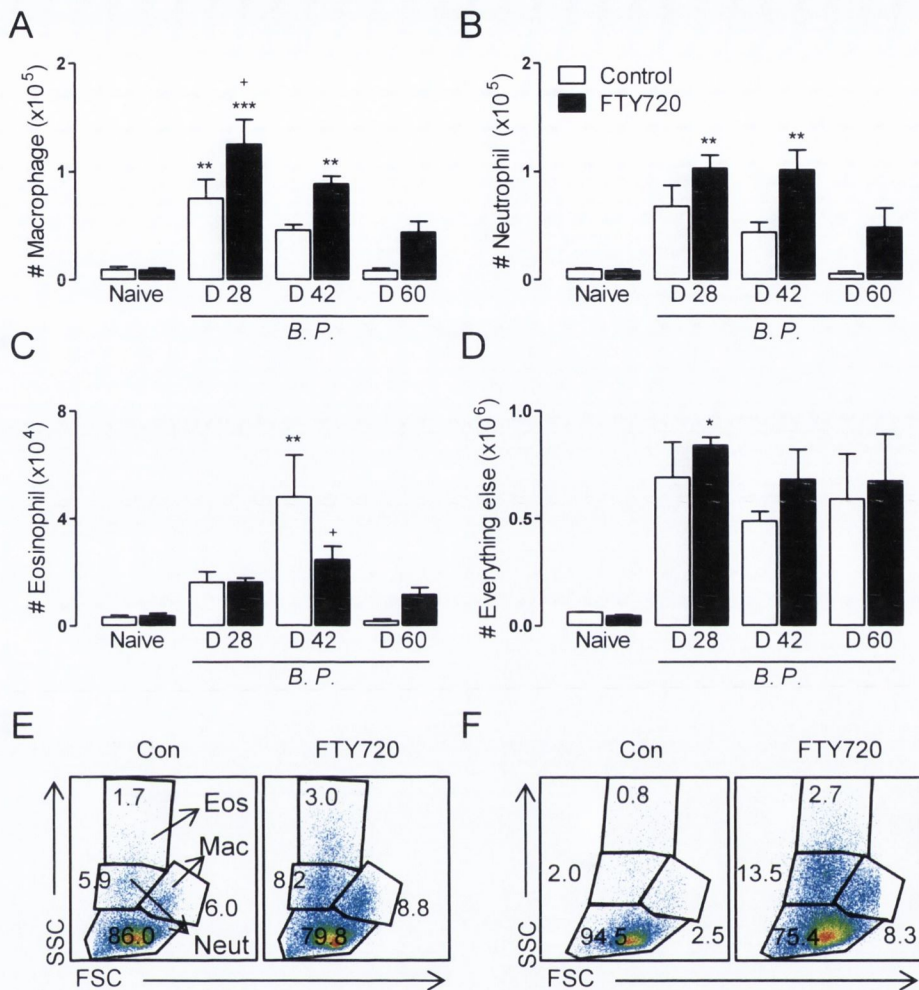


Figure 5.17 FTY720 treatment increases innate cell infiltration into the lungs of *B. pertussis*-infected mice.

(A) Macrophages were identified as CD3⁺CD19⁺SSC^{int}FSC^{high}, (B) Neutrophils were CD3⁺CD19⁺SSC^{int}FSC^{int} (C) Eosinophils were CD3⁺CD19⁺SSC^{high}FSC^{int}. Results are mean absolute numbers of the indicated cells in the lung and the diagrams are sample FACS plots of Macrophages, Neutrophils or Eosinophils from (E) day 42 or (F) day 60 post-challenge where numbers in quadrants are percentage of positive cells. * $p < 0.05$, ** $p < 0.01$, *** $p < 0.001$ in comparison to relevant uninfected control; + $p < 0.05$ in comparison to relevant infected vehicle control mice; Newman-Keuls post hoc. Data represent means \pm SEM, $n = 4$ per time point. Con, control; *B.P.*, *B. pertussis*; D, Day; FTY, FTY720, Eos, Eosinophils; Mac, Macrophage; Neut, Neutrophil; SSC, Side Scatter; FSC, Forward Scatter.

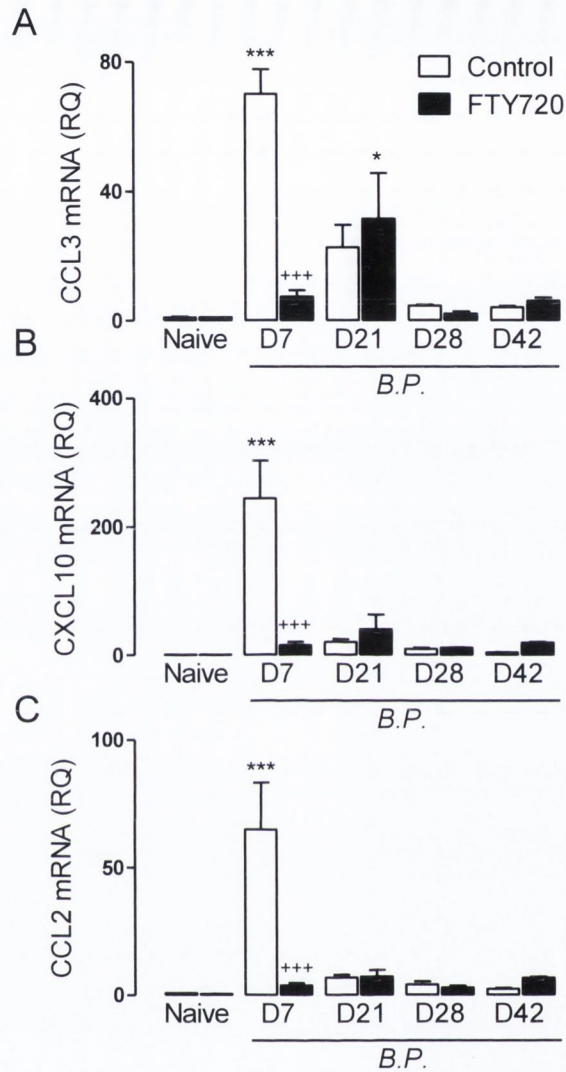


Figure 5.18 Decreased chemokine expression in the lungs of FTY720-treated infected mice.

RNA was extracted from snap-frozen lung tissue and assessed for (A) CCL3, (B) CXCL10, and (C) CCL2 expression. Values are expressed as relative quantities (RQ) normalized to the endogenous control gene, 18S, and relative to the averaged naïve vehicle control mice. * $p < 0.05$, *** $p < 0.001$ in comparison to relevant naïve uninfected mice; *** $p < 0.001$, in comparison to relevant *B. pertussis*-infected vehicle control mice; Newman-Keuls post hoc. Data represent means \pm SEM, $n = 4$ per time point. *B.P.*, *B. pertussis*; D, Day.

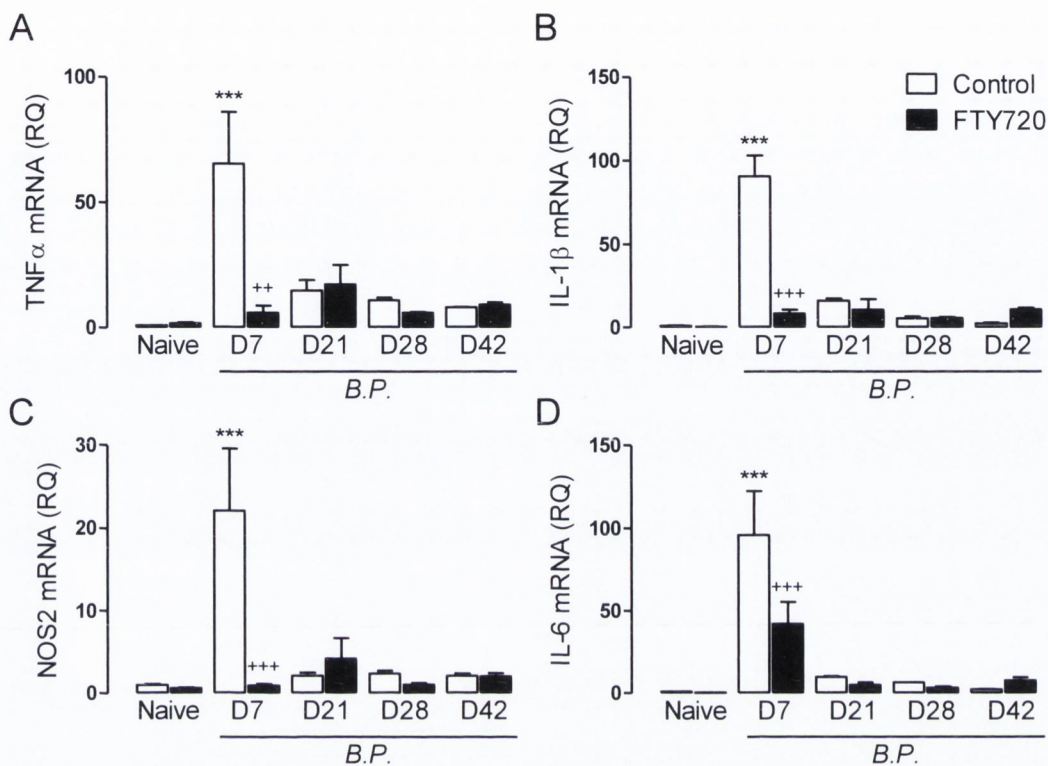


Figure 5.19 Decreased cytokine expression in the lungs of FTY720-treated infected mice.

RNA was extracted from snap-frozen lung tissue and assessed for (A) TNF α , (B) IL-1 β , (C) NOS2 and (D) IL-6 expression. Values are expressed as relative quantities (RQ) normalized to the endogenous control gene, 18S, and relative to the averaged naïve vehicle control mice. *** $p < 0.001$ in comparison to naïve uninfected mice; ** $p < 0.01$, +++ $p < 0.001$ in comparison to relevant *B. pertussis*-infected vehicle control mice; Newman-Keuls post hoc. Data represent means \pm SEM, $n = 4$ per time point. *B.P.*, *B. pertussis*; D, Day.

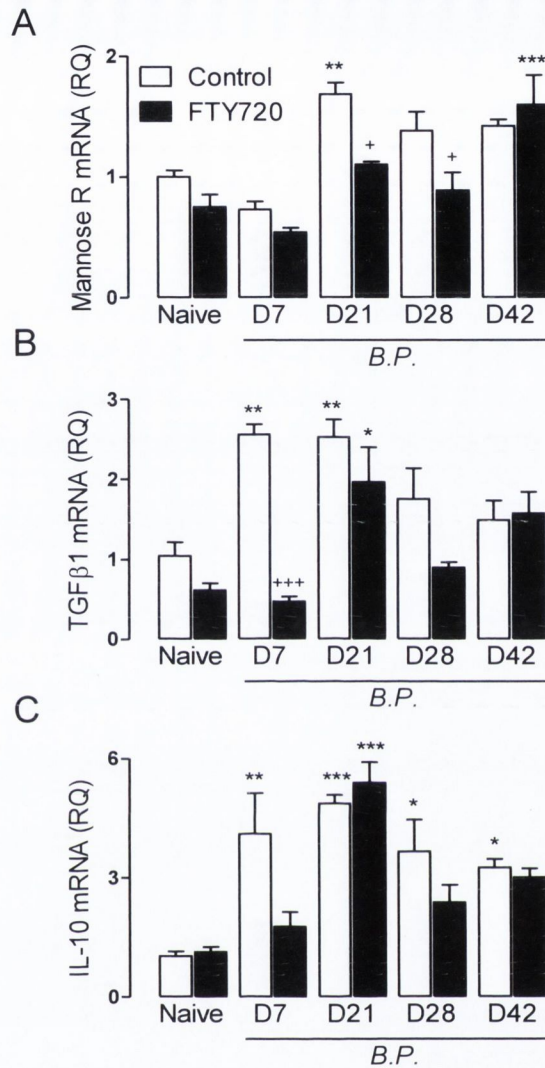


Figure 5.20 Delayed anti-inflammatory cytokine expression in the lungs of FTY720-treated infected mice.

RNA was extracted from snap-frozen lung tissue and assessed for (A) Mannose receptor, (B) TGF β 1, and (C) IL-10 expression. Values are expressed as relative quantities (RQ) normalized to the endogenous control gene, 18S, and relative to the averaged naïve vehicle control mice. * $p < 0.05$, ** $p < 0.01$, *** $p < 0.001$ in comparison to relevant naïve uninfected mice; + $p < 0.05$, +++ $p < 0.001$ in comparison to relevant *B. pertussis*-infected vehicle control mice; Newman-Keuls post hoc. Data represent means \pm SEM, $n = 4$ per time point. *B.P.*, *B. pertussis*; D, Day.

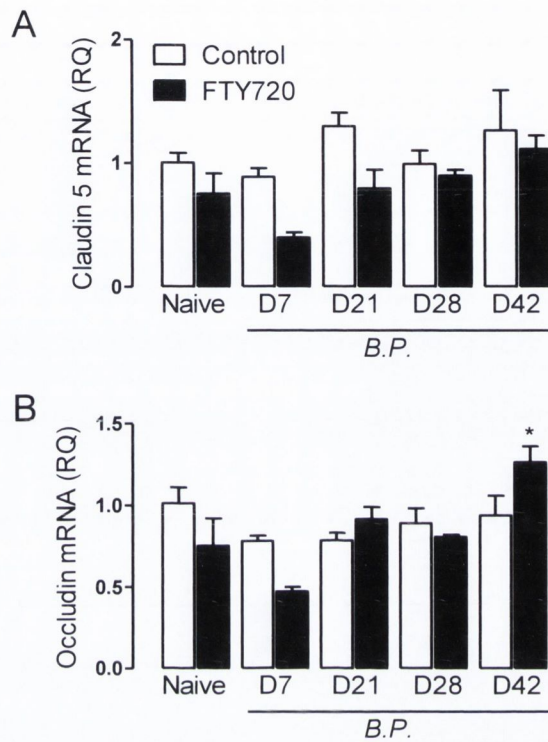


Figure 5.21 Expression of tight junction proteins in the lungs of *B. pertussis*-infected mice.

RNA was extracted from snap-frozen lung tissue and assessed for (A) Claudin 5 and (B) Occludin expression. Values are expressed as relative quantities (RQ) normalized to the endogenous control gene, 18S, and relative to the averaged naïve vehicle control mice. * $p < 0.05$ in comparison to relevant naïve uninfected mice; Newman-Keuls post hoc. Data represent means \pm SEM, $n = 4$ per time point. *B.P.*, *B. pertussis*; D, Day.

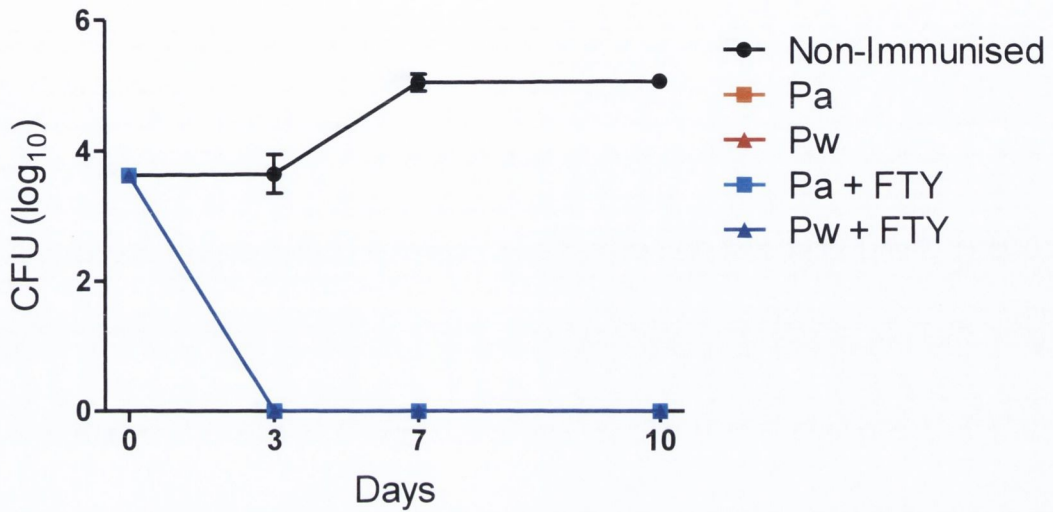


Figure 5.22 FTY720 treatment does not affect the protective efficacy of Pa or Pw in mice.

Mice were immunised with Pa or Pw (acellular or whole cell pertussis vaccine respectively) on day 0, boosted on day 28, on day 35 a group of mice began treatment with FTY720 (0.3 mg/kg/day). On day 45 vehicle control- and FTY720-treated mice were infected with *B. pertussis* at 5×10^8 CFU/ml and culled on day 3, 7 and 10 post-infection, a group of non-immunised vehicle control mice were also infected with *B. pertussis* and culled. CFU counts were determined on lung homogenate. Data represent means \pm SEM, n = 4 per time point. Con, control; Pa, acellular pertussis vaccine; Pw, whole cell pertussis vaccine; FTY, FTY720.

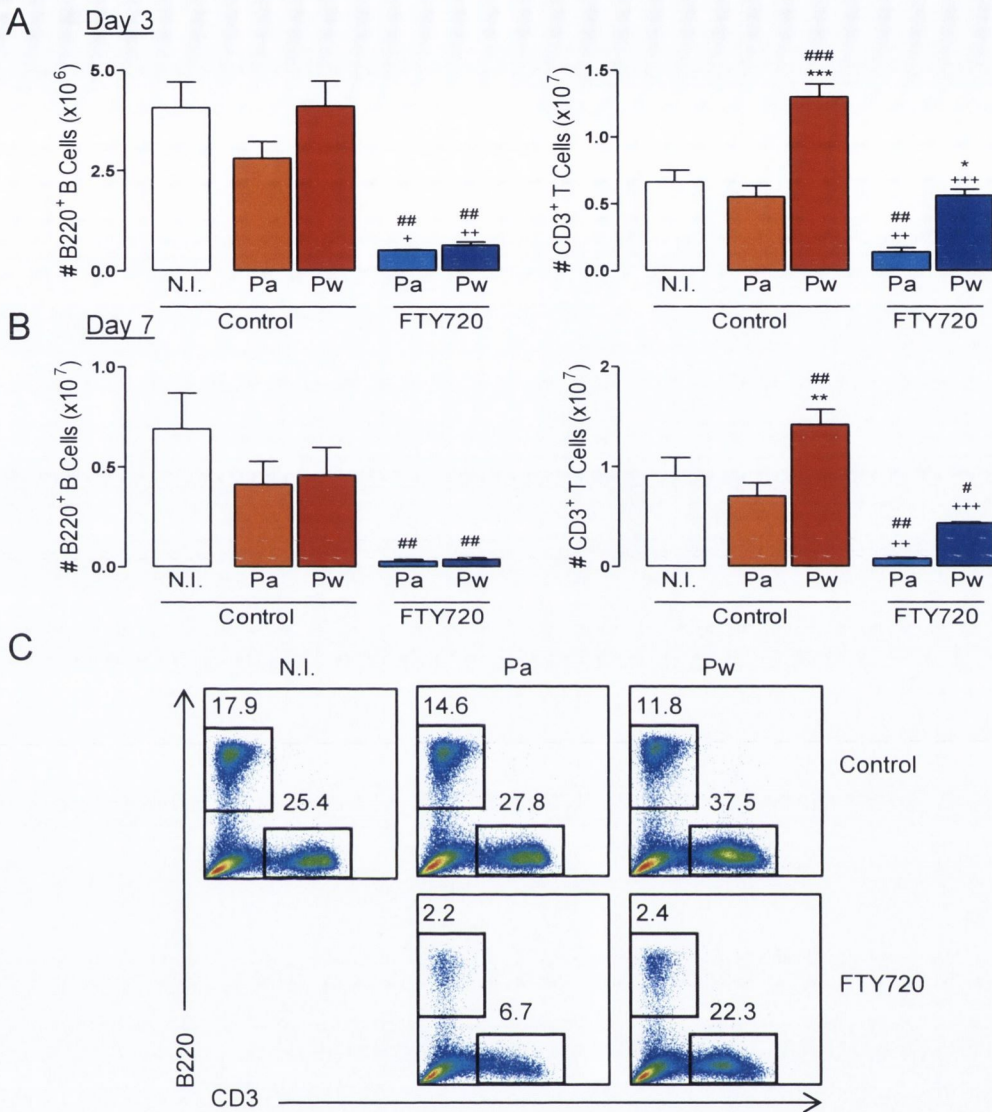


Figure 5.23 FTY720 treatment suppresses B cell and T cell infiltration into the lungs of immunised *B. pertussis*-infected mice.

Mice were immunised and infected with *B. pertussis* as described in Figure 22. Cells were isolated from the lungs of mice, stained with LIVE/DEAD, and surface-stained for B220 and CD3. Flow cytometric analysis was performed. Results are mean absolute numbers of the indicated cells in the lung from day 3 (A), day 7 (B) with sample FACS plots of (C) B220⁺ B cells or CD3⁺ T cells where numbers in quadrants are percentage of positive cells. * $p < 0.05$, ** $p < 0.01$, *** $p < 0.001$ Pa- in comparison to Pw-immunised mice; + $p < 0.05$, ++ $p < 0.01$, +++ $p < 0.001$ FTY720 treatment in comparison to relevant vehicle control mice; # $p < 0.05$, ## $p < 0.01$, ### $p < 0.001$ immunised mice in comparison with non-immunised control; Newman-Keuls post hoc. Data represent means \pm SEM, $n = 4$ per time point. Con, control; Pa, acellular pertussis vaccine; Pw, whole cell pertussis vaccine; N.I., Non-immunised mice.

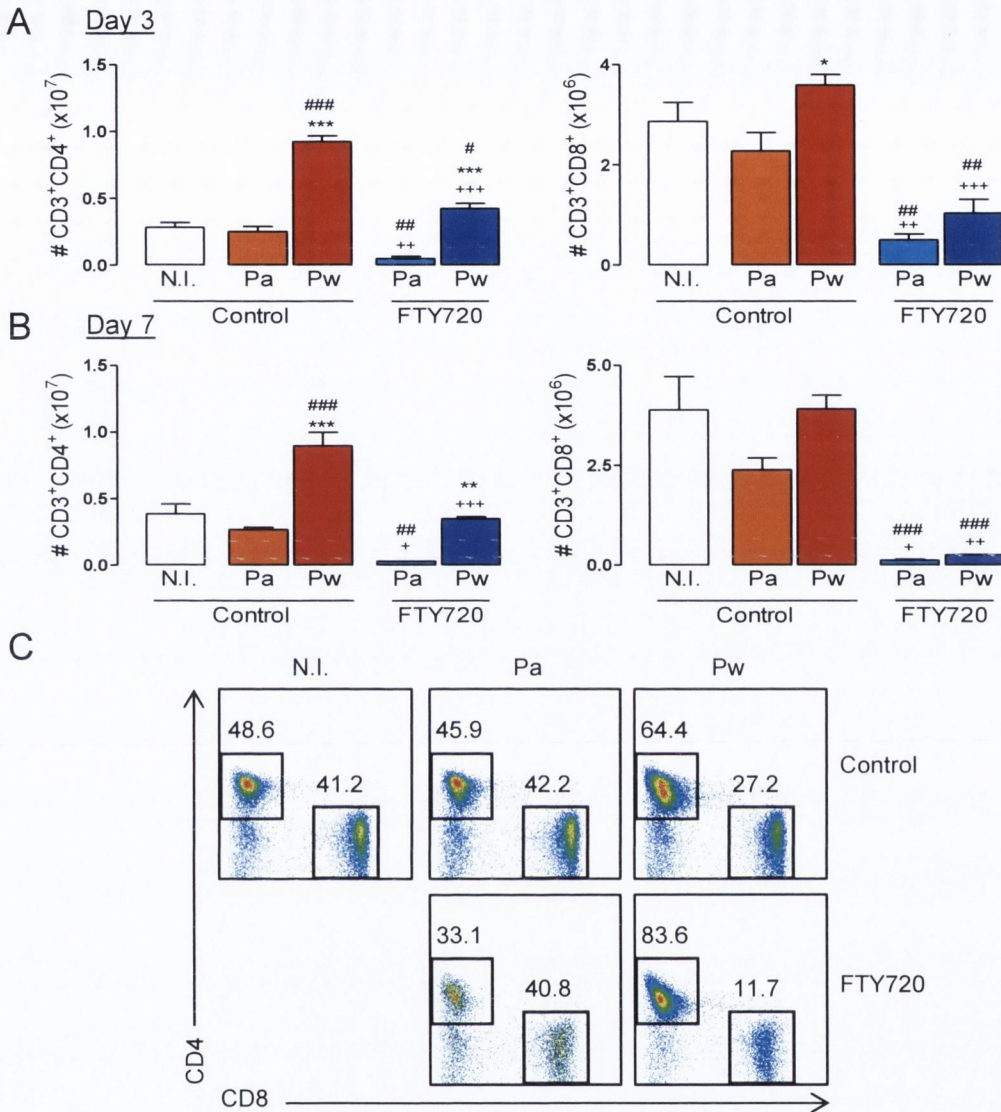


Figure 5.24 Immunization with Pw increases recruitment of CD4⁺ T cells into the lung following *B. pertussis* infection, and this is suppressed by FTY720.

Mice were immunised and infected with *B. pertussis* as described in Figure 22. CD3⁺ T cells were surface-stained with CD4 or CD8 and assessed by flow cytometry. Results are mean absolute numbers of the indicated cells in the lung from day 3 (A), day 7 (B) with sample FACS plots of (C) CD3⁺CD4⁺ T cells or CD3⁺CD8⁺ T cells where numbers in quadrants are percentage of positive cells. *** p < 0.001 Pa- in comparison to Pw-immunised mice; + p < 0.05, ** p < 0.01, *** p < 0.001 FTY720 treatment in comparison to relevant vehicle control mice; # p < 0.05, ## p < 0.01, ### p < 0.001 immunised mice in comparison with non-immunised control; Newman-Keuls post hoc. Data represent means ± SEM, n = 4 per time point. Con, control; Pa, acellular pertussis vaccine; Pw, whole cell pertussis vaccine; N.I., Non-immunised mice.

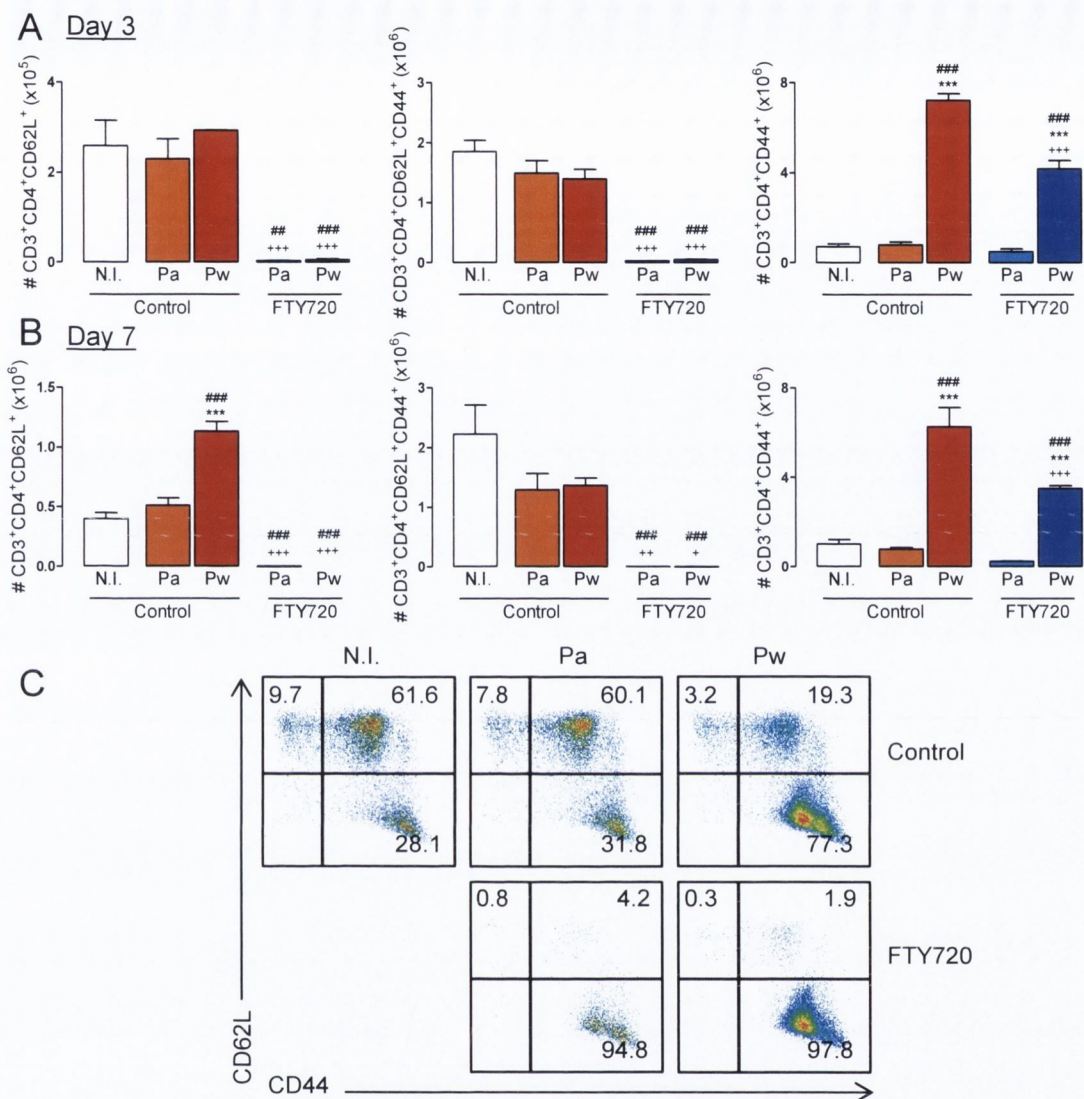


Figure 5.25 Immunization with Pw increases effector memory T cell infiltration into the lungs of *B. pertussis*-infected mice.

Mice were immunised and infected with *B. pertussis* as described in Figure 22. CD3⁺CD4⁺T cells were surface-stained with CD62L and CD44 and assessed by flow cytometry. Results are mean absolute numbers of the indicated cells in the lung from day 3 (A), day 7 (B) and with sample FACS plots (C) where numbers in quadrants are percentage of positive cells. *** p < 0.001 Pa- in comparison to Pw-immunised mice; + p < 0.05, ++ p < 0.01, +++ p < 0.001 FTY720 treatment in comparison to relevant vehicle control mice; ### p < 0.01, #### p < 0.001 immunised mice in comparison with non-immunised control; Newman-Keuls post hoc. Data represent means ± SEM, n = 4 per time point. Con, control; Pa, acellular pertussis vaccine; Pw, whole cell pertussis vaccine; N.I., Non-immunised mice.

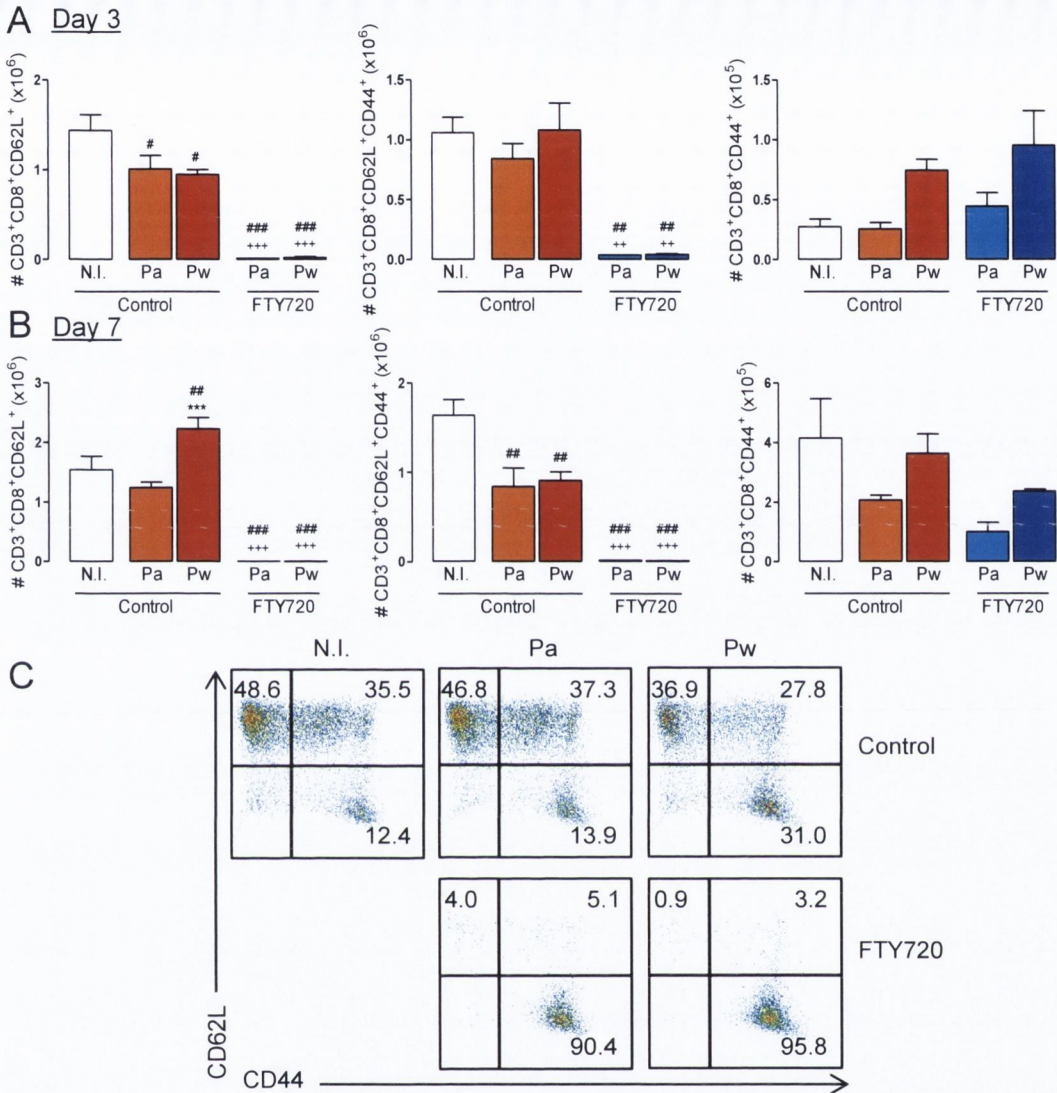


Figure 5.26 FTY720 treatment suppresses naïve and central memory CD8⁺T cell infiltration into the lungs of *B. pertussis*-infected mice.

Mice were immunised and infected with *B. pertussis* as described in Figure 22. CD3⁺CD8⁺T cells were surface-stained with CD62L and CD44 and assessed by flow cytometry. Results are mean absolute numbers of the indicated cells in the lung from day 3 (A), day 7 (B) with sample FACS plots (C) where numbers in quadrants are percentage of positive cells. *** p < 0.001 Pa- in comparison to Pw-immunised mice; ** p < 0.01, *** p < 0.001 FTY720 treatment in comparison to relevant vehicle control mice; ## p < 0.01, ### p < 0.001 immunised mice in comparison with non-immunised control; Newman-Keuls post hoc. Data represent means ± SEM, n = 4 per time point. Con, control; Pa, acellular pertussis vaccine; Pw, whole cell pertussis vaccine; N.I., Non-immunised mice.

5.3 Discussion

FTY720 is a recently approved therapy for MS, and successfully reduces the relapse rate, MRI endpoints and risk of disability progression in patients with relapse-remitting MS. However, results from clinical trials have shown that lower respiratory tract infections are almost twice as frequent in FTY720-treated patients when compared with patients taking the placebo (Cohen et al., 2010; Kappos et al., 2006; Kappos et al., 2010). The present study set out to investigate the effect of FTY720 on the clearance of a respiratory infection with the Gram-negative bacteria *B. pertussis*, and to establish whether infiltration of immune cells, especially T cells, to the lung was altered with chronic FTY720 treatment. The data demonstrate that FTY720 impaired the ability of mice to clear a primary infection with *B. pertussis* and this significant delay in bacterial clearance persisted long after vehicle control mice resolved the infection. There was a significant reduction in infiltration of T cells and B cells into the lungs of FTY720-treated *B. pertussis*-infected mice. Importantly this reduction reflected a decrease in the number of both memory and Ag-specific T cells. Mice immunised with Pa or Pw rapidly cleared *B. pertussis* following aerosol challenge. In the case of Pw, this was associated with influx of CD4⁺CD44⁺ T_{EM} cells into the lung. Importantly, FTY720 treatment in immunised mice did not affect their ability to clear infection with *B. pertussis*.

FTY720 obtained FDA approval in 2010 after numerous clinical trials (Cohen et al., 2010; Kappos et al., 2006; Kappos et al., 2010). The immunomodulatory drug had improved efficacy in MS patients in comparison to IFN-β1a, an established first line therapy, as assessed by MRI measures and relapse rate (Cohen et al., 2010). The evidence for a continued effect of FTY720 is up to 4 years treatment, and the average age of participants at the beginning of the study was 35-38 years old (Kappos et al., 2015). It has not been established whether FTY720 is as effective in older participants or the elderly. Reported adverse events with FTY720 include transient bradycardia and macular oedema (in <1% of patients). This is thought to be caused predominantly through the action of FTY720 at S1P₁ receptors, which are expressed on a variety of cell types, including those of the heart, brain and endothelium (Brinkmann et al.,

2010). The increased incidence of respiratory infections with FTY720 treatment was associated with an increase in bronchitis and pneumonia (Cohen et al., 2010; Kappos et al., 2010), which are predominantly caused by viral or bacterial infections respectively (Knutson and Braun, 2002; Mandell et al., 2007).

The present study demonstrates that chronic treatment with FTY720 impairs the clearance of the respiratory pathogen *B. pertussis*. This is consistent with previous reports that demonstrate FTY720 impairs the clearance of infections with the gut pathogen *Citrobacter rodentium* (Murphy et al., 2012) or with the helminth parasite *Nippostrongylus brasiliensis* (Thawer et al., 2014). In addition to an impaired bacterial clearance in FTY720-treated mice, the number of lung infiltrating T cells and B cells was considerably reduced throughout the period after infection. It has been proposed that FTY720 mediates its effects on T cells by inducing retention in the lymph node through functional antagonism of the S1P receptor, thus trapping the T cells (Matloubian et al., 2004). However, as T_{EM} cells lack CCR7, they do not require S1P signalling for lymph node egress, and are spared from the effects of FTY720 (Brinkmann et al., 2010; Mehling et al., 2008). As a result, effector T cells should, in theory, expand as normal in response to infection. It has been suggested that the pathogenic T cells in MS are T_{CM} cells, therefore selective retention of these in the lymphoid organs would prove an ideal therapy for this disease (Brinkmann et al., 2010). In the present study, the numbers of naïve and T_{CM} cells in the lung were significantly increased following infection with *B. pertussis*. In contrast, influx of both populations into the lung was lower in FTY720-treated infected mice. T_{EM} cells made up more than 90% of the CD4⁺ T cells in the lung of FTY720-treated *B. pertussis*-infected mice; although it was weeks before these mice had a number of T_{EM} cells in the lung that was comparable to that of vehicle control-treated infected mice. This reduced effector memory response is in agreement with previous reports on the effects of the parasite *Nippostrongylus brasiliensis* (Thawer et al., 2014), however, this is the first study to demonstrate the phenomenon during FTY720-treatment in a bacterial respiratory infection.

Following initial treatment with FTY720, the number of T cells in the blood rapidly decreases which concurs with the previously-reported transient

increase in the number of T cells in the lymph nodes and spleen (Chiba et al., 1998; Morris et al., 2005). However, with prolonged use, the total number of lymphocytes in the body was significantly reduced (Morris et al., 2005). It has been suggested that this could, in part, be due to the inhibition of T cell egress from the thymus (Matloubian et al., 2004; Morris et al., 2005; Rosen et al., 2003; Yagi et al., 2000). In addition, naïve T cells require regular cell contact with DCs for survival, an interaction which likely occurs on T cell entry into the lymphoid organ (Feuillet et al., 2005; Marrack and Kappler, 2004; Sprent et al., 2008). As FTY720 induces T cell retention in the lymph node and prevents their circulation, this limits potential T cell: DC interaction and cell viability. In this study, the number of CD4⁺ and CD8⁺ naïve and T_{CM} cells was reduced by 60-69% in the mediastinal lymph nodes of uninfected mice after treatment with FTY720. The data revealed that the number of T cells in the lymph nodes increased significantly after infection with *B. pertussis*, perhaps due to T cell expansion in response to the respiratory pathogen. However, FTY720 prevented the expansion of T cells in the lymph node following infection with *B. pertussis*. In particular, the CD4⁺ naïve and T_{CM} populations were unchanged in the lymph nodes of FTY720-treated mice on day 28 post-challenge which mirrored the decreased number of these cells in the lungs of FTY720-treated mice following infection with *B. pertussis*. In line with this, the *B. pertussis* Ag-specific response of T cells in both the mediastinal lymph node and the lung was reduced following FTY720 treatment, though FTY720 does not affect T cell proliferation *in vitro* (Brinkmann et al., 2001; Mehling et al., 2008; Xie et al., 2003). Together, this suggests that preventing the circulation of naïve T cells affects adequate T cell expansion in the lymph nodes resulting in a suppressed Ag-specific immune response, perhaps as a direct result of limiting the number of naïve T cells and therefore, the T cell repertoire, available for activation during immune challenge.

The results of this study are consistent with a previous study in an Ag-challenged mouse model (Xie et al., 2003), where FTY720-treated mice had a reduced Ag-specific T cell response. It has been suggested that lymphocytes treated with PT are resistant to the effects of FTY720 (Brinkmann et al., 2000), although PT is a toxin secreted by *B. pertussis*, its production was not sufficient

to overcome the immunosuppressive effects of FTY720 in *B. pertussis*-infected mice. It is important to note that DCs generated in the presence of FTY720 have an impaired ability to stimulate T cells, with a shift in cytokine production from IL-12 to IL-10 resulting in decreased IFN- γ -producing T cells (Muller et al., 2005). While this effect has not been demonstrated *in vivo*, it has been observed that FTY720 can impair DC migration *in vitro* and *in vivo* (Czeloth et al., 2005), providing an alternative explanation for the delayed T cell expansion in FTY720-treated *B. pertussis*-infected mice.

In the present study, there was an increase in the number of T_{EM} cells in the mediastinal lymph node of FTY720-treated infected mice 60 days after challenge. This was mirrored by an increase in T_{EM} cells in the lungs of FTY720-treated mice on day 60 post-challenge which, at this time point only, was comparable to vehicle control-treated *B. pertussis*-infected mice. It appears that 60 days after initial challenge, FTY720-treated mice are finally in the process of establishing an immune response through the expansion of effector memory cells in the draining lymph node and subsequent migration to the lung. This suggests that the immunosuppressive effect of FTY720 can eventually be overcome by the host, though the mice still had a considerable bacterial burden at this time point. Interestingly, CD3⁺ T cells typically infiltrate the lungs of untreated mice from day 7 post-challenge (McGuirk et al., 1998), with clearance of *B. pertussis* on day 42 post-infection (Dunne et al., 2010; Ross et al., 2013). While it has previously been demonstrated that FTY720 can impair the clearance of a mucosal infection due to suppression of the immune response (Murphy et al., 2012), changes were examined up to 14 days post-challenge and did not investigate whether FTY720 was associated with chronic infection in the weeks afterwards when vehicle control mice were infection-free. However, a recent study by Thawer and colleagues using *Nippostrongylus brasiliensis* infection (Thawer et al., 2014) suggested that FTY720 had no effect on re-infection of mice though, critically, the mice were given an anti-helminthic drug to clear the primary infection. Additionally, vaccinated mice treated with FTY720 during infectious challenge only, were as protected from BCG mycobacterial infection as vehicle control vaccinated mice (Connor et al., 2010).

Immunization of mice facilitates rapid clearance of infection with *B. pertussis*, which is mediated by protective immunity induced by T cells, yet the full mechanism is still unclear. Immunization with Pw induced Th1 and Th17 responses in mice, whereas immunization with Pa induced Th17 cells, but predominantly Th2 responses with clearance of infection mediated largely via humoral immunity (Barnard et al., 1996; Higgins et al., 2006; Mills et al., 1993; Redhead et al., 1993; Ross et al., 2013). These studies also demonstrated that Pw- is more effective than Pa-immunization, by inducing quicker clearance of infection with *B. pertussis*.

Immunization against *B. pertussis* began in the 1940s using Pw, but due to the side effects caused by this vaccine it was replaced by Pa in the late 1990s. However, a recent study has demonstrated that the immunity induced by Pa is short lived; protection wanes in children just 5 years after the last vaccine dose (Klein et al., 2012). The significant finding from the present experiments is that Pw induces a significant influx of CD4⁺ T_{EM} cells into the lung following challenge with *B. pertussis*, which is several-fold higher than that observed in Pa-immunised mice. The generation of this large pool of effector CD4⁺ T cells may be one mechanism for the increased effectiveness of Pw- over Pa-immunization. Importantly, chronic treatment with FTY720, which began after immunization but before bacterial challenge, did not impair the ability of mice to clear infection with *B. pertussis*. Bacterial clearance was still associated with a marked increase in CD4⁺ T_{EM} cell infiltration into the lung of Pw- compared with Pa-immunised mice. It appears that FTY720 treatment considerably impairs the development of an Ag-specific immune response during primary infection, however, once this effector memory population is established (either by primary challenge or as in this study, immunization) efficient clearance of the pathogen occurs.

An effective Th1 response is required for clearance of *B. pertussis*. Furthermore, IFN- γ from NK cells and $\gamma\delta$ T cells also contribute to protection. Studies in murine models reveal $\gamma\delta$ T cells, which are a source of IFN- γ , are recruited to the lung early in infection (McGuirk et al., 1998). In addition, $\gamma\delta$ TCR^{-/-} mice infected with *B. pertussis* have increased lung pathology in comparison to wild-type controls (Zachariadis et al., 2006). IFN- γ -secreting Th1 cells are induced

following infection with *B. pertussis* (Dunne et al., 2010; Mills et al., 1993; Ross et al., 2013), and IFN- γ ^{-/-} mice and IFN- γ R^{-/-} mice had reduced pathogen clearance, with many IFN- γ R^{-/-} mice succumbing to lethal infection (Barbic et al., 1997; Mahon et al., 1997). Macrophages are also crucial in the resolution of *B. pertussis* infection (Carbonetti et al., 2007) and, activation of macrophages by IFN- γ is important for NO production and subsequent killing of *B. pertussis* (Mahon and Mills, 1999). The impaired T cell response in FTY720-treated mice can reduce IFN- γ production by Th cells, constraining protective immunity through activation of bacterial killing by macrophages in the lung; this is reflected by the prolonged respiratory infection observed in FTY720-treated mice. This hypothesis is supported by the decreased expression of NOS2 and pro-inflammatory cytokines in the lungs of FTY720-treated *B. pertussis* infected mice.

Along with IFN- γ ⁺ T cells, IL-17 secreting Th17 cells are induced in mice infected with *B. pertussis* (Dunne et al., 2010; Ross et al., 2013). Furthermore, IL-17A^{-/-} mice have significantly impaired bacterial clearance (Ross et al., 2013), which was associated with decreased neutrophil recruitment to the lung. Although it is established that IL-17 can function in neutrophil recruitment (Laan et al., 1999; McKinley et al., 2008; Miyamoto et al., 2003) it also has a role in activating macrophages to kill *B. pertussis* (Higgins et al., 2006). This is consistent with the observation that depletion of neutrophils does not affect bacterial load post-infection with *B. pertussis* (Andreasen and Carbonetti, 2009; Harvill et al., 1999).

While the effect of FTY720 on T cells is profound, this drug has also been shown to affect B cell circulation (Morris et al., 2005) and migration of marginal zone B cells to the follicles (Cinamon et al., 2004). In addition, FTY720 prevents the production of high-affinity, class-switched antibodies due to inhibition of germinal centre formation in the lymph node (Han et al., 2004). In the present study, the absolute number of B cells in the lung of *B. pertussis*-infected mice was significantly reduced with FTY720 treatment. This was mirrored by a significant decrease in B cells in the lymph node in FTY720-treated *B. pertussis*-infected mice. It is possible that the enhanced duration of infection in FTY720-treated mice is, in part, due to the reduction in B cell number and in class-

switched antibodies in the lung. This is consistent with previous reports which document a requirement for B cells in the resolution of infection with *B. pertussis* (Hendrikx et al., 2011; Leef et al., 2000; Mahon et al., 1997).

FTY720 (and S1P) can promote vascular endothelial barrier integrity (Finney et al., 2011; Peng et al., 2004; Sanchez et al., 2003), by enhancing the distribution of the TJ proteins of endothelial cells (Brinkmann et al., 2004; Lee et al., 2006; Peng et al., 2004). In MS, restricting T cell entry is thought to be the major mechanism for the therapeutic benefits of FTY720 (Miron et al., 2008). The enhanced effect of FTY720 on TJ proteins has also been demonstrated in a model of experimental autoimmune uveoretinitis, where it promotes the integrity of the blood-ocular barrier (Copland et al., 2012) and it promotes vascular integrity in a model of cerebral malaria (Finney et al., 2011). However, FTY720 had little effect on the expression of the TJ proteins claudin-5 and occludin, both of which are expressed throughout the lung endothelium (Morita et al., 1999; Saitou et al., 1997). Together these findings suggest the reduced T cell number in the lung may be due to the effect of FTY720 on the initial expansion of Ag-specific, effector T cells in the draining lymph nodes and trafficking of these cells out of the lymph node to the lung, as opposed to an inability of the cells to cross the endothelial barriers and enter the lung.

In conclusion, treatment of mice with FTY720 reduced their ability to clear a primary infection with *B. pertussis*, with an increase in the bacterial load especially from 42 to 60 days post-challenge. The number of lung-infiltrating T cells and B cells was suppressed in FTY720-treated *B. pertussis*-infected mice, and reflected a decreased Ag-specific response in both the lungs and mediastinal lymph node. These findings may explain the increased rate of respiratory tract infections observed in patients with autoimmune disease during treatment with certain immunomodulatory drugs, and highlight the importance of both vaccination and early detection of infection in patients taking FTY720.

Chapter 6

**FTY720 treatment during infection with
B. pertussis attenuates the infection-
induced increase in AD-pathology in
APP/PS1 mice**

6.1 Introduction

Neuroinflammation is a common feature of neurodegenerative diseases, including AD (Akiyama et al., 2000). Numerous studies have demonstrated that pro-inflammatory signalling is enhanced in AD; the mRNA or protein expression of IL-1 β , IL-6 and IL-18 is increased in the brain (Griffin et al., 1989; Ojala et al., 2009; Wood et al., 1993), circulation or CSF of AD patients along with TNF α and IL-12p40 (Akiyama et al., 2000; Brosseron et al., 2014; Vom Berg et al., 2012). Indeed, inflammation has been implicated in the progression of AD at least in terms of A β accumulation, as pro-inflammatory cytokines can enhance the expression and activity of β -secretases and γ -secretases (Liao et al., 2004; Sastre et al., 2008) and inhibit phagocytosis of A β (Koenigsknecht-Talboo and Landreth, 2005; Pan et al., 2011). TNF α and IL-1 β decreases the expression of BBB TJ proteins *in vitro* (Kebir et al., 2007; Minagar and Alexander, 2003), as does A β (Carrano et al., 2011; Marco and Skaper, 2006; Tai et al., 2010), and it has been reported that AD patients have increased BBB permeability (Farrall and Wardlaw, 2009), with decreased expression of claudin-5, occludin and ZO-1 TJ proteins in A β -associated vessels (Carrano et al., 2011). A leaky BBB facilitates infiltration of peripheral immune cells, including T cells and macrophages, into the brain. A number of studies have documented T cells in the brains of AD patients (Hartwig, 1995; McGeer et al., 1989; Parachikova et al., 2007; Pirttila et al., 1992; Rogers et al., 1988; Togo et al., 2002; Town et al., 2005), along with macrophages, whose infiltration was at sites of disrupted TJs in vascular endothelial cells (Fiala et al., 2002). Consistent with the infiltration of T cells, microglia in the AD brain express MHC class II and CD40 (McGeer et al., 1989; McGeer et al., 1987; Perlmutter et al., 1992; Togo et al., 2000), indicating enhanced APC function.

Infection has also been implicated as a risk factor for the development of AD. It has been demonstrated that infection is associated with cognitive decline in AD patients (Holmes et al., 2009; Holmes et al., 2003). A recent study found that viral or bacterial infectious burden (for CMV, HSV-1, *B. burgdorferi*, *C. pneumonia* or *H. pylori*) was associated with AD, indeed more AD patients were positive for 4 or 5 pathogens than aged-matched controls (Bu et al., 2014). *C.*

pneumonia and HSV-1 have been detected in the post-mortem AD brain (Honjo et al., 2009), where infectious burden with *C. pneumonia* was higher in carriers of the *APOE4* allele (Gérard et al., 2005) and HSV-1 is also a risk factor for development of AD in *APOE4* carriers (Honjo et al., 2009). Infection with other pathogens including spirochetes (Maheshwari and Eslick, 2014), CMV (Barnes et al., 2014) and *H. pylori* (Roubaud-Baudron et al., 2012) have also been implicated with AD progression and are often associated with reduced MMSE scores. As demonstrated in Chapter 4, infection of older APP/PS1 mice with a common respiratory pathogen induces T cell infiltration, microglial activation and ultimately results in enhanced A β accumulation in the brain. Therefore, preventing T cell infiltration into the brain during the period of infection could prove an ideal therapy for the prevention of infection-induced amyloid deposition.

FTY720 is a derivative of the fungus *Isaria sinclairii* and has immunosuppressant effects (Adachi et al., 1995; Suzuki et al., 1996). FTY720 is structurally similar to S1P and acts as a “functional antagonist” of the S1P₁ receptor, resulting in receptor internalization which prevents S1P₁ from responding to S1P, which traps T cells in lymphoid organs (Brinkmann et al., 2010), and reduces T cell number in the circulation (Morris et al., 2005). FTY720 treatment reduced symptoms of disease in EAE (Brinkmann et al., 2002; Foster et al., 2007) and in MS patients (Kappos et al., 2006; Kappos et al., 2010), which is believed to be a direct result of reduced T cell infiltration into the brain (Brinkmann et al., 2010), though effects of FTY720 on astrocyte activation have also been reported (Choi et al., 2011). FTY720 has also proved beneficial in animal models of AD where treatment reversed behavioural deficits associated with injection of A β (Asle-Rousta et al., 2013; Fukumoto et al., 2014; Hemmati et al., 2013), however, the effect of long-term FTY720 treatment in transgenic AD models has not yet been examined.

While the results in Chapter 5 demonstrated that FTY720 enhanced the duration of infection with *B. pertussis*, this was associated with significantly reduced T cell influx into the lung with reduced lung inflammation. Therefore, FTY720 was used as a chronic treatment in APP/PS1 mice in an effort to reduce T

cell infiltration to the brain during infection and thereby reduce the T cell-associated inflammatory response that may lead to enhanced A β burden in the brain.

Study aims

The aims of this study were:

- 1) To establish whether FTY720 is neuroprotective in APP/PS1 mice.
- 2) To determine whether FTY720 can reduce T cell infiltration into the APP/PS1 mouse brain during infection with *B. pertussis*.
- 3) To investigate whether FTY720 can attenuate any infection-induced changes in AD-like pathology.

6.2 Results

6.2.1 Chronic treatment with FTY720 during infection with *B. pertussis* significantly reduces infection-induced neuroinflammation

C57BL/6 mice were infected with *B. pertussis* by aerosol challenge. One group was given FTY720 (0.3 mg/kg) daily for the duration of the experiment. Treatment began 10 days before mice were infected with *B. pertussis*. Vehicle control- and FTY720-treated mice were culled at 3 h, 7, 21, 28, 42 and 60 days post-challenge. The expression of pro- and anti-inflammatory markers was assessed using RNA extracted from snap-frozen cortical tissue. The expression of TCR β J, IL-17a, TNF α and CD40 all increased significantly in the brain after infection with *B. pertussis* (Fig 6.1). The expression of TCR β J did not increase with infection in mice treated with FTY720, while the expression of IL-17a, TNF α and CD40 were significantly decreased in the brains of FTY720-treated *B. pertussis*-infected mice in comparison with vehicle control-treated infected mice (Fig 6.1). The expression of IL-4 increased significantly in the cortex of *B. pertussis*-infected FTY720-treated mice on day 21 post-challenge (Fig 6.2A). The expression of IL-10 and arginase-1 increased with FTY720 treatment in infected mice, however, this did not reach statistical significance (Fig 6.2B, C).

6.2.2 Infection of APP/PS1 mice with *B. pertussis*

Older (9-10 months) WT and APP/PS1 mice were infected with *B. pertussis* by aerosol challenge with live bacteria. A group of WT and APP/PS1 mice were given FTY720 (0.3 mg/kg) daily for the duration of the experiment, treatment began 3 days before infection with *B. pertussis*. Evidence of successful infection was provided by performing CFU counts on lung homogenates removed from a group of mice at 3 h after challenge, the mean CFU counts were \log_{10} 4.4 (Fig 6.3), which is consistent with results described in Chapter 4 and 5 and is in agreement with studies from this laboratory (Dunne et al., 2010; Ross et al., 2013). Vehicle control- and FTY720-treated mice were free from infection by day 70 post-challenge (Fig 6.3).

A group of vehicle control WT and APP/PS1 mice infected with *B. pertussis* were culled on day 35 post-challenge to determine whether there was any genotype effect in their ability to resolve infection with *B. pertussis*. The splenocytes of WT and APP/PS1 mice were isolated and incubated with medium only, heat killed *B. pertussis*, or stimulated with α CD3/PMA for 72 h to investigate the Ag-specific T cell response (Fig 6.4). IFN- γ and IL-17 was quantified in the supernatants using ELISA. Re-stimulation of splenocytes from *B. pertussis* infected mice with heat killed *B. pertussis* induced significant IFN- γ and IL-17 production (Fig 6.4), as did α CD3/PMA. Importantly there was no genotype effect to the Ag-specific responses in the spleens of APP/PS1 mice.

6.2.3 Respiratory infection induces T cell infiltration into the brains of APP/PS1 mice

FTY720- and vehicle control-treated, infected WT and APP/PS1 mice, along with non-infected controls, were culled 70 days post-infection and brain tissue was prepared for flow cytometry to assess infiltration of immune cells. Mice were culled on day 70 post-challenge, rather than day 56 as in Chapter 4, due to the results from Chapter 5 which demonstrated that chronic treatment with FTY720 enhanced the duration of infection in mice. The proportion of CD3⁺CD4⁺ T cells was decreased in the brains of FTY720-treated mice (Fig 6.5A). In addition, the percentage, as opposed to the absolute number, of CD3⁺CD4⁺ and CD3⁺CD8⁺ T cells was increased in mice infected with *B. pertussis*, especially vehicle control-treated APP/PS1 mice (Fig 6.5A, B). Intracellular cytokine staining revealed that many of the CD4⁺ T cells in the brain were IFN- γ ⁺ (Fig 6.6A). Consistent with the results described in Chapter 4, there was a significant increase in IL-17⁺ and IFN- γ ⁺IL-17⁺ CD4⁺ T cells in *B. pertussis*-infected APP/PS1 mice (Fig 6.6B, C). CD8⁺ T cells revealed similar changes, with an infection-induced increase in the proportion of IL-17⁺ and IFN- γ ⁺IL-17⁺ CD8⁺ T cells in the brain (Fig 6.7B, C). To determine the extent of T cell infiltration into the brain parenchyma, cryostat sections were prepared and stained with CD3 before assessment by confocal microscopy. CD3⁺ T cells were found in the hippocampus of most mice, however there was a significant increase in the numbers of T cells which had infiltrated

into the hippocampus parenchyma of APP/PS1 vehicle control, infected and non-infected mice (Fig 6.8). Interestingly, a proportion of the T cells in APP/PS1 mice were found in close apposition to other brain cells (Fig 6.9). FTY720 significantly reduced the number of T cells in the hippocampus of both WT and APP/PS1 mice, even after infection with *B. pertussis*. While the FACS data demonstrated an FTY720-induced reduction in the proportion of CD4⁺ T cells in the brain, immunohistochemical analysis indicated that FTY720 prevented T infiltration into the brain parenchyma (Fig 6.8). Importantly, many of the T cells in WT or FTY720-treated mice were localised within ventricles or blood vessels (Fig 6.8A).

The expression of chemokines was assessed using RNA extracted from snap-frozen cortical tissue. Expression of CCL2 and CXCL1 was significantly increased in the brain following infection with *B. pertussis* (Fig 6.10A, D). CCL3 and CXCL10 were significantly increased in all APP/PS1 mice (Fig 6.10B, E) and CCL5 expression was also increased in APP/PS1 mice, however, this was the only chemokine reduced after treatment with FTY720 (Fig 6.10C).

6.2.4 FTY720 promotes BBB integrity in APP/PS1 mice

It has previously been suggested that FTY720 can increase the expression of TJ proteins of endothelial cells (Natarajan et al., 2013), therefore the leakage of fibrinogen into the hippocampus was assessed as a measure of BBB permeability. Fibrinogen immunoreactivity was found in the ventricles of mice, however, greater fibrinogen leakage from the ventricle into the hippocampus was observed in vehicle control, infected and non-infected APP/PS1 mice (Fig 6.11A). The dentate gyrus of the hippocampus also revealed similar changes (Fig 6.11B), which were quantified (Fig 6.11C). The fibrinogen leakage into the dentate gyrus was increased in vehicle control APP/PS1 mice and was significantly greater in APP/PS1 mice previously infected with *B. pertussis*, however, treatment with FTY720 significantly attenuated the extravasation of this plasma protein into the brain (Fig 6.11C). In addition, the expression of the TJ protein, occludin, was significantly increased in the cortex of non-infected mice after treatment with FTY720 (Fig 6.11D).

6.2.5 FTY720 reduces neuroinflammation in *B. pertussis*-infected APP/PS1 mice

Having demonstrated that FTY720 improves the integrity of the BBB, and reduces infiltration of T cells into the hippocampus, the effect of FTY720 on markers of neuroinflammation was assessed. Consistent with the results demonstrated in Chapter 4, older APP/PS1 mice had increased GFAP expression, indicating astrocyte activation, along with increased IL-6, CD68 and CD86 mRNA (Fig 6.12). In addition, CD68 and CD86 mRNA was increased further in vehicle control APP/PS1 mice that were previously infected with *B. pertussis* (Fig 6.12C, D). The effect of infection on the levels of mRNA expression was not as robust as observed in Chapter 4, likely due to the later time point of analysis at day 70 post-challenge for this study as opposed to day 56 in Chapter 4. However, FTY720 significantly reduced the expression of GFAP, IL-6 and CD86. APP/PS1 mice also had reduced expression of nerve growth factor (NGF) as previously reported (Minogue et al., 2014), and treatment with FTY720 significantly increased NGF mRNA (Fig 6.12). Together the data describe an FTY720-induced shift away from neuroinflammation in *B. pertussis*-infected APP/PS1 mice.

6.2.6 FTY720 reduces A β burden in *B. pertussis*-infected APP/PS1 mice

Consistent with the findings in Chapter 4, A β -containing plaques were found in the hippocampus, cortex and the frontal cortex in cryostat sections prepared from 12 month-old mice and the number of A β -containing plaques was further increased in all brain regions assessed post-infection with *B. pertussis* (Fig 6.13A-D). Interestingly, the number of A β -plaques was significantly lower in the hippocampus and cortex of *B. pertussis*-infected mice chronically treated with FTY720. The concentration of insoluble A β_{40} and A β_{42} were both increased in tissue prepared from the frontal cortex of *B. pertussis*-infected APP/PS1 mice (Fig 6.14C, D). Soluble A β_{40} and A β_{42} were also increased following infection in APP/PS1 mice, although this was significantly attenuated by treatment of APP/PS1 mice with FTY720 for the duration of the experiment (Fig 6.14A, B). These findings demonstrate that a peripheral infection of older APP/PS1 mice results in enhanced A β burden, however, treatment with FTY720 attenuates the

infection-induced increase in AD-pathology, which may be in part mediated by the BBB-promoting effects of FTY720 and reduced infiltration of T cells into the APP/PS1 brain during infection.

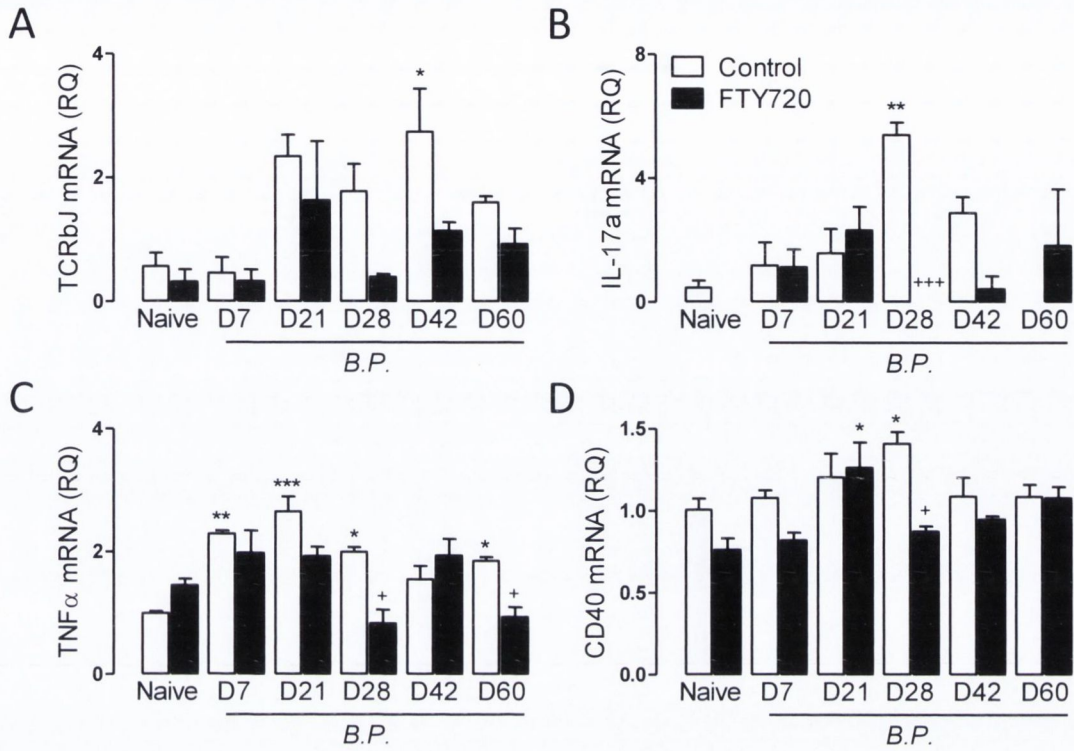


Figure 6.1 Chronic treatment with FTY720 during infection with *B. pertussis* reduces infection-induced neuroinflammation.

Mice were treated with FTY720 daily starting from day -10, control- and FTY720-treated mice were infected with *B. pertussis* at 5×10^8 CFU/ml on day 0 and sacrificed at various time points after *B. pertussis* infection. RNA was extracted from snap-frozen cortical tissue and assessed for (A) TCRbJ, (B) IL-17, (C) TNF α and (D) CD40 expression. Values are expressed as relative quantities (RQ) normalized to the endogenous control gene, 18S, and relative to the averaged naïve untreated mice. * $p < 0.05$, ** $p < 0.01$ in comparison to relevant naïve untreated mice; + $p < 0.05$, *** $p < 0.001$, in comparison to relevant untreated *B. pertussis*-infected mice; 1-way ANOVA with Newman-Keuls post hoc. Data represent means \pm SEM, $n = 4$ per time point. *B.P.*, *B. pertussis*; D, Day.

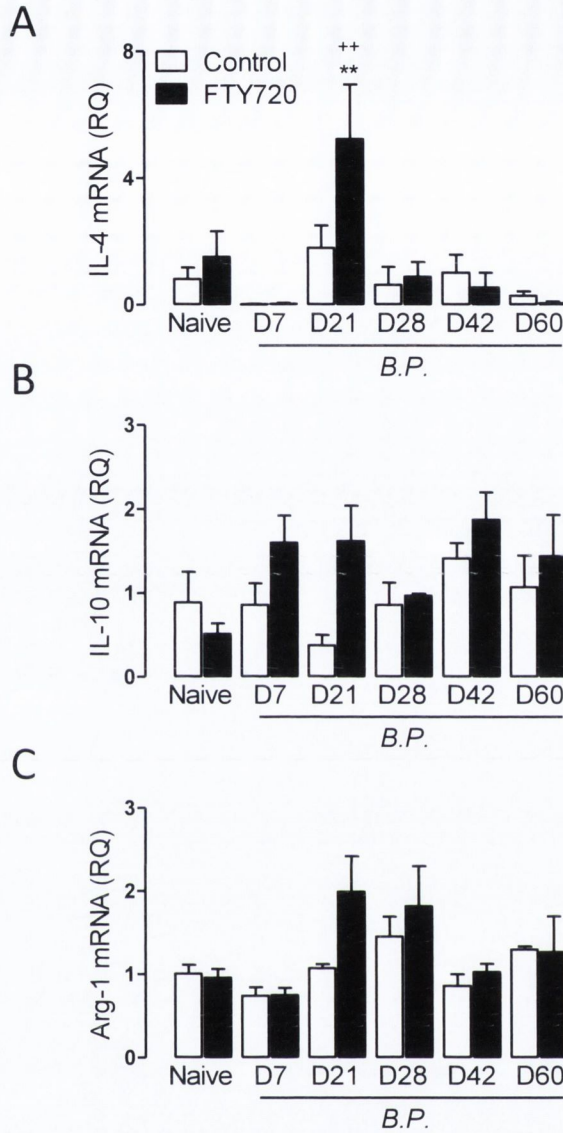


Figure 6.2 FTY720 induces the expression of IL-4 in the brain during infection with *B. pertussis*.

Mice were infected with *B. pertussis* and treated with FTY720 as described in Fig 6.1. RNA was extracted from snap-frozen cortical tissue and assessed for (A) IL-4, (B) IL-10 and (C) arginase-1 expression. Values are expressed as relative quantities (RQ) normalized to the endogenous control gene, 18S, and relative to the averaged naïve untreated group. ** $p < 0.01$ in comparison to relevant naïve untreated mice; ** $p < 0.01$, in comparison to relevant untreated *B. pertussis*-infected mice; 1-way ANOVA with Newman-Keuls post hoc. Data represent means \pm SEM, $n = 4$ per time point. *B.P.*, *B. pertussis*; D, Day.

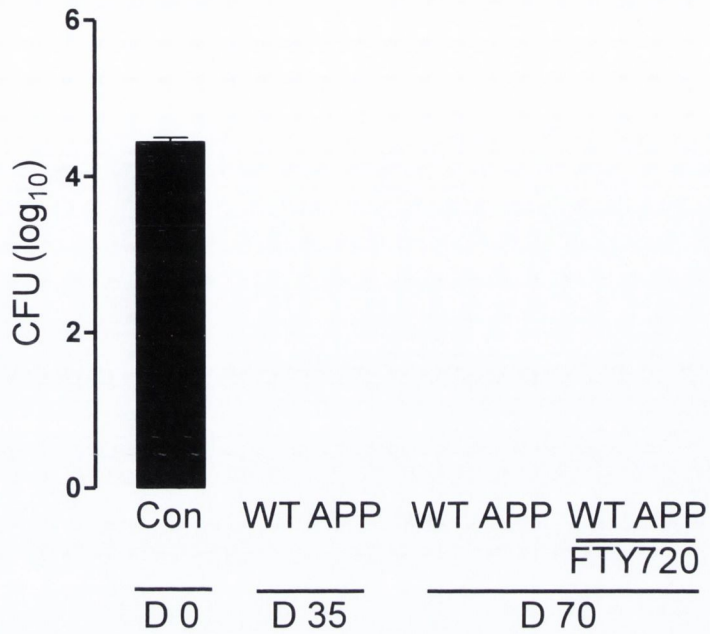


Figure 6.3 Challenge with *B. pertussis* induces transient infection in mice.

Mice were treated with FTY720 daily, starting from day -3. Control- and FTY720-treated WT and APP/PS1 mice were infected with *B. pertussis* at 5×10^8 CFU/ml on day 0 and sacrificed at various time points after *B. pertussis* infection. CFU counts were determined on the lung homogenate. Data represent means \pm SEM, n = 4-8. Con, control; APP, APP/PS1; D, Day.

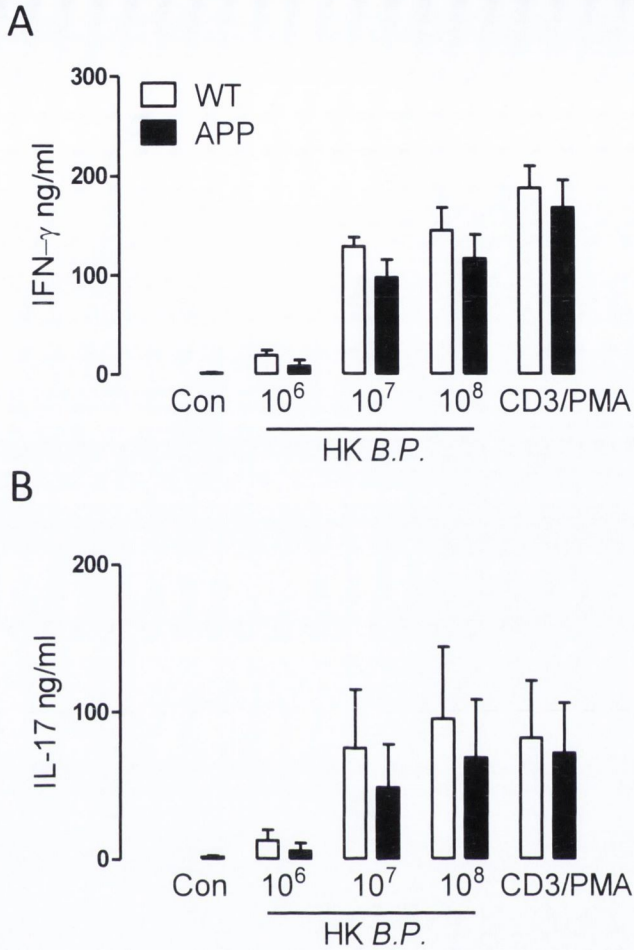


Figure 6.4 No evidence of genotype effect in response to *B. pertussis*-infection.

WT and APP/PS1 mice were infected with *B. pertussis* at 5×10^8 CFU/ml on day 0 and sacrificed on day 35 after *B. pertussis* infection. Cells prepared from the spleen were incubated medium only, HK *B.P.* (at 10^6 , 10^7 or 10^8 CFU/ml) or an α CD3/PMA cocktail for 72 h. IFN- γ and IL-17 was assessed in supernatant samples using ELISA. (A) IFN- γ ELISA: treatment effect *** $p < 0.001$; 2-way ANOVA. (B) IL-17 ELISA: treatment effect * $p < 0.05$; 2-way ANOVA. Data represent means \pm SEM, $n = 4$. Con, control; APP, APP/PS1; HK *B.P.*, heat killed *B. pertussis*.

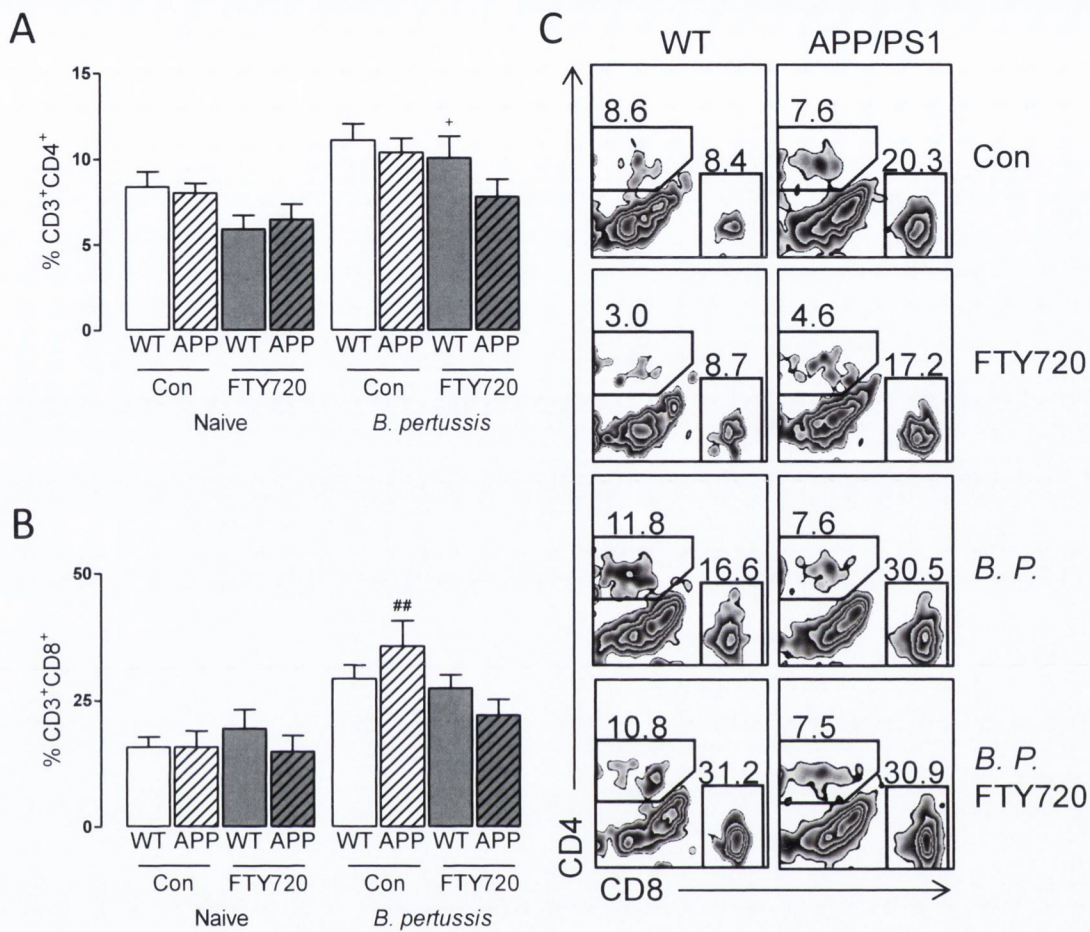


Figure 6.5 Infection induces CD4 and CD8 T cell trafficking to the brains of APP/PS1 mice.

Mice were infected with *B. pertussis* and treated with FTY720 as described in Fig 6.3. CD3⁺ T cells were surface stained for CD4 and CD8. Flow cytometric analysis was performed. Results are percentage of CD4⁺ (A) or CD8⁺ (B) T cells in the brain with sample FACS plots of CD4⁺CD8⁻ T cells and CD4⁺CD8⁺ T cells (C). (A) CD4⁺ T cells; FTY720 effect * $p < 0.05$, $F_{(1,49)}=6.24$, infection effect *** $p < 0.001$, $F_{(1,49)}=12.87$; 3-way ANOVA. (B) CD8⁺ T cells; Infection effect *** $p < 0.001$, $F_{(1,50)}=28.32$; 3-way ANOVA. + $p < 0.05$ in comparison to relevant FTY720 treatment control; ## $p < 0.01$ in comparison to relevant infection control; Newman-Keuls post hoc. Data represent means \pm SEM, $n = 8-10$. Con, Control; *B.P.*, *B. pertussis*.

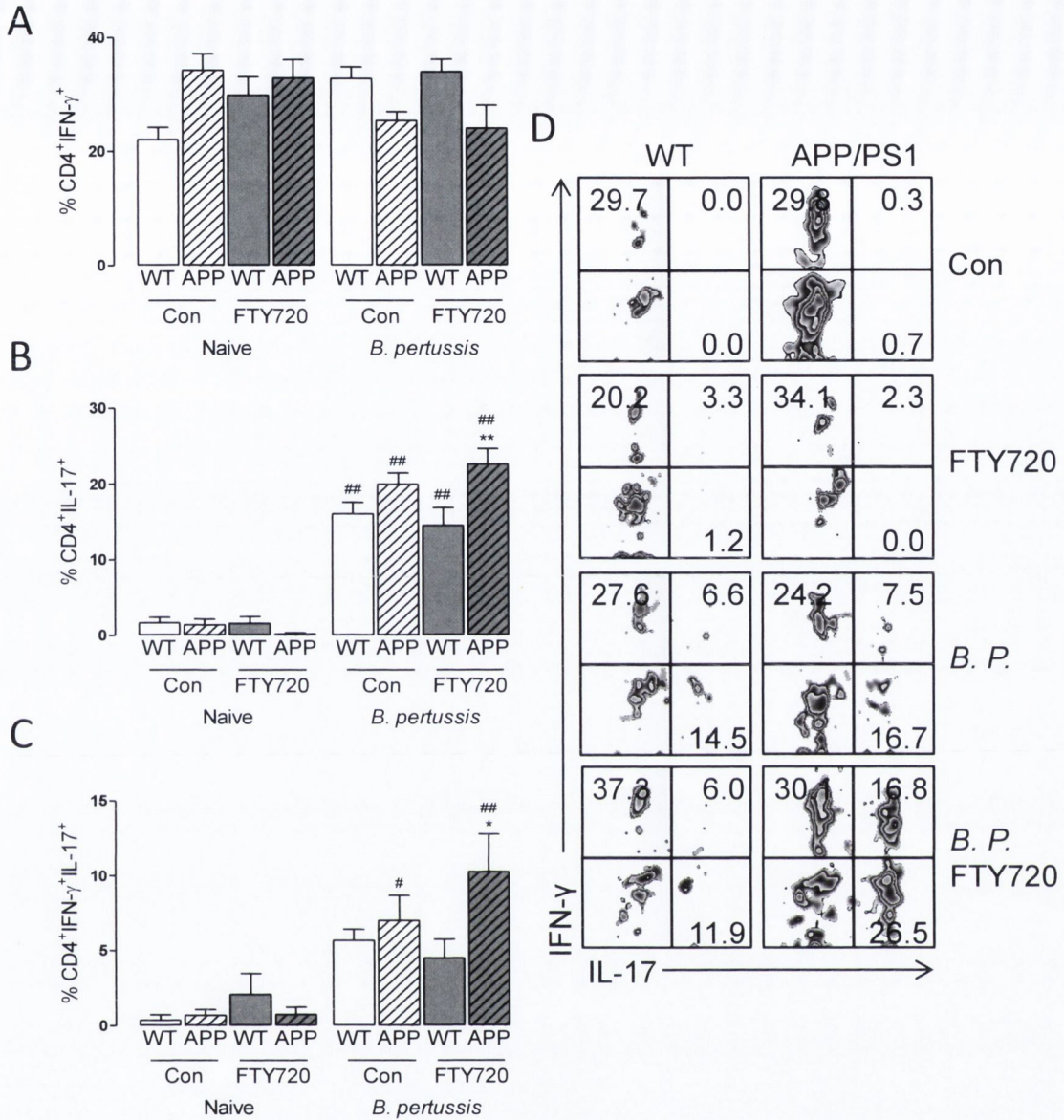


Figure 6.6 Increased IFN- γ ⁺ and IL-17⁺ CD4⁺ T cells in the brains of APP/PS1 mice following *B. pertussis*-infection.

CD4⁺ T cells were intracellularly stained for IFN- γ and IL-17 and assessed by flow cytometry. Results are percentage of CD4⁺ producing IFN- γ ⁺ (A), IL-17⁺ (B) or IFN- γ ⁺IL-17⁺ (C) in the brain. (A) CD4⁺IFN- γ ⁺; Genotype x infection interaction *** $p < 0.001$, $F_{(1,47)}=14.4$; 3-way ANOVA. (B) CD4⁺IL-17⁺; Genotype x infection interaction ** $p < 0.01$, $F_{(1,49)}=11.23$; 3-way ANOVA. (C) CD4⁺IFN- γ ⁺IL-17⁺; Genotype x infection interaction * $p < 0.05$, $F_{(1,50)}=4.45$; 3-way ANOVA. * $p < 0.05$, ** $p < 0.01$ in comparison to relevant genotype control; # $p < 0.05$, ## $p < 0.01$ in comparison to relevant infection control; Newman-Keuls post hoc. Sample FACS plots of IFN- γ ⁺ and IL-17⁺ CD4⁺ T cells (D). Data represent means \pm SEM $n = 8-10$. Con, Control; *B.P.*, *B. pertussis*.

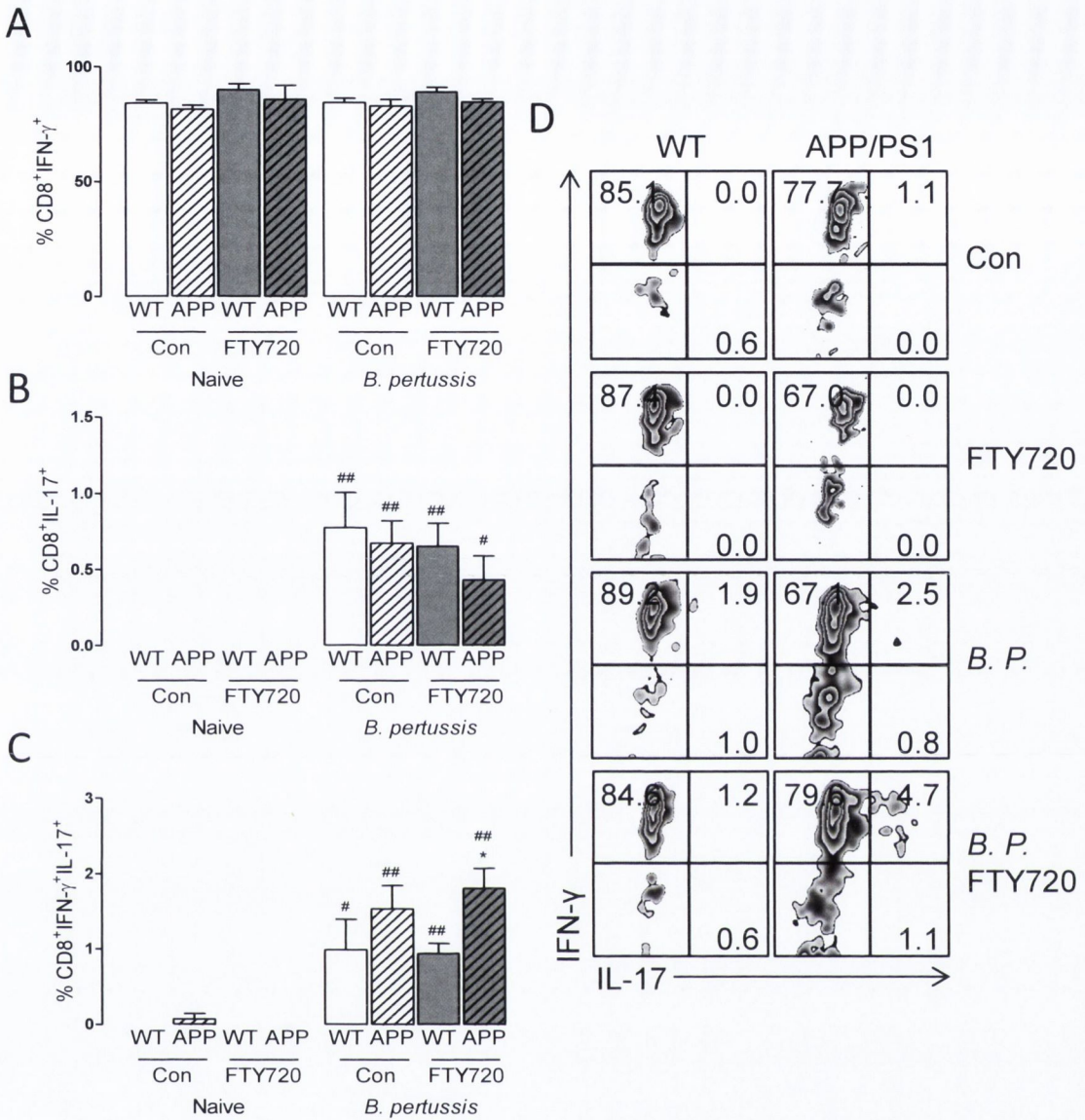


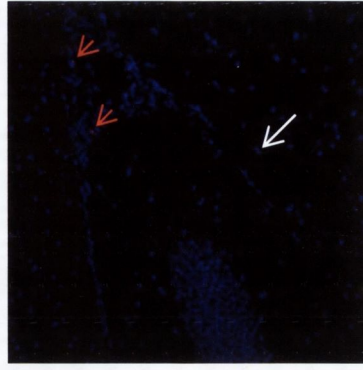
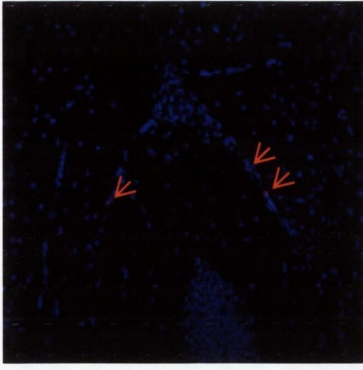
Figure 6.7 Increased IFN- γ ⁺ and IL-17⁺ CD8⁺ T cells in the brains of APP/PS1 mice following infection with *B. pertussis*.

CD8⁺ T cells were intracellularly stained for IFN- γ and IL-17 and assessed by flow cytometry. Results are mean percentage of CD8⁺ cells producing IFN- γ ⁺ (A), IL-17⁺ (B) or IFN- γ ⁺IL-17⁺ (C). (B) CD8⁺IL-17⁺; Infection effect *** $p < 0.001$, $F_{(1,51)}=50.6$; 3-way ANOVA. (C) CD8⁺IFN- γ ⁺IL-17⁺; Genotype x infection interaction * $p < 0.05$, $F_{(1,50)}=5.1$; 3-way ANOVA. * $p < 0.05$ in comparison to relevant genotype control; # $p < 0.05$, ## $p < 0.01$ in comparison to relevant infection control; Newman-Keuls post hoc. Sample FACS plots of IFN- γ ⁺ and IL-17⁺ CD8⁺ T cells (D). Data represent means \pm SEM $n = 8-10$. Con, Control; *B.P.*, *B. pertussis*.

A

WT

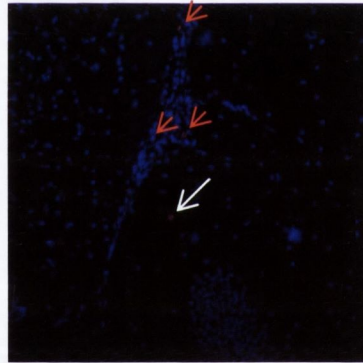
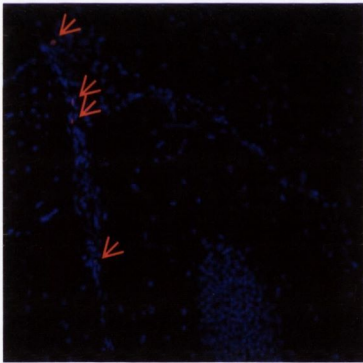
APP/PS1



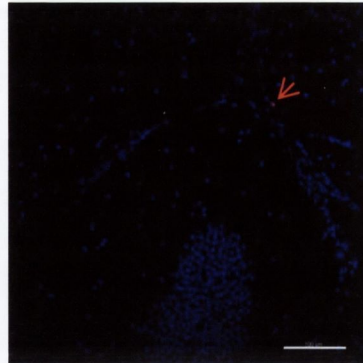
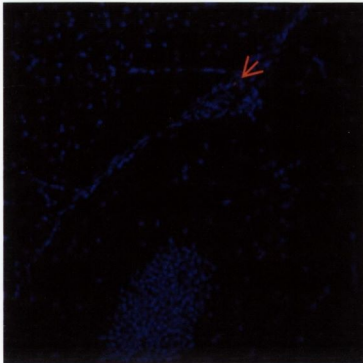
Con



FTY720



B. pertussis

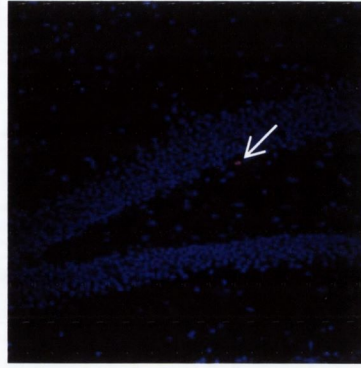
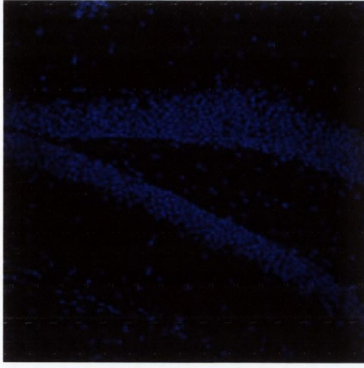


B. pertussis
FTY720

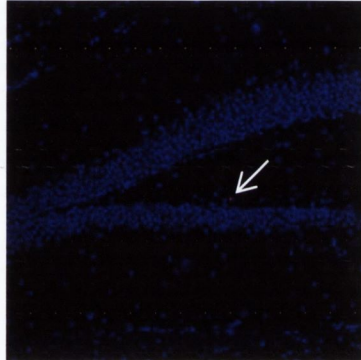
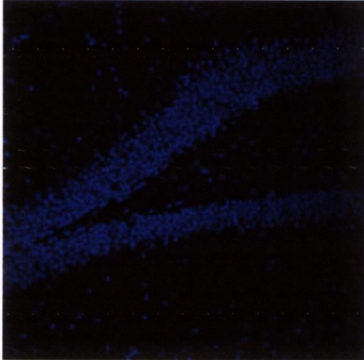
B

WT

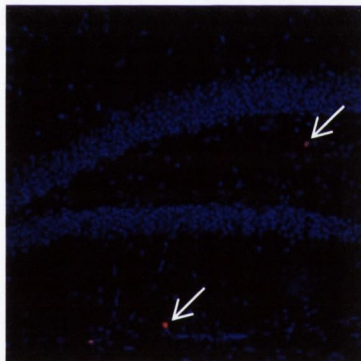
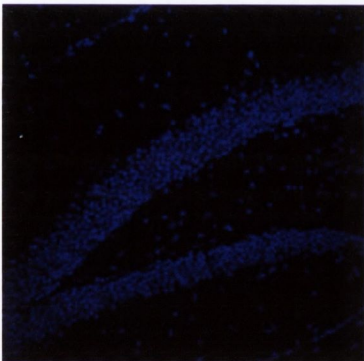
APP/PS1



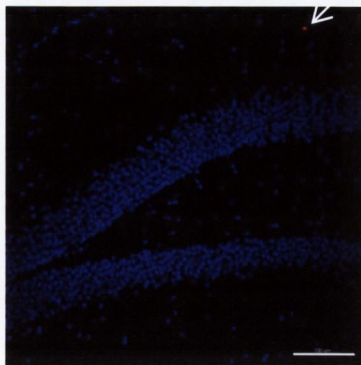
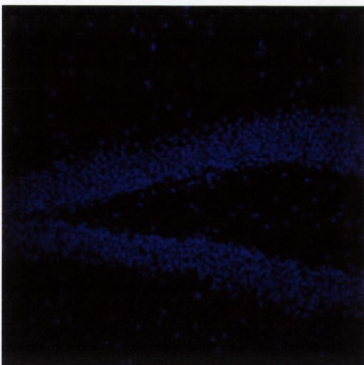
Con



FTY720



B. pertussis



B. pertussis
FTY720

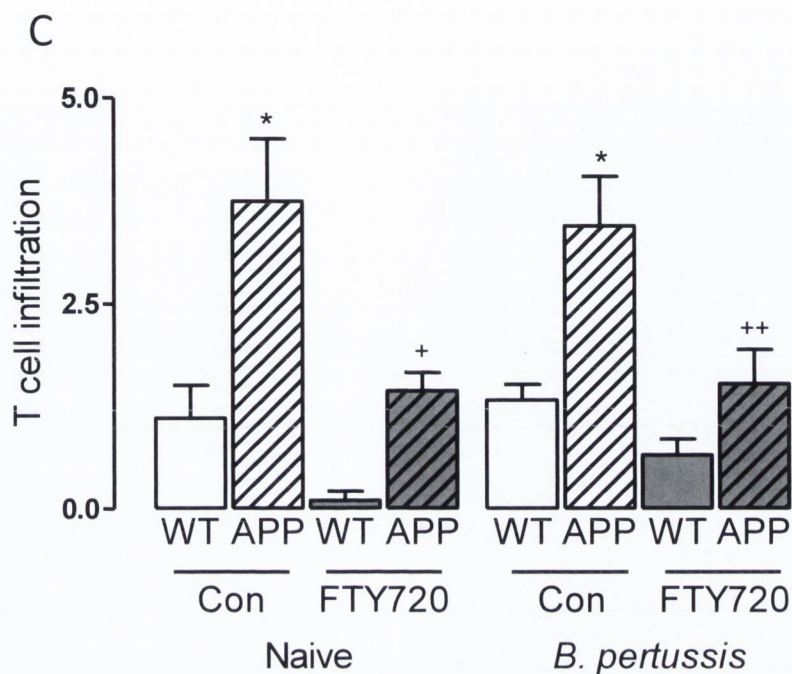


Figure 6.8 FTY720 reduces T cell infiltration into the hippocampus of APP/PS1 mice.

Mice were infected with *B. pertussis* and culled 70 days post-infection. Cryostat sections were stained with CD3 to assess T cell infiltration from the ventricle (A) into the hippocampus (B), the average number of T cells per hippocampus per mouse was recorded (C). Genotype effect *** $p < 0.001$, $F_{(1,20)}=25.55$; FTY720 effect *** $p < 0.001$, $F_{(1,20)}=18.31$; 3-way ANOVA. * $p < 0.05$ in comparison to relevant genotype control; + $p < 0.05$, ++ $p < 0.01$ in comparison to relevant FTY720 treatment control; Newman-Keuls post hoc. White arrows indicate T cell infiltration into the hippocampus parenchyma, red arrows are T cells in the ventricles. Scale bar = 100 μm . Data represent means \pm SEM, $n = 3-5$. Con, Control.

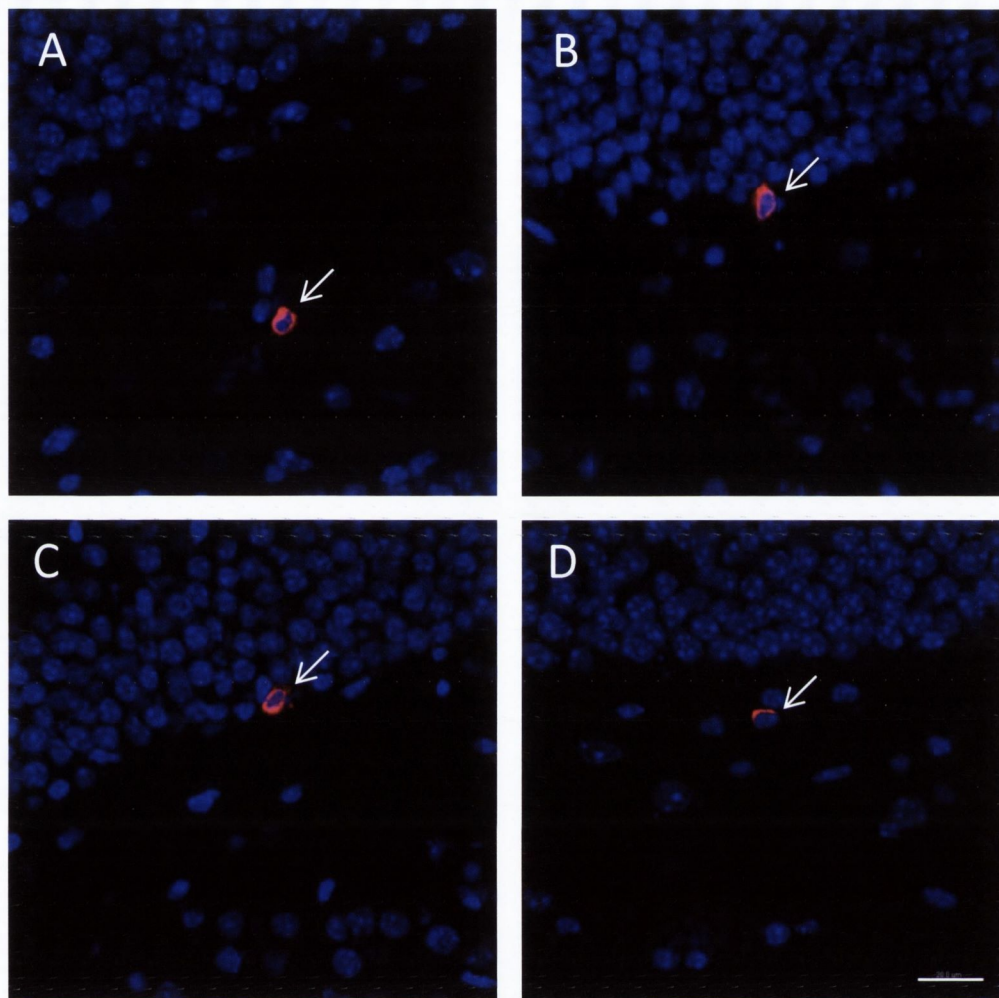


Figure 6.9 T cells found in close apposition to other brain cells in the hippocampus of APP/PS1 mice.

Mice were infected with *B. pertussis* and culled 70 days post-infection. Cryostat sections were stained with CD3 to assess T cell infiltration into the hippocampus, infiltrating T cells are found in close contact with other brain cells. (A, B) Untreated, non-infected APP/PS1 mice. (C, D) Untreated *B. pertussis*-infected APP/PS1 mice. White arrows indicate T cell infiltration into the hippocampus parenchyma, scale bar = 20 μm . Data represent means \pm SEM, n = 3-5.

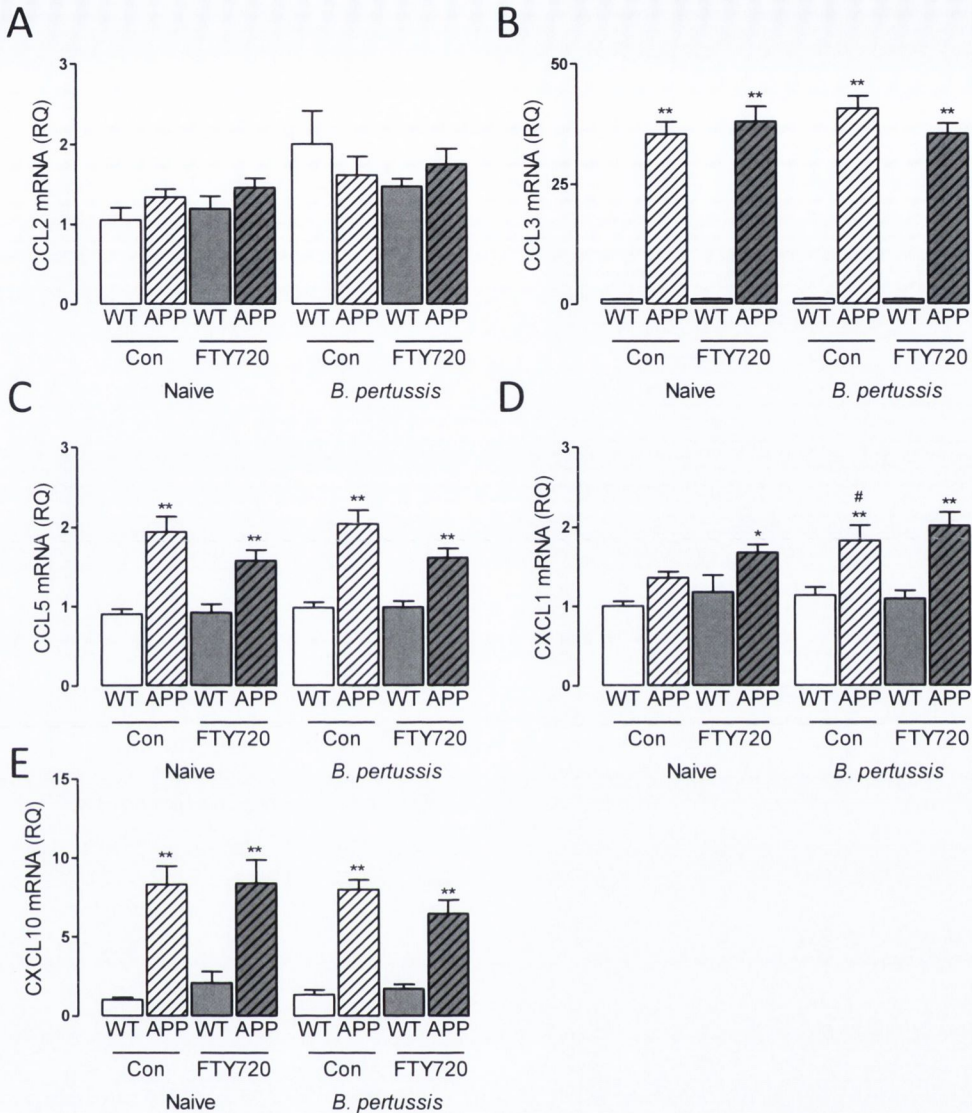


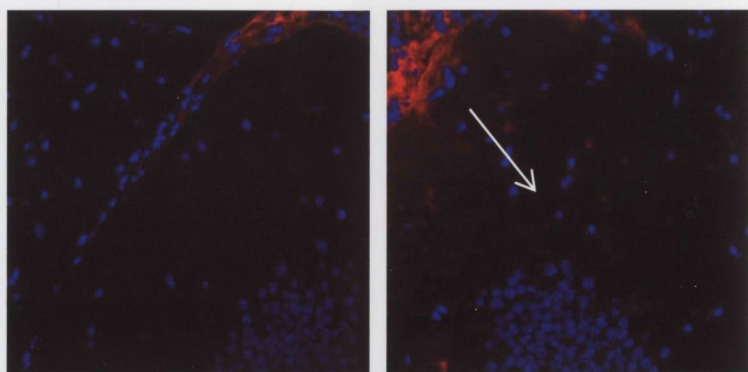
Figure 6.10 Increased chemokine expression in APP/PS1 mice.

RNA was extracted from snap-frozen cortical tissue and assessed for (A) CCL2 (B) CCL3, (C) CCL5, (D) CXCL1 and (E) CXCL10 expression. Values are expressed as relative quantities (RQ) normalised to the endogenous control gene, 18S, and relative to the averaged WT uninfected control group. (A) Infection effect ** $p < 0.01$, $F_{(1,50)}=8.4$; 3-way ANOVA. (B) Genotype effect *** $p < 0.001$, $F_{(1,47)}=814.83$; 3-way ANOVA. (C) FTY720 x genotype interaction * $p < 0.05$, $F_{(1,50)}=5.00$; 3-way ANOVA. (D) Genotype x infection interaction $p = 0.05$, $F_{(1,49)}=4.0$, genotype effect *** $p < 0.001$, $F_{(1,49)}=42.37$, infection effect * $p < 0.05$, $F_{(1,49)}=5.1$; 3-way ANOVA. (E) Genotype effect *** $p < 0.001$, $F_{(1,50)}=106.26$; 3-way ANOVA. ** $p < 0.01$ in comparison to relevant genotype control; # $p < 0.05$ in comparison to relevant infection control; Newman-Keuls post hoc. Data represent means \pm SEM, $n = 8-10$. Con, Control.

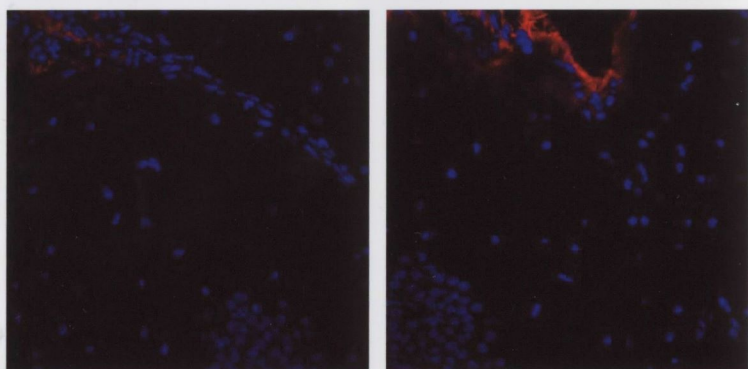
A

WT

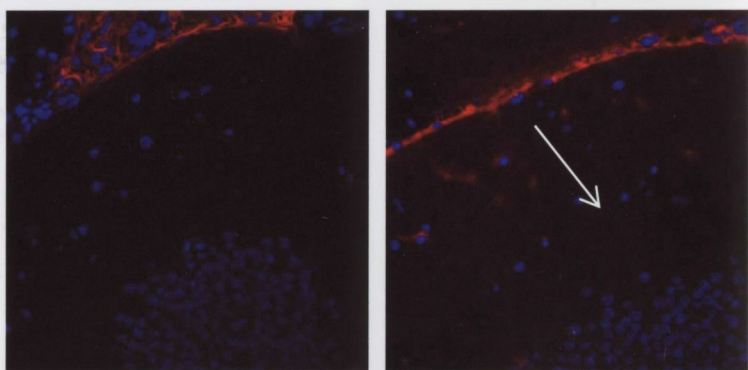
APP/PS1



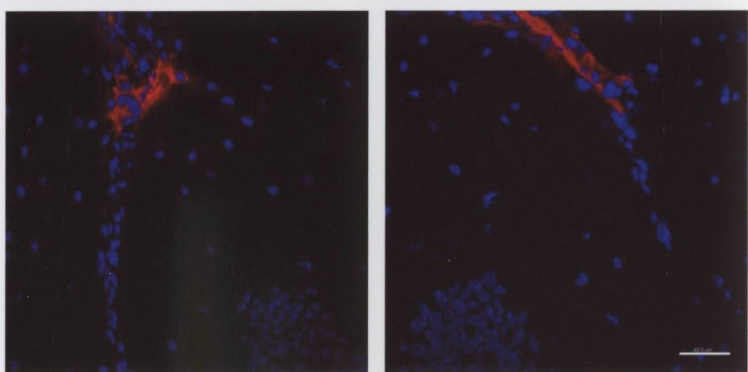
Con



FTY720



B. pertussis

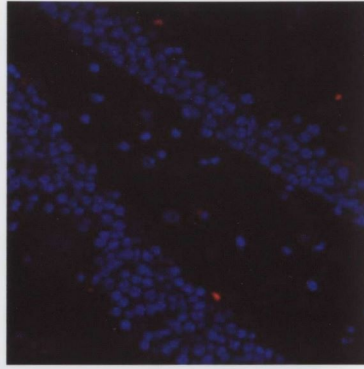
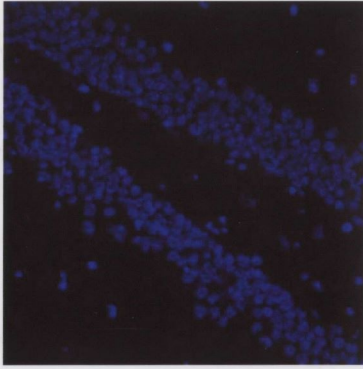


B. pertussis
FTY720

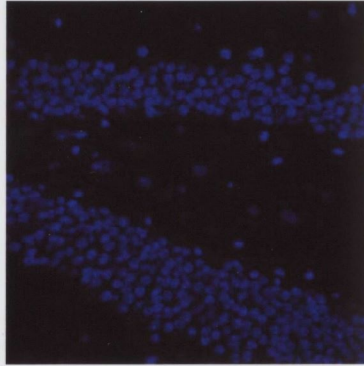
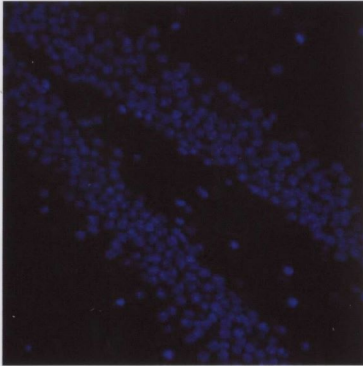
B

WT

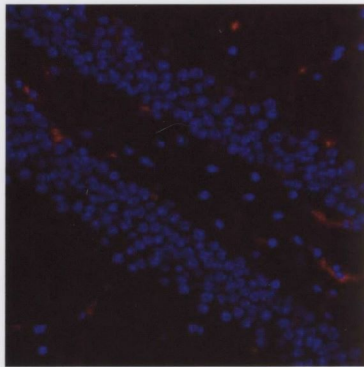
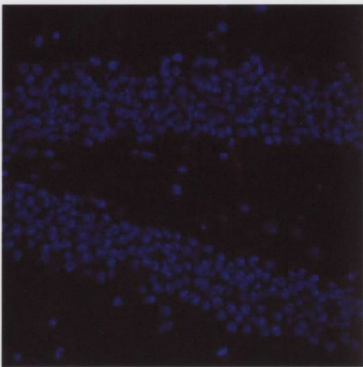
APP/PS1



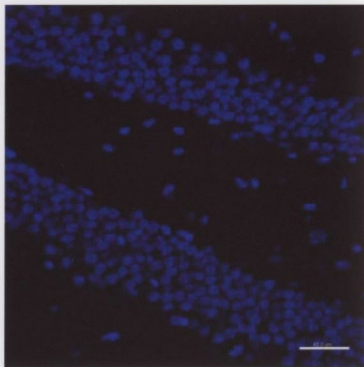
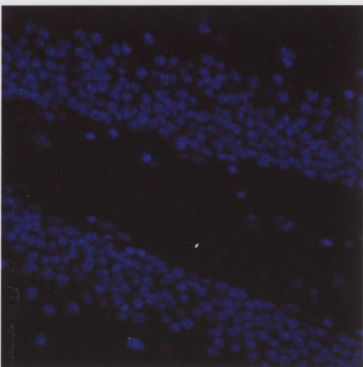
Con



FTY720



B. pertussis



B. pertussis
FTY720

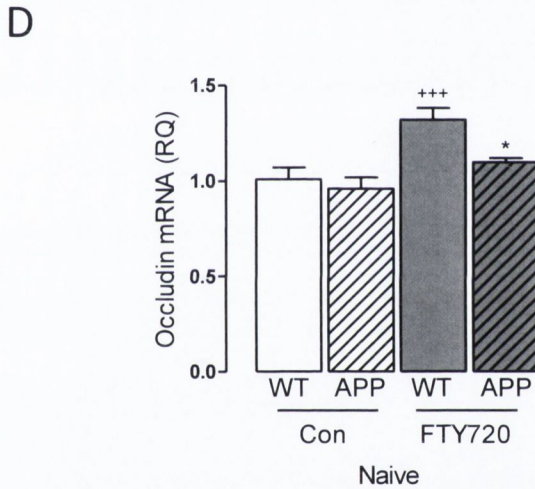
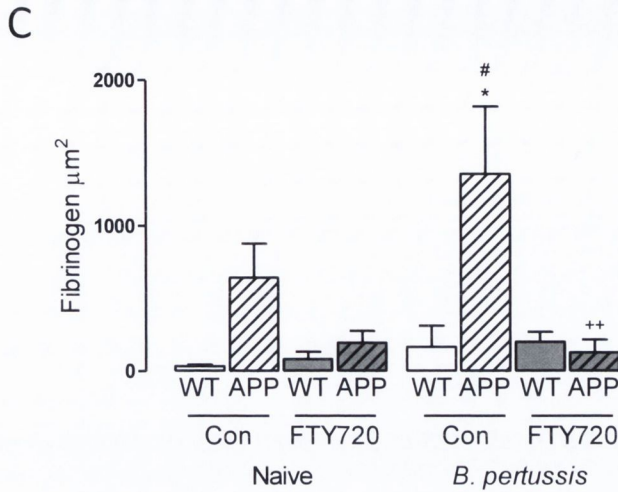


Figure 6.11 FTY720 promotes BBB integrity, reducing fibrinogen immunoreactivity in the hippocampus of APP/PS1 mice.

Cryostat sections were stained with fibrinogen to assess blood-brain barrier permeability at the ventricle (A) or hippocampus (B), and the average area of fibrinogen leakage into the hippocampus per mouse was quantified (C). (C) FTY720 x genotype interaction * $p < 0.05$, $F_{(1,22)}=5.63$; 3-way ANOVA. (D) RNA was extracted from snap-frozen cortical tissue and assessed for occludin; FTY720 effect *** $p < 0.001$, genotype effect * $p < 0.05$; 2-way ANOVA. (C) * $p < 0.05$ in comparison to relevant genotype control; ** $p < 0.01$, *** $p < 0.001$ in comparison to relevant FTY720 treatment control; # $p < 0.05$ in comparison to relevant infection control; Newman-Keuls post hoc. (D) * $p < 0.05$ in comparison to relevant genotype control; *** $p < 0.001$ in comparison to relevant FTY720 treatment control; Bonferroni post hoc. White arrow in (A) indicates direction of fibrinogen leakage, scale bar = 100 μm . Data represent means \pm SEM, $n = 3-6$. Con, Control.

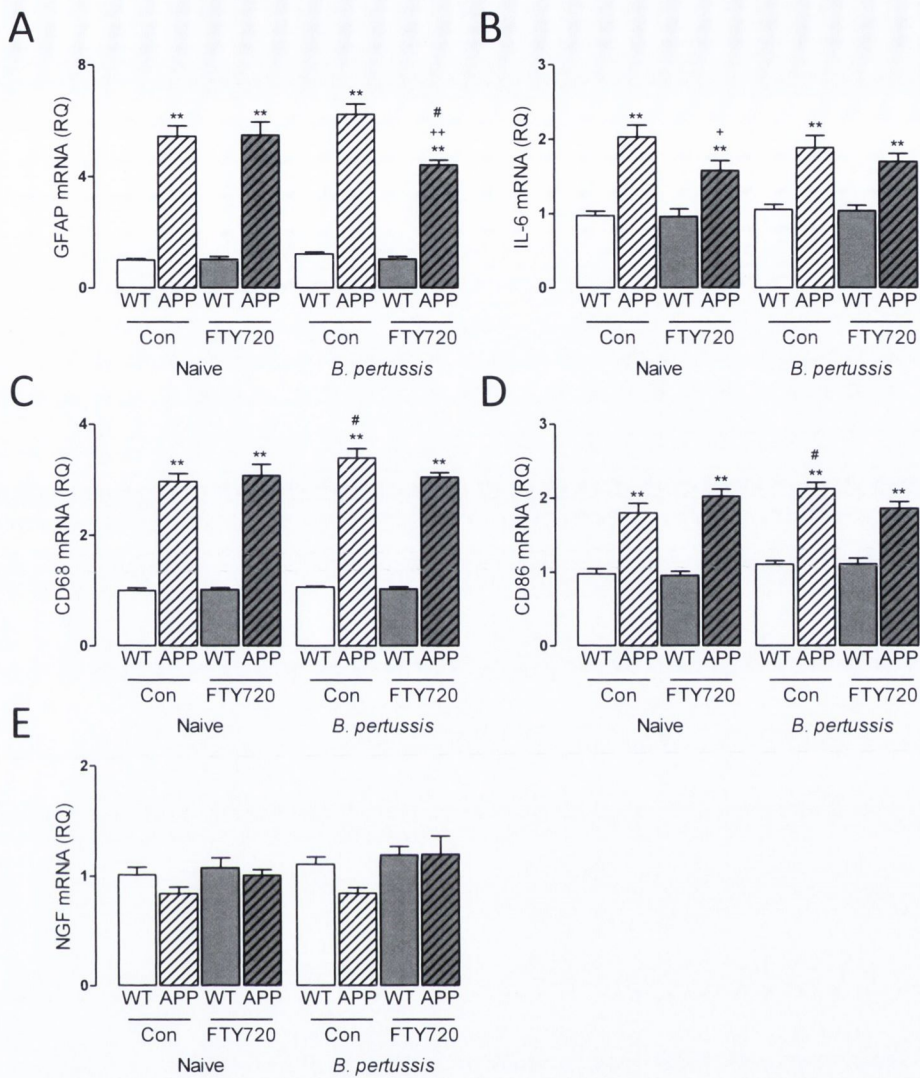


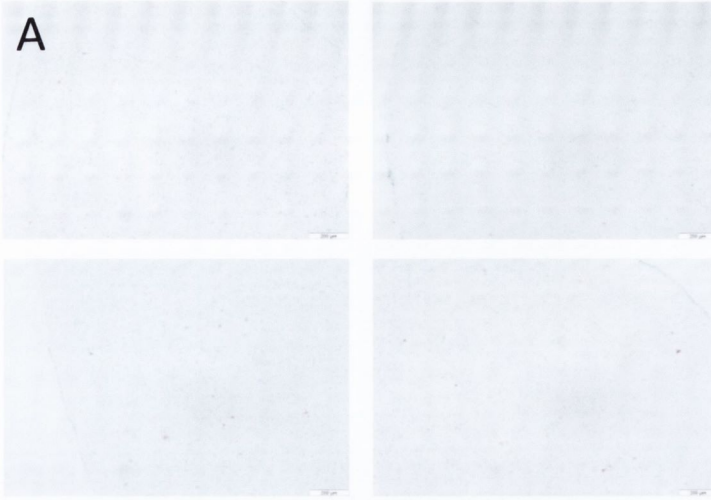
Figure 6.12 FTY720 treatment attenuates neuroinflammation in APP/PS1 mice.

RNA was extracted from snap-frozen cortical tissue and assessed for (A) GFAP (B) IL-6, (C) CD68, (D) CD86 and (E) NGF expression. Values are expressed as relative quantities (RQ) normalised to the endogenous control gene, 18S, and relative to the averaged WT uninfected control group. (A) FTY720 x genotype x infection interaction * $p < 0.05$, $F_{(1,48)}=4.85$; 3-way ANOVA. (B) FTY720 effect * $p < 0.05$, $F_{(1,49)}=4.49$, genotype effect *** $p < 0.001$, $F_{(1,49)}=98.85$, FTY720 x genotype interaction $p = 0.06$, $F_{(1,43)}=3.64$; 3-way ANOVA. (C) Genotype effect *** $p < 0.001$, $F_{(1,45)}=675.67$; 3-way ANOVA. (D) FTY720 x genotype x infection interaction * $p < 0.05$, $F_{(1,48)}=4.47$; 3-way ANOVA. (E) FTY720 effect * $p < 0.05$, $F_{(1,48)}=6.4$, genotype effect $p = 0.06$, $F_{(1,48)}=3.62$; 3-way ANOVA. ** $p < 0.01$ in comparison to relevant genotype control; + $p < 0.05$, ** $p < 0.01$ in comparison to relevant FTY720 control; # $p < 0.05$ in comparison to relevant infection control; Newman-Keuls post hoc. Data represent means \pm SEM, $n = 8-10$. Con, Control; *B.P.*, *B. pertussis*.

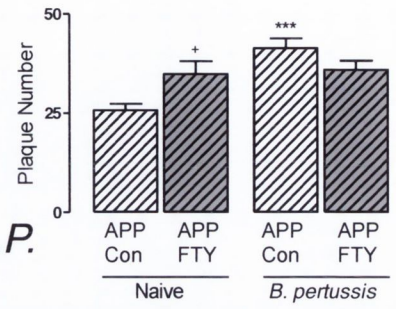
Con

FTY720

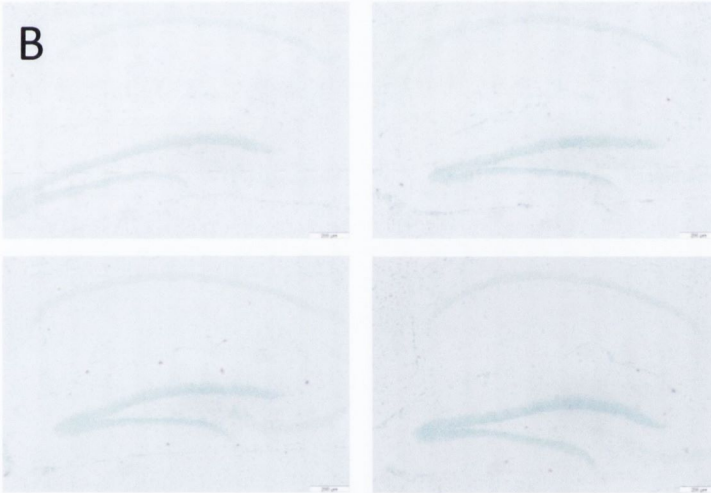
A



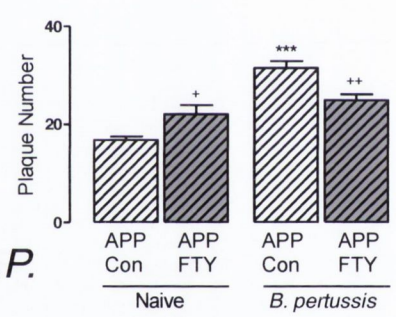
N



B.P.



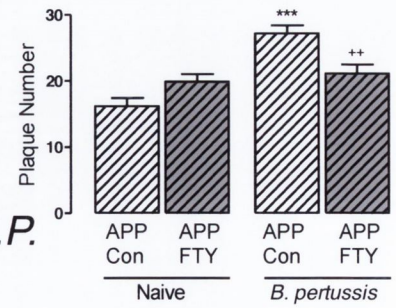
N



B.P.



N



B.P.

D

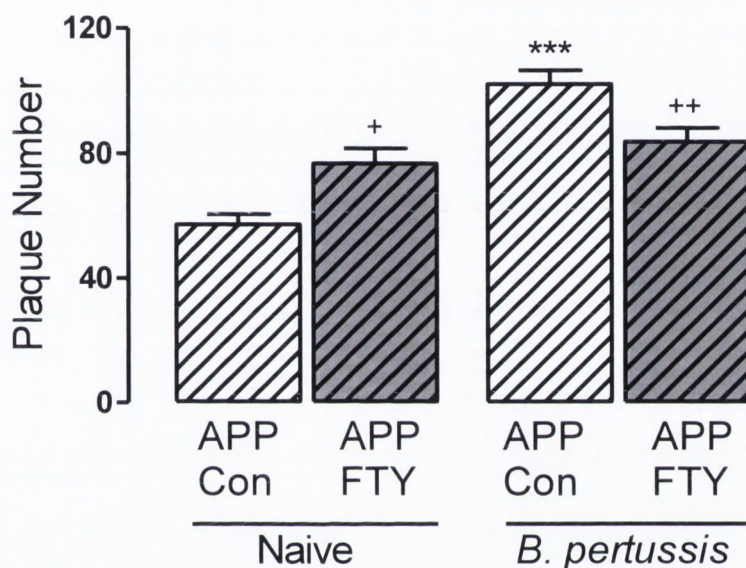


Figure 6.13 FTY720 treatment attenuates infection-induced A β deposition in APP/PS1 mice.

Cryostat sections were stained with Congo red to assess A β plaques in the frontal cortex (A), hippocampus (B) and cortex (C), the average number of plaques per area of interest per mouse was recorded. (A) Mean number in the frontal cortex; FTY720 x genotype interaction ** $p < 0.01$; 2-way ANOVA. (B) Mean number of plaques in the hippocampus; FTY720 x genotype interaction *** $p < 0.001$; 2-way ANOVA. (C) Mean number in the cortex; FTY720 x genotype interaction *** $p < 0.001$; 2-way ANOVA. (D) Combined counts for the three areas; FTY720 x genotype interaction *** $p < 0.001$; 2-way ANOVA. *** $p < 0.01$ in comparison to relevant infection control; + $p < 0.05$, ++ $p < 0.01$ in comparison to relevant FTY720 control; Bonferroni post hoc. Data represent means \pm SEM, $n = 8-10$, scale bar = 200 μm . Con, Control; *B.P.*, *B. pertussis*; N, Naïve.

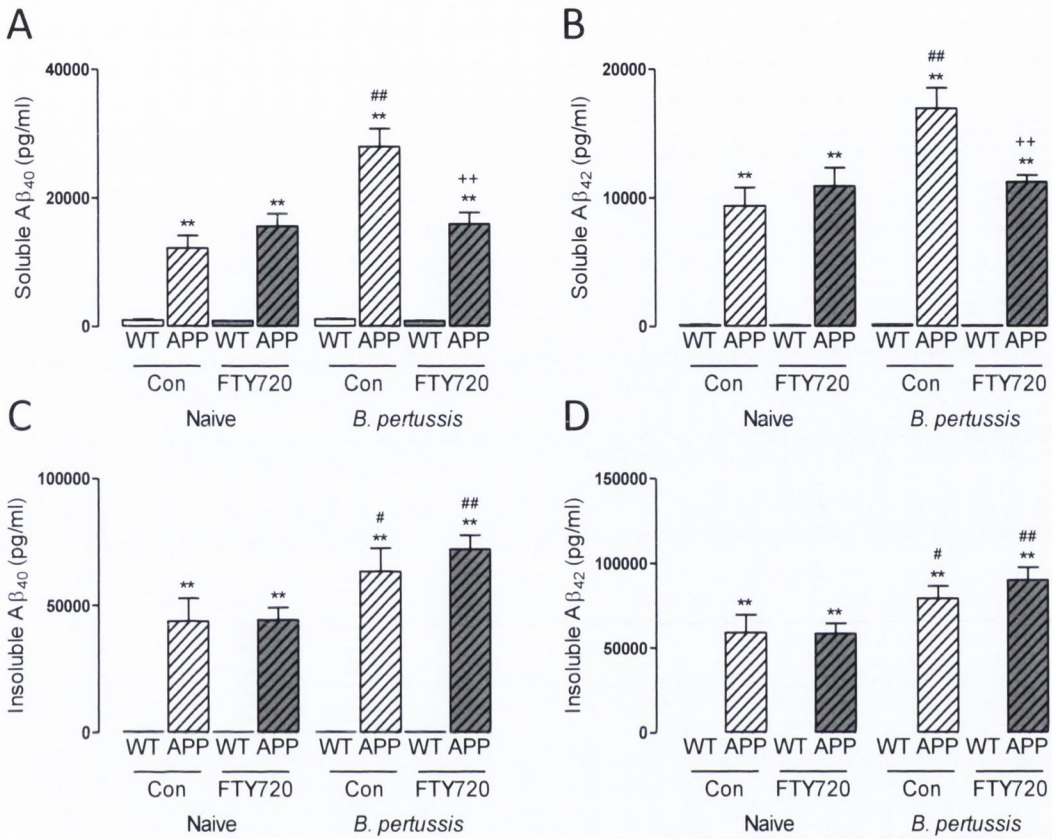


Figure 6.14 FTY720 treatment attenuates infection-induced production of soluble A β_{40} and A β_{42} in APP/PS1 mice.

Mice were infected with *B. pertussis* and culled 70 days post-infection. Amyloid levels were determined by Meso Scale from snap-frozen frontal cortical tissue. The concentrations of soluble A β_{40} (A) and A β_{42} (B), insoluble A β_{40} (C) and A β_{42} (D) were established with reference to the standard curves. (A) FTY720 x genotype x infection interaction *** $p < 0.001$, $F_{(1,49)}=12.31$; 3-way ANOVA. (B) FTY720 x genotype x infection interaction ** $p < 0.01$, $F_{(1,46)}=8.62$; 3-way ANOVA. (C) Genotype x infection interaction ** $p < 0.01$, $F_{(1,47)}=10.52$; 3-way ANOVA. (D) Genotype x infection interaction ** $p < 0.01$, $F_{(1,47)}=10.05$; 3-way ANOVA. ** $p < 0.01$ in comparison to relevant genotype control; ++ $p < 0.01$ in comparison to relevant FTY720 control; # $p < 0.05$, ## $p < 0.01$ in comparison to relevant infection control; Newman-Keuls post hoc. Data represent means \pm SEM, $n = 8-10$. Con, Control.

6.3 Discussion

The results in Chapter 4 demonstrated that older APP/PS1 mice were more vulnerable to the effects of a respiratory infection than their younger, or WT counterparts when assessed 56 day post-challenge. The aim of this present study was to examine whether preventing T cell infiltration into the brain during the period of infection could attenuate the infection-induced changes in AD-pathology. However, as the results in Chapter 5 demonstrated FTY720 enhanced the duration of infection, in this series of experiments mice were culled 70 days post-challenge with *B. pertussis*. Infection of APP/PS1 mice increased BBB permeability demonstrated by enhanced fibrinogen leakage into the hippocampus and, as shown in Chapter 4, infection increased the accumulation of A β -plaques throughout the brain. It was observed that the chronic treatment of APP/PS1 mice with FTY720 reduced the proportion of CD3⁺CD4⁺ T cells, reduced T cell infiltration into the hippocampus of WT and APP/PS1 mice as assessed by immunohistochemistry, and improved the BBB integrity of APP/PS1 mice by attenuating the infection-induced increase in fibrinogen extravasation into the hippocampus. Ultimately, FTY720 treatment reduced the infection-induced accumulation of A β -plaques in the hippocampus and cortex, and the concentration of soluble A β . These findings strengthen the hypothesis that infection is an important risk factor in the progression of AD, and suggest treatment with an immunomodulating drug like FTY720 could protect the brain from infection by improving the stability of the BBB, reducing T cell infiltration and thus may be a potential therapy for this disease.

Consistent with the findings from Chapter 4, infection of mice with *B. pertussis* increased the proportion of IL-17⁺ T cells in the brain. Importantly, these changes were observed 70 days following challenge with *B. pertussis*, and more than 35 days after clearance of bacteria in vehicle control mice, demonstrating a persistent genotype-related susceptibility to infection in APP/PS1 mice. IL-17 is important in the control and clearance of *B. pertussis* infection, as mice deficient in IL-17 have increased bacterial burden at later stages of infection, with delayed clearance (Ross et al., 2013). The T cells of AD

patients have an A β -induced Th17 phenotype (Saresella et al., 2011), in addition, A β -specific Th17 cells induce microglial activation in mixed glial cultures (McQuillan et al., 2010) and also cause astrocyte activation (Chapter 3). Transfer of A β -specific Th17 cells into 6-7 month old APP/PS1 mice resulted in increased CD11b immunoreactivity in the cortex of APP/PS1 mice, however Th17 cells alone did not enhance plaque deposition three weeks following transfer (Browne et al., 2013). Transfer of A β -specific Th1 cells enhanced amyloid deposition in APP/PS1 mice, which was attenuated by neutralising IFN- γ (Browne et al., 2013). In the present study, IFN- γ ⁺ T cells were also found in the brains of mice and together with the IL-17⁺ T cell population, suggest peripheral infection induces a window of enhanced T cell infiltration into the brain that persists for weeks after clearance of bacteria in older APP/PS1 mice. Staining cryostat sections for CD3 confirmed APP/PS1 mice have increased T cell influx into the parenchyma and FTY720 significantly reduced the number of T cells infiltrating into the hippocampus of APP/PS1 mice, to a number comparable with WT mice. Importantly, many of the T cells in WT or FTY720-treated mice were confined to the ventricles. This is consistent with reports demonstrating FTY720 decreases T cell number in the circulation (Morris et al., 2005) and was protective in EAE by reducing the number of T cells in the CNS (Kataoka et al., 2005). In addition, FTY720 induces selective retention of naïve T cells and T_{CM} over T_{EM} (Brinkmann et al., 2010). It has been demonstrated that two-thirds of CD4⁺ T cells in the CSF are T_{CM} (Kivisakk et al., 2003), and it is believed that T_{CM} are the pathogenic T cell in MS (Brinkmann et al., 2010). FTY720 had little effect on the expression of chemokines within the APP/PS1 brain, thus the FTY720-induced reduction in T cell infiltration into the parenchyma may be a direct result of lymphocyte sequestration in lymphoid organs or the enhanced BBB blocking entry, as opposed to a reduction in chemotactic signalling. It is possible that the mechanism of FTY720-mediated neuroprotection in APP/PS1 mice is by reducing T cell infiltration into the brain parenchyma, limiting T cell induced activation of microglia and astrocytes during the period of infection which perhaps prevents the infection-induced increase in amyloid as a result. While the antigen specificity of T cells in the CNS was not assessed, a proportion of T cells from C57BL/6 and APP/PS1 mice are responsive to A β (Toly-Ndour et al., 2011). The

presence of amyloid plaques in the APP/PS1 brain could allow for local re-stimulation of these cells, which may have further consequences for mice exposed to *B. pertussis* where enhanced T cell infiltration and amyloid deposition was observed.

The S1P receptor is expressed by many cells in the CNS (Dev et al., 2008), and it has been shown that FTY720 exerts a protective effect in EAE by acting on S1P₁ receptors on astrocytes, as EAE severity was reduced and FTY720 efficacy lost in mice lacking astrocyte S1P₁ (Choi et al., 2011). A recent study observed FTY720 reduced astrocyte activation in EAE (Colombo et al., 2014). Colombo and colleagues also found that IL-1 and IL-17 induced NF- κ B translocation to the nucleus with NO production in astrocytes, which was inhibited with FTY720 treatment, preventing astrocyte-induced neurodegeneration as a result (Colombo et al., 2014). In the present study astrocyte activation, as assessed by GFAP expression, was reduced in *B. pertussis*-infected FTY720-treated APP/PS1 mice. Within the CNS, astrocytes are the predominant source of IL-6 (Van Wagoner et al., 1999), and FTY720 also reduced the expression of IL-6 in all FTY720-treated APP/PS1 mice. Expression of the neurotrophic factor, NGF, was reduced in APP/PS1 mice which is consistent with previous reports (Minogue et al., 2014), and it was observed that FTY720 increased the expression of NGF in treated mice. Astrocytes are a major source of NGF in the CNS (Eddleston and Mucke, 1993). Moreover, anti-inflammatory cytokines including IL-4 and IL-10 can enhance NGF production by astrocytes, which is inhibited by IFN- γ (Brodie, 1996; Brodie et al., 1998). FTY720 can also induce BDNF mRNA and protein expression in neuronal cultures *in vitro* (Doi et al., 2013). This is of importance in the context of AD, as astrocyte mediated inflammation has been implicated in AD (Garwood et al., 2011), along with decreased levels of neurotrophic factors (Hock et al., 2000). Furthermore, it has been suggested that FTY720 may have dual functions in astrocytes, inhibiting S1P-induced cell proliferation and IL-1-induced calcium signalling without affecting IL-1 induced CXCL10 production (Wu et al., 2013), thus FTY720 impairs some specific functions in astrocytes without inhibiting all astrocytic responses.

APP/PS1 mice had enhanced fibrinogen immunoreactivity in the hippocampus, which was exacerbated after infection with *B. pertussis*, importantly this plasma protein was still elevated 70 days post-challenge indicating a genotype co-morbidity in BBB dysfunction after exposure to infection. However, treatment of APP/PS1 mice with FTY720 significantly attenuated fibrinogen leakage into the hippocampus. Previous results from this laboratory have demonstrated increased BBB permeability in 14 month-old APP/PS1, compared with WT, mice evidenced by enhanced gadolinium extravasation into the brain by MRI (Minogue et al., 2014). Leakage of the plasma proteins fibrinogen, thrombin and prothrombin has also been demonstrated in post-mortem tissue from AD patients, and were often associated with activated microglia or A β deposits (Akiyama et al., 1992; Berzin et al., 2000; Fiala et al., 2002; Ryu and McLarnon, 2009). Indeed injection of A β into the rat hippocampus induced fibrinogen extravasation into the parenchyma that co-localised with A β and activated microglia (Ryu and McLarnon, 2009). Fibrinogen has also been directly implicated in BBB damage and neuroinflammation. Fibrinogen accumulation correlated with A β deposition in transgenic AD-mice, mice with just one functional fibrinogen gene had reduced BBB permeability, and treatment of AD-transgenic mice with anicrod, which depleted circulating fibrinogen attenuated microglial activation and vascular changes (Paul et al., 2007). FTY720 reversed BBB damage in EAE (Foster et al., 2009) and significantly improved MRI endpoints in MS patients, as patients treated with FTY720 had significantly reduced gadolinium-enhanced lesions (Kappos et al., 2010). In other models of inflammation, FTY720 attenuated LPS-induced barrier permeability (Peng et al., 2004) and restored vascular integrity in a model of experimental autoimmune uveoretinitis, promoting the expression of occludin, claudin and ZO-1 at the blood-ocular barrier (Copland et al., 2012). However, this is the first study to demonstrate that FTY720 improves BBB integrity in APP/PS1 mice.

In the present study, infection with *B. pertussis* induced a significant increase in A β accumulation throughout the brain, which was accompanied by an increased concentration of insoluble A β . This is in agreement with the results in

Chapter 4, however, on day 70 post-challenge the levels of soluble A β were also significantly greater in previously infected, vehicle control APP/PS1 mice. Treatment with FTY720 for the duration of infection significantly attenuated the infection-induced increase in soluble A β in the frontal cortex, and prevented A β deposition in the hippocampus and cortex. On production, A β forms soluble oligomers which can aggregate, becoming insoluble fibrils. A β can cause physical insult to neuronal processes by aggregating in the extracellular space (Vickers et al., 2000), however, oligomeric A β is 10-fold more neurotoxic than fibrillar A β (Dahlgren et al., 2002). In addition, oligomeric A β induces a significantly greater pro-inflammatory environment than fibrillar A β , and also inhibits microglial phagocytosis (Pan et al., 2011). The decreased AD-pathology in FTY720-treated mice may be a direct result of reducing T cell infiltration, and fibrinogen extravasation into the brain during the period of infection, although direct effects of FTY720 on amyloid processing have been reported. FTY720 reduced neuronal A β production *in vitro* and decreased A β ₄₀, but increased A β ₄₂ *in vivo* after 6 days treatment in a mouse AD-model (Takasugi et al., 2013). It has also been reported that FTY720 can protect neurons *in vitro* from oligomeric A β -induced cell death, which was mediated by BDNF (Doi et al., 2013). FTY720 also protects against A β induced neurotoxicity *in vivo*, which was mediated by caspase-3 inhibition (Asle-Rousta et al., 2013), increased BDNF production (Fukumoto et al., 2014) and was associated with reduced expression of pro-apoptotic genes (Hemmati et al., 2013). In addition, FTY720 attenuated the A β -induced impairment in spatial learning and memory in the Morris water maze, passive avoidance test, novel object recognition and conditioned-fear learning test (Asle-Rousta et al., 2013; Fukumoto et al., 2014; Hemmati et al., 2013).

Together this study demonstrates that infection causes lasting changes in the APP/PS1 brain, inducing enhanced BBB permeability and infiltration of IL-17⁺ T cells that are still apparent 70 days post-challenge, and together results in increased A β accumulation. Treatment with FTY720 restores BBB integrity in APP/PS1 mice, reducing fibrinogen leakage into the parenchyma and decreases T cell infiltration into the hippocampus, importantly FTY720 attenuated the infection-induced increase in AD-pathology. It is clear that FTY720 is a drug with

multiple targets, including lymphocyte sequestration, astrocyte and BBB modulation with direct effects on A β neurotoxicity. Due to its wide mechanistic action, FTY720 could prove an ideal therapy in AD where multiple pathways appear to be involved in disease progression.

Chapter 7

General Discussion

7.1 General Discussion

The brain has developed a tightly regulated immunosurveillance system that can mount an appropriate response to pathogens, while protecting the neuronal environment from unnecessary inflammation which can be neurotoxic. This system is predominantly non-inflammatory, relies on activation of resident microglia in the brain and T cells in the CSF and blood, whose entry into the brain parenchyma occurs infrequently under normal conditions due to the BBB. However, the relative immune privilege the brain has declines with age and in inflammatory or infectious conditions, and this is often associated with increased BBB permeability which has also been reported in AD (Farrall and Wardlaw, 2009). It is known that AD patients are vulnerable to the effects of peripheral infection, which negatively impacts on cognitive function (Holmes et al., 2009; Holmes et al., 2003). However, the mechanism mediating the infection-induced changes remains unclear. This study examined the possibility that infection-induced T cell infiltration into the brain was key to these changes. The results demonstrate that T cells cause microglial and astrocytic activation *in vitro* and that T cell infiltration in APP/PS1 mice was associated with A β deposition *in vivo*. Infection exacerbated A β -pathology in older APP/PS1 mice, and this was associated with enhanced BBB permeability and infiltration of IFN- γ ⁺ cells, including T cells into the brain. This sequence of events might explain why AD patients are often cognitively impaired after infection. Preventing T cell infiltration into the brain during infection with *B. pertussis* attenuated the infection-induced changes in A β -plaque deposition in older APP/PS1 mice, thus drugs which target T cell influx could prove a potential therapy in AD.

One of the significant findings described in this thesis is that Th1 cells cause microglial and astrocytic activation *in vitro*, and when transferred to mice with AD-like pathology, increased numbers of Th1 cells infiltrated the brain and resulted in enhanced A β -plaque deposition *in vivo*. Few studies have examined the impact of T cells on glial activation, particularly in the context of AD, although it was recently demonstrated that A β -specific T cells cause microglial activation in mixed glial cultures (McQuillan et al., 2010). The absence of research into this

area has had serious implications, particularly in relation to the AN1792 AD clinical trial. Research into immunotherapy as a way to remove the increasing burden of A β in the AD brain began over 15 years ago. Activating the immune system by immunising with A β stimulated T cell immune responses (Schenk, 2002) and produced exciting results in animal models, reducing A β burden and attenuating behavioural deficits (Janus et al., 2000; Schenk et al., 1999), which led to the development of the AN1792 clinical trial. However, at that time, the ability of A β -specific T cells to induce microglial or astrocytic activation had not been examined. The AN1792 trial had to be terminated because of the meningoencephalitis which developed in 6% of patients, possibly a result of QS-21, the adjuvant used, which stimulates Th1 responses (Wilcock and Colton, 2008). The results in this thesis go some way to explain why meningoencephalitis developed in a subset of patients, and suggest an anti-inflammatory, Th2-type adjuvant may be more appropriate for an AD vaccine, as Th2 cells do not cause pro-inflammatory activation of glia. Indeed A β immunization with other adjuvants such as alum, which favours a Th2 response (Asuni et al., 2006) or with IL-4 and GM-CSF (DaSilva et al., 2006) significantly reduced A β -plaques in the brains of AD-transgenic mice, and may have a better translation to AD patients.

Recent studies suggest bacterial and viral infections are a risk factor in the progression of AD. Due to changes in the immune system, the elderly are vulnerable to infection (Kovaiou et al., 2007), which is associated with lower MMSE scores (Katan et al., 2013), and progression to dementia (Shah et al., 2013). In those with AD, infection results in cognitive decline (Holmes et al., 2009; Holmes et al., 2003) and a number of specific infections have been associated with AD progression including CMV, HSV-1, *B. burgdorferi*, *C. pneumonia* and *H. pylori* (Bu et al., 2014; Honjo et al., 2009). However, there is little evidence to explain why young adults and the healthy elderly are unaffected by infection, whereas patients with AD are vulnerable to infection-induced cognitive decline. In addition, no study has examined whether there is an age-related susceptibility to infection in AD-transgenic mouse models. Due to the re-emergence of whooping cough, *B. pertussis* was used as a model of respiratory infection in this study. Infection of mice with *B. pertussis* is also well-

characterised, and activates both the innate and adaptive immune system over a 35-42 day period.

The results revealed that infection induced lasting changes in older, but not younger, APP/PS1 mice by exacerbating A β deposition in the brain. The impact of peripheral stimulation on AD-pathology is relatively unstudied, but it has been demonstrated that repeated administration of LPS in AD-transgenic mice increased the concentration of A β (Sheng et al., 2003) or tau tangle pathology (Kitazawa et al., 2005). MHV infection also induced tau pathology in 3xTg-AD mice (Sy et al., 2011). However, *B. pertussis* is a typical Gram-negative bacteria which continuously produces toxins and virulence factors in the lung before natural resolution of infection unlike LPS injections, and thus, closely reflects the course of infection observed in humans. The enhanced A β -pathology described here was associated with IFN- γ ⁺ and IL-17⁺ T cell infiltration into the brain, a change that was still apparent weeks after clearance of *B. pertussis*. Interestingly, CD3⁺ T cell infiltration into the brains of APP/PS1 mice correlated with the expression of CCL3 ($r=0.75$, $r^2=0.56$) and CCL5 ($r=0.74$, $r^2=0.54$). Therefore, the increased chemokine expression may, in part, explain why T cell infiltration was further enhanced in older APP/PS1 mice after infection.

Microglia and macrophages in the brains of APP/PS1 mice had an APC phenotype post-infection; it is possible that T cell influx induced local APC activation and that this contributed to the observed neuroinflammation and A β -plaque deposition. This is in line with suggestions that microglia in an APC phenotype are inflammatory, and can contribute to AD-pathology (Town et al., 2005; Townsend et al., 2005).

It has been reported that microglia in the AD brain are chronically activated by the constant and increasing presence of A β , and it is possible that further activation by T cells may trigger persistent changes. The mechanism of T cell entry into the CNS is largely based *in vitro* and *in vivo* studies, thus it remains to be established whether similar interactions occur in the human brain. Due to the presence of the BBB, T cell migration to the human CNS is minimal in healthy individuals (Hickey, 2001; Ousman and Kubes, 2012), however, T cell infiltration

into the CNS is increased in AD (Togo et al., 2002). Consistently, T cells are rarely found in the CNS parenchyma of mice, however, infiltration increases with age in APP/PS1 mice. In *B. pertussis*-infected APP/PS1 mice, pro-inflammatory T cells were located in a CNS parenchyma that was already undergoing chronic inflammatory stimulation by A β . It is possible that this could lead to a feed-forward cycle of microglial activation and cytokine secretion, which can increase the activity of β - and γ -secretases (Liao et al., 2004; Sastre et al., 2008), thus contributing to the enhanced production of A β . Tan and colleagues have investigated the effect of neuroinflammation on subsequent T cell-induced glial activation; A β -stimulated microglia treated with CD40L induced greater pro-inflammatory cytokine release and neuronal injury than A β or CD40L stimulation alone (Tan et al., 1999; Townsend et al., 2005). In addition, APP^{swe} mice that lack CD40L or the CD40 receptor have significantly reduced amyloid pathology throughout the brain with decreased glial activation (Laporte et al., 2006; Tan et al., 2002). In relation to AD patients, it has been demonstrated that their T cells have increased reactivity to A β (Monsonogo et al., 2003; Saresella et al., 2010; Saresella et al., 2012) and T cell infiltration into the brain is enhanced in AD, where T cells were found in close apposition to microglia (Togo et al., 2002), which have an APC phenotype (McGeer et al., 1989; McGeer et al., 1987; Perlmutter et al., 1992; Togo et al., 2000). Together, these findings suggest that, in AD, a connection exists between T cells, microglial activation and amyloid pathology, which is consistent with the current data demonstrating parallel increases in T cell infiltration, microglial activation, and increased A β accumulation, particularly post-infection. It has been suggested that infiltration of peripheral immune cells may be protective in AD; macrophages could mediate A β -removal (Town et al., 2008) and anti-inflammatory T cells may be beneficial in the resolution of neuroinflammation (Schwartz and Baruch, 2014). In this current study, it is proposed that infection and pro-inflammatory T cell infiltration combine to enhance A β deposition in older APP/PS1 mice, which are vulnerable to the stimulation due to the heightened state of glial activation already induced by A β .

The progression of AD-pathology in older APP/PS1 mice may be compared with the “two-hit hypothesis” where amyloid-induced microglial activation and peripheral infection may each reflect an insult or “hit”. While each event in isolation can have adverse effects on the brain, together, they rapidly exacerbate disease pathogenesis. In the A β -induced neuroinflammatory environment, the threshold for activation is lower and it appears that the brain cannot efficiently handle the “second hit” i.e. the peripheral infection and subsequent infiltration of immune cells, and ultimately this results in greater plaque deposition in older APP/PS1 mice. Interestingly, this novel finding provides further insight into events that may be occurring in the AD brain and explain why AD patients are vulnerable to the effects of infection. Importantly this study highlights the need for early detection and treatment of infections in the elderly.

The enhanced T cell infiltration post-infection in older APP/PS1 mice and the associated inflammation and pathology predicts that blocking influx of these cells may be protective. Consistent with this prediction, treatment with FTY720, which reduced T cell infiltration into the lungs of C57BL/6 mice during infection with *B. pertussis*, decreased T cell infiltration into the brain and neuroinflammation. Importantly, chronic treatment of APP/PS1 mice with FTY720 during the period of infection with *B. pertussis* attenuated the infection-induced increase in soluble A β and the deposition of A β in many regions of the brain, as predicted. In AD, it is believed that soluble A β is more detrimental than insoluble A β , although A β aggregates can cause physical disruption to neuronal processes. This is the first time that protective effects of FTY720 have been demonstrated in AD-transgenic mice, although FTY720 can inhibit neuronal A β production *in vitro* (Takasugi et al., 2013), and prevent A β -induced neurotoxicity *in vivo* (Asle-Rousta et al., 2013; Fukumoto et al., 2014; Hemmati et al., 2013). It is important to note that while A β deposition is a feature of AD, plaque deposition occurs years before the onset of clinical symptoms and therefore in patients, A β load does not necessarily correlate with the degree of cognitive decline (Hampel, 2013). Indeed a stronger correlate of cognitive deficits in AD is synaptic loss (Terry et al., 1991).

There was evidence of BBB breakdown in older APP/PS1 mice; this can facilitate the infiltration of peripheral immune cells, and was enhanced in APP/PS1 mice previously exposed to *B. pertussis*. Previous studies have shown that APP/PS1 mice have a compromised BBB and that this developed with age (Minogue et al., 2014) and LPS also increased BBB leakage in APP^{swe} mice (Takeda et al., 2013). The present data show that FTY720 significantly improved the BBB integrity, and prevented infiltration of T cells into the brain, which is consistent with reports on the mechanism of FTY720-mediated protection in EAE and MS (Brinkmann et al., 2010). Protecting the brain from inflammatory infiltrates may help avoid over-stimulation of the A β -activated microglia and astrocytes. This could potentially negate the “second hit” induced by infection in the two-hit hypothesis, thus preventing the increase in A β pathology post-infection in APP/PS1 mice. Indeed as FTY720 had little effect in uninfected APP/PS1 mice, it appears that its protective effects are predominantly evident in the context of infection, at least in this model.

It remains to be established whether infection induces behavioural deficits in older APP/PS1 mice, although due to the wide range of pro-inflammatory changes, and increased soluble and insoluble A β , it seems likely that learning or memory impairments would be observed. While few studies have examined the effect of infection on behaviour in AD models, LPS administered i.p. enhanced sickness behaviour (Takeda et al., 2013) and cognitive impairments (Sy et al., 2011) in APP^{swe} or 3xTg-AD mice. Furthermore, infection of young and aged adult mice with *Mycobacterium bovis*, *Bacillus Calmette-Guérin* (BCG) induced prolonged sickness and depressive behaviour in aged mice only (Kelley et al., 2013). Behavioural assessment of FTY720-treated *B. pertussis*-infected APP/PS1 mice might also delineate whether FTY720 could attenuate any possible deficits induced by exposure to infection and if successful, might correlate with the FTY720-related attenuation in A β accumulation post-challenge. A clear result would certainly make FTY720 a potentially attractive therapy in the treatment of AD.

The current drug therapies available for AD treat the symptoms as opposed to slowing disease progression and fall into two categories; those that

inhibit cholinesterase (e.g. donepezil) or block N-methyl-d-aspartate (NMDA) receptors (e.g. memantine) and can temporarily help memory or language problems. At present there are just 5 drugs available for the treatment of AD and it has been over 10 years since a new treatment was identified. While there are many ongoing clinical trials investigating AD therapies, these have not translated to the clinic. It is clear AD patients have a compromised BBB (Farrall and Wardlaw, 2009) with increased chemokine expression in the CNS (Streit et al., 2001; Tripathy et al., 2007, 2010; Xia et al., 2000; Xia et al., 1998). In addition, plasma proteins and peripheral immune cells are found in the AD brain (Akiyama et al., 1992; Berzin et al., 2000; Fiala et al., 2002; Ryu and McLarnon, 2009; Togo et al., 2002), which can contribute to neuroinflammation, therefore interrupting this cycle could provide new targets in the treatment of AD.

To date, there are no clinical trials underway which aim to improve BBB integrity in AD and protect the brain from unnecessary inflammatory stimulation and peripheral cell infiltration. The present findings suggest that restoring BBB integrity may protect the brain from the inflammatory events that occur in the periphery, particularly during the period of infection. This could prevent the infection-induced inflammation and A β accumulation. A key aim of therapy in AD is to prevent disease progression and as demonstrated here, infection is a significant driving factor in A β accumulation. It has been suggested that if a new therapy or intervention could slow the progression of dementia by 25% or 50%, this would reduce the proportion of people with severe dementia in 2050 to just 8% or 2% respectively (www.alzheimersresearchuk.org). As the current projection estimates that 14% of AD patients will have severe dementia in 2050, this could have a substantial impact on the quality of life of AD patients. FTY720 is already a licensed drug for MS, therefore it could be directly translated to an AD clinical trial. Indeed, as AD is a neurodegenerative disease with many pathways and factors at play, a drug like FTY720, which has numerous targets may prove ideal.

The key findings presented here is that peripheral infection is a significant additional factor in the progression of AD pathology in APP/PS1 mice. Infection triggers BBB permeability and infiltration of IFN- γ ⁺ and IL-17⁺ T cells into the

brains of older APP/PS1 mice, which are capable of inducing microglial and astrocyte activation (Fig 7.1). These effects last for weeks after the infection is cleared, and exposure to *B. pertussis* ultimately exacerbates A β -pathology. This novel finding has serious implications for the AD population, and identifies new targets in the treatment of AD that could slow or delay disease progression. Overall, the data suggest FTY720 is a drug which warrants further investigation as a therapy in AD, and future experiments are required to determine the exact mechanism by which FTY720 is protective.

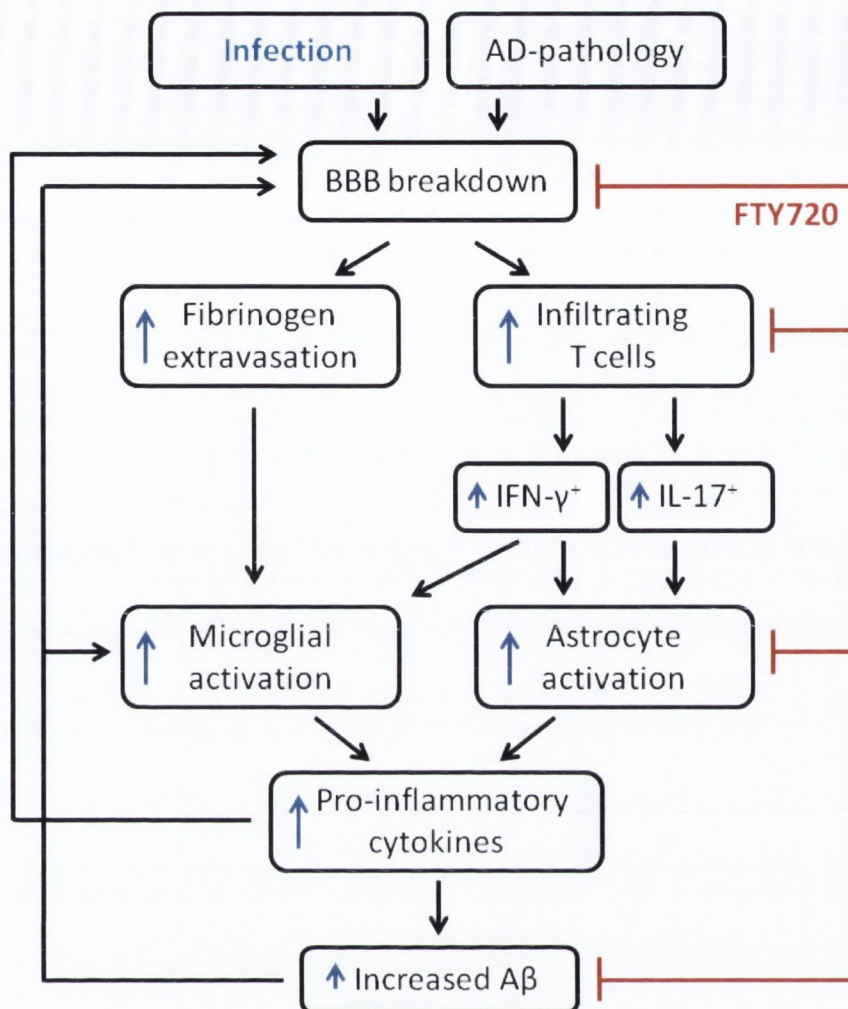


Figure 7.1 Proposed sequence of events leading to the increased deposition of A β in APP/PS1 mice during infection, and possible targets of FTY720

*This proposed sequence of events suggests that BBB permeability accompanies the accumulation of A β in APP/PS1 mice, facilitating fibrinogen leakage into the parenchyma, which can contribute to microglial activation. With the increased expression of chemokines and BBB permeability, IFN- γ^+ and IL-17 $^+$ T cell infiltration is also increased. These cells cause activation of microglia and astrocytes, resulting in increased expression of pro-inflammatory cytokines which can enhance the activity of β - and γ -secretases, increasing the production of A β . An inflammatory environment also prevents phagocytosis and microglia are poor phagocytes when in an APC state, together contributing to the accumulation of A β . Increasing presence of A β can enhance glial activation and further disrupt the BBB leading to a vicious cycle of events. Exposure to infection increases BBB permeability and results in significantly increased numbers of IFN- γ^+ and IL-17 $^+$ T cells gaining access to the brain, changes which persist for a long period of time after the infection is resolved. Importantly, infection with *B. pertussis* results in a significant increase in A β deposition in the brain. Treatment of APP/PS1 mice with FTY720 appears to interrupt this cycle; FTY720 improves BBB integrity preventing fibrinogen leakage, and significantly reduces T cell infiltration into the brain. Furthermore, FTY720 significantly attenuates the infection-induced increase in A β . Blue arrows reflect changes which occur in the brain after infection with *B. pertussis*.*

7.2 Limitations of the study

While every effort was made to ensure the experimental design, and the studies themselves were carried out to the highest standard, there are a number of limitations to the results described in this thesis. APP/PS1 mice are genetically developed to increase production of A β , with evidence of plaques by 6 months of age. While these mice develop learning and memory impairments, neuroinflammation and synaptic loss, other features of AD are not recapitulated, such as the substantial neuronal loss that is observed in AD patients. To date, there are no animal models of AD where genetic manipulation of APP and PS1 alone induces neuronal loss however, it has been established that deletion of NOS2 in APP^{swe} mice, or replacement with human NOS2 results in a significant loss of neurons in the brains of transgenic mice (Colton et al., 2014). The impact of peripheral infection on neuroinflammation and neurodegeneration in this model would undoubtedly be interesting.

Cryostat sections were stained with CD3 to identify T cells in the CNS, however, the use of a vascular marker would further clarify the extent to which the cells migrated into the parenchyma. Indeed staining the cryostat sections with a microglia or macrophage marker along with CD3, and viewing at a higher magnification would determine whether the T cells were found in close proximity to APCs in the brain.

In the current series of experiments the memory and learning behaviour of mice was not examined following infection with *B. pertussis*. However, the impact of infection on these parameters would further determine the extent to which the older mice are vulnerable to the effects of infection. It would be interesting to then compare whether FTY720 can in fact negate any infection-induced deficits in cognition. Analysing the levels of synaptic proteins would also complement any observed changes in learning or memory in mice. This data could more closely align with what is observed in AD patients following infection, and would delineate whether the infection-induced increase in T cell infiltration and A β -deposition can impact cognitive function in the older APP/PS1 mice.

7.3 Future work

The results described in this thesis demonstrate that older APP/PS1 mice are vulnerable to the effects of a respiratory infection. Infection with *B. pertussis* induced persistent changes in the brains of older APP/PS1 mice with enhanced infiltration of T cells, glial activation and ultimately resulted in greater A β deposition when assessed 56 days after challenge with bacteria. Future experiments could include enough mice to do a full time course of the study. Culling a group of WT and APP/PS1 mice weekly after challenge with *B. pertussis* would determine the sequence of events of T cell infiltration and microglial activation which leads to the development of A β -plaques in the brains of the APP/PS1 mice. Further information on the timing of T cell infiltration, and perhaps any genotype differences between the WT and APP/PS1 mice during the course of infection, could help develop new therapies for this disease by pinpointing the most appropriate therapeutic window for treatment of these mice. Furthermore, a time course experiment would allow delineation of the beneficial effects of FTY720 in this model during the entire course of the infection.

Repeating the infection experiment would also allow for animal behaviour to be performed on the mice, to investigate the effect of infection on cognitive function. In turn this could be matched with changes in synaptic proteins in the brains of the mice or even changes in long term potentiation. Although neuronal loss is not observed in APP/PS1 mice it would be worthwhile to examine whether infection with *B. pertussis* could affect neurodegeneration in this model.

Chapter 8

Bibliography

- (CDC), C. f. D. C. a. P., 2012, Pertussis epidemic--Washington, 2012: MMWR Morb Mortal Wkly Rep, v. 61, p. 517-22.
- Adachi, K., T. Kohara, N. Nakao, K. Chiba, T. Mishina, S. Sasaki, and T. Fujita, 1995, Design, synthesis, and structure-activity relationships of 2-substituted-2-amino-1,3-propanediols: Discovery of a novel immunosuppressant, FTY720, v. 5, p. 853-856.
- Agostini, C., M. Facco, M. Siviero, D. Carollo, S. Galvan, A. M. Cattelan, R. Zambello, L. Trentin, and G. Semenzato, 2000, CXC chemokines IP-10 and mig expression and direct migration of pulmonary CD8+/CXCR3+ T cells in the lungs of patients with HIV infection and T-cell alveolitis: Am J Respir Crit Care Med, v. 162, p. 1466-73.
- Agrawal, S., P. Anderson, M. Durbeej, N. van Rooijen, F. Ivars, G. Opdenakker, and L. M. Sorokin, 2006, Dystroglycan is selectively cleaved at the parenchymal basement membrane at sites of leukocyte extravasation in experimental autoimmune encephalomyelitis: J Exp Med, v. 203, p. 1007-19.
- Aguzzi, A., B. A. Barres, and M. L. Bennett, 2013, Microglia: scapegoat, saboteur, or something else?: Science, v. 339, p. 156-61.
- Ajami, B., J. L. Bennett, C. Krieger, K. M. McNagny, and F. M. Rossi, 2011, Infiltrating monocytes trigger EAE progression, but do not contribute to the resident microglia pool, Nat Neurosci, v. 14: United States, p. 1142-9.
- Ajami, B., J. L. Bennett, C. Krieger, W. Tetzlaff, and F. M. Rossi, 2007, Local self-renewal can sustain CNS microglia maintenance and function throughout adult life, Nat Neurosci, v. 10: United States, p. 1538-43.
- Akiyama, H., S. Barger, S. Barnum, B. Bradt, J. Bauer, G. M. Cole, N. R. Cooper, P. Eikelenboom, M. Emmerling, B. L. Fiebich, C. E. Finch, S. Frautschy, W. S. Griffin, H. Hampel, M. Hull, G. Landreth, L. Lue, R. Mrak, I. R. Mackenzie, P. L. McGeer, M. K. O'Banion, J. Pachter, G. Pasinetti, C. Plata-Salaman, J. Rogers, R. Rydel, Y. Shen, W. Streit, R. Strohmeyer, I. Tooyama, F. L. Van Muiswinkel, R. Veerhuis, D. Walker, S. Webster, B. Wegrzyniak, G. Wenk, and T. Wyss-Coray, 2000, Inflammation and Alzheimer's disease: Neurobiol Aging, v. 21, p. 383-421.
- Akiyama, H., K. Ikeda, H. Kondo, and P. L. McGeer, 1992, Thrombin accumulation in brains of patients with Alzheimer's disease: Neurosci Lett, v. 146, p. 152-4.
- Akiyama, H., T. Kawamata, T. Yamada, I. Tooyama, T. Ishii, and P. L. McGeer, 1993, Expression of intercellular adhesion molecule (ICAM)-1 by a subset of astrocytes in Alzheimer disease and some other degenerative neurological disorders: Acta Neuropathol, v. 85, p. 628-34.
- Aloisi, F., R. De Simone, S. Columba-Cabezas, G. Penna, and L. Adorini, 2000a, Functional maturation of adult mouse resting microglia into an APC is promoted by granulocyte-macrophage colony-stimulating factor and interaction with Th1 cells.: J Immunol, v. 164, p. 1705-12.
- Aloisi, F., F. Ria, and L. Adorini, 2000b, Regulation of T-cell responses by CNS antigen-presenting cells: different roles for microglia and astrocytes: Immunol Today, v. 21, p. 141-7.

- Aloisi, F., F. Ria, G. Penna, and L. Adorini, 1998, Microglia are more efficient than astrocytes in antigen processing and in Th1 but not Th2 cell activation.: *J Immunol*, v. 160, p. 4671-80.
- Anderson, J. M., and C. M. Van Itallie, 2009, Physiology and Function of the Tight Junction, *Cold Spring Harb Perspect Biol*, v. 1.
- Andreasen, C., and N. H. Carbonetti, 2009, Role of neutrophils in response to *Bordetella pertussis* infection in mice: *Infect Immun*, v. 77, p. 1182-8.
- Appel, S. H., D. R. Beers, and J. S. Henkel, 2010, T cell-microglial dialogue in Parkinson's disease and amyotrophic lateral sclerosis: are we listening?, *Trends Immunol*, v. 31: England, p. 7-17.
- Appelt, D. M., M. R. Roupas, D. S. Way, M. G. Bell, E. V. Albert, C. J. Hammond, and B. J. Balin, 2008, Inhibition of apoptosis in neuronal cells infected with *Chlamydia (Chlamydia) pneumoniae*: *BMC Neurosci*, v. 9, p. 13.
- Armulik, A., G. Genove, and C. Betsholtz, 2011, Pericytes: developmental, physiological, and pathological perspectives, problems, and promises, *Dev Cell*, v. 21: United States, 2011 Elsevier Inc, p. 193-215.
- Armulik, A., G. Genove, M. Mae, M. H. Nisancioglu, E. Wallgard, C. Niaudet, L. He, J. Norlin, P. Lindblom, K. Strittmatter, B. R. Johansson, and C. Betsholtz, 2010, Pericytes regulate the blood-brain barrier, *Nature*, v. 468: England, p. 557-61.
- Asahi, M., X. Wang, T. Mori, T. Sumii, J. C. Jung, M. A. Moskowitz, M. E. Fini, and E. H. Lo, 2001, Effects of matrix metalloproteinase-9 gene knock-out on the proteolysis of blood-brain barrier and white matter components after cerebral ischemia: *J Neurosci*, v. 21, p. 7724-32.
- Asle-Rousta, M., Z. Kolahdooz, S. Oryan, A. Ahmadiani, and L. Dargahi, 2013, FTY720 (fingolimod) attenuates beta-amyloid peptide (A β 42)-induced impairment of spatial learning and memory in rats: *J Mol Neurosci*, v. 50, p. 524-32.
- Asuni, A. A., A. Boutajangout, H. Scholtzova, E. Knudsen, Y. S. Li, D. Quartermain, B. Frangione, T. Wisniewski, and E. M. Sigurdsson, 2006, Vaccination of Alzheimer's model mice with A β derivative in alum adjuvant reduces A β burden without microhemorrhages: *Eur J Neurosci*, v. 24, p. 2530-42.
- Azevedo, F. A., L. R. Carvalho, L. T. Grinberg, J. M. Farfel, R. E. Ferretti, R. E. Leite, W. Jacob Filho, R. Lent, and S. Herculano-Houzel, 2009, Equal numbers of neuronal and nonneuronal cells make the human brain an isometrically scaled-up primate brain: *J Comp Neurol*, v. 513, p. 532-41.
- Baglio, F., M. Saresella, M. G. Preti, M. Cabinio, L. Griffanti, I. Marventano, F. Piancone, E. Calabrese, R. Nemni, and M. Clerici, 2013, Neuroinflammation and brain functional disconnection in Alzheimer's disease: *Front Aging Neurosci*, v. 5, p. 81.
- Balabanov, R., T. Beaumont, and P. Dore-Duffy, 1999, Role of central nervous system microvascular pericytes in activation of antigen-primed splenic T-lymphocytes: *J Neurosci Res*, v. 55, p. 578-87.
- Balin, B. J., H. C. Gérard, E. J. Arking, D. M. Appelt, P. J. Branigan, J. T. Abrams, J. A. Whittum-Hudson, and A. P. Hudson, 1998, Identification and localization of

- Chlamydia pneumoniae in the Alzheimer's brain: *Med Microbiol Immunol*, v. 187, p. 23-42.
- Balin, B. J., C. S. Little, C. J. Hammond, D. M. Appelt, J. A. Whittum-Hudson, H. C. Gérard, and A. P. Hudson, 2008, Chlamydia pneumoniae and the etiology of late-onset Alzheimer's disease: *J Alzheimers Dis*, v. 13, p. 371-80.
- Bamberger, M. E., M. E. Harris, D. R. McDonald, J. Husemann, and G. E. Landreth, 2003, A cell surface receptor complex for fibrillar beta-amyloid mediates microglial activation: *J Neurosci*, v. 23, p. 2665-74.
- Barbic, J., M. F. Leef, D. L. Burns, and R. D. Shahin, 1997, Role of gamma interferon in natural clearance of Bordetella pertussis infection: *Infect Immun*, v. 65, p. 4904-8.
- Barker, W. H., H. Borisute, and C. Cox, 1998, A study of the impact of influenza on the functional status of frail older people: *Arch Intern Med*, v. 158, p. 645-50.
- Barnard, A., B. P. Mahon, J. Watkins, K. Redhead, and K. H. Mills, 1996, Th1/Th2 cell dichotomy in acquired immunity to Bordetella pertussis: variables in the in vivo priming and in vitro cytokine detection techniques affect the classification of T-cell subsets as Th1, Th2 or Th0: *Immunology*, v. 87, p. 372-80.
- Barnes, L. L., A. W. Capuano, A. E. Aiello, A. D. Turner, R. H. Yolken, E. F. Torrey, and D. A. Bennett, 2014, Cytomegalovirus Infection and Risk of Alzheimer Disease in Older Black and White Individuals: *J Infect Dis*.
- Barret, A. S., A. Ryan, A. Breslin, L. Cullen, A. Murray, J. Grogan, S. Bourke, and S. Cotter, 2010, Pertussis outbreak in northwest Ireland, January - June 2010: *Euro Surveill*, v. 15.
- Bateman, R. J., C. Xiong, T. L. Benzinger, A. M. Fagan, A. Goate, N. C. Fox, D. S. Marcus, N. J. Cairns, X. Xie, T. M. Blazey, D. M. Holtzman, A. Santacruz, V. Buckles, A. Oliver, K. Moulder, P. S. Aisen, B. Ghetti, W. E. Klunk, E. McDade, R. N. Martins, C. L. Masters, R. Mayeux, J. M. Ringman, M. N. Rossor, P. R. Schofield, R. A. Sperling, S. Salloway, and J. C. Morris, 2012, Clinical and biomarker changes in dominantly inherited Alzheimer's disease: *N Engl J Med*, v. 367, p. 795-804.
- Becher, B., and J. P. Antel, 1996, Comparison of phenotypic and functional properties of immediately ex vivo and cultured human adult microglia: *Glia*, v. 18, p. 1-10.
- Becher, B., A. Prat, and J. P. Antel, 2000, Brain-immune connection: immuno-regulatory properties of CNS-resident cells.: *Glia*, v. 29, p. 293-304.
- Bechmann, I., I. Galea, and V. H. Perry, 2007, What is the blood-brain barrier (not)?: *Trends Immunol*, v. 28, p. 5-11.
- Bell, R. D., E. A. Winkler, A. P. Sagare, I. Singh, B. LaRue, R. Deane, and B. V. Zlokovic, 2010, Pericytes control key neurovascular functions and neuronal phenotype in the adult brain and during brain aging, *Neuron*, v. 68: United States, 2010 Elsevier Inc, p. 409-27.
- Bell, R. D., E. A. Winkler, I. Singh, A. P. Sagare, R. Deane, Z. Wu, D. M. Holtzman, C. Betsholtz, A. Armulik, J. Sallstrom, B. C. Berk, and B. V. Zlokovic, 2012, Apolipoprotein E controls cerebrovascular integrity via cyclophilin A: *Nature*, v. 485, p. 512-6.

- Benveniste, E. N., V. T. Nguyen, and D. R. Wesemann, 2004, Molecular regulation of CD40 gene expression in macrophages and microglia: *Brain Behav Immun*, v. 18, p. 7-12.
- Berzin, T. M., B. D. Zipser, M. S. Rafii, V. Kuo-Leblanc, G. D. Yancopoulos, D. J. Glass, J. R. Fallon, and E. G. Stopa, 2000, Agrin and microvascular damage in Alzheimer's disease: *Neurobiol Aging*, v. 21, p. 349-55.
- Berzins, S. P., M. J. Smyth, and A. G. Baxter, 2011, Presumed guilty: natural killer T cell defects and human disease: *Nat Rev Immunol*, v. 11, p. 131-42.
- Beydoun, M. A., H. A. Beydoun, M. R. Shroff, M. H. Kitner-Triolo, and A. B. Zonderman, 2013, *Helicobacter pylori* seropositivity and cognitive performance among US adults: evidence from a large national survey: *Psychosom Med*, v. 75, p. 486-96.
- Biron, K. E., D. L. Dickstein, R. Gopaul, and W. A. Jefferies, 2011, Amyloid triggers extensive cerebral angiogenesis causing blood brain barrier permeability and hypervascularity in Alzheimer's disease: *PLoS One*, v. 6, p. e23789.
- Black, R. E., S. Cousens, H. L. Johnson, J. E. Lawn, I. Rudan, D. G. Bassani, P. Jha, H. Campbell, C. F. Walker, R. Cibulskis, T. Eisele, L. Liu, C. Mathers, and C. H. E. R. G. o. W. a. UNICEF, 2010, Global, regional, and national causes of child mortality in 2008: a systematic analysis: *Lancet*, v. 375, p. 1969-87.
- Blau, C. W., T. R. Cowley, J. O'Sullivan, B. Grehan, T. C. Browne, L. Kelly, A. Birch, N. Murphy, A. M. Kelly, C. M. Kerskens, and M. A. Lynch, 2012, The age-related deficit in LTP is associated with changes in perfusion and blood-brain barrier permeability: *Neurobiol Aging*, v. 33, p. 1005 e23-35.
- Boche, D., and J. A. Nicoll, 2008, The role of the immune system in clearance of Abeta from the brain: *Brain Pathol*, v. 18, p. 267-78.
- Bolton, S. J., D. C. Anthony, and V. H. Perry, 1998, Loss of the tight junction proteins occludin and zonula occludens-1 from cerebral vascular endothelium during neutrophil-induced blood-brain barrier breakdown in vivo: *Neuroscience*, v. 86, p. 1245-57.
- Boockvar, K. S., and M. S. Lachs, 2003, Predictive value of nonspecific symptoms for acute illness in nursing home residents: *J Am Geriatr Soc*, v. 51, p. 1111-5.
- Boven, L. A., J. Middel, J. Verhoef, C. J. De Groot, and H. S. Nottet, 2000, Monocyte infiltration is highly associated with loss of the tight junction protein zonula occludens in HIV-1-associated dementia: *Neuropathol Appl Neurobiol*, v. 26, p. 356-60.
- Bowman, C. C., A. Rasley, S. L. Tranguch, and I. Marriott, 2003, Cultured astrocytes express toll-like receptors for bacterial products: *Glia*, v. 43, p. 281-91.
- Brinkmann, V., 2007, Sphingosine 1-phosphate receptors in health and disease: mechanistic insights from gene deletion studies and reverse pharmacology, *Pharmacol Ther*, v. 115: England, p. 84-105.
- Brinkmann, V., A. Billich, T. Baumruker, P. Heining, R. Schmouder, G. Francis, S. Aradhye, and P. Burtin, 2010, Fingolimod (FTY720): discovery and development of an oral drug to treat multiple sclerosis: *Nat Rev Drug Discov*, v. 9, p. 883-97.

- Brinkmann, V., S. Chen, L. Feng, D. Pinschewer, Z. Nikolova, and R. Hof, 2001, FTY720 alters lymphocyte homing and protects allografts without inducing general immunosuppression: *Transplant Proc*, v. 33, p. 530-1.
- Brinkmann, V., J. G. Cyster, and T. Hla, 2004, FTY720: sphingosine 1-phosphate receptor-1 in the control of lymphocyte egress and endothelial barrier function: *Am J Transplant*, v. 4, p. 1019-25.
- Brinkmann, V., M. D. Davis, C. E. Heise, R. Albert, S. Cottens, R. Hof, C. Bruns, E. Prieschl, T. Baumruker, P. Hiestand, C. A. Foster, M. Zollinger, and K. R. Lynch, 2002, The immune modulator FTY720 targets sphingosine 1-phosphate receptors: *J Biol Chem*, v. 277, p. 21453-7.
- Brinkmann, V., and K. R. Lynch, 2002, FTY720: targeting G-protein-coupled receptors for sphingosine 1-phosphate in transplantation and autoimmunity: *Curr Opin Immunol*, v. 14, p. 569-75.
- Brinkmann, V., D. Pinschewer, K. Chiba, and L. Feng, 2000, FTY720: a novel transplantation drug that modulates lymphocyte traffic rather than activation: *Trends Pharmacol Sci*, v. 21, p. 49-52.
- Brodie, C., 1996, Differential effects of Th1 and Th2 derived cytokines on NGF synthesis by mouse astrocytes: *FEBS Lett*, v. 394, p. 117-20.
- Brodie, C., N. Goldreich, T. Haiman, and G. Kazimirsky, 1998, Functional IL-4 receptors on mouse astrocytes: IL-4 inhibits astrocyte activation and induces NGF secretion: *J Neuroimmunol*, v. 81, p. 20-30.
- Brosseron, F., M. Krauthausen, M. Kummer, and M. T. Heneka, 2014, Body fluid cytokine levels in mild cognitive impairment and Alzheimer's disease: a comparative overview: *Mol Neurobiol*, v. 50, p. 534-44.
- Browne, T. C., K. McQuillan, R. M. McManus, J. A. O'Reilly, K. H. Mills, and M. A. Lynch, 2013, IFN- γ Production by amyloid β -specific Th1 cells promotes microglial activation and increases plaque burden in a mouse model of Alzheimer's disease: *J Immunol*, v. 190, p. 2241-51.
- Bu, X. L., X. Q. Yao, S. S. Jiao, F. Zeng, Y. H. Liu, Y. Xiang, C. R. Liang, Q. H. Wang, X. Wang, H. Y. Cao, X. Yi, B. Deng, C. H. Liu, J. Xu, L. L. Zhang, C. Y. Gao, Z. Q. Xu, M. Zhang, L. Wang, X. L. Tan, X. Xu, H. D. Zhou, and Y. J. Wang, 2014, A study on the association between infectious burden and Alzheimer's disease: *Eur J Neurol*.
- Buljevac, D., H. Z. Flach, W. C. Hop, D. Hijdra, J. D. Laman, H. F. Savelkoul, F. G. van Der Meché, P. A. van Doorn, and R. Q. Hintzen, 2002, Prospective study on the relationship between infections and multiple sclerosis exacerbations: *Brain*, v. 125, p. 952-60.
- Buljevac, D., W. C. Hop, W. Reedeker, A. C. Janssens, F. G. van der Meché, P. A. van Doorn, and R. Q. Hintzen, 2003, Self reported stressful life events and exacerbations in multiple sclerosis: prospective study: *BMJ*, v. 327, p. 646.
- Burgos, J. S., C. Ramirez, I. Sastre, M. J. Bullido, and F. Valdivieso, 2003, ApoE4 is more efficient than E3 in brain access by herpes simplex virus type 1: *Neuroreport*, v. 14, p. 1825-7.

- Burgos, J. S., C. Ramirez, I. Sastre, and F. Valdivieso, 2006, Effect of apolipoprotein E on the cerebral load of latent herpes simplex virus type 1 DNA: *J Virol*, v. 80, p. 5383-7.
- Butovsky, O., M. Koronyo-Hamaoui, G. Kunis, E. Ophir, G. Landa, H. Cohen, and M. Schwartz, 2006, Glatiramer acetate fights against Alzheimer's disease by inducing dendritic-like microglia expressing insulin-like growth factor 1: *Proc Natl Acad Sci U S A*, v. 103, p. 11784-9.
- Butovsky, O., G. Kunis, M. Koronyo-Hamaoui, and M. Schwartz, 2007, Selective ablation of bone marrow-derived dendritic cells increases amyloid plaques in a mouse Alzheimer's disease model: *Eur J Neurosci*, v. 26, p. 413-6.
- Byrne, P., P. McGuirk, S. Todryk, and K. H. Mills, 2004, Depletion of NK cells results in disseminating lethal infection with *Bordetella pertussis* associated with a reduction of antigen-specific Th1 and enhancement of Th2, but not Tr1 cells: *Eur J Immunol*, v. 34, p. 2579-88.
- Büla, C. J., G. Ghilardi, V. Wietlisbach, C. Petignat, and P. Francioli, 2004, Infections and functional impairment in nursing home residents: a reciprocal relationship: *J Am Geriatr Soc*, v. 52, p. 700-6.
- Cagnin, A., D. J. Brooks, A. M. Kennedy, R. N. Gunn, R. Myers, F. E. Turkheimer, T. Jones, and R. B. Banati, 2001, In-vivo measurement of activated microglia in dementia: *Lancet*, v. 358, p. 461-7.
- Calingasan, N. Y., H. A. Erdely, and C. A. Altar, 2002, Identification of CD40 ligand in Alzheimer's disease and in animal models of Alzheimer's disease and brain injury: *Neurobiol Aging*, v. 23, p. 31-9.
- Caljouw, M. A., S. J. Kruijdenberg, A. J. de Craen, H. J. Cools, W. P. den Elzen, and J. Gussekloo, 2013, Clinically diagnosed infections predict disability in activities of daily living among the oldest-old in the general population: the Leiden 85-plus Study: *Age Ageing*, v. 42, p. 482-8.
- Campos, F., T. Qin, J. Castillo, J. H. Seo, K. Arai, E. H. Lo, and C. Waeber, 2013, Fingolimod reduces hemorrhagic transformation associated with delayed tissue plasminogen activator treatment in a mouse thromboembolic model: *Stroke*, v. 44, p. 505-11.
- Cao, C., G. W. Arendash, A. Dickson, M. B. Mamcarz, X. Lin, and D. W. Ethell, 2009, Abeta-specific Th2 cells provide cognitive and pathological benefits to Alzheimer's mice without infiltrating the CNS: *Neurobiol Dis*, v. 34, p. 63-70.
- Cao, D., H. Lu, T. L. Lewis, and L. Li, 2007, Intake of sucrose-sweetened water induces insulin resistance and exacerbates memory deficits and amyloidosis in a transgenic mouse model of Alzheimer disease: *J Biol Chem*, v. 282, p. 36275-82.
- Carare, R. O., M. Bernardes-Silva, T. A. Newman, A. M. Page, J. A. Nicoll, V. H. Perry, and R. O. Weller, 2008, Solutes, but not cells, drain from the brain parenchyma along basement membranes of capillaries and arteries: significance for cerebral amyloid angiopathy and neuroimmunology: *Neuropathol Appl Neurobiol*, v. 34, p. 131-44.

- Carbone, I., T. Lazzarotto, M. Ianni, E. Porcellini, P. Forti, E. Masliah, L. Gabrielli, and F. Licastro, 2014, Herpes virus in Alzheimer's disease: relation to progression of the disease: *Neurobiol Aging*, v. 35, p. 122-9.
- Carbonetti, N. H., G. V. Artamonova, N. Van Rooijen, and V. I. Ayala, 2007, Pertussis toxin targets airway macrophages to promote *Bordetella pertussis* infection of the respiratory tract: *Infect Immun*, v. 75, p. 1713-20.
- Carman, C. V., 2009, Mechanisms for transcellular diapedesis: probing and pathfinding by 'invadosome-like protrusions': *J Cell Sci*, v. 122, p. 3025-35.
- Carrano, A., J. J. Hoozemans, S. M. van der Vies, A. J. Rozemuller, J. van Horsen, and H. E. de Vries, 2011, Amyloid Beta induces oxidative stress-mediated blood-brain barrier changes in capillary amyloid angiopathy: *Antioxid Redox Signal*, v. 15, p. 1167-78.
- Carter, S. L., M. Muller, P. M. Manders, and I. L. Campbell, 2007, Induction of the genes for Cxcl9 and Cxcl10 is dependent on IFN-gamma but shows differential cellular expression in experimental autoimmune encephalomyelitis and by astrocytes and microglia in vitro: *Glia*, v. 55, p. 1728-39.
- Cartier, L., O. Hartley, M. Dubois-Dauphin, and K. H. Krause, 2005, Chemokine receptors in the central nervous system: role in brain inflammation and neurodegenerative diseases: *Brain Res Brain Res Rev*, v. 48, p. 16-42.
- Castellano, J. M., J. Kim, F. R. Stewart, H. Jiang, R. B. DeMattos, B. W. Patterson, A. M. Fagan, J. C. Morris, K. G. Mawuenyega, C. Cruchaga, A. M. Goate, K. R. Bales, S. M. Paul, R. J. Bateman, and D. M. Holtzman, 2011, Human apoE isoforms differentially regulate brain amyloid-beta peptide clearance: *Sci Transl Med*, v. 3, p. 89ra57.
- Castle, S. C., 2000, Clinical relevance of age-related immune dysfunction: *Clin Infect Dis*, v. 31, p. 578-85.
- Catron, D. M., L. K. Rusch, J. Hataye, A. A. Itano, and M. K. Jenkins, 2006, CD4+ T cells that enter the draining lymph nodes after antigen injection participate in the primary response and become central-memory cells, *J Exp Med*, v. 203, p. 1045-54.
- Chastain, E. M., D. S. Duncan, J. M. Rodgers, and S. D. Miller, 2011, The role of antigen presenting cells in multiple sclerosis: *Biochim Biophys Acta*, v. 1812, p. 265-74.
- Chen, L., and D. B. Flies, 2013, Molecular mechanisms of T cell co-stimulation and co-inhibition, *Nat Rev Immunol*, v. 13: England, p. 227-42.
- Cherry, J. D., 2012, Epidemic pertussis in 2012--the resurgence of a vaccine-preventable disease: *N Engl J Med*, v. 367, p. 785-7.
- Chiba, K., Y. Hoshino, C. Suzuki, Y. Masubuchi, Y. Yanagawa, M. Ohtsuki, S. Sasaki, and T. Fujita, 1996, FTY720, a novel immunosuppressant possessing unique mechanisms. I. Prolongation of skin allograft survival and synergistic effect in combination with cyclosporine in rats: *Transplant Proc*, v. 28, p. 1056-9.
- Chiba, K., H. Kataoka, N. Seki, K. Shimano, M. Koyama, A. Fukunari, K. Sugahara, and T. Sugita, 2011, Fingolimod (FTY720), sphingosine 1-phosphate receptor modulator, shows superior efficacy as compared with interferon- β in mouse

experimental autoimmune encephalomyelitis: *Int Immunopharmacol*, v. 11, p. 366-72.

- Chiba, K., Y. Yanagawa, Y. Masubuchi, H. Kataoka, T. Kawaguchi, M. Ohtsuki, and Y. Hoshino, 1998, FTY720, a novel immunosuppressant, induces sequestration of circulating mature lymphocytes by acceleration of lymphocyte homing in rats. I. FTY720 selectively decreases the number of circulating mature lymphocytes by acceleration of lymphocyte homing: *J Immunol*, v. 160, p. 5037-44.
- Choi, J. W., S. E. Gardell, D. R. Herr, R. Rivera, C. W. Lee, K. Noguchi, S. T. Teo, Y. C. Yung, M. Lu, G. Kennedy, and J. Chun, 2011, FTY720 (fingolimod) efficacy in an animal model of multiple sclerosis requires astrocyte sphingosine 1-phosphate receptor 1 (S1P1) modulation: *Proc Natl Acad Sci U S A*, v. 108, p. 751-6.
- Cinamon, G., M. Matloubian, M. J. Lesneski, Y. Xu, C. Low, T. Lu, R. L. Proia, and J. G. Cyster, 2004, Sphingosine 1-phosphate receptor 1 promotes B cell localization in the splenic marginal zone: *Nat Immunol*, v. 5, p. 713-20.
- Citron, M., T. Oltersdorf, C. Haass, L. McConlogue, A. Y. Hung, P. Seubert, C. Vigo-Pelfrey, i. Lieberburg, and D. J. Selkoe, 1992, Mutation of the beta-amyloid precursor protein in familial Alzheimer's disease increases beta-protein production: *Nature*, v. 360, p. 672-4.
- Clarke, R. M., F. O'Connell, A. Lyons, and M. A. Lynch, 2007, The HMG-CoA reductase inhibitor, atorvastatin, attenuates the effects of acute administration of amyloid-beta1-42 in the rat hippocampus in vivo: *Neuropharmacology*, v. 52, p. 136-45.
- Clayton, T. C., M. Thompson, and T. W. Meade, 2008, Recent respiratory infection and risk of cardiovascular disease: case-control study through a general practice database: *Eur Heart J*, v. 29, p. 96-103.
- Cohen, J. A., F. Barkhof, G. Comi, H. P. Hartung, B. O. Khatri, X. Montalban, J. Pelletier, R. Capra, P. Gallo, G. Izquierdo, K. Tiel-Wilck, A. de Vera, J. Jin, T. Stites, S. Wu, S. Aradhye, and L. Kappos, 2010, Oral fingolimod or intramuscular interferon for relapsing multiple sclerosis: *N Engl J Med*, v. 362, p. 402-15.
- Colombo, E., M. Di Dario, E. Capitolo, L. Chaabane, J. Newcombe, G. Martino, and C. Farina, 2014, Fingolimod may support neuroprotection via blockade of astrocyte nitric oxide: *Ann Neurol*, v. 76, p. 325-37.
- Colton, C. A., J. G. Wilson, A. Everhart, D. M. Wilcock, J. Puolivali, T. Heikkinen, J. Oksman, O. Jaaskelainen, K. Lehtimaki, T. Laitinen, N. Vartiainen, and M. P. Vitek, 2014, mNos2 deletion and human NOS2 replacement in Alzheimer disease models: *J Neuropathol Exp Neurol*, v. 73, p. 752-69.
- Connor, L. M., M. C. Harvie, F. J. Rich, K. M. Quinn, V. Brinkmann, G. Le Gros, and J. R. Kirman, 2010, A key role for lung-resident memory lymphocytes in protective immune responses after BCG vaccination: *Eur J Immunol*, v. 40, p. 2482-92.
- Constantinescu, C. S., M. Tani, R. M. Ransohoff, M. Wysocka, B. Hilliard, T. Fujioka, S. Murphy, P. J. Tighe, J. Das Sarma, G. Trinchieri, and A. Rostami, 2005, Astrocytes as antigen-presenting cells: expression of IL-12/IL-23: *J Neurochem*, v. 95, p. 331-40.

- Cook, D. G., J. B. Leverenz, P. J. McMillan, J. J. Kulstad, S. Ericksen, R. A. Roth, G. D. Schellenberg, L. W. Jin, K. S. Kovacina, and S. Craft, 2003, Reduced hippocampal insulin-degrading enzyme in late-onset Alzheimer's disease is associated with the apolipoprotein E-epsilon4 allele: *Am J Pathol*, v. 162, p. 313-9.
- Copland, D. A., J. Liu, L. P. Schewitz-Bowers, V. Brinkmann, K. Anderson, L. B. Nicholson, and A. D. Dick, 2012, Therapeutic dosing of fingolimod (FTY720) prevents cell infiltration, rapidly suppresses ocular inflammation, and maintains the blood-ocular barrier: *Am J Pathol*, v. 180, p. 672-81.
- Cortese, M. M., A. L. Baughman, K. Brown, and P. Srivastava, 2007, A "new age" in pertussis prevention new opportunities through adult vaccination: *Am J Prev Med*, v. 32, p. 177-185.
- Cox, F. F., D. Carney, A. M. Miller, and M. A. Lynch, 2012, CD200 fusion protein decreases microglial activation in the hippocampus of aged rats: *Brain Behav Immun*, v. 26, p. 789-96.
- Cribbs, D. H., A. Ghochikyan, V. Vasilevko, M. Tran, I. Petrushina, N. Sadzikava, D. Babikyan, P. Kessler, T. Kieber-Emmons, C. W. Cotman, and M. G. Agadjanyan, 2003, Adjuvant-dependent modulation of Th1 and Th2 responses to immunization with beta-amyloid: *Int Immunol*, v. 15, p. 505-14.
- Crossley, K. B., and P. K. Peterson, 1996, Infections in the elderly: *Clin Infect Dis*, v. 22, p. 209-15.
- Czeloth, N., G. Bernhardt, F. Hofmann, H. Genth, and R. Forster, 2005, Sphingosine-1-phosphate mediates migration of mature dendritic cells: *J Immunol*, v. 175, p. 2960-7.
- Dahlgren, K. N., A. M. Manelli, W. B. Stine, Jr., L. K. Baker, G. A. Krafft, and M. J. LaDu, 2002, Oligomeric and fibrillar species of amyloid-beta peptides differentially affect neuronal viability: *J Biol Chem*, v. 277, p. 32046-53.
- Daneman, R., L. Zhou, A. A. Kebede, and B. A. Barres, 2010, Pericytes are required for blood-brain barrier integrity during embryogenesis, *Nature*, v. 468: England, p. 562-6.
- DaSilva, K., M. E. Brown, D. Westaway, and J. McLaurin, 2006, Immunization with amyloid-beta using GM-CSF and IL-4 reduces amyloid burden and alters plaque morphology: *Neurobiol Dis*, v. 23, p. 433-44.
- Davis, D. H., G. Muniz Terrera, H. Keage, T. Rahkonen, M. Oinas, F. E. Matthews, C. Cunningham, T. Polvikoski, R. Sulkava, A. M. MacLulich, and C. Brayne, 2012, Delirium is a strong risk factor for dementia in the oldest-old: a population-based cohort study: *Brain*, v. 135, p. 2809-16.
- Dawson, G. R., G. R. Seabrook, H. Zheng, D. W. Smith, S. Graham, G. O'Dowd, B. J. Bowery, S. Boyce, M. E. Trumbauer, H. Y. Chen, L. H. Van der Ploeg, and D. J. Sirinathsinghji, 1999, Age-related cognitive deficits, impaired long-term potentiation and reduction in synaptic marker density in mice lacking the beta-amyloid precursor protein: *Neuroscience*, v. 90, p. 1-13.
- de Bont, N., M. G. Netea, P. N. Demacker, I. Verschueren, B. J. Kullberg, K. W. van Dijk, J. W. van der Meer, and A. F. Stalenhoef, 1999, Apolipoprotein E knock-out mice

are highly susceptible to endotoxemia and *Klebsiella pneumoniae* infection: *J Lipid Res*, v. 40, p. 680-5.

- De Chiara, G., M. E. Marcocci, L. Civitelli, R. Argnani, R. Piacentini, C. Ripoli, R. Manservigi, C. Grassi, E. Garaci, and A. T. Palamara, 2010, APP processing induced by herpes simplex virus type 1 (HSV-1) yields several APP fragments in human and rat neuronal cells: *PLoS One*, v. 5, p. e13989.
- De Strooper, B., 2007, Loss-of-function presenilin mutations in Alzheimer disease. Talking Point on the role of presenilin mutations in Alzheimer disease: *EMBO Rep*, v. 8, p. 141-6.
- den Braber, I., T. Mugwagwa, N. Vrisekoop, L. Westera, R. Mogling, A. B. de Boer, N. Willems, E. H. Schrijver, G. Spierenburg, K. Gaiser, E. Mul, S. A. Otto, A. F. Ruiten, M. T. Ackermans, F. Miedema, J. A. Borghans, R. J. de Boer, and K. Tesselaar, 2012, Maintenance of peripheral naive T cells is sustained by thymus output in mice but not humans: *Immunity*, v. 36, p. 288-97.
- den Hartigh, L. J., R. Altman, R. Hutchinson, J. Petrlova, M. S. Budamagunta, S. D. Tetali, J. O. Lagerstedt, J. C. Voss, and J. C. Rutledge, 2012, Postprandial apoE isoform and conformational changes associated with VLDL lipolysis products modulate monocyte inflammation: *PLoS One*, v. 7, p. e50513.
- Denieffe, S., R. J. Kelly, C. McDonald, A. Lyons, and M. A. Lynch, 2013, Classical activation of microglia in CD200-deficient mice is a consequence of blood brain barrier permeability and infiltration of peripheral cells: *Brain Behav Immun*, v. 34, p. 86-97.
- Dev, K. K., F. Mullershausen, H. Mattes, R. R. Kuhn, G. Bilbe, D. Hoyer, and A. Mir, 2008, Brain sphingosine-1-phosphate receptors: implication for FTY720 in the treatment of multiple sclerosis: *Pharmacol Ther*, v. 117, p. 77-93.
- Di Pietro, M., S. Filardo, F. De Santis, and R. Sessa, 2013, *Chlamydia pneumoniae* infection in atherosclerotic lesion development through oxidative stress: a brief overview: *Int J Mol Sci*, v. 14, p. 15105-20.
- Dick, A. D., M. Pell, B. J. Brew, E. Foulcher, and J. D. Sedgwick, 1997, Direct ex vivo flow cytometric analysis of human microglial cell CD4 expression: examination of central nervous system biopsy specimens from HIV-seropositive patients and patients with other neurological disease: *AIDS*, v. 11, p. 1699-708.
- Doi, Y., H. Takeuchi, H. Horiuchi, T. Hanyu, J. Kawanokuchi, S. Jin, B. Parajuli, Y. Sonobe, T. Mizuno, and A. Suzumura, 2013, Fingolimod phosphate attenuates oligomeric amyloid beta-induced neurotoxicity via increased brain-derived neurotrophic factor expression in neurons: *PLoS One*, v. 8, p. e61988.
- Dominguez, M. R., J. Ersching, R. Lemos, A. V. Machado, O. Bruna-Romero, M. M. Rodrigues, and J. R. de Vasconcelos, 2012, Re-circulation of lymphocytes mediated by sphingosine-1-phosphate receptor-1 contributes to resistance against experimental infection with the protozoan parasite *Trypanosoma cruzi*: *Vaccine*, v. 30, p. 2882-91.
- Dong, Y., and E. N. Benveniste, 2001, Immune function of astrocytes: *Glia*, v. 36, p. 180-90.

- Dong, Y., W. M. Rohn, and E. N. Benveniste, 1999, IFN-gamma regulation of the type IV class II transactivator promoter in astrocytes: *J Immunol*, v. 162, p. 4731-9.
- Downer, E. J., T. R. Cowley, F. Cox, F. O. Maher, V. Berezin, E. Bock, and M. A. Lynch, 2009, A synthetic NCAM-derived mimetic peptide, FGL, exerts anti-inflammatory properties via IGF-1 and interferon-gamma modulation: *J Neurochem*, v. 109, p. 1516-25.
- Duff, K., C. Eckman, C. Zehr, X. Yu, C. M. Prada, J. Perez-tur, M. Hutton, L. Buee, Y. Harigaya, D. Yager, D. Morgan, M. N. Gordon, L. Holcomb, L. Refolo, B. Zenk, J. Hardy, and S. Younkin, 1996, Increased amyloid-beta42(43) in brains of mice expressing mutant presenilin 1: *Nature*, v. 383, p. 710-3.
- Dungan, L. S., N. C. McGuinness, L. Boon, M. A. Lynch, and K. H. Mills, 2014, Innate IFN-gamma promotes development of experimental autoimmune encephalomyelitis: A role for NK cells and M1 macrophages: *Eur J Immunol*, v. 44, p. 2903-2917.
- Dunn, N., M. Mullee, V. H. Perry, and C. Holmes, 2005, Association between dementia and infectious disease: evidence from a case-control study: *Alzheimer Dis Assoc Disord*, v. 19, p. 91-4.
- Dunne, A., P. J. Ross, E. Pospisilova, J. Masin, A. Meaney, C. E. Sutton, Y. Iwakura, J. Tschopp, P. Sebo, and K. H. Mills, 2010, Inflammasome activation by adenylate cyclase toxin directs Th17 responses and protection against *Bordetella pertussis*: *J Immunol*, v. 185, p. 1711-9.
- Dunne, P. J., B. Moran, R. C. Cummins, and K. H. Mills, 2009, CD11c+CD8alpha+ dendritic cells promote protective immunity to respiratory infection with *Bordetella pertussis*: *J Immunol*, v. 183, p. 400-10.
- Dénes, A., N. Humphreys, T. E. Lane, R. Grecis, and N. Rothwell, 2010, Chronic systemic infection exacerbates ischemic brain damage via a CCL5 (regulated on activation, normal T-cell expressed and secreted)-mediated proinflammatory response in mice: *J Neurosci*, v. 30, p. 10086-95.
- Ebert, S., M. Goos, L. Rollwagen, D. Baake, W. D. Zech, H. Esselmann, J. Wiltfang, B. Mollenhauer, R. Schliebs, J. Gerber, and R. Nau, 2010, Recurrent systemic infections with *Streptococcus pneumoniae* do not aggravate the course of experimental neurodegenerative diseases: *J Neurosci Res*, v. 88, p. 1124-36.
- Eddleston, M., and L. Mucke, 1993, Molecular profile of reactive astrocytes--implications for their role in neurologic disease: *Neuroscience*, v. 54, p. 15-36.
- El Khoury, J., M. Toft, S. E. Hickman, T. K. Means, K. Terada, C. Geula, and A. D. Luster, 2007, *Ccr2* deficiency impairs microglial accumulation and accelerates progression of Alzheimer-like disease: *Nat Med*, v. 13, p. 432-8.
- Emsley, H. C., and S. J. Hopkins, 2008, Acute ischaemic stroke and infection: recent and emerging concepts: *Lancet Neurol*, v. 7, p. 341-53.
- Engelhardt, B., and R. M. Ransohoff, 2005, The ins and outs of T-lymphocyte trafficking to the CNS: anatomical sites and molecular mechanisms: *Trends Immunol*, v. 26, p. 485-95.
- Engelhardt, B., and R. M. Ransohoff, 2012, Capture, crawl, cross: the T cell code to breach the blood-brain barriers: *Trends Immunol*, v. 33, p. 579-89.

- Engelhardt, B., K. Wolburg-Buchholz, and H. Wolburg, 2001, Involvement of the choroid plexus in central nervous system inflammation: *Microsc Res Tech*, v. 52, p. 112-29.
- Engelhart, S. T., L. Hanes-Derendorf, M. Exner, and M. H. Kramer, 2005, Prospective surveillance for healthcare-associated infections in German nursing home residents: *J Hosp Infect*, v. 60, p. 46-50.
- Erickson, M. A., and W. A. Banks, 2011, Cytokine and chemokine responses in serum and brain after single and repeated injections of lipopolysaccharide: multiplex quantification with path analysis: *Brain Behav Immun*, v. 25, p. 1637-48.
- Farrall, A. J., and J. M. Wardlaw, 2009, Blood-brain barrier: ageing and microvascular disease--systematic review and meta-analysis: *Neurobiol Aging*, v. 30, p. 337-52.
- Fessler, J., A. Ficjan, C. Duftner, and C. Dejaco, 2013, The impact of aging on regulatory T-cells: *Front Immunol*, v. 4, p. 231.
- Feuillet, V., B. Lucas, J. P. Di Santo, G. Bismuth, and A. Trautmann, 2005, Multiple survival signals are delivered by dendritic cells to naive CD4+ T cells: *Eur J Immunol*, v. 35, p. 2563-72.
- Fiala, M., J. Lin, J. Ringman, V. Kermani-Arab, G. Tsao, A. Patel, A. S. Lossinsky, M. C. Graves, A. Gustavson, J. Sayre, E. Sofroni, T. Suarez, F. Chiappelli, and G. Bernard, 2005, Ineffective phagocytosis of amyloid-beta by macrophages of Alzheimer's disease patients.: *J Alzheimers Dis*, v. 7, p. 221-32; discussion 255-62.
- Fiala, M., Q. N. Liu, J. Sayre, V. Pop, V. Brahmandam, M. C. Graves, and H. V. Vinters, 2002, Cyclooxygenase-2-positive macrophages infiltrate the Alzheimer's disease brain and damage the blood-brain barrier: *Eur J Clin Invest*, v. 32, p. 360-71.
- Fiala, M., L. Zhang, X. Gan, B. Sherry, D. Taub, M. C. Graves, S. Hama, D. Way, M. Weinand, M. Witte, D. Lorton, Y. M. Kuo, and A. E. Roher, 1998, Amyloid-beta induces chemokine secretion and monocyte migration across a human blood--brain barrier model: *Mol Med*, v. 4, p. 480-9.
- Fick, D. M., J. V. Agostini, and S. K. Inouye, 2002, Delirium superimposed on dementia: a systematic review: *J Am Geriatr Soc*, v. 50, p. 1723-32.
- Filiano, A. J., S. P. Gadani, and J. Kipnis, 2014, Interactions of innate and adaptive immunity in brain development and function: *Brain Res*.
- Finkelstein, A., G. Kunis, A. Seksenyan, A. Ronen, T. Berkutzki, D. Azoulay, M. Koronyo-Hamaoui, and M. Schwartz, 2011, Abnormal changes in NKT cells, the IGF-1 axis, and liver pathology in an animal model of ALS: *PLoS One*, v. 6, p. e22374.
- Finlay, C. M., K. P. Walsh, and K. H. Mills, 2014, Induction of regulatory cells by helminth parasites: exploitation for the treatment of inflammatory diseases: *Immunol Rev*, v. 259, p. 206-30.
- Finney, C. A., C. A. Hawkes, D. C. Kain, A. Dhabangi, C. Musoke, C. Cserti-Gazdewich, T. Oravec, W. C. Liles, and K. C. Kain, 2011, S1P is associated with protection in human and experimental cerebral malaria: *Mol Med*, v. 17, p. 717-25.
- Finsen, B. R., T. Sorensen, B. Castellano, E. B. Pedersen, and J. Zimmer, 1991, Leukocyte infiltration and glial reactions in xenografts of mouse brain tissue undergoing

rejection in the adult rat brain. A light and electron microscopical immunocytochemical study: *J Neuroimmunol*, v. 32, p. 159-83.

Fisher, Y., I. Strominger, S. Biton, A. Nemirovsky, R. Baron, and A. Monsonego, 2014, Th1 polarization of T cells injected into the cerebrospinal fluid induces brain immunosurveillance: *J Immunol*, v. 192, p. 92-102.

Fitzpatrick, A. L., L. H. Kuller, O. L. Lopez, C. H. Kawas, and W. Jagust, 2005, Survival following dementia onset: Alzheimer's disease and vascular dementia: *J Neurol Sci*, v. 229-230, p. 43-9.

Flanary, B. E., N. W. Sammons, C. Nguyen, D. Walker, and W. J. Streit, 2007, Evidence that aging and amyloid promote microglial cell senescence: *Rejuvenation Res*, v. 10, p. 61-74.

Fletcher, J. M., S. J. Lalor, C. M. Sweeney, N. Tubridy, and K. H. Mills, 2010, T cells in multiple sclerosis and experimental autoimmune encephalomyelitis: *Clin Exp Immunol*, v. 162, p. 1-11.

Fong, T. G., R. N. Jones, P. Shi, E. R. Marcantonio, L. Yap, J. L. Rudolph, F. M. Yang, D. K. Kiely, and S. K. Inouye, 2009, Delirium accelerates cognitive decline in Alzheimer disease: *Neurology*, v. 72, p. 1570-5.

Foster, C. A., L. M. Howard, A. Schweitzer, E. Persohn, P. C. Hiestand, B. Balatoni, R. Reuschel, C. Beerli, M. Schwartz, and A. Billich, 2007, Brain penetration of the oral immunomodulatory drug FTY720 and its phosphorylation in the central nervous system during experimental autoimmune encephalomyelitis: consequences for mode of action in multiple sclerosis: *J Pharmacol Exp Ther*, v. 323, p. 469-75.

Foster, C. A., D. Mechtcheriakova, M. K. Storch, B. Balatoni, L. M. Howard, F. Bornancin, A. Wlachos, J. Sobanov, A. Kinnunen, and T. Baumruker, 2009, FTY720 rescue therapy in the dark agouti rat model of experimental autoimmune encephalomyelitis: expression of central nervous system genes and reversal of blood-brain-barrier damage: *Brain Pathol*, v. 19, p. 254-66.

Frackowiak, J., H. M. Wisniewski, J. Wegiel, G. S. Merz, K. Iqbal, and K. C. Wang, 1992, Ultrastructure of the microglia that phagocytose amyloid and the microglia that produce beta-amyloid fibrils: *Acta Neuropathol*, v. 84, p. 225-33.

Franceschi, C., M. Bonafè, and S. Valensin, 2000, Human immunosenescence: the prevailing of innate immunity, the failing of clonotypic immunity, and the filling of immunological space: *Vaccine*, v. 18, p. 1717-20.

Franceschi, C., and J. Campisi, 2014, Chronic inflammation (inflammaging) and its potential contribution to age-associated diseases, *J Gerontol A Biol Sci Med Sci*, v. 69 Suppl 1: United States, The Author 2014. Published by Oxford University Press on behalf of The Gerontological Society of America For permissions, please e-mail: journals.permissions@oup.com., p. S4-9.

Frautschy, S. A., G. M. Cole, and A. Baird, 1992, Phagocytosis and deposition of vascular beta-amyloid in rat brains injected with Alzheimer beta-amyloid: *Am J Pathol*, v. 140, p. 1389-99.

- Frautschy, S. A., F. Yang, L. Calderon, and G. M. Cole, 1996, Rodent models of Alzheimer's disease: rat A beta infusion approaches to amyloid deposits: *Neurobiol Aging*, v. 17, p. 311-21.
- Friedl, P., and M. Gunzer, 2001, Interaction of T cells with APCs: the serial encounter model: *Trends Immunol*, v. 22, p. 187-91.
- Friese, M. A., and L. Fugger, 2005, Autoreactive CD8+ T cells in multiple sclerosis: a new target for therapy?, *Brain*, v. 128: England, p. 1747-63.
- Fukumoto, K., H. Mizoguchi, H. Takeuchi, H. Horiuchi, J. Kawanokuchi, S. Jin, T. Mizuno, and A. Suzumura, 2014, Fingolimod increases brain-derived neurotrophic factor levels and ameliorates amyloid beta-induced memory impairment: *Behav Brain Res*, v. 268, p. 88-93.
- Galea, I., I. Bechmann, and V. H. Perry, 2007, What is immune privilege (not)?: *Trends Immunol*, v. 28, p. 12-8.
- Gallagher, J. J., M. E. Finnegan, B. Grehan, J. Dobson, J. F. Collingwood, and M. A. Lynch, 2012, Modest amyloid deposition is associated with iron dysregulation, microglial activation, and oxidative stress: *J Alzheimers Dis*, v. 28, p. 147-61.
- Gallagher, J. J., A. M. Minogue, and M. A. Lynch, 2013, Impaired performance of female APP/PS1 mice in the Morris water maze is coupled with increased A β accumulation and microglial activation: *Neurodegener Dis*, v. 11, p. 33-41.
- Gamblin, T. C., F. Chen, A. Zambrano, A. Abraha, S. Lagalwar, A. L. Guillozet, M. Lu, Y. Fu, F. Garcia-Sierra, N. LaPointe, R. Miller, R. W. Berry, L. I. Binder, and V. L. Cryns, 2003, Caspase cleavage of tau: Linking amyloid and neurofibrillary tangles in Alzheimer's disease, *Proc Natl Acad Sci U S A*, v. 100, p. 10032-7.
- Gardner, E. M., E. W. Gonzalez, S. Nogusa, and D. M. Murasko, 2006, Age-related changes in the immune response to influenza vaccination in a racially diverse, healthy elderly population: *Vaccine*, v. 24, p. 1609-14.
- Garwood, C. J., A. M. Pooler, J. Atherton, D. P. Hanger, and W. Noble, 2011, Astrocytes are important mediators of A β -induced neurotoxicity and tau phosphorylation in primary culture: *Cell Death Dis*, v. 2, p. e167.
- Gengler, S., A. Hamilton, and C. Hölscher, 2010, Synaptic plasticity in the hippocampus of a APP/PS1 mouse model of Alzheimer's disease is impaired in old but not young mice: *PLoS One*, v. 5, p. e9764.
- Ginhoux, F., M. Greter, M. Leboeuf, S. Nandi, P. See, S. Gokhan, M. F. Mehler, S. J. Conway, L. G. Ng, E. R. Stanley, I. M. Samokhvalov, and M. Merad, 2010, Fate Mapping Analysis Reveals That Adult Microglia Derive from Primitive Macrophages: *Science*, v. 330, p. 841-5.
- Girvin, A. M., K. B. Gordon, C. J. Welsh, N. A. Clipstone, and S. D. Miller, 2002, Differential abilities of central nervous system resident endothelial cells and astrocytes to serve as inducible antigen-presenting cells: *Blood*, v. 99, p. 3692-701.
- Glass, C. K., K. Saijo, B. Winner, M. C. Marchetto, and F. H. Gage, 2010, Mechanisms underlying inflammation in neurodegeneration: *Cell*, v. 140, p. 918-34.

- Glenner, G. G., and C. W. Wong, 1984, Alzheimer's disease: initial report of the purification and characterization of a novel cerebrovascular amyloid protein: *Biochem Biophys Res Commun*, v. 120, p. 885-90.
- Goldeck, D., A. Larbi, M. Pellicano, I. Alam, I. Zerr, C. Schmidt, T. Fulop, and G. Pawelec, 2013, Enhanced Chemokine Receptor Expression on Leukocytes of Patients with Alzheimer's Disease: *PLoS One*, v. 8, p. e66664.
- Goldmann, T., and M. Prinz, 2013, Role of microglia in CNS autoimmunity: *Clin Dev Immunol*, v. 2013, p. 208093.
- Gonzalez-Velasquez, F. J., and M. A. Moss, 2008, Soluble aggregates of the amyloid-beta protein activate endothelial monolayers for adhesion and subsequent transmigration of monocyte cells: *J Neurochem*, v. 104, p. 500-13.
- Gotz, J., F. Chen, J. van Dorpe, and R. M. Nitsch, 2001, Formation of neurofibrillary tangles in P301l tau transgenic mice induced by Abeta 42 fibrils: *Science*, v. 293, p. 1491-5.
- Gotz, J., and L. M. Ittner, 2008, Animal models of Alzheimer's disease and frontotemporal dementia: *Nat Rev Neurosci*, v. 9, p. 532-44.
- Gotz, J., A. Schild, F. Hoerndli, and L. Pennanen, 2004, Amyloid-induced neurofibrillary tangle formation in Alzheimer's disease: insight from transgenic mouse and tissue-culture models: *Int J Dev Neurosci*, v. 22, p. 453-65.
- Grau, A. J., C. Urbanek, and F. Palm, 2010, Common infections and the risk of stroke: *Nat Rev Neurol*, v. 6, p. 681-94.
- Greter, M., F. L. Heppner, M. P. Lemos, B. M. Odermatt, N. Goebels, T. Laufer, R. J. Noelle, and B. Becher, 2005, Dendritic cells permit immune invasion of the CNS in an animal model of multiple sclerosis: *Nat Med*, v. 11, p. 328-34.
- Griffin, W. S., L. C. Stanley, C. Ling, L. White, V. MacLeod, L. J. Perrot, C. L. White, and C. Araoz, 1989, Brain interleukin 1 and S-100 immunoreactivity are elevated in Down syndrome and Alzheimer disease: *Proc Natl Acad Sci U S A*, v. 86, p. 7611-5.
- Grubeck-Loebenstien, B., and G. Wick, 2002, The aging of the immune system: *Adv Immunol*, v. 80, p. 243-84.
- Grundke-Iqbal, I., K. Iqbal, Y. C. Tung, M. Quinlan, H. M. Wisniewski, and L. I. Binder, 1986, Abnormal phosphorylation of the microtubule-associated protein tau (tau) in Alzheimer cytoskeletal pathology: *Proc Natl Acad Sci U S A*, v. 83, p. 4913-7.
- Guerra, C., W. T. Linde-Zwirble, and H. Wunsch, 2012, Risk factors for dementia after critical illness in elderly Medicare beneficiaries: *Crit Care*, v. 16, p. R233.
- Guillemin, G. J., and B. J. Brew, 2004, Microglia, macrophages, perivascular macrophages, and pericytes: a review of function and identification, *J Leukoc Biol*, v. 75: United States, p. 388-97.
- Gérard, H. C., U. Dreses-Werringloer, K. S. Wildt, S. Deka, C. Oszust, B. J. Balin, W. H. Frey, E. Z. Bodayo, J. A. Whittum-Hudson, and A. P. Hudson, 2006, *Chlamydia pneumoniae* in the Alzheimer's brain: *FEMS Immunol Med Microbiol*, v. 48, p. 355-66.

- Gérard, H. C., K. L. Wildt, J. A. Whittum-Hudson, Z. Lai, J. Ager, and A. P. Hudson, 2005, The load of *Chlamydia pneumoniae* in the Alzheimer's brain varies with APOE genotype: *Microb Pathog*, v. 39, p. 19-26.
- Haass, C., C. Kaether, G. Thinakaran, and S. Sisodia, 2012, Trafficking and proteolytic processing of APP: *Cold Spring Harb Perspect Med*, v. 2, p. a006270.
- Haass, C., and D. J. Selkoe, 2007, Soluble protein oligomers in neurodegeneration: lessons from the Alzheimer's amyloid beta-peptide: *Nat Rev Mol Cell Biol*, v. 8, p. 101-12.
- Halle, A., V. Hornung, G. C. Petzold, C. R. Stewart, B. G. Monks, T. Reinheckel, K. A. Fitzgerald, E. Latz, K. J. Moore, and D. T. Golenbock, 2008, The NALP3 inflammasome is involved in the innate immune response to amyloid-beta: *Nat Immunol*, v. 9, p. 857-65.
- Hammond, C. J., L. R. Hallock, R. J. Howanski, D. M. Appelt, C. S. Little, and B. J. Balin, 2010, Immunohistological detection of *Chlamydia pneumoniae* in the Alzheimer's disease brain: *BMC Neurosci*, v. 11, p. 121.
- Hampel, H., 2013, Amyloid-beta and cognition in aging and Alzheimer's disease: molecular and neurophysiological mechanisms, *J Alzheimers Dis*, v. 33 Suppl 1: Netherlands, p. S79-86.
- Han, S., X. Zhang, G. Wang, H. Guan, G. Garcia, P. Li, L. Feng, and B. Zheng, 2004, FTY720 suppresses humoral immunity by inhibiting germinal center reaction: *Blood*, v. 104, p. 4129-33.
- Handels, R. L., C. A. Wolfs, P. Aalten, M. A. Joore, F. R. Verhey, and J. L. Severens, 2013, Diagnosing Alzheimer's disease: A systematic review of economic evaluations: *Alzheimers Dement*.
- Harada, J., M. Foley, M. A. Moskowitz, and C. Waeber, 2004, Sphingosine-1-phosphate induces proliferation and morphological changes of neural progenitor cells: *J Neurochem*, v. 88, p. 1026-39.
- Hardy, J., and D. J. Selkoe, 2002, The amyloid hypothesis of Alzheimer's disease: progress and problems on the road to therapeutics.: *Science*, v. 297, p. 353-6.
- Harkness, K. A., P. Adamson, J. D. Sussman, G. A. Davies-Jones, J. Greenwood, and M. N. Woodroffe, 2000, Dexamethasone regulation of matrix metalloproteinase expression in CNS vascular endothelium: *Brain*, v. 123 (Pt 4), p. 698-709.
- Harrington, L. E., R. D. Hatton, P. R. Mangan, H. Turner, T. L. Murphy, K. M. Murphy, and C. T. Weaver, 2005, Interleukin 17-producing CD4+ effector T cells develop via a lineage distinct from the T helper type 1 and 2 lineages: *Nat Immunol*, v. 6, p. 1123-32.
- Hartwig, M., 1995, Immune ageing and Alzheimer's disease: *Neuroreport*, v. 6, p. 1274-6.
- Harty, J. T., A. R. Tinnereim, and D. W. White, 2000, CD8+ T cell effector mechanisms in resistance to infection: *Annu Rev Immunol*, v. 18, p. 275-308.
- Harvill, E. T., P. A. Cotter, and J. F. Miller, 1999, Pregenomic comparative analysis between *Bordetella bronchiseptica* RB50 and *Bordetella pertussis* tohama I in murine models of respiratory tract infection: *Infect Immun*, v. 67, p. 6109-18.

- Hawkins, B. T., and T. P. Davis, 2005, The blood-brain barrier/neurovascular unit in health and disease: *Pharmacol Rev*, v. 57, p. 173-85.
- Haynes, L., and S. L. Swain, 2006, Why aging T cells fail: implications for vaccination: *Immunity*, v. 24, p. 663-6.
- Hellstrom, M., H. Gerhardt, M. Kalen, X. Li, U. Eriksson, H. Wolburg, and C. Betsholtz, 2001, Lack of pericytes leads to endothelial hyperplasia and abnormal vascular morphogenesis: *J Cell Biol*, v. 153, p. 543-53.
- Hellwig, S. M., W. L. Hazenbos, J. G. van de Winkel, and F. R. Mooi, 1999, Evidence for an intracellular niche for *Bordetella pertussis* in broncho-alveolar lavage cells of mice: *FEMS Immunol Med Microbiol*, v. 26, p. 203-7.
- Hemmati, F., L. Dargahi, S. Nasoohi, R. Omidbakhsh, Z. Mohamed, Z. Chik, M. Naidu, and A. Ahmadiani, 2013, Neurorestorative effect of FTY720 in a rat model of Alzheimer's disease: Comparison with Memantine: *Behav Brain Res*, v. 252C, p. 415-421.
- Hendriks, L. H., M. K. Felderhof, K. Ozturk, L. G. de Rond, M. A. van Houten, E. A. Sanders, G. A. Berbers, and A. M. Buisman, 2011, Enhanced memory B-cell immune responses after a second acellular pertussis booster vaccination in children 9 years of age: *Vaccine*, v. 30, p. 51-8.
- Heneka, M. T., M. P. Kummer, and E. Latz, 2014, Innate immune activation in neurodegenerative disease: *Nat Rev Immunol*, v. 14, p. 463-77.
- Heneka, M. T., M. P. Kummer, A. Stutz, A. Delekate, S. Schwartz, A. Saecker, A. Griep, D. Axt, A. Remus, T. C. Tzeng, E. Gelpi, A. Halle, M. Korte, E. Latz, and D. Golenbock, 2013, NLRP3 is activated in Alzheimer's disease and contributes to pathology in APP/PS1 mice: *Nature*, v. 493, p. 674-678.
- Heneka, M. T., J. J. Rodriguez, and A. Verkhratsky, 2010, Neuroglia in neurodegeneration, *Brain Res Rev*, v. 63: Netherlands, 2009 Elsevier B.V, p. 189-211.
- Herrmann, I., M. Kellert, H. Schmidt, A. Mildner, U. K. Hanisch, W. Brück, M. Prinz, and R. Nau, 2006, *Streptococcus pneumoniae* Infection aggravates experimental autoimmune encephalomyelitis via Toll-like receptor 2: *Infect Immun*, v. 74, p. 4841-8.
- Hickey, W. F., 2001, Basic principles of immunological surveillance of the normal central nervous system: *Glia*, v. 36, p. 118-24.
- Higgins, S. C., A. G. Jarnicki, E. C. Lavelle, and K. H. Mills, 2006, TLR4 mediates vaccine-induced protective cellular immunity to *Bordetella pertussis*: role of IL-17-producing T cells: *J Immunol*, v. 177, p. 7980-9.
- Higgins, S. C., E. C. Lavelle, C. McCann, B. Keogh, E. McNeela, P. Byrne, B. O'Gorman, A. Jarnicki, P. McGuirk, and K. H. Mills, 2003, Toll-like receptor 4-mediated innate IL-10 activates antigen-specific regulatory T cells and confers resistance to *Bordetella pertussis* by inhibiting inflammatory pathology: *J Immunol*, v. 171, p. 3119-27.
- Higgs, R., S. C. Higgins, P. J. Ross, and K. H. Mills, 2012, Immunity to the respiratory pathogen *Bordetella pertussis*: *Mucosal Immunol*, v. 5, p. 485-500.

- Hock, C., K. Heese, C. Hulette, C. Rosenberg, and U. Otten, 2000, Region-specific neurotrophin imbalances in Alzheimer disease: decreased levels of brain-derived neurotrophic factor and increased levels of nerve growth factor in hippocampus and cortical areas: *Arch Neurol*, v. 57, p. 846-51.
- Hodgson, N. A., L. N. Gitlin, L. Winter, and K. Czekanski, 2011, Undiagnosed illness and neuropsychiatric behaviors in community residing older adults with dementia: *Alzheimer Dis Assoc Disord*, v. 25, p. 109-15.
- Holmes, C., D. Boche, D. Wilkinson, G. Yadegarfar, V. Hopkins, A. Bayer, R. W. Jones, R. Bullock, S. Love, J. W. Neal, E. Zotova, and J. A. Nicoll, 2008, Long-term effects of Abeta42 immunisation in Alzheimer's disease: follow-up of a randomised, placebo-controlled phase I trial.: *Lancet*, v. 372, p. 216-23.
- Holmes, C., C. Cunningham, E. Zotova, J. Woolford, C. Dean, S. Kerr, D. Culliford, and V. H. Perry, 2009, Systemic inflammation and disease progression in Alzheimer disease: *Neurology*, v. 73, p. 768-74.
- Holmes, C., M. El-Okli, A. L. Williams, C. Cunningham, D. Wilcockson, and V. H. Perry, 2003, Systemic infection, interleukin 1beta, and cognitive decline in Alzheimer's disease.: *J Neurol Neurosurg Psychiatry*, v. 74, p. 788-9.
- Honjo, K., R. van Reekum, and N. P. Verhoeff, 2009, Alzheimer's disease and infection: do infectious agents contribute to progression of Alzheimer's disease?: *Alzheimers Dement*, v. 5, p. 348-60.
- Hsiao, K., P. Chapman, S. Nilsen, C. Eckman, Y. Harigaya, S. Younkin, F. Yang, and G. Cole, 1996, Correlative memory deficits, Abeta elevation, and amyloid plaques in transgenic mice: *Science*, v. 274, p. 99-102.
- Iezzi, G., I. Sonderegger, F. Ampenberger, N. Schmitz, B. J. Marsland, and M. Kopf, 2009, CD40-CD40L cross-talk integrates strong antigenic signals and microbial stimuli to induce development of IL-17-producing CD4+ T cells: *Proc Natl Acad Sci U S A*, v. 106, p. 876-81.
- Itzhaki, R. F., W. R. Lin, D. Shang, G. K. Wilcock, B. Faragher, and G. A. Jamieson, 1997, Herpes simplex virus type 1 in brain and risk of Alzheimer's disease: *Lancet*, v. 349, p. 241-4.
- Itzhaki, R. F., and M. A. Wozniak, 2006, Herpes simplex virus type 1, apolipoprotein E, and cholesterol: a dangerous liaison in Alzheimer's disease and other disorders: *Prog Lipid Res*, v. 45, p. 73-90.
- Itzhaki, R. F., M. A. Wozniak, D. M. Appelt, and B. J. Balin, 2004, Infiltration of the brain by pathogens causes Alzheimer's disease: *Neurobiol Aging*, v. 25, p. 619-27.
- Jack, C. S., N. Arbour, J. Manusow, V. Montgrain, M. Blain, E. McCrea, A. Shapiro, and J. P. Antel, 2005, TLR signaling tailors innate immune responses in human microglia and astrocytes: *J Immunol*, v. 175, p. 4320-30.
- Jackson, J. C., S. M. Gordon, R. P. Hart, R. O. Hopkins, and E. W. Ely, 2004, The association between delirium and cognitive decline: a review of the empirical literature: *Neuropsychol Rev*, v. 14, p. 87-98.
- Jamieson, G. A., N. J. Maitland, G. K. Wilcock, J. Craske, and R. F. Itzhaki, 1991, Latent herpes simplex virus type 1 in normal and Alzheimer's disease brains: *J Med Virol*, v. 33, p. 224-7.

- Jamieson, G. A., N. J. Maitland, G. K. Wilcock, C. M. Yates, and R. F. Itzhaki, 1992, Herpes simplex virus type 1 DNA is present in specific regions of brain from aged people with and without senile dementia of the Alzheimer type: *J Pathol*, v. 167, p. 365-8.
- Jankowsky, J. L., D. J. Fadale, J. Anderson, G. M. Xu, V. Gonzales, N. A. Jenkins, N. G. Copeland, M. K. Lee, L. H. Younkin, S. L. Wagner, S. G. Younkin, and D. R. Borchelt, 2004, Mutant presenilins specifically elevate the levels of the 42 residue beta-amyloid peptide in vivo: evidence for augmentation of a 42-specific gamma secretase: *Hum Mol Genet*, v. 13, p. 159-70.
- Jankowsky, J. L., T. Melnikova, D. J. Fadale, G. M. Xu, H. H. Slunt, V. Gonzales, L. H. Younkin, S. G. Younkin, D. R. Borchelt, and A. V. Savonenko, 2005, Environmental enrichment mitigates cognitive deficits in a mouse model of Alzheimer's disease: *J Neurosci*, v. 25, p. 5217-24.
- Jansson, D., J. Rustenhoven, S. Feng, D. Hurley, R. L. Oldfield, P. S. Bergin, E. W. Mee, R. L. Faull, and M. Dragunow, 2014, A role for human brain pericytes in neuroinflammation, *J Neuroinflammation*, v. 11: England, p. 104.
- Janus, C., J. Pearson, J. McLaurin, P. M. Mathews, Y. Jiang, S. D. Schmidt, M. A. Chishti, P. Horne, D. Heslin, J. French, H. T. Mount, R. A. Nixon, M. Mercken, C. Bergeron, P. E. Fraser, P. St George-Hyslop, and D. Westaway, 2000, A beta peptide immunization reduces behavioural impairment and plaques in a model of Alzheimer's disease.: *Nature*, v. 408, p. 979-82.
- Jimenez, S., D. Baglietto-Vargas, C. Caballero, I. Moreno-Gonzalez, M. Torres, R. Sanchez-Varo, D. Ruano, M. Vizuete, A. Gutierrez, and J. Vitorica, 2008, Inflammatory response in the hippocampus of PS1M146L/APP751SL mouse model of Alzheimer's disease: age-dependent switch in the microglial phenotype from alternative to classic: *J Neurosci*, v. 28, p. 11650-61.
- Jin, M., N. Shepardson, T. Yang, G. Chen, D. Walsh, and D. J. Selkoe, 2011, Soluble amyloid beta-protein dimers isolated from Alzheimer cortex directly induce Tau hyperphosphorylation and neuritic degeneration: *Proc Natl Acad Sci U S A*, v. 108, p. 5819-24.
- Jones, R. S., A. M. Minogue, T. J. Connor, and M. A. Lynch, 2013, Amyloid- β -induced astrocytic phagocytosis is mediated by CD36, CD47 and RAGE: *J Neuroimmune Pharmacol*, v. 8, p. 301-11.
- Josefowicz, S. Z., L. F. Lu, and A. Y. Rudensky, 2012, Regulatory T cells: mechanisms of differentiation and function: *Annu Rev Immunol*, v. 30, p. 531-64.
- Jung, B. K., K. H. Pyo, K. Y. Shin, Y. S. Hwang, H. Lim, S. J. Lee, J. H. Moon, S. H. Lee, Y. H. Suh, J. Y. Chai, and E. H. Shin, 2012, Toxoplasma gondii infection in the brain inhibits neuronal degeneration and learning and memory impairments in a murine model of Alzheimer's disease: *PLoS One*, v. 7, p. e33312.
- Kamer, A. R., R. G. Craig, A. P. Dasanayake, M. Brys, L. Glodzik-Sobanska, and M. J. de Leon, 2008, Inflammation and Alzheimer's disease: possible role of periodontal diseases: *Alzheimers Dement*, v. 4, p. 242-50.
- Kang, I., M. S. Hong, H. Nolasco, S. H. Park, J. M. Dan, J. Y. Choi, and J. Craft, 2004, Age-associated change in the frequency of memory CD4+ T cells impairs long term CD4+ T cell responses to influenza vaccine: *J Immunol*, v. 173, p. 673-81.

- Kappos, L., J. Antel, G. Comi, X. Montalban, P. O'Connor, C. H. Polman, T. Haas, A. A. Korn, G. Karlsson, E. W. Radue, and F. D. S. Group, 2006, Oral fingolimod (FTY720) for relapsing multiple sclerosis: *N Engl J Med*, v. 355, p. 1124-40.
- Kappos, L., P. O'Connor, E. W. Radue, C. Polman, R. Hohlfeld, K. Selmaj, S. Ritter, R. Schlosshauer, P. von Rosenstiel, L. Zhang-Auberson, and G. Francis, 2015, Long-term effects of fingolimod in multiple sclerosis: The randomized FREEDOMS extension trial: *Neurology*.
- Kappos, L., E. W. Radue, P. O'Connor, C. Polman, R. Hohlfeld, P. Calabresi, K. Selmaj, C. Agoropoulou, M. Leyk, L. Zhang-Auberson, P. Burtin, and F. S. Group, 2010, A placebo-controlled trial of oral fingolimod in relapsing multiple sclerosis: *N Engl J Med*, v. 362, p. 387-401.
- Katan, M., Y. P. Moon, M. C. Paik, R. L. Sacco, C. B. Wright, and M. S. Elkind, 2013, Infectious burden and cognitive function: the Northern Manhattan Study: *Neurology*, v. 80, p. 1209-15.
- Kataoka, H., K. Sugahara, K. Shimano, K. Teshima, M. Koyama, A. Fukunari, and K. Chiba, 2005, FTY720, sphingosine 1-phosphate receptor modulator, ameliorates experimental autoimmune encephalomyelitis by inhibition of T cell infiltration: *Cell Mol Immunol*, v. 2, p. 439-48.
- Kawanokuchi, J., K. Shimizu, A. Nitta, K. Yamada, T. Mizuno, H. Takeuchi, and A. Suzumura, 2008, Production and functions of IL-17 in microglia: *J Neuroimmunol*, v. 194, p. 54-61.
- Kebir, H., K. Kreymborg, I. Ifergan, A. Dodelet-Devillers, R. Cayrol, M. Bernard, F. Giuliani, N. Arbour, B. Becher, and A. Prat, 2007, Human TH17 lymphocytes promote blood-brain barrier disruption and central nervous system inflammation: *Nat Med*, v. 13, p. 1173-5.
- Keir, M. E., M. J. Butte, G. J. Freeman, and A. H. Sharpe, 2008, PD-1 and its ligands in tolerance and immunity: *Annu Rev Immunol*, v. 26, p. 677-704.
- Kelley, K. W., J. C. O'Connor, M. A. Lawson, R. Dantzer, S. L. Rodriguez-Zas, and R. H. McCusker, 2013, Aging leads to prolonged duration of inflammation-induced depression-like behavior caused by *Bacillus Calmette-Guerin*: *Brain Behav Immun*, v. 32, p. 63-9.
- Kelly, R. J., A. M. Minogue, A. Lyons, R. S. Jones, T. C. Browne, D. A. Costello, S. Denieffe, C. O'Sullivan, T. J. Connor, and M. A. Lynch, 2013, Glial Activation in A β PP/PS1 Mice is Associated with Infiltration of IFN γ -Producing Cells: *J Alzheimers Dis*, v. 37, p. 63-75.
- Khan, N., N. Shariff, M. Cobbold, R. Bruton, J. A. Ainsworth, A. J. Sinclair, L. Nayak, and P. A. Moss, 2002, Cytomegalovirus seropositivity drives the CD8 T cell repertoire toward greater clonality in healthy elderly individuals: *J Immunol*, v. 169, p. 1984-92.
- Kim, D. Y., G. U. Hong, and J. Y. Ro, 2011, Signal pathways in astrocytes activated by cross-talk between of astrocytes and mast cells through CD40-CD40L: *J Neuroinflammation*, v. 8, p. 25.
- Kipnis, J., H. Cohen, M. Cardon, Y. Ziv, and M. Schwartz, 2004, T cell deficiency leads to cognitive dysfunction: implications for therapeutic vaccination for schizophrenia

- and other psychiatric conditions, *Proc Natl Acad Sci U S A*, v. 101: United States, p. 8180-5.
- Kirk, J., J. Plumb, M. Mirakhur, and S. McQuaid, 2003, Tight junctional abnormality in multiple sclerosis white matter affects all calibres of vessel and is associated with blood-brain barrier leakage and active demyelination: *J Pathol*, v. 201, p. 319-27.
- Kitazawa, M., S. Oddo, T. R. Yamasaki, K. N. Green, and F. M. LaFerla, 2005, Lipopolysaccharide-induced inflammation exacerbates tau pathology by a cyclin-dependent kinase 5-mediated pathway in a transgenic model of Alzheimer's disease: *J Neurosci*, v. 25, p. 8843-53.
- Kivisakk, P., D. J. Mahad, M. K. Callahan, C. Trebst, B. Tucky, T. Wei, L. Wu, E. S. Baekkevold, H. Lassmann, S. M. Staugaitis, J. J. Campbell, and R. M. Ransohoff, 2003, Human cerebrospinal fluid central memory CD4+ T cells: evidence for trafficking through choroid plexus and meninges via P-selectin: *Proc Natl Acad Sci U S A*, v. 100, p. 8389-94.
- Klein, N., J. Bartlett, A. Rowhani-Rahbar, B. Fireman, and R. Baxter, 2012, Waning Protection after Fifth Dose of Acellular Pertussis Vaccine in Children: *The New England Journal of Medicine*, p. 1012-1019.
- Knutson, D., and C. Braun, 2002, Diagnosis and management of acute bronchitis: *Am Fam Physician*, v. 65, p. 2039-44.
- Koenen, P., S. Heinzel, E. M. Carrington, L. Happo, W. S. Alexander, J.-G. Zhang, M. J. Herold, C. L. Scott, A. M. Lew, A. Strasser, and P. D. Hodgkin, 2013, Mutually exclusive regulation of T cell survival by IL-7R and antigen receptor-induced signals: *Nature Communications*, v. 4, p. 1735.
- Koenigsknecht-Talboo, J., and G. E. Landreth, 2005, Microglial phagocytosis induced by fibrillar beta-amyloid and IgGs are differentially regulated by proinflammatory cytokines.: *J Neurosci*, v. 25, p. 8240-9.
- Komiyama, Y., S. Nakae, T. Matsuki, A. Nambu, H. Ishigame, S. Kakuta, K. Sudo, and Y. Iwakura, 2006, IL-17 plays an important role in the development of experimental autoimmune encephalomyelitis: *J Immunol*, v. 177, p. 566-73.
- Kook, S. Y., H. S. Hong, M. Moon, C. M. Ha, S. Chang, and I. Mook-Jung, 2012, Abeta(1)-(4)(2)-RAGE interaction disrupts tight junctions of the blood-brain barrier via Ca(2)(+)-calcineurin signaling: *J Neurosci*, v. 32, p. 8845-54.
- Kort, J. J., K. Kawamura, L. Fugger, R. Weissert, and T. G. Forsthuber, 2006, Efficient presentation of myelin oligodendrocyte glycoprotein peptides but not protein by astrocytes from HLA-DR2 and HLA-DR4 transgenic mice: *J Neuroimmunol*, v. 173, p. 23-34.
- Kountouras, J., M. Boziki, E. Gavalas, C. Zavos, G. Deretzi, S. Chatzigeorgiou, P. Katsinelos, N. Grigoriadis, E. Giartza-Taxidou, and I. Venizelos, 2010, Five-year survival after *Helicobacter pylori* eradication in Alzheimer disease patients: *Cogn Behav Neurol*, v. 23, p. 199-204.
- Kountouras, J., M. Boziki, E. Gavalas, C. Zavos, G. Deretzi, N. Grigoriadis, M. Tsolaki, D. Chatzopoulos, P. Katsinelos, D. Tzilves, A. Zabouri, and I. Michailidou, 2009a,

- Increased cerebrospinal fluid *Helicobacter pylori* antibody in Alzheimer's disease: *Int J Neurosci*, v. 119, p. 765-77.
- Kountouras, J., M. Boziki, E. Gavalas, C. Zavos, N. Grigoriadis, G. Deretzi, D. Tzilves, P. Katsinelos, M. Tsolaki, D. Chatzopoulos, and I. Venizelos, 2009b, Eradication of *Helicobacter pylori* may be beneficial in the management of Alzheimer's disease: *J Neurol*, v. 256, p. 758-67.
- Kountouras, J., M. Tsolaki, E. Gavalas, M. Boziki, C. Zavos, P. Karatzoglou, D. Chatzopoulos, and I. Venizelos, 2006, Relationship between *Helicobacter pylori* infection and Alzheimer disease: *Neurology*, v. 66, p. 938-40.
- Kovaiou, R. D., D. Herndler-Brandstetter, and B. Grubeck-Loebenstien, 2007, Age-related changes in immunity: implications for vaccination in the elderly: *Expert Rev Mol Med*, v. 9, p. 1-17.
- Krabbe, G., A. Halle, V. Matyash, J. L. Rinnenthal, G. D. Eom, U. Bernhardt, K. R. Miller, S. Prokop, H. Kettenmann, and F. L. Heppner, 2013, Functional impairment of microglia coincides with Beta-amyloid deposition in mice with Alzheimer-like pathology: *PLoS One*, v. 8, p. e60921.
- Krstic, D., A. Madhusudan, J. Doehner, P. Vogel, T. Notter, C. Imhof, A. Manalastas, M. Hilfiker, S. Pfister, C. Schwerdel, C. Riether, U. Meyer, and I. Knuesel, 2012, Systemic immune challenges trigger and drive Alzheimer-like neuropathology in mice: *J Neuroinflammation*, v. 9, p. 151.
- Kuhn, P. H., H. Wang, B. Dislich, A. Colombo, U. Zeitschel, J. W. Ellwart, E. Kremmer, S. Rossner, and S. F. Lichtenthaler, 2010, ADAM10 is the physiologically relevant, constitutive alpha-secretase of the amyloid precursor protein in primary neurons: *Embo j*, v. 29, p. 3020-32.
- Kummer, M. P., and M. T. Heneka, 2014, Truncated and modified amyloid-beta species: *Alzheimers Res Ther*, v. 6, p. 28.
- Laan, M., Z. H. Cui, H. Hoshino, J. Lotvall, M. Sjostrand, D. C. Gruenert, B. E. Skoogh, and A. Linden, 1999, Neutrophil recruitment by human IL-17 via C-X-C chemokine release in the airways: *J Immunol*, v. 162, p. 2347-52.
- Lages, C. S., I. Suffia, P. A. Velilla, B. Huang, G. Warshaw, D. A. Hildeman, Y. Belkaid, and C. Chougnet, 2008, Functional Regulatory T Cells Accumulate in Aged Hosts and Promote Chronic Infectious Disease Reactivation1: *J Immunol*, v. 181, p. 1835-48.
- Lalor, S. J., L. S. Dungan, C. E. Sutton, S. A. Basdeo, J. M. Fletcher, and K. H. Mills, 2011, Caspase-1-processed cytokines IL-1beta and IL-18 promote IL-17 production by gammadelta and CD4 T cells that mediate autoimmunity: *J Immunol*, v. 186, p. 5738-48.
- Lamberti, Y. A., J. A. Hayes, M. L. Perez Vidakovics, E. T. Harvill, and M. E. Rodriguez, 2010, Intracellular Trafficking of *Bordetella pertussis* in Human Macrophages: *Infect Immun*, v. 78, p. 907-13.
- Lambracht-Washington, D., and R. N. Rosenberg, 2013, Anti-amyloid beta to tau - based immunization: Developments in immunotherapy for Alzheimer disease: *Immunotargets Ther*, v. 2013, p. 105-114.

- Landreth, G. E., and E. G. Reed-Geaghan, 2009, Toll-like receptors in Alzheimer's disease.: *Curr Top Microbiol Immunol*, v. 336, p. 137-53.
- Langrish, C. L., Y. Chen, W. M. Blumenschein, J. Mattson, B. Basham, J. D. Sedgwick, T. McClanahan, R. A. Kastelein, and D. J. Cua, 2005, IL-23 drives a pathogenic T cell population that induces autoimmune inflammation: *J Exp Med*, v. 201, p. 233-40.
- Lanzavecchia, A., and F. Sallusto, 2005, Understanding the generation and function of memory T cell subsets: *Curr Opin Immunol*, v. 17, p. 326-32.
- Laporte, V., G. Ait-Ghezala, C. H. Volmar, and M. Mullan, 2006, CD40 deficiency mitigates Alzheimer's disease pathology in transgenic mouse models, *J Neuroinflammation*, v. 3, p. 3.
- Larbi, A., G. Pawelec, J. M. Witkowski, H. M. Schipper, E. Derhovanessian, D. Goldeck, and T. Fulop, 2009, Dramatic shifts in circulating CD4 but not CD8 T cell subsets in mild Alzheimer's disease.: *J Alzheimers Dis*, v. 17, p. 91-103.
- Lee, J. F., Q. Zeng, H. Ozaki, L. Wang, A. R. Hand, T. Hla, E. Wang, and M. J. Lee, 2006, Dual roles of tight junction-associated protein, zonula occludens-1, in sphingosine 1-phosphate-mediated endothelial chemotaxis and barrier integrity: *J Biol Chem*, v. 281, p. 29190-200.
- Lee, J. W., Y. K. Lee, D. Y. Yuk, D. Y. Choi, S. B. Ban, K. W. Oh, and J. T. Hong, 2008, Neuroinflammation induced by lipopolysaccharide causes cognitive impairment through enhancement of beta-amyloid generation: *J Neuroinflammation*, v. 5, p. 37.
- Leech, S., J. Kirk, J. Plumb, and S. McQuaid, 2007, Persistent endothelial abnormalities and blood-brain barrier leak in primary and secondary progressive multiple sclerosis: *Neuropathol Appl Neurobiol*, v. 33, p. 86-98.
- Leef, M., K. L. Elkins, J. Barbic, and R. D. Shahin, 2000, Protective immunity to *Bordetella pertussis* requires both B cells and CD4(+) T cells for key functions other than specific antibody production: *J Exp Med*, v. 191, p. 1841-52.
- Leissring, M. A., W. Farris, A. Y. Chang, D. M. Walsh, X. Wu, X. Sun, M. P. Frosch, and D. J. Selkoe, 2003, Enhanced proteolysis of beta-amyloid in APP transgenic mice prevents plaque formation, secondary pathology, and premature death: *Neuron*, v. 40, p. 1087-93.
- Lewandowski, M., 1900, Zur Lehre von der Cerebrospinalflüssigkeit. [On the cerebrospinal fluid.], *Z. Klein Forsch*, p. 480-494.
- Li, M., D. S. Shang, W. D. Zhao, L. Tian, B. Li, W. G. Fang, L. Zhu, S. M. Man, and Y. H. Chen, 2009, Amyloid beta interaction with receptor for advanced glycation end products up-regulates brain endothelial CCR5 expression and promotes T cells crossing the blood-brain barrier.: *J Immunol*, v. 182, p. 5778-88.
- Liao, Y. F., B. J. Wang, H. T. Cheng, L. H. Kuo, and M. S. Wolfe, 2004, Tumor necrosis factor-alpha, interleukin-1beta, and interferon-gamma stimulate gamma-secretase-mediated cleavage of amyloid precursor protein through a JNK-dependent MAPK pathway: *J Biol Chem*, v. 279, p. 49523-32.

- Linhares, I., T. Raposo, A. Rodrigues, and A. Almeida, 2013, Frequency and antimicrobial resistance patterns of bacteria implicated in community urinary tract infections: a ten-year surveillance study (2000-2009): *BMC Infect Dis*, v. 13, p. 19.
- Linthicum, D. S., J. J. Munoz, and A. Blaskett, 1982, Acute experimental autoimmune encephalomyelitis in mice. I. Adjuvant action of *Bordetella pertussis* is due to vasoactive amine sensitization and increased vascular permeability of the central nervous system: *Cell Immunol*, v. 73, p. 299-310.
- Little, C. S., C. J. Hammond, A. MacIntyre, B. J. Balin, and D. M. Appelt, 2004, *Chlamydia pneumoniae* induces Alzheimer-like amyloid plaques in brains of BALB/c mice: *Neurobiol Aging*, v. 25, p. 419-29.
- Liu, C. C., T. Kanekiyo, H. Xu, and G. Bu, 2013, Apolipoprotein E and Alzheimer disease: risk, mechanisms, and therapy: *Nat Rev Neurol*, v. 9, p. 106-18.
- Liu, Y. J., D. W. Guo, L. Tian, D. S. Shang, W. D. Zhao, B. Li, W. G. Fang, L. Zhu, and Y. H. Chen, 2010, Peripheral T cells derived from Alzheimer's disease patients overexpress CXCR2 contributing to its transendothelial migration, which is microglial TNF-alpha-dependent.: *Neurobiol Aging*, v. 31, p. 175-88.
- Livengood, J. A., and R. D. Gilmore, 2006, Invasion of human neuronal and glial cells by an infectious strain of *Borrelia burgdorferi*: *Microbes Infect*, v. 8, p. 2832-40.
- Loeb, M. B., D. W. Molloy, M. Smieja, T. Standish, C. H. Goldsmith, J. Mahony, S. Smith, M. Borrie, E. Decoteau, W. Davidson, A. McDougall, J. Gnarpe, M. O'Donnell, and M. Chernesky, 2004, A randomized, controlled trial of doxycycline and rifampin for patients with Alzheimer's disease: *J Am Geriatr Soc*, v. 52, p. 381-7.
- London, A., M. Cohen, and M. Schwartz, 2013, Microglia and monocyte-derived macrophages: functionally distinct populations that act in concert in CNS plasticity and repair: *Front Cell Neurosci*, v. 7, p. 34.
- Lopes, C. T., D. M. de Paula, P. M. Cury, V. B. Valero-Lapchik, and V. Bueno, 2010, *Leishmania (Leishmania) amazonensis* infection in mice treated with FTY720: *Transplant Proc*, v. 42, p. 578-81.
- Lorenzl, S., D. S. Albers, N. Relkin, T. Ngyuen, S. L. Hilgenberg, J. Chirichigno, M. E. Cudkowicz, and M. F. Beal, 2003, Increased plasma levels of matrix metalloproteinase-9 in patients with Alzheimer's disease: *Neurochem Int*, v. 43, p. 191-6.
- Lue, L. F., R. Rydel, E. F. Brigham, L. B. Yang, H. Hampel, G. M. Murphy, Jr., L. Brachova, S. D. Yan, D. G. Walker, Y. Shen, and J. Rogers, 2001, Inflammatory repertoire of Alzheimer's disease and nondemented elderly microglia in vitro: *Glia*, v. 35, p. 72-9.
- Lurain, N. S., B. A. Hanson, J. Martinson, S. E. Leurgans, A. L. Landay, D. A. Bennett, and J. A. Schneider, 2013, Virological and immunological characteristics of human cytomegalovirus infection associated with Alzheimer disease: *J Infect Dis*, v. 208, p. 564-72.
- Lutz, W., W. Sanderson, and S. Scherbov, 1997, Doubling of world population unlikely: *Nature*, v. 387, p. 803-5.
- Lynch, J. R., W. Tang, H. Wang, M. P. Vitek, E. R. Bennett, P. M. Sullivan, D. S. Warner, and D. T. Laskowitz, 2003, APOE genotype and an ApoE-mimetic peptide modify

- the systemic and central nervous system inflammatory response: *J Biol Chem*, v. 278, p. 48529-33.
- Lynch, M. A., 2009, The multifaceted profile of activated microglia.: *Mol Neurobiol*, v. 40, p. 139-56.
- Lynch, M. A., 2014, The impact of neuroimmune changes on development of amyloid pathology; relevance to Alzheimer's disease: *Immunology*, v. 141, p. 292-301.
- Lyons, A., E. J. Downer, S. Crotty, Y. M. Nolan, K. H. Mills, and M. A. Lynch, 2007a, CD200 ligand receptor interaction modulates microglial activation in vivo and in vitro: a role for IL-4: *J Neurosci*, v. 27, p. 8309-13.
- Lyons, A., R. J. Griffin, C. E. Costelloe, R. M. Clarke, and M. A. Lynch, 2007b, IL-4 attenuates the neuroinflammation induced by amyloid-beta in vivo and in vitro: *J Neurochem*, v. 101, p. 771-81.
- Löppönen, M. K., R. E. Isoaho, I. J. Räihä, T. J. Vahlberg, S. M. Loikas, T. I. Takala, H. Puolijoki, K. M. Irjala, and S. L. Kivelä, 2004, Undiagnosed diseases in patients with dementia--a potential target group for intervention: *Dement Geriatr Cogn Disord*, v. 18, p. 321-9.
- Ma, X., S. L. Reynolds, B. J. Baker, X. Li, E. N. Benveniste, and H. Qin, 2010, IL-17 enhancement of the IL-6 signaling cascade in astrocytes: *J Immunol*, v. 184, p. 4898-906.
- MacDonald, A. B., 2007, Alzheimer's neuroborreliosis with trans-synaptic spread of infection and neurofibrillary tangles derived from intraneuronal spirochetes: *Med Hypotheses*, v. 68, p. 822-5.
- Mackall, C. L., T. A. Fleisher, M. R. Brown, M. P. Andrich, C. C. Chen, I. M. Feuerstein, M. E. Horowitz, I. T. Magrath, A. T. Shad, and S. M. Steinberg, 1995, Age, thymopoiesis, and CD4+ T-lymphocyte regeneration after intensive chemotherapy: *N Engl J Med*, v. 332, p. 143-9.
- Mackall, C. L., and R. E. Gress, 1997, Thymic aging and T-cell regeneration: *Immunol Rev*, v. 160, p. 91-102.
- Mackall, C. L., F. T. Hakim, and R. E. Gress, 1997, T-cell regeneration: all repertoires are not created equal: *Immunol Today*, v. 18, p. 245-51.
- MacLulich, A. M., A. Beaglehole, R. J. Hall, and D. J. Meagher, 2009, Delirium and long-term cognitive impairment: *Int Rev Psychiatry*, v. 21, p. 30-42.
- Maheshwari, P., and G. D. Eslick, 2014, Bacterial Infection and Alzheimer's Disease: A Meta-Analysis: *J Alzheimers Dis*, v. 43, p. 957-66.
- Mahon, B. P., and K. H. Mills, 1999, Interferon-gamma mediated immune effector mechanisms against *Bordetella pertussis*: *Immunol Lett*, v. 68, p. 213-7.
- Mahon, B. P., B. J. Sheahan, F. Griffin, G. Murphy, and K. H. Mills, 1997, Atypical disease after *Bordetella pertussis* respiratory infection of mice with targeted disruptions of interferon-gamma receptor or immunoglobulin mu chain genes: *J Exp Med*, v. 186, p. 1843-51.

- Majumdar, A., H. Chung, G. Dolios, R. Wang, N. Asamoah, P. Lobel, and F. R. Maxfield, 2008, Degradation of fibrillar forms of Alzheimer's amyloid beta-peptide by macrophages: *Neurobiol Aging*, v. 29, p. 707-15.
- Malaguarnera, M., R. Bella, G. Alagona, R. Ferri, A. Carnemolla, and G. Pennisi, 2004, *Helicobacter pylori* and Alzheimer's disease: a possible link: *Eur J Intern Med*, v. 15, p. 381-386.
- Malchinkhuu, E., K. Sato, T. Muraki, K. Ishikawa, A. Kuwabara, and F. Okajima, 2003, Assessment of the role of sphingosine 1-phosphate and its receptors in high-density lipoprotein-induced stimulation of astroglial cell function: *Biochem J*, v. 370, p. 817-27.
- Man, S. M., Y. R. Ma, D. S. Shang, W. D. Zhao, B. Li, D. W. Guo, W. G. Fang, L. Zhu, and Y. H. Chen, 2007, Peripheral T cells overexpress MIP-1alpha to enhance its transendothelial migration in Alzheimer's disease.: *Neurobiol Aging*, v. 28, p. 485-96.
- Mandala, S., R. Hajdu, J. Bergstrom, E. Quackenbush, J. Xie, J. Milligan, R. Thornton, G. J. Shei, D. Card, C. Keohane, M. Rosenbach, J. Hale, C. L. Lynch, K. Rupprecht, W. Parsons, and H. Rosen, 2002, Alteration of lymphocyte trafficking by sphingosine-1-phosphate receptor agonists: *Science*, v. 296, p. 346-9.
- Mandell, L. A., R. G. Wunderink, A. Anzueto, J. G. Bartlett, G. D. Campbell, N. C. Dean, S. F. Dowell, T. M. File, Jr., D. M. Musher, M. S. Niederman, A. Torres, and C. G. Whitney, 2007, Infectious Diseases Society of America/American Thoracic Society consensus guidelines on the management of community-acquired pneumonia in adults: *Clin Infect Dis*, v. 44 Suppl 2, p. S27-72.
- Mandrekar-Colucci, S., J. C. Karlo, and G. E. Landreth, 2012, Mechanisms underlying the rapid peroxisome proliferator-activated receptor-gamma-mediated amyloid clearance and reversal of cognitive deficits in a murine model of Alzheimer's disease: *J Neurosci*, v. 32, p. 10117-28.
- Mangan, P. R., L. E. Harrington, D. B. O'Quinn, W. S. Helms, D. C. Bullard, C. O. Elson, R. D. Hatton, S. M. Wahl, T. R. Schoeb, and C. T. Weaver, 2006, Transforming growth factor-beta induces development of the T(H)17 lineage: *Nature*, v. 441, p. 231-4.
- Mantovani, A., S. K. Biswas, M. R. Galdiero, A. Sica, and M. Locati, 2013, Macrophage plasticity and polarization in tissue repair and remodelling: *J Pathol*, v. 229, p. 176-85.
- Marco, S., and S. D. Skaper, 2006, Amyloid beta-peptide1-42 alters tight junction protein distribution and expression in brain microvessel endothelial cells: *Neurosci Lett*, v. 401, p. 219-24.
- Marrack, P., and J. Kappler, 2004, Control of T cell viability: *Annu Rev Immunol*, v. 22, p. 765-87.
- Mars, L. T., A. S. Gautron, J. Novak, L. Beaudoin, J. Diana, R. S. Liblau, and A. Lehen, 2008, Invariant NKT cells regulate experimental autoimmune encephalomyelitis and infiltrate the central nervous system in a CD1d-independent manner: *J Immunol*, v. 181, p. 2321-9.

- Martinez, F. O., and S. Gordon, 2014, The M1 and M2 paradigm of macrophage activation: time for reassessment, *F1000Prime Rep*, v. 6.
- Mathiisen, T. M., K. P. Lehre, N. C. Danbolt, and O. P. Ottersen, 2010, The perivascular astroglial sheath provides a complete covering of the brain microvessels: an electron microscopic 3D reconstruction: *Glia*, v. 58, p. 1094-103.
- Matloubian, M., C. G. Lo, G. Cinamon, M. J. Lesneski, Y. Xu, V. Brinkmann, M. L. Allende, R. L. Proia, and J. G. Cyster, 2004, Lymphocyte egress from thymus and peripheral lymphoid organs is dependent on S1P receptor 1: *Nature*, v. 427, p. 355-60.
- Mattson, M. P., 2004, Pathways towards and away from Alzheimer's disease: *Nature*, v. 430, p. 631-9.
- Maurer, K., S. Volk, and H. Gerbaldo, 1997, Auguste D and Alzheimer's disease: *Lancet*, v. 349, p. 1546-9.
- Mayo, L., F. J. Quintana, and H. L. Weiner, 2012, The innate immune system in demyelinating disease: *Immunol Rev*, v. 248, p. 170-87.
- McCloskey, R. M., 2004, Caring for patients with dementia in an acute care environment: *Geriatr Nurs*, v. 25, p. 139-44.
- McGeer, P. L., H. Akiyama, S. Itagaki, and E. G. McGeer, 1989, Immune system response in Alzheimer's disease: *Can J Neurol Sci*, v. 16, p. 516-27.
- McGeer, P. L., S. Itagaki, H. Tago, and E. G. McGeer, 1987, Reactive microglia in patients with senile dementia of the Alzheimer type are positive for the histocompatibility glycoprotein HLA-DR.: *Neurosci Lett*, v. 79, p. 195-200.
- McGuinness, C. B., J. Hill, E. Fonseca, G. Hess, W. Hitchcock, and G. Krishnarajah, 2013, The disease burden of pertussis in adults 50 years old and older in the United States: a retrospective study: *BMC Infect Dis*, v. 13, p. 32.
- McGuirk, P., B. P. Mahon, F. Griffin, and K. H. Mills, 1998, Compartmentalization of T cell responses following respiratory infection with *Bordetella pertussis*: hyporesponsiveness of lung T cells is associated with modulated expression of the co-stimulatory molecule CD28: *Eur J Immunol*, v. 28, p. 153-63.
- McGuirk, P., C. McCann, and K. H. Mills, 2002, Pathogen-specific T regulatory 1 cells induced in the respiratory tract by a bacterial molecule that stimulates interleukin 10 production by dendritic cells: a novel strategy for evasion of protective T helper type 1 responses by *Bordetella pertussis*: *J Exp Med*, v. 195, p. 221-31.
- McGuirk, P., and K. H. Mills, 2000, Direct anti-inflammatory effect of a bacterial virulence factor: IL-10-dependent suppression of IL-12 production by filamentous hemagglutinin from *Bordetella pertussis*: *Eur J Immunol*, v. 30, p. 415-22.
- McKinley, L., J. F. Alcorn, A. Peterson, R. B. Dupont, S. Kapadia, A. Logar, A. Henry, C. G. Irvin, J. D. Piganelli, A. Ray, and J. K. Kolls, 2008, TH17 cells mediate steroid-resistant airway inflammation and airway hyperresponsiveness in mice: *J Immunol*, v. 181, p. 4089-97.

- McQuillan, K., M. A. Lynch, and K. H. Mills, 2010, Activation of mixed glia by Abeta-specific Th1 and Th17 cells and its regulation by Th2 cells.: *Brain Behav Immun*, v. 24, p. 598-607.
- Medawar, P. B., 1948, Immunity to Homologous Grafted Skin. III. The Fate of Skin Homographs Transplanted to the Brain, to Subcutaneous Tissue, and to the Anterior Chamber of the Eye: *Br J Exp Pathol*, v. 29, p. 58-69.
- Mehling, M., V. Brinkmann, J. Antel, A. Bar-Or, N. Goebels, C. Vedrine, C. Kristofic, J. Kuhle, R. L. Lindberg, and L. Kappos, 2008, FTY720 therapy exerts differential effects on T cell subsets in multiple sclerosis: *Neurology*, v. 71, p. 1261-7.
- Merlini, M., E. P. Meyer, A. Ulmann-Schuler, and R. M. Nitsch, 2011, Vascular beta-amyloid and early astrocyte alterations impair cerebrovascular function and cerebral metabolism in transgenic arcAbeta mice: *Acta Neuropathol*, v. 122, p. 293-311.
- Michaud, J. P., M. Hallé, A. Lampron, P. Thériault, P. Préfontaine, M. Filali, P. Tribout-Jover, A. M. Lanteigne, R. Jodoin, C. Cluff, V. Brichard, R. Palmantier, A. Pilorget, D. Larocque, and S. Rivest, 2013, Toll-like receptor 4 stimulation with the detoxified ligand monophosphoryl lipid A improves Alzheimer's disease-related pathology: *Proc Natl Acad Sci U S A*, v. 110, p. 1941-6.
- Michelucci, A., T. Heurtaux, L. Grandbarbe, E. Morga, and P. Heuschling, 2009, Characterization of the microglial phenotype under specific pro-inflammatory and anti-inflammatory conditions: Effects of oligomeric and fibrillar amyloid-beta: *J Neuroimmunol*, v. 210, p. 3-12.
- Miklossy, J., 1993, Alzheimer's disease--a spirochetosis?: *Neuroreport*, v. 4, p. 841-8.
- Miklossy, J., 2011, Alzheimer's disease - a neurospirochetosis. Analysis of the evidence following Koch's and Hill's criteria: *J Neuroinflammation*, v. 8, p. 90.
- Miklossy, J., S. Kasas, R. C. Janzer, F. Ardizzoni, and H. Van der Loos, 1994, Further ultrastructural evidence that spirochaetes may play a role in the aetiology of Alzheimer's disease: *Neuroreport*, v. 5, p. 1201-4.
- Miklossy, J., K. Khalili, L. Gern, R. L. Ericson, P. Darekar, L. Bolle, J. Hurlimann, and B. J. Paster, 2004, *Borrelia burgdorferi* persists in the brain in chronic lyme neuroborreliosis and may be associated with Alzheimer disease: *J Alzheimers Dis*, v. 6, p. 639-49; discussion 673-81.
- Miklossy, J., A. Kis, A. Radenovic, L. Miller, L. Forro, R. Martins, K. Reiss, N. Darbinian, P. Darekar, L. Mihaly, and K. Khalili, 2006, Beta-amyloid deposition and Alzheimer's type changes induced by *Borrelia spirochetes*: *Neurobiol Aging*, v. 27, p. 228-36.
- Miljkovic, D., M. Momcilovic, I. Stojanovic, S. Stosic-Grujicic, Z. Ramic, and M. Mostarica-Stojkovic, 2007, Astrocytes stimulate interleukin-17 and interferon-gamma production in vitro: *J Neurosci Res*, v. 85, p. 3598-606.
- Miller, K. R., and W. J. Streit, 2007, The effects of aging, injury and disease on microglial function: a case for cellular senescence: *Neuron Glia Biol*, v. 3, p. 245-53.
- Mills, K. H., 2004, Regulatory T cells: friend or foe in immunity to infection?: *Nat Rev Immunol*, v. 4, p. 841-55.

- Mills, K. H., 2008, Induction, function and regulation of IL-17-producing T cells.: *Eur J Immunol*, v. 38, p. 2636-49.
- Mills, K. H., A. Barnard, J. Watkins, and K. Redhead, 1993, Cell-mediated immunity to *Bordetella pertussis*: role of Th1 cells in bacterial clearance in a murine respiratory infection model: *Infect Immun*, v. 61, p. 399-410.
- Mills, K. H., P. J. Ross, A. C. Allen, and M. M. Wilk, 2014, Do we need a new vaccine to control the re-emergence of pertussis?: *Trends Microbiol*, v. 22, p. 49-52.
- Minagar, A., and J. S. Alexander, 2003, Blood-brain barrier disruption in multiple sclerosis: *Mult Scler*, v. 9, p. 540-9.
- Minogue, A. M., R. S. Jones, R. J. Kelly, C. L. McDonald, T. J. Connor, and M. A. Lynch, 2014, Age-associated dysregulation of microglial activation is coupled with enhanced blood-brain barrier permeability and pathology in APP/PS1 mice: *Neurobiol Aging*, v. 35, p. 1442-52.
- Miron, V. E., A. Schubart, and J. P. Antel, 2008, Central nervous system-directed effects of FTY720 (fingolimod): *J Neurol Sci*, v. 274, p. 13-7.
- Mirra, S. S., J. R. Murrell, M. Gearing, M. G. Spillantini, M. Goedert, R. A. Crowther, A. I. Levey, R. Jones, J. Green, J. M. Shoffner, B. H. Wainer, M. L. Schmidt, J. Q. Trojanowski, and B. Ghetti, 1999, Tau pathology in a family with dementia and a P301L mutation in tau: *J Neuropathol Exp Neurol*, v. 58, p. 335-45.
- Miyamoto, M., O. Prause, M. Sjostrand, M. Laan, J. Lotvall, and A. Linden, 2003, Endogenous IL-17 as a mediator of neutrophil recruitment caused by endotoxin exposure in mouse airways: *J Immunol*, v. 170, p. 4665-72.
- Mizugishi, K., T. Yamashita, A. Olivera, G. F. Miller, S. Spiegel, and R. L. Proia, 2005, Essential role for sphingosine kinases in neural and vascular development: *Mol Cell Biol*, v. 25, p. 11113-21.
- Mizwicki, M. T., D. Menegaz, J. Zhang, A. Barrientos-Durán, S. Tse, J. R. Cashman, P. R. Griffin, and M. Fiala, 2012, Genomic and nongenomic signaling induced by 1 α ,25(OH) $_2$ -vitamin D $_3$ promotes the recovery of amyloid- β phagocytosis by Alzheimer's disease macrophages: *J Alzheimers Dis*, v. 29, p. 51-62.
- Monson, N. L., S. J. Ireland, A. J. Ligocki, D. Chen, W. H. Rounds, M. Li, R. M. Huebinger, C. Munro Cullum, B. M. Greenberg, A. M. Stowe, and R. Zhang, 2014, Elevated CNS inflammation in patients with preclinical Alzheimer's disease: *J Cereb Blood Flow Metab*, v. 34, p. 30-3.
- Monsonogo, A., V. Zota, A. Karni, J. I. Krieger, A. Bar-Or, G. Bitan, A. E. Budson, R. Sperling, D. J. Selkoe, and H. L. Weiner, 2003, Increased T cell reactivity to amyloid beta protein in older humans and patients with Alzheimer disease: *J Clin Invest*, v. 112, p. 415-22.
- Moon, H., J. Chon, J. Joo, D. Kim, J. In, H. Lee, J. Park, and J. Choi, 2013, FTY720 preserved islet β -cell mass by inhibiting apoptosis and increasing survival of β -cells in db/db mice: *Diabetes Metab Res Rev*, v. 29, p. 19-24.
- Morita, K., H. Sasaki, M. Furuse, and S. Tsukita, 1999, Endothelial claudin: claudin-5/TMVCF constitutes tight junction strands in endothelial cells: *J Cell Biol*, v. 147, p. 185-94.

- Morris, M. A., D. R. Gibb, F. Picard, V. Brinkmann, M. Straume, and K. Ley, 2005, Transient T cell accumulation in lymph nodes and sustained lymphopenia in mice treated with FTY720: *Eur J Immunol*, v. 35, p. 3570-80.
- Muhammad, S., E. Haasbach, M. Kotchourko, A. Strigli, A. Krenz, D. A. Ridder, A. B. Vogel, H. H. Marti, Y. Al-Abed, O. Planz, and M. Schwaninger, 2011, Influenza virus infection aggravates stroke outcome: *Stroke*, v. 42, p. 783-91.
- Mullan, M., F. Crawford, K. Axelman, H. Houlden, L. Lilius, B. Winblad, and L. Lannfelt, 1992, A pathogenic mutation for probable Alzheimer's disease in the APP gene at the N-terminus of beta-amyloid: *Nat Genet*, v. 1, p. 345-7.
- Muller, H., S. Hofer, N. Kaneider, H. Neuwirt, B. Mosheimer, G. Mayer, G. Konwalinka, C. Heufler, and M. Tiefenthaler, 2005, The immunomodulator FTY720 interferes with effector functions of human monocyte-derived dendritic cells: *Eur J Immunol*, v. 35, p. 533-45.
- Murooka, T. T., R. Rahbar, L. C. Platanias, and E. N. Fish, 2008, CCL5-mediated T-cell chemotaxis involves the initiation of mRNA translation through mTOR/4E-BP1: *Blood*, v. 111, p. 4892-901.
- Murphy, A. C., S. J. Lalor, M. A. Lynch, and K. H. Mills, 2010, Infiltration of Th1 and Th17 cells and activation of microglia in the CNS during the course of experimental autoimmune encephalomyelitis: *Brain Behav Immun*, v. 24, p. 641-51.
- Murphy, C. T., L. J. Hall, G. Hurley, A. Quinlan, J. MacSharry, F. Shanahan, K. Nally, and S. Melgar, 2012, The sphingosine-1-phosphate analogue FTY720 impairs mucosal immunity and clearance of the enteric pathogen *Citrobacter rodentium*: *Infect Immun*, v. 80, p. 2712-23.
- Murphy, J. B., and E. Sturm, 1923, CONDITIONS DETERMINING THE TRANSPLANTABILITY OF TISSUES IN THE BRAIN: *J Exp Med*, v. 38, p. 183-97.
- Nacer, A., A. Movila, K. Baer, S. A. Mikolajczak, S. H. Kappe, and U. Frevert, 2012, Neuroimmunological blood brain barrier opening in experimental cerebral malaria: *PLoS Pathog*, v. 8, p. e1002982.
- Nagele, R. G., J. Wegiel, V. Venkataraman, H. Imaki, and K. C. Wang, 2004, Contribution of glial cells to the development of amyloid plaques in Alzheimer's disease: *Neurobiol Aging*, v. 25, p. 663-74.
- Nair, A., T. J. Frederick, and S. D. Miller, 2008, Astrocytes in multiple sclerosis: a product of their environment: *Cell Mol Life Sci*, v. 65, p. 2702-20.
- Nakagawa, S., M. A. Deli, H. Kawaguchi, T. Shimizudani, T. Shimono, A. Kittel, K. Tanaka, and M. Niwa, 2009, A new blood-brain barrier model using primary rat brain endothelial cells, pericytes and astrocytes, *Neurochem Int*, v. 54: England, p. 253-63.
- Nakamura, S., N. Murayama, T. Noshita, H. Annoura, and T. Ohno, 2001, Progressive brain dysfunction following intracerebroventricular infusion of beta(1-42)-amyloid peptide: *Brain Res*, v. 912, p. 128-36.
- Natalwala, A., R. Potluri, H. Uppal, and R. Heun, 2008, Reasons for hospital admissions in dementia patients in Birmingham, UK, during 2002-2007: *Dement Geriatr Cogn Disord*, v. 26, p. 499-505.

- Natarajan, V., S. M. Dudek, J. R. Jacobson, L. Moreno-Vinasco, L. S. Huang, T. Abassi, B. Mathew, Y. Zhao, L. Wang, R. Bittman, R. Weichselbaum, E. Berdyshev, and J. G. Garcia, 2013, Sphingosine-1-phosphate, FTY720, and sphingosine-1-phosphate receptors in the pathobiology of acute lung injury: *Am J Respir Cell Mol Biol*, v. 49, p. 6-17.
- Nave, K. A., 2010, Myelination and support of axonal integrity by glia: *Nature*, v. 468, p. 244-52.
- Naylor, K., G. Li, A. N. Vallejo, W. W. Lee, K. Koetz, E. Bryl, J. Witkowski, J. Fulbright, C. M. Weyand, and J. J. Goronzy, 2005, The influence of age on T cell generation and TCR diversity: *J Immunol*, v. 174, p. 7446-52.
- Nguyen, V. T., and E. N. Benveniste, 2002, Critical role of tumor necrosis factor-alpha and NF-kappa B in interferon-gamma -induced CD40 expression in microglia/macrophages: *J Biol Chem*, v. 277, p. 13796-803.
- Nicoll, J. A., M. Yamada, J. Frackowiak, B. Mazur-Kolecka, and R. O. Weller, 2004, Cerebral amyloid angiopathy plays a direct role in the pathogenesis of Alzheimer's disease. Pro-CAA position statement: *Neurobiol Aging*, v. 25, p. 589-97; discussion 603-4.
- Nikcevic, K. M., K. B. Gordon, L. Tan, S. D. Hurst, J. F. Kroepfl, M. Gardinier, T. A. Barrett, and S. D. Miller, 1997, IFN-gamma-activated primary murine astrocytes express B7 costimulatory molecules and prime naive antigen-specific T cells: *J Immunol*, v. 158, p. 614-21.
- Nimmerjahn, A., F. Kirchhoff, and F. Helmchen, 2005, Resting microglial cells are highly dynamic surveillants of brain parenchyma in vivo: *Science*, v. 308, p. 1314-8.
- Nitta, T., M. Hata, S. Gotoh, Y. Seo, H. Sasaki, N. Hashimoto, M. Furuse, and S. Tsukita, 2003, Size-selective loosening of the blood-brain barrier in claudin-5-deficient mice: *J Cell Biol*, v. 161, p. 653-60.
- Ntranos, A., O. Hall, D. P. Robinson, I. V. Grishkan, J. T. Schott, D. M. Tosi, S. L. Klein, P. A. Calabresi, and A. R. Gocke, 2014, FTY720 impairs CD8 T-cell function independently of the sphingosine-1-phosphate pathway: *J Neuroimmunol*, v. 270, p. 13-21.
- Nunan, J., and D. H. Small, 2000, Regulation of APP cleavage by alpha-, beta- and gamma-secretases: *FEBS Lett*, v. 483, p. 6-10.
- O'Connor, R. A., C. T. Prendergast, C. A. Sabatos, C. W. Lau, M. D. Leech, D. C. Wraith, and S. M. Anderton, 2008, Cutting edge: Th1 cells facilitate the entry of Th17 cells to the central nervous system during experimental autoimmune encephalomyelitis: *J Immunol*, v. 181, p. 3750-4.
- Oddo, S., A. Caccamo, J. D. Shepherd, M. P. Murphy, T. E. Golde, R. Kaye, R. Metherate, M. P. Mattson, Y. Akbari, and F. M. LaFerla, 2003, Triple-transgenic model of Alzheimer's disease with plaques and tangles: intracellular Abeta and synaptic dysfunction: *Neuron*, v. 39, p. 409-21.
- Ojala, J., I. Alafuzoff, S. K. Herukka, T. van Groen, H. Tanila, and T. Pirttilä, 2009, Expression of interleukin-18 is increased in the brains of Alzheimer's disease patients.: *Neurobiol Aging*, v. 30, p. 198-209.

- Okello, A., P. Edison, H. A. Archer, F. E. Turkheimer, J. Kennedy, R. Bullock, Z. Walker, A. Kennedy, N. Fox, M. Rossor, and D. J. Brooks, 2009, Microglial activation and amyloid deposition in mild cognitive impairment: a PET study: *Neurology*, v. 72, p. 56-62.
- Olkhanud, P. B., M. Mughal, K. Ayukawa, E. Malchinkhuu, M. Bodogai, N. Feldman, S. Rothman, J. H. Lee, S. Chigurupati, E. Okun, K. Nagashima, M. P. Mattson, and A. Biragyn, 2012, DNA immunization with HBsAg-based particles expressing a B cell epitope of amyloid β -peptide attenuates disease progression and prolongs survival in a mouse model of Alzheimer's disease: *Vaccine*, v. 30, p. 1650-8.
- Olson, J. K., A. M. Girvin, and S. D. Miller, 2001, Direct activation of innate and antigen-presenting functions of microglia following infection with Theiler's virus: *J Virol*, v. 75, p. 9780-9.
- Olson, J. K., and S. D. Miller, 2004, Microglia initiate central nervous system innate and adaptive immune responses through multiple TLRs: *J Immunol*, v. 173, p. 3916-24.
- Ousman, S. S., and P. Kubes, 2012, Immune surveillance in the central nervous system, *Nat Neurosci*, v. 15: United States, p. 1096-101.
- Owens, T., I. Bechmann, and B. Engelhardt, 2008, Perivascular spaces and the two steps to neuroinflammation: *J Neuropathol Exp Neurol*, v. 67, p. 1113-21.
- Paddock, C. D., G. N. Sanden, J. D. Cherry, A. A. Gal, C. Langston, K. M. Tatti, K. H. Wu, C. S. Goldsmith, P. W. Greer, J. L. Montague, M. T. Eliason, R. C. Holman, J. Guarner, W. J. Shieh, and S. R. Zaki, 2008, Pathology and pathogenesis of fatal *Bordetella pertussis* infection in infants: *Clin Infect Dis*, v. 47, p. 328-38.
- Pan, X. D., Y. G. Zhu, N. Lin, J. Zhang, Q. Y. Ye, H. P. Huang, and X. C. Chen, 2011, Microglial phagocytosis induced by fibrillar beta-amyloid is attenuated by oligomeric beta-amyloid: implications for Alzheimer's disease: *Mol Neurodegener*, v. 6, p. 45.
- Panek, R. B., H. Moses, J. P. Ting, and E. N. Benveniste, 1992, Tumor necrosis factor alpha response elements in the HLA-DRA promoter: identification of a tumor necrosis factor alpha-induced DNA-protein complex in astrocytes: *Proc Natl Acad Sci U S A*, v. 89, p. 11518-22.
- Panossian, L. A., V. R. Porter, H. F. Valenzuela, X. Zhu, E. Reback, D. Masterman, J. L. Cummings, and R. B. Effros, 2003, Telomere shortening in T cells correlates with Alzheimer's disease status: *Neurobiol Aging*, v. 24, p. 77-84.
- Parachikova, A., M. G. Agadjanyan, D. H. Cribbs, M. Blurton-Jones, V. Perreau, J. Rogers, T. G. Beach, and C. W. Cotman, 2007, Inflammatory changes parallel the early stages of Alzheimer disease: *Neurobiol Aging*, v. 28, p. 1821-33.
- Paul, J., S. Strickland, and J. P. Melchor, 2007, Fibrin deposition accelerates neurovascular damage and neuroinflammation in mouse models of Alzheimer's disease: *J Exp Med*, v. 204, p. 1999-2008.
- Paul, W. E., and J. Zhu, 2010, How are TH2-type immune responses initiated and amplified?: *Nat Rev Immunol*, v. 10, p. 225-35.
- Pawelec, G., A. Akbar, C. Caruso, R. Effros, B. Grubeck-Loebenstein, and A. Wikby, 2004, Is immunosenescence infectious?: *Trends Immunol*, v. 25, p. 406-10.

- Pawelec, G., Y. Barnett, R. Forsey, D. Frasca, A. Globerson, J. McLeod, C. Caruso, C. Franceschi, T. Fülöp, S. Gupta, E. Mariani, E. Mocchegiani, and R. Solana, 2002, T cells and aging, January 2002 update: *Front Biosci*, v. 7, p. d1056-183.
- Pellicano, M., M. Bulati, S. Buffa, M. Barbagallo, A. Di Prima, G. Misiano, P. Picone, M. Di Carlo, D. Nuzzo, G. Candore, S. Vasto, D. Lio, C. Caruso, and G. Colonna-Romano, 2010, Systemic immune responses in Alzheimer's disease: in vitro mononuclear cell activation and cytokine production: *J Alzheimers Dis*, v. 21, p. 181-92.
- Pellicanò, M., A. Larbi, D. Goldeck, G. Colonna-Romano, S. Buffa, M. Bulati, G. Rubino, F. Lemolo, G. Candore, C. Caruso, E. Derhovanessian, and G. Pawelec, 2012, Immune profiling of Alzheimer patients: *J Neuroimmunol*, v. 242, p. 52-9.
- Penaranda, C., Q. Tang, N. H. Ruddle, and J. A. Bluestone, 2010, Prevention of diabetes by FTY720-mediated stabilization of peri-islet tertiary lymphoid organs: *Diabetes*, v. 59, p. 1461-8.
- Peng, X., P. M. Hassoun, S. Sammani, B. J. McVerry, M. J. Burne, H. Rabb, D. Pearse, R. M. Tuder, and J. G. Garcia, 2004, Protective effects of sphingosine 1-phosphate in murine endotoxin-induced inflammatory lung injury: *Am J Respir Crit Care Med*, v. 169, p. 1245-51.
- Perez-Tur, J., S. Froelich, G. Prihar, R. Crook, M. Baker, K. Duff, M. Wragg, F. Busfield, C. Lendon, and R. F. Clark, 1995, A mutation in Alzheimer's disease destroying a splice acceptor site in the presenilin-1 gene: *Neuroreport*, v. 7, p. 297-301.
- Perlmutter, L. S., S. A. Scott, E. Barron, and H. C. Chui, 1992, MHC class II-positive microglia in human brain: association with Alzheimer lesions: *J Neurosci Res*, v. 33, p. 549-58.
- Perrin, R. J., A. M. Fagan, and D. M. Holtzman, 2009, Multimodal techniques for diagnosis and prognosis of Alzheimer's disease: *Nature*, v. 461, p. 916-22.
- Perry, V. H., C. Cunningham, and C. Holmes, 2007, Systemic infections and inflammation affect chronic neurodegeneration.: *Nat Rev Immunol*, v. 7, p. 161-7.
- Pfeifer, M., S. Boncristiano, L. Bondolfi, A. Stalder, T. Deller, M. Staufenbiel, P. M. Mathews, and M. Jucker, 2002, Cerebral hemorrhage after passive anti-Abeta immunotherapy: *Science*, v. 298, p. 1379.
- Piacentini, R., L. Civitelli, C. Ripoli, M. E. Marcocci, G. De Chiara, E. Garaci, G. B. Azzena, A. T. Palamara, and C. Grassi, 2011, HSV-1 promotes Ca²⁺-mediated APP phosphorylation and Aβ accumulation in rat cortical neurons: *Neurobiol Aging*, v. 32, p. 2323.e13-26.
- Pirttila, T., S. Mattinen, and H. Frey, 1992, The decrease of CD8-positive lymphocytes in Alzheimer's disease: *J Neurol Sci*, v. 107, p. 160-5.
- Plumb, J., S. McQuaid, M. Mirakhur, and J. Kirk, 2002, Abnormal endothelial tight junctions in active lesions and normal-appearing white matter in multiple sclerosis: *Brain Pathol*, v. 12, p. 154-69.
- Poole, S., S. K. Singhrao, L. Kesavalu, M. A. Curtis, and S. Crean, 2013, Determining the presence of periodontopathic virulence factors in short-term postmortem Alzheimer's disease brain tissue: *J Alzheimers Dis*, v. 36, p. 665-77.

- Prajeeth, C. K., K. Lohr, S. Floess, J. Zimmermann, R. Ulrich, V. Gudi, A. Beineke, W. Baumgartner, M. Müller, J. Huehn, and M. Stangel, 2014, Effector molecules released by Th1 but not Th17 cells drive an M1 response in microglia: *Brain Behav Immun*, v. 37, p. 248-59.
- Prince, M., E. Albanese, M. Guerchet, and M. Prina, 2014, *World Alzheimer Report 2014: Dementia and Risk Reduction: An Analysis of Protective and Modifiable Factors*, Alzheimer's Disease International.
- Pébay, A., M. Toutant, J. Prémont, C. F. Calvo, L. Venance, J. Cordier, J. Glowinski, and M. Tencé, 2001, Sphingosine-1-phosphate induces proliferation of astrocytes: regulation by intracellular signalling cascades: *Eur J Neurosci*, v. 13, p. 2067-76.
- Qin, L., X. Wu, M. L. Block, Y. Liu, G. R. Breese, J. S. Hong, D. J. Knapp, and F. T. Crews, 2007, Systemic LPS causes chronic neuroinflammation and progressive neurodegeneration: *Glia*, v. 55, p. 453-62.
- Radjavi, A., I. Smirnov, and J. Kipnis, 2014, Brain antigen-reactive CD4⁺ T cells are sufficient to support learning behavior in mice with limited T cell repertoire: *Brain Behav Immun*, v. 35, p. 58-63.
- Rahkonen, T., U. Eloniemi-Sulkava, P. Halonen, A. Verkkoniemi, L. Niinistö, I. L. Notkola, and R. Sulkava, 2001, Delirium in the non-demented oldest old in the general population: risk factors and prognosis: *Int J Geriatr Psychiatry*, v. 16, p. 415-21.
- Rahkonen, T., R. Luukkainen-Markkula, S. Paanila, J. Sivenius, and R. Sulkava, 2000, Delirium episode as a sign of undetected dementia among community dwelling elderly subjects: a 2 year follow up study: *J Neurol Neurosurg Psychiatry*, v. 69, p. 519-21.
- Rao, J. S., S. I. Rapoport, and H. W. Kim, 2011, Altered neuroinflammatory, arachidonic acid cascade and synaptic markers in postmortem Alzheimer's disease brain, *Transl Psychiatry*, v. 1, p. e31.
- Reale, M., C. Iarlori, C. Feliciani, and D. Gambi, 2008, Peripheral chemokine receptors, their ligands, cytokines and Alzheimer's disease: *J Alzheimers Dis*, v. 14, p. 147-59.
- Reboldi, A., C. Coisne, D. Baumjohann, F. Benvenuto, D. Bottinelli, S. Lira, A. Uccelli, A. Lanzavecchia, B. Engelhardt, and F. Sallusto, 2009, C-C chemokine receptor 6-regulated entry of TH-17 cells into the CNS through the choroid plexus is required for the initiation of EAE: *Nat Immunol*, v. 10, p. 514-23.
- Redhead, K., J. Watkins, A. Barnard, and K. H. Mills, 1993, Effective immunization against *Bordetella pertussis* respiratory infection in mice is dependent on induction of cell-mediated immunity: *Infect Immun*, v. 61, p. 3190-8.
- Reed-Geaghan, E. G., J. C. Savage, A. G. Hise, and G. E. Landreth, 2009, CD14 and toll-like receptors 2 and 4 are required for fibrillar A β -stimulated microglial activation.: *J Neurosci*, v. 29, p. 11982-92.
- Riviere, G. R., K. H. Riviere, and K. S. Smith, 2002, Molecular and immunological evidence of oral *Treponema* in the human brain and their association with Alzheimer's disease: *Oral Microbiol Immunol*, v. 17, p. 113-8.

- Rock, R. B., S. Hu, A. Deshpande, S. Munir, B. J. May, C. A. Baker, P. K. Peterson, and V. Kapur, 2005, Transcriptional response of human microglial cells to interferon-gamma: *Genes Immun*, v. 6, p. 712-9.
- Rodriguez, J. J., M. Olabarria, A. Chvatal, and A. Verkhratsky, 2009, Astroglia in dementia and Alzheimer's disease: *Cell Death Differ*, v. 16, p. 378-85.
- Rogers, J., J. Lubner-Narod, S. D. Styren, and W. H. Civin, 1988, Expression of immune system-associated antigens by cells of the human central nervous system: relationship to the pathology of Alzheimer's disease: *Neurobiol Aging*, v. 9, p. 339-49.
- Rogers, J., R. Strohmeyer, C. J. Kovelowski, and R. Li, 2002, Microglia and inflammatory mechanisms in the clearance of amyloid beta peptide.: *Glia*, v. 40, p. 260-9.
- Rolland, W. B., T. Lekic, P. R. Krafft, Y. Hasegawa, O. Altay, R. Hartman, R. Ostrowski, A. Manaenko, J. Tang, and J. H. Zhang, 2013, Fingolimod reduces cerebral lymphocyte infiltration in experimental models of rodent intracerebral hemorrhage: *Exp Neurol*, v. 241, p. 45-55.
- Rollins, B. J., 1997, Chemokines: *Blood*, v. 90, p. 909-28.
- Roper, K., and O. f. o. H. P. Surveillance Branch, 2009, Outbreak of pertussis, 1 January to 31 March 2009: *Commun Dis Intell Q Rep*, v. 33, p. 36-7.
- Rosen, H., C. Alfonso, C. D. Surh, and M. G. McHeyzer-Williams, 2003, Rapid induction of medullary thymocyte phenotypic maturation and egress inhibition by nanomolar sphingosine 1-phosphate receptor agonist: *Proc Natl Acad Sci U S A*, v. 100, p. 10907-12.
- Rosen, H., and E. J. Goetzl, 2005, Sphingosine 1-phosphate and its receptors: an autocrine and paracrine network, *Nat Rev Immunol*, v. 5: England, p. 560-70.
- Ross, P. J., E. C. Lavelle, K. H. Mills, and A. P. Boyd, 2004, Adenylate cyclase toxin from *Bordetella pertussis* synergizes with lipopolysaccharide to promote innate interleukin-10 production and enhances the induction of Th2 and regulatory T cells: *Infect Immun*, v. 72, p. 1568-79.
- Ross, P. J., C. E. Sutton, S. Higgins, A. C. Allen, K. Walsh, A. Misiak, E. C. Lavelle, R. M. McLoughlin, and K. H. Mills, 2013, Relative Contribution of Th1 and Th17 Cells in Adaptive Immunity to *Bordetella pertussis*: Towards the Rational Design of an Improved Acellular Pertussis Vaccine: *PLoS Pathog*, v. 9, p. e1003264.
- Roubaud Baudron, C., L. Letenneur, A. Langlais, A. Buissonnière, F. Mégraud, J. F. Dartigues, N. Salles, and P. A. Q. Study, 2013, Does *Helicobacter pylori* infection increase incidence of dementia? The Personnes Agées QUID Study: *J Am Geriatr Soc*, v. 61, p. 74-8.
- Roubaud-Baudron, C., P. Krolak-Salmon, I. Quadrio, F. Mégraud, and N. Salles, 2012, Impact of chronic *Helicobacter pylori* infection on Alzheimer's disease: preliminary results: *Neurobiol Aging*, v. 33, p. 1009.e11-9.
- Rudd, C. E., A. Taylor, and H. Schneider, 2009, CD28 and CTLA-4 coreceptor expression and signal transduction, *Immunol Rev*, v. 229: Denmark, p. 12-26.

- Ryu, J. K., and J. G. McLarnon, 2009, A leaky blood-brain barrier, fibrinogen infiltration and microglial reactivity in inflamed Alzheimer's disease brain: *J Cell Mol Med*, v. 13, p. 2911-25.
- Saijo, K., and C. K. Glass, 2011, Microglial cell origin and phenotypes in health and disease: *Nat Rev Immunol*, v. 11, p. 775-87.
- Saitou, M., Y. Ando-Akatsuka, M. Itoh, M. Furuse, J. Inazawa, K. Fujimoto, and S. Tsukita, 1997, Mammalian occludin in epithelial cells: its expression and subcellular distribution: *Eur J Cell Biol*, v. 73, p. 222-31.
- Sanchez, T., T. Estrada-Hernandez, J. H. Paik, M. T. Wu, K. Venkataraman, V. Brinkmann, K. Claffey, and T. Hla, 2003, Phosphorylation and action of the immunomodulator FTY720 inhibits vascular endothelial cell growth factor-induced vascular permeability: *J Biol Chem*, v. 278, p. 47281-90.
- Saresella, M., E. Calabrese, I. Marventano, F. Piancone, A. Gatti, M. Alberoni, R. Nemni, and M. Clerici, 2011, Increased activity of Th-17 and Th-9 lymphocytes and a skewing of the post-thymic differentiation pathway are seen in Alzheimer's disease: *Brain Behav Immun*, v. 25, p. 539-47.
- Saresella, M., E. Calabrese, I. Marventano, F. Piancone, A. Gatti, M. G. Calvo, R. Nemni, and M. Clerici, 2010, PD1 negative and PD1 positive CD4+ T regulatory cells in mild cognitive impairment and Alzheimer's disease: *J Alzheimers Dis*, v. 21, p. 927-38.
- Saresella, M., E. Calabrese, I. Marventano, F. Piancone, A. Gatti, E. Farina, M. Alberoni, and M. Clerici, 2012, A potential role for the PD1/PD-L1 pathway in the neuroinflammation of Alzheimer's disease: *Neurobiol Aging*, v. 33, p. 624.e11-22.
- Sarma, J. D., B. Ciric, R. Marek, S. Sadhukhan, M. L. Caruso, J. Shafagh, D. C. Fitzgerald, K. S. Shindler, and A. Rostami, 2009, Functional interleukin-17 receptor A is expressed in central nervous system glia and upregulated in experimental autoimmune encephalomyelitis, *J Neuroinflammation*, v. 6, p. 14.
- Sastre, M., J. Walter, and S. M. Gentleman, 2008, Interactions between APP secretases and inflammatory mediators: *J Neuroinflammation*, v. 5, p. 25.
- Schall, T. J., K. Bacon, R. D. Camp, J. W. Kaspari, and D. V. Goeddel, 1993, Human macrophage inflammatory protein alpha (MIP-1 alpha) and MIP-1 beta chemokines attract distinct populations of lymphocytes: *J Exp Med*, v. 177, p. 1821-6.
- Schenk, D., 2002, Amyloid-beta immunotherapy for Alzheimer's disease: the end of the beginning.: *Nat Rev Neurosci*, v. 3, p. 824-8.
- Schenk, D., R. Barbour, W. Dunn, G. Gordon, H. Grajeda, T. Guido, K. Hu, J. Huang, K. Johnson-Wood, K. Khan, D. Kholodenko, M. Lee, Z. Liao, I. Lieberburg, R. Motter, L. Mutter, F. Soriano, G. Shopp, N. Vasquez, C. Vandever, S. Walker, M. Wogulis, T. Yednock, D. Games, and P. Seubert, 1999, Immunization with amyloid-beta attenuates Alzheimer-disease-like pathology in the PDAPP mouse: *Nature*, v. 400, p. 173-7.

- Schiffenbauer, J., H. M. Johnson, E. J. Butfiloski, L. Wegrzyn, and J. M. Soos, 1993, Staphylococcal enterotoxins can reactivate experimental allergic encephalomyelitis: *Proc Natl Acad Sci U S A*, v. 90, p. 8543-6.
- Schindowski, K., A. Eckert, J. Peters, C. Gorriz, U. Schramm, T. Weinandi, K. Maurer, L. Frölich, and W. E. Müller, 2007, Increased T-cell reactivity and elevated levels of CD8+ memory T-cells in Alzheimer's disease-patients and T-cell hyporeactivity in an Alzheimer's disease-mouse model: implications for immunotherapy.: *Neuromolecular Med*, v. 9, p. 340-54.
- Schwartz, M., and K. Baruch, 2014, The resolution of neuroinflammation in neurodegeneration: leukocyte recruitment via the choroid plexus: *Embo j*, v. 33, p. 7-22.
- Sedgwick, J. D., S. Schwender, H. Imrich, R. Dörries, G. W. Butcher, and V. ter Meulen, 1991, Isolation and direct characterization of resident microglial cells from the normal and inflamed central nervous system: *Proc Natl Acad Sci U S A*, v. 88, p. 7438-42.
- Selkoe, D. J., 2001, Alzheimer's disease results from the cerebral accumulation and cytotoxicity of amyloid beta-protein: *J Alzheimers Dis*, v. 3, p. 75-80.
- Selkoe, D. J., 2012, Preventing Alzheimer's disease: *Science*, v. 337, p. 1488-92.
- Sengillo, J. D., E. A. Winkler, C. T. Walker, J. S. Sullivan, M. Johnson, and B. V. Zlokovic, 2013, Deficiency in mural vascular cells coincides with blood-brain barrier disruption in Alzheimer's disease: *Brain Pathol*, v. 23, p. 303-10.
- Shah, F. A., F. Pike, K. Alvarez, D. Angus, A. B. Newman, O. Lopez, J. Tate, V. Kapur, A. Wilsdon, J. A. Krishnan, N. Hansel, D. Au, M. Avdalovic, V. S. Fan, R. G. Barr, and S. Yende, 2013, Bidirectional relationship between cognitive function and pneumonia: *Am J Respir Crit Care Med*, v. 188, p. 586-92.
- Sheng, J. G., S. H. Bora, G. Xu, D. R. Borchelt, D. L. Price, and V. E. Koliatsos, 2003, Lipopolysaccharide-induced-neuroinflammation increases intracellular accumulation of amyloid precursor protein and amyloid beta peptide in APPswe transgenic mice: *Neurobiol Dis*, v. 14, p. 133-45.
- Shirai, Y., 1921, On the transplantation of the rat sarcoma in adult heterogenous animals., *Jap. Med. World*, p. 14-15.
- Sibley, W. A., C. R. Bamford, and K. Clark, 1985, Clinical viral infections and multiple sclerosis: *Lancet*, v. 1, p. 1313-5.
- Simard, A. R., D. Soulet, G. Gowing, J. P. Julien, and S. Rivest, 2006, Bone marrow-derived microglia play a critical role in restricting senile plaque formation in Alzheimer's disease: *Neuron*, v. 49, p. 489-502.
- Simpson, J. E., P. G. Ince, G. Lace, G. Forster, P. J. Shaw, F. Matthews, G. Savva, C. Brayne, S. B. Wharton, and M. C. F. a. A. N. S. Group, 2010, Astrocyte phenotype in relation to Alzheimer-type pathology in the ageing brain: *Neurobiol Aging*, v. 31, p. 578-90.
- Sly, L. M., R. F. Krzesicki, J. R. Brashler, A. E. Buhl, D. D. McKinley, D. B. Carter, and J. E. Chin, 2001, Endogenous brain cytokine mRNA and inflammatory responses to lipopolysaccharide are elevated in the Tg2576 transgenic mouse model of Alzheimer's disease: *Brain Res Bull*, v. 56, p. 581-8.

- Smeeth, L., S. L. Thomas, A. J. Hall, R. Hubbard, P. Farrington, and P. Vallance, 2004, Risk of myocardial infarction and stroke after acute infection or vaccination: *N Engl J Med*, v. 351, p. 2611-8.
- Sofroniew, M. V., and H. V. Vinters, 2010, Astrocytes: biology and pathology: *Acta Neuropathol*, v. 119, p. 7-35.
- Soos, J. M., T. A. Ashley, J. Morrow, J. C. Patarroyo, B. E. Szente, and S. S. Zamvil, 1999, Differential expression of B7 co-stimulatory molecules by astrocytes correlates with T cell activation and cytokine production: *Int Immunol*, v. 11, p. 1169-79.
- Soos, J. M., J. Morrow, T. A. Ashley, B. E. Szente, E. K. Bikoff, and S. S. Zamvil, 1998, Astrocytes express elements of the class II endocytic pathway and process central nervous system autoantigen for presentation to encephalitogenic T cells: *J Immunol*, v. 161, p. 5959-66.
- Sorensen, S. D., O. Nicole, R. D. Peavy, L. M. Montoya, C. J. Lee, T. J. Murphy, S. F. Traynelis, and J. R. Hepler, 2003, Common signaling pathways link activation of murine PAR-1, LPA, and S1P receptors to proliferation of astrocytes: *Mol Pharmacol*, v. 64, p. 1199-209.
- Speciale, L., E. Calabrese, M. Saresella, C. Tinelli, C. Mariani, L. Sanvito, R. Longhi, and P. Ferrante, 2007, Lymphocyte subset patterns and cytokine production in Alzheimer's disease patients: *Neurobiol Aging*, v. 28, p. 1163-9.
- Sprent, J., J. H. Cho, O. Boyman, and C. D. Surh, 2008, T cell homeostasis: *Immunol Cell Biol*, v. 86, p. 312-9.
- Stahl, T., C. Reimers, R. Johne, R. Schliebs, and J. Seeger, 2006, Viral-induced inflammation is accompanied by beta-amyloid plaque reduction in brains of amyloid precursor protein transgenic Tg2576 mice: *Eur J Neurosci*, v. 24, p. 1923-34.
- Strandberg, T. E., K. H. Pitkala, K. Linnavuori, and R. S. Tilvis, 2004, Cognitive impairment and infectious burden in the elderly: *Arch Gerontol Geriatr Suppl*, p. 419-23.
- Streit, W. J., J. R. Conde, and J. K. Harrison, 2001, Chemokines and Alzheimer's disease: *Neurobiol Aging*, v. 22, p. 909-13.
- Sutton, C. E., S. J. Lalor, C. M. Sweeney, C. F. Brereton, E. C. Lavelle, and K. H. Mills, 2009, Interleukin-1 and IL-23 induce innate IL-17 production from gammadelta T cells, amplifying Th17 responses and autoimmunity: *Immunity*, v. 31, p. 331-41.
- Suzuki, S., X. K. Li, S. Enosawa, and T. Shinomiya, 1996, A new immunosuppressant, FTY720, induces bcl-2-associated apoptotic cell death in human lymphocytes: *Immunology*, v. 89, p. 518-23.
- Sy, M., M. Kitazawa, R. Medeiros, L. Whitman, D. Cheng, T. E. Lane, and F. M. Laferla, 2011, Inflammation induced by infection potentiates tau pathological features in transgenic mice: *Am J Pathol*, v. 178, p. 2811-22.
- Séguin, R., K. Biernacki, A. Prat, K. Wosik, H. J. Kim, M. Blain, E. McCrea, A. Bar-Or, and J. P. Antel, 2003, Differential effects of Th1 and Th2 lymphocyte supernatants on human microglia.: *Glia*, v. 42, p. 36-45.
- Tahara, K., H. D. Kim, J. J. Jin, J. A. Maxwell, L. Li, and K. Fukuchi, 2006, Role of toll-like receptor signalling in Abeta uptake and clearance: *Brain*, v. 129, p. 3006-19.

- Tai, L. M., K. A. Holloway, D. K. Male, A. J. Loughlin, and I. A. Romero, 2010, Amyloid-beta-induced occludin down-regulation and increased permeability in human brain endothelial cells is mediated by MAPK activation: *J Cell Mol Med*, v. 14, p. 1101-12.
- Takasugi, N., T. Sasaki, I. Ebinuma, S. Osawa, H. Isshiki, K. Takeo, T. Tomita, and T. Iwatsubo, 2013, FTY720/fingolimod, a sphingosine analogue, reduces amyloid-beta production in neurons: *PLoS One*, v. 8, p. e64050.
- Takeda, S., N. Sato, K. Ikimura, H. Nishino, H. Rakugi, and R. Morishita, 2013, Increased blood-brain barrier vulnerability to systemic inflammation in an Alzheimer disease mouse model: *Neurobiol Aging*, v. 34, p. 2064-70.
- Tal, S., V. Guller, A. Gurevich, and S. Levi, 2002, Fever of unknown origin in the elderly: *J Intern Med*, v. 252, p. 295-304.
- Tan, J., T. Town, F. Crawford, T. Mori, A. DelleDonne, R. Crescentini, D. Obregon, R. A. Flavell, and M. J. Mullan, 2002, Role of CD40 ligand in amyloidosis in transgenic Alzheimer's mice: *Nat Neurosci*, v. 5, p. 1288-93.
- Tan, J., T. Town, D. Paris, T. Mori, Z. Suo, F. Crawford, M. P. Mattson, R. A. Flavell, and M. Mullan, 1999, Microglial activation resulting from CD40-CD40L interaction after beta-amyloid stimulation: *Science*, v. 286, p. 2352-5.
- Tan, L., K. B. Gordon, J. P. Mueller, L. A. Matis, and S. D. Miller, 1998, Presentation of proteolipid protein epitopes and B7-1-dependent activation of encephalitogenic T cells by IFN-gamma-activated SJL/J astrocytes: *J Immunol*, v. 160, p. 4271-9.
- Teige, I., Y. Liu, and S. Issazadeh-Navikas, 2006, IFN-beta inhibits T cell activation capacity of central nervous system APCs: *J Immunol*, v. 177, p. 3542-53.
- Terry, R. D., E. Masliah, D. P. Salmon, N. Butters, R. DeTeresa, R. Hill, L. A. Hansen, and R. Katzman, 1991, Physical basis of cognitive alterations in Alzheimer's disease: synapse loss is the major correlate of cognitive impairment: *Ann Neurol*, v. 30, p. 572-80.
- Thawer, S. G., W. G. Horsnell, M. Darby, J. C. Hoving, B. Dewals, A. J. Cutler, D. Lang, and F. Brombacher, 2014, Lung-resident CD4(+) T cells are sufficient for IL-4Ralpha-dependent recall immunity to *Nippostrongylus brasiliensis* infection: *Mucosal Immunol*, v. 7, p. 239-48.
- Thies, W., and L. Bleiler, 2013, 2013 Alzheimer's disease facts and figures: *Alzheimers Dement*, v. 9, p. 208-45.
- Tigges, U., A. Boroujerdi, J. V. Welser-Alves, and R. Milner, 2013, TNF-alpha promotes cerebral pericyte remodeling in vitro, via a switch from alpha1 to alpha2 integrins, *J Neuroinflammation*, v. 10: England, p. 33.
- Tilvis, R. S., M. H. Kähönen-Väre, J. Jolkkonen, J. Valvanne, K. H. Pitkala, and T. E. Strandberg, 2004, Predictors of cognitive decline and mortality of aged people over a 10-year period: *J Gerontol A Biol Sci Med Sci*, v. 59, p. 268-74.
- Togo, T., H. Akiyama, E. Iseki, H. Kondo, K. Ikeda, M. Kato, T. Oda, K. Tsuchiya, and K. Kosaka, 2002, Occurrence of T cells in the brain of Alzheimer's disease and other neurological diseases: *J Neuroimmunol*, v. 124, p. 83-92.

- Togo, T., H. Akiyama, H. Kondo, K. Ikeda, M. Kato, E. Iseki, and K. Kosaka, 2000, Expression of CD40 in the brain of Alzheimer's disease and other neurological diseases: *Brain Res*, v. 885, p. 117-21.
- Toly-Ndour, C., G. Lui, M. M. Nunes, M. Bruley-Rosset, P. Aucouturier, and G. Dorothee, 2011, MHC-independent genetic factors control the magnitude of CD4+ T cell responses to amyloid-beta peptide in mice through regulatory T cell-mediated inhibition, *J Immunol*, v. 187: United States, p. 4492-500.
- Town, T., Y. Laouar, C. Pittenger, T. Mori, C. A. Szekely, J. Tan, R. S. Duman, and R. A. Flavell, 2008, Blocking TGF-beta-Smad2/3 innate immune signaling mitigates Alzheimer-like pathology: *Nat Med*, v. 14, p. 681-7.
- Town, T., J. Tan, R. A. Flavell, and M. Mullan, 2005, T-cells in Alzheimer's disease: *Neuromolecular Med*, v. 7, p. 255-64.
- Townsend, K. P., T. Town, T. Mori, L. F. Lue, D. Shytle, P. R. Sanberg, D. Morgan, F. Fernandez, R. A. Flavell, and J. Tan, 2005, CD40 signaling regulates innate and adaptive activation of microglia in response to amyloid beta-peptide: *Eur J Immunol*, v. 35, p. 901-10.
- Tripathy, D., L. Thirumangalakudi, and P. Grammas, 2007, Expression of macrophage inflammatory protein 1-alpha is elevated in Alzheimer's vessels and is regulated by oxidative stress: *J Alzheimers Dis*, v. 11, p. 447-55.
- Tripathy, D., L. Thirumangalakudi, and P. Grammas, 2010, RANTES upregulation in the Alzheimer's disease brain: a possible neuroprotective role: *Neurobiol Aging*, v. 31, p. 8-16.
- Turner, P. R., K. O'Connor, W. P. Tate, and W. C. Abraham, 2003, Roles of amyloid precursor protein and its fragments in regulating neural activity, plasticity and memory: *Prog Neurobiol*, v. 70, p. 1-32.
- Tyas, S. L., J. Manfreda, L. A. Strain, and P. R. Montgomery, 2001, Risk factors for Alzheimer's disease: a population-based, longitudinal study in Manitoba, Canada.: *Int J Epidemiol*, v. 30, p. 590-7.
- Urosevic, N., and R. N. Martins, 2008, Infection and Alzheimer's disease: the APOE epsilon4 connection and lipid metabolism: *J Alzheimers Dis*, v. 13, p. 421-35.
- Van Dijk, P. T., D. W. Dippel, J. H. Van Der Meulen, and J. D. Habbema, 1996, Comorbidity and its effect on mortality in nursing home patients with dementia: *J Nerv Ment Dis*, v. 184, p. 180-7.
- Van Wagoner, N. J., J. W. Oh, P. Repovic, and E. N. Benveniste, 1999, Interleukin-6 (IL-6) production by astrocytes: autocrine regulation by IL-6 and the soluble IL-6 receptor: *J Neurosci*, v. 19, p. 5236-44.
- Vass, K., and H. Lassmann, 1990, Intrathecal application of interferon gamma. Progressive appearance of MHC antigens within the rat nervous system: *Am J Pathol*, v. 137, p. 789-800.
- Vasto, S., G. Colonna-Romano, A. Larbi, A. Wikby, C. Caruso, and G. Pawelec, 2007, Role of persistent CMV infection in configuring T cell immunity in the elderly: *Immun Ageing*, v. 4, p. 2.

- Veldhoen, M., R. J. Hocking, C. J. Atkins, R. M. Locksley, and B. Stockinger, 2006, TGFbeta in the context of an inflammatory cytokine milieu supports de novo differentiation of IL-17-producing T cells: *Immunity*, v. 24, p. 179-89.
- Vellas, B., R. Black, L. J. Thal, N. C. Fox, M. Daniels, G. McLennan, C. Tompkins, C. Leibman, M. Pomfret, M. Grundman, and A. Q.-S. Team, 2009, Long-term follow-up of patients immunized with AN1792: reduced functional decline in antibody responders.: *Curr Alzheimer Res*, v. 6, p. 144-51.
- Verreault, R., D. Laurin, J. Lindsay, and G. De Serres, 2001, Past exposure to vaccines and subsequent risk of Alzheimer's disease.: *CMAJ*, v. 165, p. 1495-8.
- Vickers, J. C., T. C. Dickson, P. A. Adlard, H. L. Saunders, C. E. King, and G. McCormack, 2000, The cause of neuronal degeneration in Alzheimer's disease.: *Prog Neurobiol*, v. 60, p. 139-65.
- Viggars, A. P., S. B. Wharton, J. E. Simpson, F. E. Matthews, C. Brayne, G. M. Savva, C. Garwood, D. Drew, P. J. Shaw, and P. G. Ince, 2011, Alterations in the blood brain barrier in ageing cerebral cortex in relationship to Alzheimer-type pathology: a study in the MRC-CFAS population neuropathology cohort: *Neurosci Lett*, v. 505, p. 25-30.
- Vom Berg, J., S. Prokop, K. R. Miller, J. Obst, R. E. Kalin, I. Lopategui-Cabezas, A. Wegner, F. Mair, C. G. Schipke, O. Peters, Y. Winter, B. Becher, and F. L. Heppner, 2012, Inhibition of IL-12/IL-23 signaling reduces Alzheimer's disease-like pathology and cognitive decline: *Nat Med*, v. 18, p. 1812-9.
- Walsh, K. B., D. Marsolais, M. J. Welch, H. Rosen, and M. B. Oldstone, 2010, Treatment with a sphingosine analog does not alter the outcome of a persistent virus infection: *Virology*, v. 397, p. 260-9.
- Walsh, K. P., and K. H. Mills, 2013, Dendritic cells and other innate determinants of T helper cell polarisation: *Trends Immunol*, v. 34, p. 521-30.
- Wang, D. S., D. W. Dickson, and J. S. Malter, 2006, beta-Amyloid degradation and Alzheimer's disease: *J Biomed Biotechnol*, v. 2006, p. 58406.
- Wang, S., R. Wang, L. Chen, D. A. Bennett, D. W. Dickson, and D. S. Wang, 2010, Expression and functional profiling of neprilysin, insulin-degrading enzyme, and endothelin-converting enzyme in prospectively studied elderly and Alzheimer's brain: *J Neurochem*, v. 115, p. 47-57.
- Wang, X. L., J. Zeng, J. Feng, Y. T. Tian, Y. J. Liu, M. Qiu, X. Yan, Y. Yang, Y. Xiong, Z. H. Zhang, Q. Wang, J. Z. Wang, and R. Liu, 2014, Helicobacter pylori filtrate impairs spatial learning and memory in rats and increases β -amyloid by enhancing expression of presenilin-2: *Front Aging Neurosci*, v. 6.
- Weiner, H. L., and D. Frenkel, 2006, Immunology and immunotherapy of Alzheimer's disease.: *Nat Rev Immunol*, v. 6, p. 404-16.
- Weiss, N., F. Miller, S. Cazaubon, and P. O. Couraud, 2009, The blood-brain barrier in brain homeostasis and neurological diseases: *Biochim Biophys Acta*, v. 1788, p. 842-57.
- Weller, R. O., E. Djuanda, H. Y. Yow, and R. O. Carare, 2009, Lymphatic drainage of the brain and the pathophysiology of neurological disease: *Acta Neuropathol*, v. 117, p. 1-14.

- Weng, N. P., Y. Araki, and K. Subedi, 2012, The molecular basis of the memory T cell response: differential gene expression and its epigenetic regulation: *Nat Rev Immunol*, v. 12, p. 306-15.
- Westendorp, R. G., 2006, What is healthy aging in the 21st century?: *Am J Clin Nutr*, v. 83, p. 404S-409S.
- Westerman, M. A., D. Cooper-Blacketer, A. Mariash, L. Kotilinek, T. Kawarabayashi, L. H. Younkin, G. A. Carlson, S. G. Younkin, and K. H. Ashe, 2002, The relationship between Abeta and memory in the Tg2576 mouse model of Alzheimer's disease: *J Neurosci*, v. 22, p. 1858-67.
- Westman, G., D. Berglund, J. Widen, M. Ingelsson, O. Korsgren, L. Lannfelt, D. Sehlin, A. K. Lidehall, and B. M. Eriksson, 2014, Increased Inflammatory Response in Cytomegalovirus Seropositive Patients with Alzheimer's Disease, *PLoS One*, v. 9.
- Weston, W. M., L. R. Friedland, X. Wu, and B. Howe, 2012, Vaccination of adults 65 years of age and older with tetanus toxoid, reduced diphtheria toxoid and acellular pertussis vaccine (Boostrix[®]): results of two randomized trials: *Vaccine*, v. 30, p. 1721-8.
- Widmann, C. N., and M. T. Heneka, 2014, Long-term cerebral consequences of sepsis: *Lancet Neurol*, v. 13, p. 630-6.
- Wiessner, C., K. H. Wiederhold, A. C. Tissot, P. Frey, S. Danner, L. H. Jacobson, G. T. Jennings, R. Luond, R. Ortman, J. Reichwald, M. Zurini, A. Mir, M. F. Bachmann, and M. Staufenbiel, 2011, The second-generation active Abeta immunotherapy CAD106 reduces amyloid accumulation in APP transgenic mice while minimizing potential side effects: *J Neurosci*, v. 31, p. 9323-31.
- Wilcock, D. M., and C. A. Colton, 2008, Anti-amyloid-beta immunotherapy in Alzheimer's disease: relevance of transgenic mouse studies to clinical trials: *J Alzheimers Dis*, v. 15, p. 555-69.
- Wilcock, D. M., M. P. Vitek, and C. A. Colton, 2009, Vascular amyloid alters astrocytic water and potassium channels in mouse models and humans with Alzheimer's disease: *Neuroscience*, v. 159, p. 1055-69.
- Wilcock, D. M., Q. Zhao, D. Morgan, M. N. Gordon, A. Everhart, J. G. Wilson, J. E. Lee, and C. A. Colton, 2011, Diverse inflammatory responses in transgenic mouse models of Alzheimer's disease and the effect of immunotherapy on these responses: *ASN Neuro*, v. 3, p. 249-58.
- Williams, M., 2009, Progress in Alzheimer's disease drug discovery: an update.: *Curr Opin Investig Drugs*, v. 10, p. 23-34.
- Wolf, S. A., U. Gimsa, I. Bechmann, and R. Nitsch, 2001, Differential expression of costimulatory molecules B7-1 and B7-2 on microglial cells induced by Th1 and Th2 cells in organotypic brain tissue.: *Glia*, v. 36, p. 414-20.
- Wong, G. H., P. F. Bartlett, I. Clark-Lewis, F. Battye, and J. W. Schrader, 1984, Inducible expression of H-2 and Ia antigens on brain cells: *Nature*, v. 310, p. 688-91.
- Wood, J. A., P. L. Wood, R. Ryan, N. R. Graff-Radford, C. Pilapil, Y. Robitaille, and R. Quirion, 1993, Cytokine indices in Alzheimer's temporal cortex: no changes in mature IL-1 beta or IL-1RA but increases in the associated acute phase proteins IL-6, alpha 2-macroglobulin and C-reactive protein: *Brain Res*, v. 629, p. 245-52.

- Wozniak, M. A., S. J. Shipley, M. Combrinck, G. K. Wilcock, and R. F. Itzhaki, 2005, Productive herpes simplex virus in brain of elderly normal subjects and Alzheimer's disease patients: *J Med Virol*, v. 75, p. 300-6.
- Wraith, D. C., and L. B. Nicholson, 2012, The adaptive immune system in diseases of the central nervous system: *J Clin Invest*, v. 122, p. 1172-9.
- Wu, C., S. Y. Leong, C. S. Moore, Q. L. Cui, P. Gris, L. P. Bernier, T. A. Johnson, P. Seguela, T. E. Kennedy, A. Bar-Or, and J. P. Antel, 2013, Dual effects of daily FTY720 on human astrocytes in vitro: relevance for neuroinflammation: *J Neuroinflammation*, v. 10, p. 41.
- WuDunn, D., and P. G. Spear, 1989, Initial interaction of herpes simplex virus with cells is binding to heparan sulfate: *J Virol*, v. 63, p. 52-8.
- Wyss-Coray, T., J. D. Loike, T. C. Brionne, E. Lu, R. Anankov, F. Yan, S. C. Silverstein, and J. Husemann, 2003, Adult mouse astrocytes degrade amyloid-beta in vitro and in situ: *Nat Med*, v. 9, p. 453-7.
- Xia, M. Q., B. J. Bacskai, R. B. Knowles, S. X. Qin, and B. T. Hyman, 2000, Expression of the chemokine receptor CXCR3 on neurons and the elevated expression of its ligand IP-10 in reactive astrocytes: in vitro ERK1/2 activation and role in Alzheimer's disease: *J Neuroimmunol*, v. 108, p. 227-35.
- Xia, M. Q., S. X. Qin, L. J. Wu, C. R. Mackay, and B. T. Hyman, 1998, Immunohistochemical study of the beta-chemokine receptors CCR3 and CCR5 and their ligands in normal and Alzheimer's disease brains: *Am J Pathol*, v. 153, p. 31-7.
- Xie, J. H., N. Nomura, S. L. Koprak, E. J. Quackenbush, M. J. Forrest, and H. Rosen, 2003, Sphingosine-1-phosphate receptor agonism impairs the efficiency of the local immune response by altering trafficking of naive and antigen-activated CD4+ T cells: *J Immunol*, v. 170, p. 3662-70.
- Yagi, H., R. Kamba, K. Chiba, H. Soga, K. Yaguchi, M. Nakamura, and T. Itoh, 2000, Immunosuppressant FTY720 inhibits thymocyte emigration: *Eur J Immunol*, v. 30, p. 1435-44.
- Yamamoto, M., T. Kiyota, M. Horiba, J. L. Buescher, S. M. Walsh, H. E. Gendelman, and T. Ikezu, 2007, Interferon-gamma and tumor necrosis factor-alpha regulate amyloid-beta plaque deposition and beta-secretase expression in Swedish mutant APP transgenic mice: *Am J Pathol*, v. 170, p. 680-92.
- Yanagawa, Y., Y. Masubuchi, and K. Chiba, 1998, FTY720, a novel immunosuppressant, induces sequestration of circulating mature lymphocytes by acceleration of lymphocyte homing in rats, III. Increase in frequency of CD62L-positive T cells in Peyer's patches by FTY720-induced lymphocyte homing: *Immunology*, v. 95, p. 591-4.
- Yoshiyama, Y., M. Higuchi, B. Zhang, S. M. Huang, N. Iwata, T. C. Saido, J. Maeda, T. Suhara, J. Q. Trojanowski, and V. M. Lee, 2007, Synapse loss and microglial activation precede tangles in a P301S tauopathy mouse model: *Neuron*, v. 53, p. 337-51.

- Zachariadis, O., J. P. Cassidy, J. Brady, and B. P. Mahon, 2006, gammadelta T cells regulate the early inflammatory response to bordetella pertussis infection in the murine respiratory tract: *Infect Immun*, v. 74, p. 1837-45.
- Zeinstra, E., N. Wilczak, and J. De Keyser, 2003, Reactive astrocytes in chronic active lesions of multiple sclerosis express co-stimulatory molecules B7-1 and B7-2: *J Neuroimmunol*, v. 135, p. 166-71.
- Zeinstra, E., N. Wilczak, C. Streefland, and J. De Keyser, 2000, Astrocytes in chronic active multiple sclerosis plaques express MHC class II molecules: *Neuroreport*, v. 11, p. 89-91.
- Zhang, K., L. Tian, L. Liu, Y. Feng, Y. B. Dong, B. Li, D. S. Shang, W. G. Fang, Y. P. Cao, and Y. H. Chen, 2013, CXCL1 contributes to beta-amyloid-induced transendothelial migration of monocytes in Alzheimer's disease: *PLoS One*, v. 8, p. e72744.
- Zheng, H., M. Jiang, M. E. Trumbauer, D. J. Sirinathsinghji, R. Hopkins, D. W. Smith, R. P. Heavens, G. R. Dawson, S. Boyce, M. W. Conner, K. A. Stevens, H. H. Slunt, S. S. Sisoda, H. Y. Chen, and L. H. Van der Ploeg, 1995, beta-Amyloid precursor protein-deficient mice show reactive gliosis and decreased locomotor activity: *Cell*, v. 81, p. 525-31.
- Zhu, Y., S. Yao, and L. Chen, 2011, Cell surface signaling molecules in the control of immune responses: a tide model, *Immunity*, v. 34: United States, 2011 Elsevier Inc, p. 466-78.
- Zipser, B. D., C. E. Johanson, L. Gonzalez, T. M. Berzin, R. Tavares, C. M. Hulette, M. P. Vitek, V. Hovanesian, and E. G. Stopa, 2007, Microvascular injury and blood-brain barrier leakage in Alzheimer's disease: *Neurobiol Aging*, v. 28, p. 977-86.
- Zlokovic, B. V., 2011, Neurovascular pathways to neurodegeneration in Alzheimer's disease and other disorders: *Nat Rev Neurosci*, v. 12, p. 723-38.

Appendix I

Solutions

Agarose Gel	1.3 g agarose 130 ml DEPC-treated dH ₂ O Heat in microwave until boiling Add: 13 µl Gel red
Ammonium chloride lysis solution (0.87%)	4.35 g ammonium chloride (NH ₄ Cl) 500 ml ddH ₂ O
Bordet-Gengou agar plates	500 ml dH ₂ O 5 ml glycerol 15 g Bordet-Gengou agar base Autoclave Add: 1 ml cephalixin (10 mg/ml) 100 ml pre-warmed sterile horse blood Pipette 23 ml into each Petri dish Allow to set overnight
Casein	6 g NaCl 10 g Casamino acid 1 L ddH ₂ O pH 7-7.2 Autoclave at 115°C, store at 4°C
Cephalexine (10 mg/ml)	0.1 g Cephalexine 10 ml dH ₂ O
Citrate buffer	2.1 g Citric acid 1 L dH ₂ O pH 6 Store at 4°C
Coating solution for glass slides	2.5 g Gelatine 0.25 g Chromium potassium sulphate 500 ml dH ₂ O Heat to 60°C, then filter Store at 4°C
Congo Red solution (0.2%)	1 g Congo red 500 ml Saturated NaCl solution Stir overnight and filter before use Add: 2 ml NaOH (1 M) per 200 ml
DEPC-treated dH ₂ O	1 L dH ₂ O 1 ml DEPC 37°C for 1 h, then autoclave

DMEM complete	500 ml DMEM 50 ml FBS 5 ml penicillin-streptomycin
EDTA (1 M)	18.61 g EDTA disodium salt 50 ml dH ₂ O pH 8
FACS Buffer	500 ml PBS 10 ml FBS 0.5 g Sodium azide (NaN ₃)
Guanidine Buffer	62.5 ml Guanidine-HCl (8 M, final concentration 5 M) 37.5 ml Tris-HCl (0.13 M pH 8, final concentration 50 mM) Add: 10 µl/ml protease inhibitor cocktail
Homogenisation Buffer (Soluble Aβ)	0.292 g NaCl 1 g SDS 100 ml dH ₂ O pH 10 Add: 10 µl/ml protease inhibitor cocktail
Immunohistochemistry wash buffer	500 ml PBS 100 µl Triton X-100
MACS Buffer	2.5 ml BSA 1 ml EDTA (1 M, final concentration 2 mM) 500 ml PBS
Methyl green solution	1 g methyl green 100 ml dH ₂ O
Neutralising buffer (Tris/HCl 0.5 M)	3.94 g Tris/HCl 50 ml dH ₂ O pH 6.8
PBS (1X)	8 g NaCl 0.2 g Potassium chloride (KCl) 1.15 g Disodium hydrogen phosphate (Na ₂ HPO ₄) 0.2 g Potassium phosphate monobasic (KH ₂ PO ₄) 1 L dH ₂ O pH 7.2-7.4
PBS-T	1 L PBS (1X) 500 µl Tween 20 pH 7.2-7.4

Percoll dilutions	<p>Stock Isotonic Percoll (SIP): dilute Percoll from bottle 9:1 with 10X PBS.</p> <p>The different gradients are as follows:</p> <p>1.030 g/ml: 21.5 ml SIP + 78.7 ml 1X PBS</p> <p>1.072 g/ml: 57 ml SIP + 43.1 ml 1X PBS</p> <p>1.088 g/ml: 70 ml SIP + 29.34 ml 1X PBS</p> <p>1.123 g/ml: 100 ml SIP</p>
PFA	<p>4 g PFA</p> <p>100 ml 1X PBS</p> <p>pH 7.4</p>
RPMI complete	<p>500 ml RPMI</p> <p>5 ml penicillin-streptomycin</p> <p>5 ml L-glutamine</p> <p>50 ml FBS</p>
Saponin	<p>1 g saponin</p> <p>200 ml 1X PBS</p>
Saturated NaCl solution	<p>50 g NaCl</p> <p>500 ml 80% ethanol in dH₂O</p> <p>Add NaCl until 5 mm resides at bottom of glass beaker</p> <p>Add: 2 ml NaOH (1 M) per 200 ml</p>
Stainer-Scholte liquid medium	<p>10.72 g L-Glutamic acid</p> <p>0.24 g L-Proline</p> <p>2.5 g NaCl</p> <p>0.5 g KH₂PO₄</p> <p>0.2 g KCl</p> <p>0.1 g Magnesium chloride hexahydrate (MgCl₂.6H₂O)</p> <p>0.02 g Calcium chloride dihydrate (CaCl₂.2H₂O)</p> <p>1.525 g Tris</p> <p>1 L ddH₂O, pH 7.3-7.4</p> <p>Autoclave and store at 4°C</p> <p>Add: 1 ml supplement per 100 ml Stainer-Scholte liquid medium for culture of <i>B. pertussis</i></p>
Sulfuric acid (ELISA stop solution)	<p>26.6 ml H₂SO₄ (18.8 M)</p> <p>473.4 ml dH₂O</p>

Supplement for Stainer-Scholte
liquid medium

0.4 g L-cystine (dissolve in 1 ml concentrated
HCl)

0.1 g Iron(II) sulfate heptahydrate
(Fe.SO₄.7H₂O)

0.2 g Ascorbic acid

0.04 g Nicotinic acid

1.0 g Glutathione (reduced)

100 ml ddH₂O

Sterilize by membrane filtration

Store at 4°C

X-Vivo complete

500 ml X-Vivo

5 ml penicillin-streptomycin

5 ml L-glutamine

2 µl β-mercaptoethanol

Appendix II

Materials

100 base pair ladder	Promega
ABI Prism 7300 instrument	Applied Biosystems
Agarose	Life Technologies
Alexa Fluor 647 goat anti-rabbit secondary IgG	Life Technologies
Ammonium chloride	Sigma-Aldrich
Amyloid β_{1-42}	Life Technologies
Anti-mouse CD3	BD Biosciences
Ascorbic acid	Sigma-Aldrich
BCA protein assay kit	Thermo Fisher Scientific
BFA	Sigma-Aldrich
Bordet Gengou Agar Base	BD Biosciences
BSA	Sigma-Aldrich
CaCl ₂ .2H ₂ O	Sigma-Aldrich
Casamino acid	BD Biosciences
Cell permeabilisation kit	Dako
Cephalexine	Sigma-Aldrich
Chromium potassium sulphate	Sigma-Aldrich
Citric acid	Sigma-Aldrich
Collagenase D	Roche
Congo red	Sigma-Aldrich
CpG	Sigma-Genosys
Cryostat	Leica
Cytokines (recombinant)	R&D Systems or Immunotools
DEPC	Sigma-Aldrich
DNase I	Sigma-Aldrich
DNase/RNase free 1.5 ml Eppendorf tubes	Sarstedt
DNeasy® blood and tissue kit	Qiagen
DPX	RA Lamb
EDTA disodium salt	Sigma-Aldrich
ELISA kits	R&D Systems
ELISA substrate solution	R&D Systems
Ethanol 96-100%	Sigma-Aldrich
Falcon tubes	Thermo Fisher Scientific
FBS	Sigma-Aldrich
Fe.SO ₄ .7H ₂ O	Sigma-Aldrich
FlowJo software	Tree Star
FTY720	Santa-Cruz Biotechnology
Gel red	Biotium
Gelatine	Fluka
Genotyping primers	Eurofins MWG Operon
Glass slides	Thermo Fisher Scientific
Glutathione (reduced)	Sigma-Aldrich
Glycerol	Sigma-Aldrich
Go Taq® qPCR Mastermix	Promega

GraphPad Prism v4.0	GraphPad Software
Guanidine	Sigma-Aldrich
Haemocytometer	Hycor Biomedical
HBSS	Sigma-Aldrich
High Capacity cDNA RT kit	Applied Biosystems
Horse Blood	Cruinn Diagnostics
Imaris imaging software	Bitplane
Ionomycin	Sigma-Aldrich
KCl	Sigma-Aldrich
KH ₂ PO ₄	Sigma-Aldrich
L-Cystine	Sigma-Aldrich
Leica SP8 confocal microscope	Leica
L-glutamic acid	Sigma-Aldrich
L-glutamine	Sigma-Aldrich
LIVE/DEAD® Fixable Aqua Dead Cell Stain kit	Life Technologies
L-Proline	Sigma-Aldrich
LSR Fortessa	BD Biosciences
MACS column	Miltenyi Biotec
MACS isolation kit	Miltenyi Biotec
Methyl green	Sigma-Aldrich
MgCl ₂ ·6H ₂ O	Sigma-Aldrich
MJ Research Peltier Thermal Cycler-200	Biosciences
MSD® 96-well multi-spot 4G8 Aβ triple ultra-sensitive assay kits	Meso Scale Discovery
MSD® Aβ peptide Panel 1 (4G8) V-PLEX kits	Meso Scale Discovery
Na ₂ HPO ₄	Sigma-Aldrich
NaCl	Sigma-Aldrich
NanoDrop Spectrophotometer	NanoDrop Technologies Inc.
NaOH	Sigma-Aldrich
Nebulizer	PARI GmbH
Nicotinic acid	Sigma-Aldrich
Normal goat serum	Vector Laboratories
Nuaire Flow CO ₂ incubator	Jencons
NucleoSpin® RNAII isolation kit	Macherey-Nagel Inc.
Nunc-Immuno plate with Maxisorp surface	Sigma-Aldrich
Nylon mesh filter	Thermo Fisher Scientific
OCT	Sakura Tissue- Tek
Olympus Ix51 light microscope	Olympus
Pa: Infanrix®-IPV	GSK
Parafilm	VWR
PBS 10X	Sigma-Aldrich
Penicillin-streptomycin	Sigma-Aldrich
Percoll	Sigma-Aldrich
Petri-dish	Sarstedt
PFA	Thermo Fisher Scientific
PI	Sigma-Aldrich
PMA	Sigma-Aldrich
Pw: Whole cell <i>B. pertussis</i> vaccine 41S NIBSC code: 94/532	NIBSC
Rabbit anti-human CD3 antibody	Dako

Rabbit-anti human fibrinogen antibody	Dako
RPMI	Sigma-Aldrich
SDS	Sigma-Aldrich
Sector Imager plate reader	Meso Scale Discovery
SensiMix™ II Probe Mastermix	Bioline
Sodium azide	Sigma-Aldrich
Sodium pentobarbital	Merial Animal Health
Sulphuric acid	Sigma-Aldrich
Summit software	Dako
T25 flasks	Sigma-Aldrich
Taqman Gene Expression Assays	Applied Biosystems
Tris	Sigma-Aldrich
Tris/HCL	Sigma-Aldrich
Triton X-100	Sigma-Aldrich
Trypan Blue	Sigma-Aldrich
Trypsin-EDTA	Sigma-Aldrich
Tween-20	Sigma-Aldrich
Ultraviolet transilluminator	Bioimaging Systems
Vectashield with DAPI	Vector Laboratories
Whatman filter paper	Whatman International
X-Vivo	Lonza
Xylene	Sigma-Aldrich
β-mercaptoethanol	Sigma-Aldrich

Appendix III

Addresses

AbD Serotec	Endeavour House Langford Lane Kidlington OX5 1GE UK
Applied Biosystems	Life Technologies GmbH Frankfurter Straye 129 B 64293 Darmstadt Germany
BD Bioscience	Edmund Halley Road Oxford Science Park OX4 4DQ Oxford UK
Bioimaging Systems	UVP, LLC 2066 W. 11th Street Upland CA 91786 US
Bioline	16 The Edge Business Centre Humber Road London NW2 6EW UK
Biosciences	3 Charlemont Terrace Crofton Rd Dun Laoghaire Co. Dublin Ireland
Biotium	Biotium, Inc. 3159 Corporate Place Hayward CA 94545 US
Bitplane	Bitplane AG Badenerstrasse 682 CH-8048 Zurich Switzerland

Cruinn Diagnostics	5b/6b Hume Centre Park West Industrial Estate Nangor Road Dublin 12 Ireland
Dako	Dako Denmark A/S Produktionsvej 42 DK-2600 Glostrup Denmark
eBioscience	2nd Floor, Titan Court 3 Bishop Square Hatfield, AL10 9NA UK
Eurofins MWG Operon	Eurofins MWG Operon Anzinger Strasse 7a D-85560 Ebersberg Germany
GraphPad	GraphPad Software, Inc. 7825 Fay Avenue, Suite 230 La Jolla CA 92037 US
GSK	GlaxoSmithKline Limited Stonemasons Way Rathfarnham Dublin 16 Ireland
Hycor Biomedical	Hycor Pentlands Science Park Bush Loan Penicuik Edinburgh EH26 0pl UK
Immunotools	Altenoyther Strasse 10 26169 Friesoythe Germany
Jencons	Unit 15 The Birches Willard Way Imberhorne Industrial Estate East Grinstead West Sussex RH19 1XZ

	UK
Leica	Laboratory Instruments & Supplies Ltd Pamaron House Ballybin Road Ashbourne Ireland
Life Technologies	Bio-Sciences 3 Charlemont Terrace Crofton Road Dun Laoghaire Co Dublin Ireland
Lonza	Lonza Group Ltd Basel Switzerland
Macherey-Nagel Inc	Macherey- Nagel GmbH & Co. KG Postfach 10 13 52 D-52313 Düren Neumann Neander Str. 6-8 D-52355 Düren Germany
Merial Animal Health Limited	Sandringham House Harlow Business Park Harlow Essex CM19 5TG UK
Meso Scale Discovery	Meso Scale Discovery 1601 Research Boulevard Rockville, MD 20850-3173 US
Miltenyi Biotec	Miltenyi Biotec Ltd. Almac House, Church Lane Bisley Bisley, Surrey GU24 9DR UK
NanoDrop Technologies Inc.	3411 Silverside Rd Wilmington DE 19810 US
NIBSC	National Institute for Biological Standards and Control

	Potters Bar Hertfordshire EN6 3QG UK
Olympus	Shinjuku Monolith 3-1 Nishi-Shinjuku 2-chome Shinjuku-ku Tokyo Japan
PARI GmbH	Specialists in effective inhalation Moosstrasse 3 D-82319 Starnberg Germany
Promega	Promega Corporation 2800 Woods Hollow Road Madison WI 53711 US
Qiagen	Skelton House Lloyd Street North Manchester M15 6SH UK
R&D Systems	R&D Systems Europe Ltd. 19 Barton Lane Abingdon Science Park Abingdon, OX14 3NB UK
Roche	Roche Ireland Limited Clarecastle Co. Clare Ireland
Sakura Tissue Tek	Sakura Finetek Europe B.V. Flemingweg 10A 2408 AV Alphen aan den Rijn P.O. Box 362 2400 AJ Alphen aan den Rijn The Netherlands
Santa-Cruz Biotechnologies	2145 Delaware Ave Santa Cruz CA 95060 US

Sarstedt	Sarstedt AG & Co. Sarstedtstraße Postfach 1220 51582 Nümbrecht Germany
Sigma-Aldrich	Sigma-Aldrich Ireland Limited Vale Road Arklow Wicklow Ireland
Thermo Fisher Scientific	Fisher Scientific Ireland Suite 3 Plaza 212 Blanchardstown Corporate Park 2 Ballycoolin, Dublin 15 Ireland
Tree Star	340 A Street Suite # 206 Ashland OR 97520 US
Vector Laboratories	Vector Laboratories Ltd 3 Accent Park Bakewell Road Orton Southgate Peterborough PE2 6XS UK
VWR	Orion Business Campus Northwest Business Park Ballycoolin Blanchardstown, Dublin 15 Ireland
Whatman	Springfield Mill Sandling Rd Maidstone ME14 2LE UK

